SPAWAR
Systems Center
San Diego

TECHNICAL REPORT 1801
August 1999

Review of Dolphin Hydrodynamics and Swimming Performance

F. E. Fish
West Chester University

J. J. Rohr
SSC San Diego

SSC San Diego

TECHNICAL REPORT 1801
August 1999

Review of Dolphin Hydrodynamics and Swimming Performance

F. E. Fish
West Chester University

J. J. Rohr
SSC San Diego

SSC San Diego
San Diego, CA 92152–5001

SSC SAN DIEGO
San Diego, California 92152–5001

E. L. Valdes, CAPT, USN
Commanding Officer

R. C. Kolb
Executive Director

ADMINISTRATIVE INFORMATION

The work detailed in this report was performed for the Defense Advanced Research Projects Agency (DARPA) by the Applied Research and Technology Branch, Code D363, Space and Naval Warfare (SPAWAR) Systems Center, San Diego (SSC San Diego) and West Chester University.

Released by
G. W. Anderson, Head
Applied Research &
Technology Branch

Under authority of
R. H. Moore, Head
Environmental
Sciences Division

SB

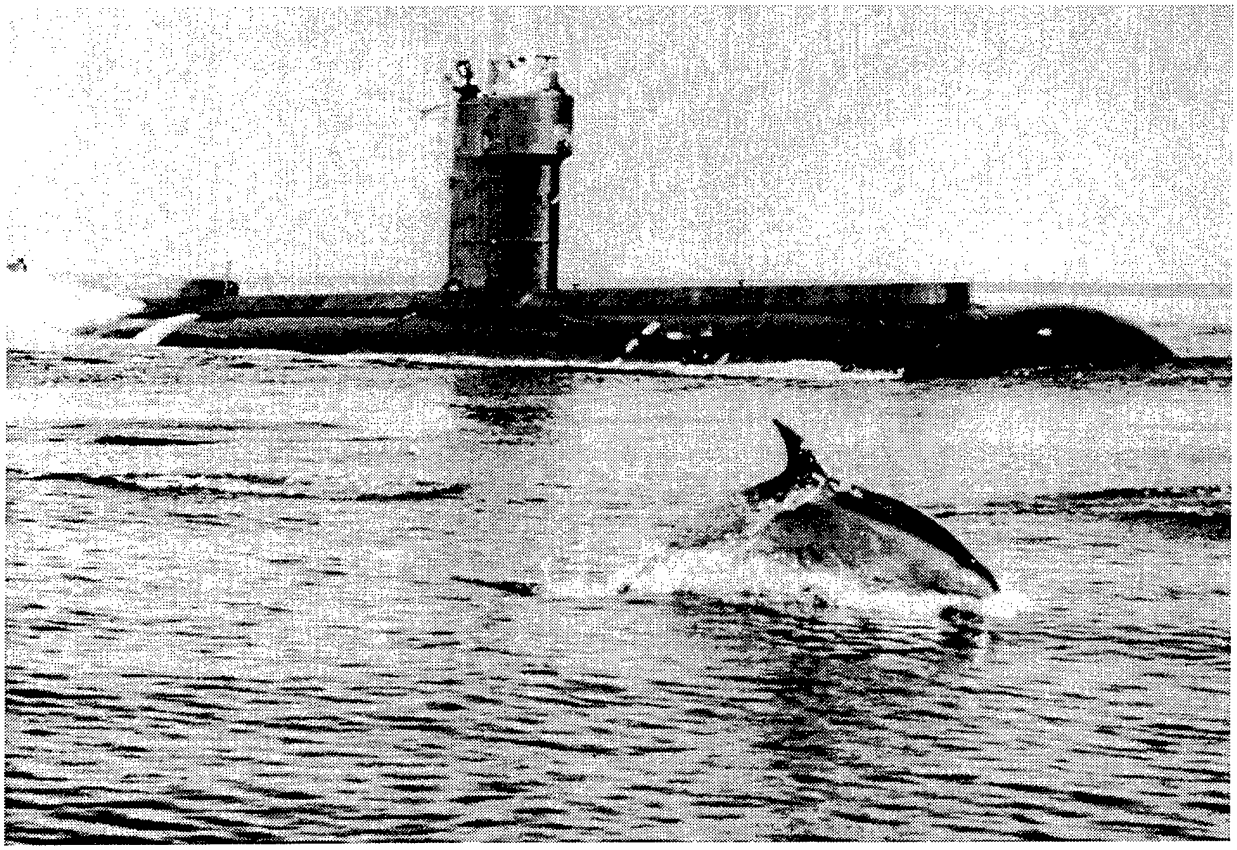

"The dolphins usually swim ahead of the ship, or sometimes alongside, but never in the ship's wake. Unlike sharks, which follow ocean liners for their refuse, dolphins merely come up to play, sometimes jumping right out of the water, darting across the bow waves and even diving under the ship. They are never covetous and never beg. On the contrary, the are the envoys of Neptune, the God of the Sea, and as such they accompany the ship and see it safe to harbour."

E. J. Slijper, 1979

EXECUTIVE SUMMARY

OBJECTIVE

The principal objective of this project was to perform a comprehensive review of performance, kinematics, and swimming hydrodynamics by dolphins and other cetaceans. This report describes information obtained from the available literature including published research and technical reports from English-speaking and Russian sources. The project team specifically studied routine and maximum swimming speeds, morphological design related to hydrodynamic performance, drag reduction, swimming kinematics, thrust production and efficiency, behavioral strategies employed for energy economy when swimming, and maneuverability.

SYNOPSIS

Research into dolphin swimming has been guided historically by the false assumptions of "effortless, high-speed" swimming. Drag-reduction hypotheses were developed from these assumptions. A survey of the reported swimming speed estimates show that speed is inversely related to duration (i.e., the faster the speed, the shorter the duration). Reported maximum speed estimates range from 8 to 15 m/s. The body and control surfaces are highly streamlined. Dolphin body and control surfaces are similar to the design of manufactured high-performance structures. Drag estimates obtained from experiments on towed models and gliding and actively swimming animals were used to investigate drag-reduction mechanisms including compliant dampening, dermal ridges, secretions, boundary layer heating, and skin folds. There is some indication that the fluke oscillations may control boundary flow and prevent premature separation although the character of the boundary layer (laminar versus turbulent) remains in dispute. Symmetrical, sinusoidal fluke oscillations in the vertical plane produce thrust. Whereas the amplitude of the stroke remains constant over a routine speed range, frequency increases directly with speed, and pitch angle and angle of attack decrease with increasing speed. Hydromechanical models provide reasonable estimates of thrust power and efficiency, although the simplified assumptions of the models (i.e., rigid planform, simple geometric design) do not provide exact solutions. Propulsive efficiencies are 0.75 to 0.90. These efficiencies occur within the optimal range of Strouhal numbers predicted for maximum efficiency. Metabolic data independently supports an assertion of high-efficiency swimming. Dolphins require additional metabolic energy when swimming to support homeothermy maintenance. Dolphins reduce the energetic cost of swimming through behavioral strategies. Drafting, wave and bow riding, gliding, porpoising, and avoiding the water surface are all mechanisms that allow for reduced swimming effort. Dolphins exhibit enhanced maneuverability because of their flexible body design and mobile control surfaces.

RECOMMENDATIONS

A comprehensive understanding of dolphin hydrodynamics will remain elusive for sometime because of the complexity of the problem and limited research opportunities. A thorough physics-based description of nonsteady, turbulent flow is presently not possible as neither is a detailed knowledge of the underlying biology. The research on swimming by dolphins has been limited because of restrictions on examining these animals and the lack of a comprehensive, coordinated investigation by biologists and engineers. None the less, trained animals, swimming flumes, and advanced technologies and computational models affords the opportunity to resolve many of the issues surrounding dolphin hydrodynamics. Even partial knowledge acquired on dolphin swimming performance has direct application to unmanned undersea vehicle (UUV) development. The per-

formance levels exhibited for speed, efficiency, stealth, and maneuverability by dolphins operating in either open ocean or confined habitats are desirable characteristics for transition to UUV technologies.

CONTENTS

Figures

Tables

LIST OF SYMBOLS

Many of the hydrodynamic terms listed below are briefly explained in Appendix A.

a	acceleration
A	planform area
a_{cg}	centripetal acceleration with respect to g
A_f	total projected area of flippers
$A_{p\text{-}p}$	peak-to-peak amplitude
AR	aspect ratio
BL	body length
c	constant
C	chord
C_D	coefficient of drag
C_L	coefficient of lift
COT	cost of transport
COT_{min}	minimum cost of transport
C_T	coefficient of thrust
d	distance between bow of vessel and tail of bow-riding dolphin
D	drag
DF	dorsal fin height
E	modulus of elasticity
f	frequency
F	Froude number
F_c	centripetal force
FL	flipper length
FR	fineness ratio
g	gravitational acceleration
h	amplitude of heave
h_e	height of the center of gravity when the tail emerges

H	maximum height of the dolphin's center of gravity from water surface
k	drag augmentation factor
L	lift
L	length of vessel
L_w	water line length
m	mass
m_v	virtual mass
M	metabolic power
MR	resting metabolic rate
P_{av}	average power
P_T	thrust power
R	resultant force
r	turning radius
RC	root chord
Re	Reynolds number
Rd	resultant drag
Rt	resultant thrust
s	distance traveled during acceleration
S	span
SP	shoulder position
St	Strouhal number
S_w	wetted surface area
t	time
t_a	acceleration period
T	thrust
T	maximum thickness
TR	thickness ratio
Vb	forward velocity of body
Vf	velocity of flukes

Vr	true velocity of flukes
U	velocity
U_c	critical velocity for leaping
U_e	water exit velocity
U_{m}	velocity of maximum range
U_{mr}	$\pm$ 10% of U_{m}
U_f	final velocity
U_i	initial velocity
α	angle of attack
α^*	pitch angle
ϕ	bank angle
η	Froude (propulsive) efficiency
η_a	aerobic efficiency
λ	added mass coefficient
Λ	sweepback angle
θ	feathering parameter
ρ	density
σ	reduced frequency
ω	radian frequency

1. INTRODUCTION

Dolphins are one of the most enigmatic of sea creatures. Even though reasonably large and restricted to the water surface to breathe, these animals dive frequently, and the depth and expanse of the oceans have limited precise observation of swimming performance. This limitation has created many erroneous conclusions regarding dolphin locomotor performance. The collection of good data on dolphin swimming capabilities has become more important as engineers and biologists have focused on dolphins and other marine organisms in developing the next generation of advanced naval technologies.

A long-standing idea is that new technologies can be developed from natural designs (Gibbs-Smith, 1962; Triantafyllou and Triantafyllou, 1995; Fish, 1998c; Vogel, 1998). Animals have inspired various technological developments including flight and robotics. Copying animals by the biomimetic approach seeks common solutions from engineering and biology for increased efficiency and specialization (Vincent, 1990). Because biological designs resulted from the evolutionary Darwinian process of "natural selection," it is assumed that animals have already performed the "cost-benefit-analysis," optimizing particular designs for specific functions. The diverse morphological specializations exhibited by animals may be targeted by engineers for technology transfer and effectively reduce the time required to develop innovative technological solutions. The development potential of new and superior technological designs for enhanced performance based on animal systems has been tantalizing, though elusive (Fish, 1998c; Vogel, 1998).

Aquatic animals are considered superior in their capabilities when compared to technologies produced from nautical engineering (Triantafyllou and Triantafyllou, 1995). Dolphins have been recorded at speeds over 11 m/s (>21 kts) (Lang, 1975). Turning maneuvers by dolphins are at rates as high as 450 deg/s with turn radii as low as 11 to 17% of body length (Fish, 1997). In addition, whales can migrate a distance of 18,000 km without feeding, dive to depths of 3195 m (2 miles), and generate sufficient force to launch their 30-ton weight out of the water (Winn and Reichley, 1985; Rice, 1989).

This report focuses on the hydrodynamics and energetics of swimming by dolphins and other whales in accordance with their varied morphological designs. The specialized adaptations used by whales and dolphins for drag reduction, thrust production, energy economy, and maneuverability are explored. These adaptations are compared with analogous engineered solutions to provide insight into the effectiveness of each system.

2. TAXONOMY OF CETACEANS

Whales and dolphins are mammals that breathe air with lungs, have hair, and nurse their young. These aquatic mammals are in the taxonomic order Cetacea. Cetaceans evolved in the Eocene epoch, approximately 50 million years ago (Thewissen, 1998). Modern cetaceans are split into two suborders: Mysticeti including the baleen whales and Odontoceti including the toothed whales (Minasian et al., 1984).

Mysticete whales (table 1) are divided into three families including the Balaenoptera (rorqual whales), Eschrichtiidae (gray whale), and Balaenidae (right whales). The mysticetes include the largest of all living animals, the blue whale (*Balaenoptera musculus*), which can grow to more than 27.4 m (90 ft) and weigh more than 136,000 kg (150 tons). These whales feed on small fish and crustaceans that they strain out of the water. The whales undertake some of the longest migrations in the animal kingdom.

Table 1. Mysticete whale species listed by taxonomic family.

Family	Species
Balaenopteridae	*Balaenoptera acutorostrata:* Minke whale
	Balaenoptera borealis: Sei whale
	Balaenoptera edeni: Bryde's whale
	Balaenoptera musculus: Blue whale
	Balaenoptera physalus: Fin whale
	Megaptera novaeangliae: Whiteback whale
Eschrichtiidae	*Eschrichtius robustus:* Gray whale
Balaenidae	*Balaena mysticetus:* Bowhead whale
	Caperea marginata: Pygmy right whale
	Eubalaena glacialis: Right whale

Odontocete whales (table 2) have 67 species that are divided into six families including the Physeteridae (sperm whales), Ziphiidae (beaked whales), Delphinidae (oceanic dolphins), Monodontidae (beluga and narwhal), Platanistidae (freshwater dolphins), and Phocoenidae (porpoises). These whales vary in size from the sperm whale (*Physter macrocephalus*) at 18.5 m and 45,000 kg to Heaviside's dolphin (*Cephalorhynchus heavisidii*) at 1.3 m and 45 kg. Odontocete whales generally feed on elusive and fast-moving prey including fish, squid, and marine mammals.

Most research has been performed on members of the Delphinidae. These animals have particular attributes that have been studied by zoos and aquaria, private foundations, and the military. In addition, these animals are extremely tractable for research because of their small size, easy mainte-

nance in captivity, and highly trainable and non-aggressive nature. The research on delphinids has focused on their large and highly complex brain, echolocation, communication, diving capability, and ability to swim at high speeds (Wood, 1973; Au, 1993).

Due to bias of previous work towards delphinids, much of this report focuses on information obtained from studies of particular members of this family, including *Tursiops*, *Stenella*, and *Lagenorhynchus*. However, data from other cetaceans will be incorporated into the text for a comprehensive review.

Table 2. Odontocete whale species listed by taxonomic family.

Family	Species
Physeteridae	*Kogia breviceps:* Pygmy sperm whale
	Kogia simus: Dwarf sperm whale
	Physter macrocephalus: Sperm whale
Ziphiidae	*Berardius arnuxii:* Arnoux's beaked whale
	Berardius bairdii: Baird's beaked whale
	Hyperoodon ampullatus: Northern bottlenose whale
	Hyperoodon planifrons: Southern bottlenose whale
	Mesoplodon bidens: Sowerby's beaked whale
	Mesoplodon bowdoini: Andrew's beaked whale
	Mesoplodon carlhubbsi: Hubb's beaked whale
	Mesoplodon densirostris: Blainville's beaked whale
	Mesoplodon europaeus: Gervais' beaked whale
	Mesoplodon ginkgodens: Ginko-toothed beaked whale
	Mesoplodon grayi: Gray's beaked whale
	Mesoplodon hectori: Hector's beaked whale
	Mesoplodon layardii: Strap-toothed whale
	Mesoplodon mirus: True's beaked whale
	Mesoplodon pacificus: Longman's beaked whale
	Mesoplodon stejnegeri: Stejneger's beaked whale
	Tasmacetus shepherd : Shepherd's beaked whale
	Ziphius cavirostris: Cuvier's beaked whale

Table 2. Odontocete whale species listed by taxonomic family. (continued)

Family	Species
Delphinidae	*Cephalorhynchus commersonii:* Commerson's dolphin
	Cephalorhynchus eutropia: Chilean dolphin
	Cephalorhynchus heavisidii: Heaviside's dolphin
	Cephalorhynchus hectori: Hector's dolphin
	Delphinus capensis: Long-beaked common dolphin
	Delphinus delphis: Common dolphin
	Feresa attenuata: Pygmy killer whale
	Grampus griseus: Risso's dolphin
	Globicephala macrorhynchus: Short-finned pilot whale
	Globicephala melaena: Long-finned pilot whale
	Lagenodelphis hosei: Fraser's dolphin
	Lagenorhynchus acutus: Atlantic white-sided dolphin
	Lagenorhynchus albirostris: White-beaked dolphin
	Lagenorhynchus australis: Peal's dolphin
	Lagenorhynchus cruciger: Hourglass dolphin
	Lagenorhynchus obliquidens: Pacific white-sided dolphin
	Lagenorhynchus obscurus: Dusky dolphin
	Lissodelphis borealis: Northern right whale dolphin
	Lissodelphis peronii: Southern right whale dolphin
	Orcaella brevirostris: Irrawaddy dolphin
	Orcinus orca: Killer whale
	Peponocephala electra: Melon-headed whale
	Pseudorca crassidens: False killer whale
	Sotalia fluvialtilis: Tucuxi dolphin
	Sousa chinensis: Indo-Pacific hump-backed dolphin
	Sousa teuszii: Atlantic hump-backed dolphin
	Stenella attenuata: Spotted dolphin
	Stenella clymene: Short-snouted dolphin
	Stenella coeruleoalba: Striped dolphin
	Stenella longirostris: Spinner dolphin

Table 2. Odontocete whale species listed by taxonomic family. (continued)

Family	Species
Delphinidae (continued)	*Stenella plagiodon:* Atlantic spotted dolphin
	Steno bredanensi: Rough-toothed dolphin
	Tursiops truncatus: Bottlenose dolphin
Monodontidae	*Delphinapterus leucas:* Beluga
	Monodon monoceros: Narwhal
Platanistidae	*Inia geoffrensis:* Amazon river dolphin
	Lipotes vexillifer: Chinese river dolphin
	Platanista gangetica: Ganges river dolphin
	Plantanista minor: Indus river dolphin
	Pontoporia blainvillei: Franciscana dolphin
Phocoenidae	*Neophocaena phocaenoides:* Finless porpoise
	Phocoena dioptrica: Spectacled porpoise
	Phocoena phocoena: Harbor porpoise
	Phocoena sinus: Gulf of California harbor porpoise
	Phocoena spinipinnis: Burmeister's porpoise
	Phocoenoides dalli: Dall's porpoise

3. HISTORICAL PERSPECTIVE AND GRAY'S PARADOX

3.1 EARLY EXAMINATIONS OF DOLPHINS

The earliest account of the swimming ability of dolphins comes from Aristotle (*Historia Animalium*), who considered dolphins the fastest of all animals and capable of leaping over the masts of large ships. A description of the dolphin swimming mechanism was given by Borelli (*De Motu Animalium*; 1680), who noted the up and down movements of the cetacean tail (Borelli, 1989). Observations of swimming by cetaceans remained largely anecdotal until the 1800s. In the years after 1859 when Charles Darwin published his book, *The Origin of the Species*, biologists concerned themselves with whale morphology and swimming movements to address evolutionary transition mechanisms (Flower, 1883; Ryder, 1885; Kükenthal, 1891; Pettigrew, 1893; Beddard, 1900; Kellogg, 1928).

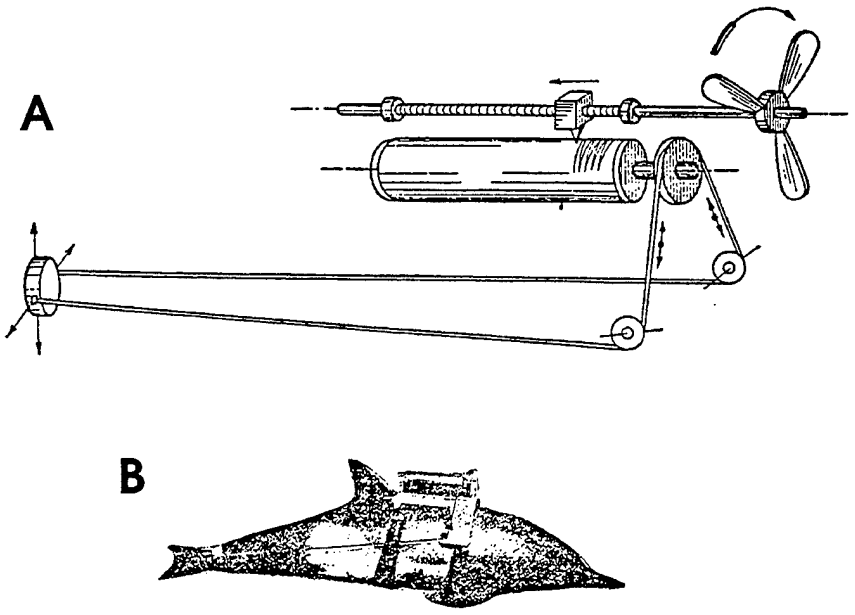

Figure 1. Device for measuring lateral tail movements by a swimming dolphin. A. Drawing of device showing tail shock bracelet connected through pulleys to a recording drum. Recordings were made from a sharp needle mounted on a nut that moved by rotation of a long screw connected to a propeller. B. Device mounted on dolphin. Redrawn from Stas (1939a).

Observations on cetaceans indicated that propulsion was accomplished by tail movement. Various descriptions disagreed on how the tail was moved with up and down, lateral, or screw-like motions (Petersen, 1925; Stas, 1939a). Direct observations of dolphin swimming motions were difficult because of the high stroke frequency and distortion of viewing through water. In one case, a device was mounted on the back and tail stock of a free-swimming dolphin to record lateral and vertical movements of the tail (figure 1; Stas, 1939a, 1939b). Although vertical motion predominated, some

lateral movement was detected that may have been an artifact of the dolphin not maintaining a straight course.

Tail movement in the vertical plane was considered analogous to the swimming motions in the horizonal plane of fast-swimming fish (Pettigrew, 1893; Howell, 1930). Indeed, the thrust performance of fish and dolphin tails was considered superior to screw propellers (Pettigrew, 1893; Petersen, 1925; Triantafyllou and Triantafyllou, 1995). Screw propellers could not conform with speed variation because of their inelastic nature. This was believed to limit the effective speed range of propellers whereas the oscillatory motions of the flexible fish and dolphin tails could adjust to velocity changes and maintain effective thrust production (Pettigrew, 1893; Petersen, 1925; Saunders, 1951, 1957).

The dolphin shape came under scurtiny by engineers in the 1800s. Cayley (circa 1800) considered the dolphin body as a solid of least-resistance design (Gibbs-Smith, 1962). The streamlined, fusiform shape of the dolphin closely matches modern low-drag airfoils (figure 2). Modern submarines since USS *Albacore* have also used a fusiform design analogous to dolphins.

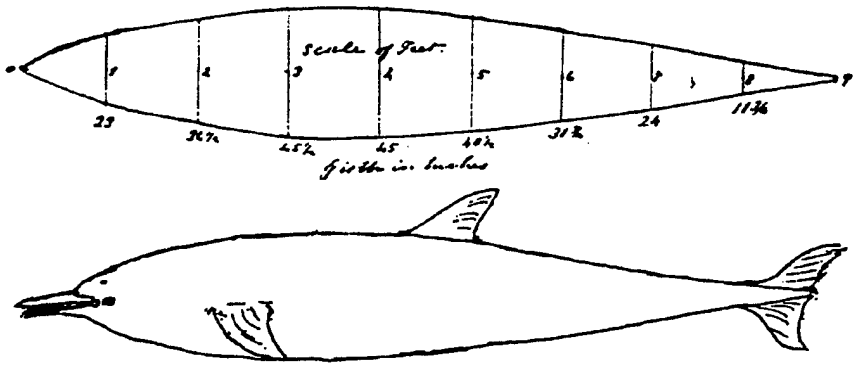

Figure 2. Sketch of dolphin and body contours by Cayley.

3.2 GRAY'S PARADOX

Of all the information on dolphin swimming, arguments surrounding the investigation and application of special mechanisms for dolphin drag reduction have been by far the most contentious (Gray, 1936; Webb, 1975; Fish and Hui, 1991, Vogel, 1994; Fein, 1998). The controversy, known as "Gray's Paradox," was the result of the first attempt to evaluate swimming energetics in animals (Gray, 1936; Webb, 1975). Sir James Gray (1936) used a simple hydrodynamic model based on a rigid body to calculate drag power and applied it to a dolphin and a porpoise swimming at speeds of 10.1 and 7.6 m/s, respectively. The results indicated that the estimated drag power could not be reconciled with the available power generated by the muscles. Gray (1936) stated:

"If the resistance of an actively swimming dolphin is equal to that of a rigid model towed at the same speed, the muscles must be capable of generating energy at a rate at least seven times greater than that of other types of mammalian muscle."

For his calculations, Gray initially assumed that turbulent boundary flow conditions existed because of the speed and size of the animals (Appendix A). Gray's resolution to the problem was that the drag on the dolphin would have to be lower. This could be achieved through maintenance of a fully laminar boundary layer. Gray proposed a mechanism whereby the dolphins' oscillating flukes would laminarize the boundary layer by accelerating the flow over the posterior half of the body (see section 7.7, BOUNDARY LAYER ACCELERATION). This mechanism was largely ignored in subsequent work, however, the basic premise that dolphins could maintain laminar boundary conditions became the focus and justification of most dolphin hydrodynamic work for the next 60 years (Gawn, 1948; Parry, 1949a; Gero, 1952; Kramer, 1960a, b; Webb, 1975; Aleyev, 1977; van Oossanen and Oosterveld, 1989; Fish and Hui, 1991; Fein, 1998; Fish, 1998c).

The basic premise of Gray's Paradox, however, was flawed because of potential errors in estimation of dolphin swimming speed and inconsistencies between dolphin swimming performance and data on muscle power outputs. Gray (1936) used a shipboard observation by E. F. Thompson, who timed a dolphin with a stopwatch as it swam along the side of the ship (length = 41.5 m) from stern to bow in 7 s (10.1 m/s). If the dolphin was swimming close enough to use the wave system of the ship, its speed may have been artificially enhanced and energetic effort reduced because of free-riding behaviors (see section 10, BEHAVIORAL STRATEGIES FOR ENERGY ECONOMY; Lang, 1966b; Williams et al., 1992). Later, Gray (1968) used speed data of 10.3 m/s for a 9-s effort from Steven (1950), but the dolphin was also swimming close to the ship.

More important than the actual speed, the observation of the dolphin swimming speeds was for sprints (7 to 9 s) and Gray used measurements for muscle power output of sustained performance (3 to 5 min) by human oarsmen (Henderson and Haggard, 1925). Muscle performance is a function of the type of muscle fibers stimulated during an activity. Fast glycolytic (FG) fibers are adapted for short burst activities with high-power output and very high intrinsic speed of shortening, whereas slow oxidative (SO) fibers are slow contracting and are suitable for slow, sustained activity (Alexander and Goldspink, 1977). The peak power outputs are 2.6 to 3 times greater for FG than SO fibers (Barclay et al., 1993; Askew and Marsh, 1997). Both FG and SO fibers are found in the musculature of cetaceans (Mankovskaya, 1975; Ponganis and Pierce, 1978; Suzuki et al., 1983; Bello et al., 1985). FG fibers are fueled primarily by anaerobic metabolism and SO fibers primarily use aerobic metabolism. Depending on the type of metabolic pathway, anaerobic metabolism has a maximum metabolic power output 2 to 17 times greater than aerobic metabolism (Hochachka, 1991).

If the dolphins were truly swimming at 10.1 m/s without interference from the ships (Gray, 1936; Steven, 1950), the short duration of the activity would have indicated use of FG fibers and higher power outputs (Webb, 1975; Fish and Hui, 1991). Gray (1936) calculated muscle power outputs of 14 W/kg for a dolphin with a low-drag laminar boundary layer and 122 W/kg with a high-drag turbulent boundary layer, respectively. With anaerobic contributions, *Tursiops truncatus* could generate an estimated 110 W/kg (Weis-Fogh and Alexander, 1977).

3.3 KRAMER

The idea that dolphins could reduce their drag by laminarizing the boundary layer was tantalizing, but elusive. However, Gray's Paradox was invigorated by the work of Max Kramer (1960a, 1960b, 1965). Kramer claimed that a laminar boundary layer without separation could be achieved at high

Reynolds number through their soft compliant skin that dampens incipient turbulence. (Webb, 1975). The Reynolds number (Re) is representative of the ratio of inertial to viscous forces; see Appendix A.

Kramer (1960a) coated a torpedo with an artificial skin based on a dolphin's skin. The dolphin integument is composed of a smooth, hairless epidermal surface forming an elastic membrane (Kramer, 1960b; Aleyev, 1977) and is anchored to the underlying dermis with its blubber layer by longitudinal dermal crest with rows of papillae, which penetrate the lower epidermis (Kramer, 1960b, 1965; Sokolov et al, 1969; Yurchenko and Babenko, 1980; Haun et al., 1983). Kramer's analogous skin was composed of a heavy rubber diaphragm supported by rubber studs with the intervening spaces filled with a viscous silicone fluid (Kramer, 1960a, 1960b, 1965). The diaphragm would be sensitive to pressure changes and transmit the pressure oscillations below to the viscous fluid. The fluid would flow beneath the diaphragm to absorb part of the turbulent energy. It was hypothesized that the coating would dampen out perturbations in the flow and prevent or delay transition. When a towed body was coated with the artificial skin, anterior of the maximum thickness, a 59% reduction in drag was achieved at $Re = 15x10^6$ compared to a rigid reference model with fully turbulent flow. Kramer (1960b) claimed to have exposed the "dolphin's secret" and provided a resolution to Gray's Paradox.

In what has been characterized as "enthusiastic optimism" (Vogel, 1994), research on dolphin hydrodynamics and compliant coatings was accelerated again during the 1960s (Aleyev, 1977; Riley et al., 1988; Fish and Hui, 1991). Attempts to verify Kramer's results subsequently failed (Landahl, 1962; Riley et al., 1988). Furthermore, in reviewing the available literature on dolphin swimming performance, Fish and Hui (1991) found no evidence for drag reduction from special mechanisms.

3.4 NAVAL RESEARCH

Naval interest in swimming by dolphins and other marine life began nearly 50 years ago. Captain Harold Saunders, USN, from the Bureau of Ships delivered a paper before the Chesapeake Section of the Society of Naval Architects and Marine Engineers discussing the propulsion systems of fish and marine mammals to learn how to increase speed and maneuverability in water craft (Saunders, 1951). Shaw (1959) put forth a number of ideas related to the study of marine organisms to search for new approaches for application to undersea vehicles. Particular interest was focused on properties associated with (1) silence, (2) speed, (3) endurance or range, (4) wakelessness, and (5) mechanical efficiency. Stealth was associated with both silence and wakelessness. Shaw (1959) considered that marine animals swimming by undulation of the body would be quiet, efficient, highly maneuverable, and almost wakeless. His report recommended a course of action pertinent to a biology-engineering technology transfer with collaboration between biologists and engineers.

The U.S. Navy's Marine Mammal Program originated in 1960 when a Pacific white-sided dolphin (*Lagenorhynchus obliquidens*) was acquired for hydrodynamic studies. This purchase was largely motivated by accounts of extraordinary swimming speeds of dolphins and the desire to reduce the hydrodynamic resistance of torpedoes and submarines. The work of Sir James Gray and Dr. Max Kramer provided a scientific context for this investigation (Wood, 1973). Kramer's studies suggested that the dolphin can achieve high swimming speeds by extending laminar flow over its body. Kramer thought that the compliant nature of its skin tended to dampen incipient turbulence. If true, and if this strategy could be applied to torpedoes, for example, 10-fold reductions in drag seemed possible (Rehman, 1961; Renwick et al., 1997).

The initial drag studies were conducted on the *Lagenorhynchus obliquidens* in a 96 m long, 3.7 m wide, and 1.8 m deep towing tank filled with seawater at the Convair Hydrodynamics Laboratory

(Lang and Daybell, 1963). The animal was trained to glide through a series of submerged hoops. Comparisons were made between swimming bouts in which the dolphin swam with and without various collars around its head. The collars were used to induce turbulent flow. These experiments demonstrated that the boundary layer over the dolphin was primarily turbulent and there were no unusual physiological or hydrodynamic phenomena. However, it was suspected that limited physical facilities and measurement capabilities may have affected the study data (Lang and Daybell, 1963). Turbulence in the water may have induced a turbulent boundary layer (Lang, 1963).

In 1964, dolphin hydrodynamic studies were resumed after dolphins were trained to work untethered outside their pens. Open-water speed-run trials were conducted in a lagoon at Coconut Island, Oahu, Hawaii, in March 1964 with a *Tursiops truncatus* (*gilli*) and in March 1965 with a *Stenella attenuata* (Lang, 1975). These trials indicated that swimming speed was indirectly related to duration (Lang and Norris, 1966). For *Tursiops*, a maximum speed of 8.3 m/s could only be maintained for 7.5 s whereas a cruising speed of 3.1 m/s could be maintained indefinitely. Maximum swimming speed for *Stenella* was 11.1 m/s during a 2-s acceleration with an estimated power output of 46.5 W/ kg total body mass (Lang and Pryor, 1966). This series of experiments by Lang and his colleagues cast further doubt on the validity of Gray's Paradox.

It was not until 1980 that dolphin hydrodynamic work was continued in the United States. This was largely motivated by increasing performance requirements of underwater vehicles (Haun et al., 1984). Drag reductions of 20 to 30% were now considered important. While Lang's work discounted large drag reductions (approximately 700%), his research was not thought to have precluded the possibility of the dolphin possessing this level of drag reduction capability. During the hiatus in hydrodynamic research on dolphins in the United States, there was a large effort ongoing in the Soviet Union (another argument to continue dolphin research in this country). In fact, Soviet research continued from the 1960s until the dissolution of the Soviet Union (Yurchenko and Babenko, 1980; Romanenko, 1976, 1981, 1995; Aleyev, 1977; Pershin, 1988). Soviet scientists, however, based their research on the assumption that Gray's Paradox was correct (Yurchenko and Babenko, 1980; Romanenko, 1976, 1981, 1995; Aleyev, 1977; Pershin, 1988).

Throughout the 1980s, dolphin hydrodynamic research focused on metabolic effort and on various hypothesized turbulent drag reduction techniques employed by dolphins* (Stone, 1980; Haun and Hendricks, 1988). Although it was found that dolphins seem to be physiologically efficient as swimmers, it did not appear that unusual metabolic changes take place (Haun and Hendricks, 1988). The drag mechanisms studied were principally both passive and active skin compliance and biopolymer addition (Haun et al., 1983, 1984). Study results, while indicating some drag reduction capability, remained inconclusive (Haun et al., 1983, 1984; Haun and Hendricks, 1988).

Since the 1960s, most Navy research has focused on biosonar studies (Au, 1993; Cranford et al., 1996) and physiological systems (Ridgway and Howard, 1979; Ridgway et al., 1984; Shaffer et al., 1997). Dolphins are used in the Navy's Marine Mammal Systems (MMS). The MMS detachments search for mines moored off the seafloor (Mk 4) and on the surface or buried under the seafloor

---

* Henricks, E. W. and J. E. Haun. 1982a. "Dolphin Hydrodynamics: A Review of the Literature." NOSC (now SSC San Diego) TN 1183. SSC San Diego, CA.

Henricks, E. W. and J. E. Haun. 1982b. "Dolphin Hydrodynamics: Instrumentation Review." NOSC (now SSC San Diego) TN 1184. SSC San Diego, CA.

(Mk 7), and detect swimmers and divers (Mk 6) (Renwick, 1997; Wilson, 1999). Most recently, research on dolphin swimming and hydrodynamics has focused on flow visualization (Rohr et al., 1998a), energetics and efficiency (Williams et al., 1992, 1993a; Fish 1998a, b; Rohr et al., 1998b; Williams, 1998), structural materials (Pabst, 1996a, b), and maneuverability (Fish, 1997). For more information on the U.S. Navy's Marine Mammal Program, see Appendix D. A list of some 700 publications,
current to 1997, can be found at the following URL:

http://guppy.nosc.mil/services/sti/publications/pubs/td/627/

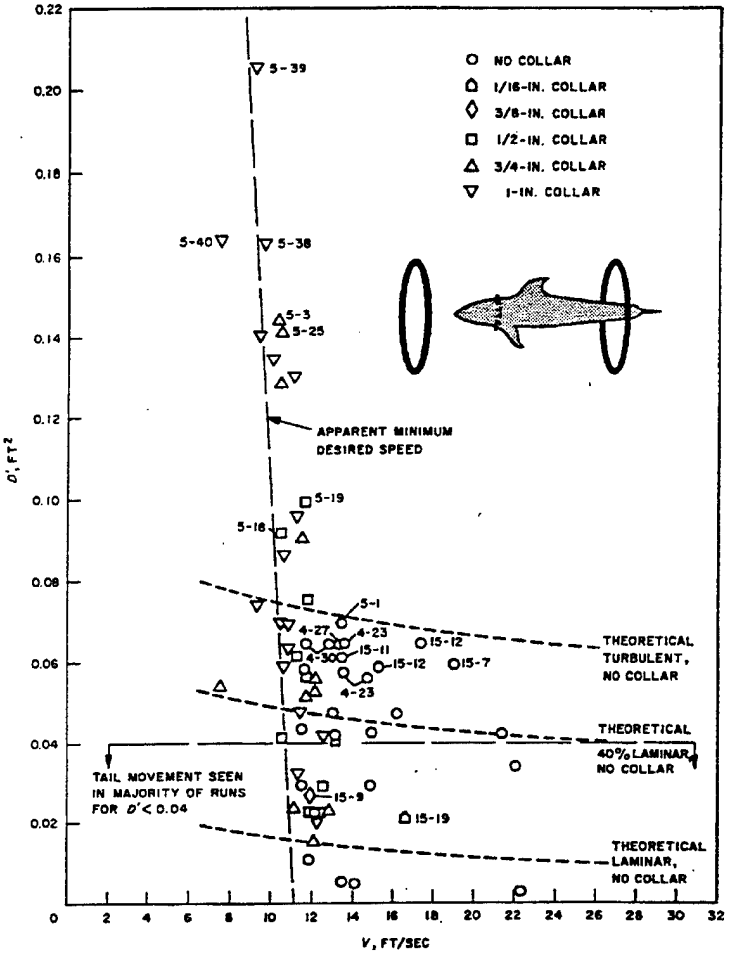

Figure 3. Drag as a function of average speed during a glide through hoops for a single *Lagenorhynchus obliquidens* with and without collars (from Lang and Daybell, 1963).

4. CETACEAN SWIMMING SPEEDS

The simplest behavioral parameter that can be controlled is swimming speed (Weihs and Webb 1983). High speeds allow increased foraging and active pursuit, but require large energy expenditures because thrust power is directly related to the cube of velocity. Low swimming speeds observed for cetaceans, while foraging and migrating (Würsig and Würsig, 1979; Sumich 1983; Lockyer and Morris 1987; Fish and Hui 1991; Hanson and Defran, 1993), would minimize transport costs and maximize the distance traveled for the work performed (Williams, 1987).

Accurate swimming speed measurements of free-ranging dolphins are rare, and when reported, often do not include the duration of the swimming effort. Reports on cetacean swimming speeds have in many instances been anecdotal and often unreliable. The reason for questioning these reports is that estimates of swimming speeds based on observations from ships, airplanes, or shorelines have often been made without fixed reference points, information on currents, or accurate timing instruments (Fish and Hui, 1991; Fein, 1998; Rohr et al., 1998b). Even with satellite tracking systems, the resolution and sampling rates are too low to accurately measure short duration swimming efforts (e.g., sprints). The diving pattern and high probability that animals do not swim in straight lines between consecutive satellite locations would skew the data towards the minimum transit speed, which is well below the routine and maximum speeds (Martin et al., 1993; Davis et al., 1996).

Appendix B lists available information of cetacean swimming speed. The data were collected by various means including boat measurements (Gray, 1936; Woodcock, 1948; Johannessen and Harder, 1960; Ridgway and Johnston, 1966), timing of captive animals (Lang and Norris, 1966; Lang and Pryor, 1966; Fish, 1993a, 1998a; Rohr et al., 1998b), radio tagged animals (Tanaka, 1987), theodolite tracking (Würsig and Würsig, 1979), sonar tracking (Ridoux et al., 1997), and observations correlated with map locations (Lockyer and Morris, 1987; Wood, 1998).

4.1 SUSTAINED SPEED

Sustained speeds are associated with performance levels described as cruising, migrating, routine, prolonged, and feeding. Webb (1975) categorizes sustained swimming, including routine and cruising speeds, as an activity level maintained for longer than 200 min. Prolonged swimming is described as an activity level maintained between 200 min and 15 s. These speeds are steady low level activities. Sustained speeds are the preferred swimming speeds and are probably minimum speeds for the most-efficient thrust generation (Fish, 1998a).

Both mysticetes and odontocetes display low sustained speeds (figure 4). For mysticetes, the low sustained speeds (0.5 to 3.6 m/s) encountered during feeding would be associated with high drag. Mysticetes obtain food by filter-feeding that involves straining water directly through the whale's baleen plates or gulping a large quantity of water (at least 60 m^3 or 70 tons) by depressing the lower jaw and filling the throat pouch (Pivorunas, 1979).

Odontocetes display a similar range of sustained swimming speeds with mysticete whales (figure 4). One record for sustained swimming by a killer whale (*Orcinus orca*), although probably incorrect, is unfortunately widespread in the literature (Kooyman, 1989). The killer whale was reported to swim for 20 min at 12.5 to 15.5 m/s (Johannessen and Harder, 1960). The data were obtained from questionnaires placed aboard a ship. Because the killer whale was "playing" around the ship, the animal was probably bow riding and thereby swimming at a higher speed with less effort (Fish, 1998a).

Without direct observation of swimming speed, physiological characteristics have been used as an indicator of sustained swimming ability. Species with greater adaptation for deep, long-duration dives are precluded from fast sustainable swimming (Hedrick and Duffield, 1991). Deep divers possess increased oxygen stores through increased hematocrit (i.e., percentage of blood occupied by cellular components) and hemoglobin concentration, but at the expense of oxygen transport capacity for rapid swimming (Ridgway and Johnston, 1966; Hedrick and Duffield, 1991; Kooyman, 1989; Shaffer et al., 1997). Belugas (*Delphinapterus leucas*) are considered slow swimmers that can dive to great depths and remain submerged for extended periods (Ridgway et al., 1984; Shaffer et al., 1997; Fish, 1998a). The hematocrit and hemoglobin concentration of these whales is greater than for the faster swimming *Cephalorhynchus commersonii*, *Lagenorhynchus obliquidens*, *Orcinus orca*, and *Tursiops truncatus* (Hedrick and Duffield, 1991).

4.2 MAXIMUM SPEED

Maximum speeds are associated with duration times of seconds and performance levels indicative of maximum effort. For free-ranging dolphins, this behavior might be associated with flight or pursuit where, presumably, motivation is high. For captive dolphins, researchers hope that similar efforts may be observed through training. Whether the motivation levels can be duplicated has been controversial (Lang, 1963; Lang and Daybell, 1963; Lang 1975).

The range of maximum speeds varies considerably (figure 4) for mysticetes (2.1 to 13.4 m/s) and odontocetes (1.5 to 15.3 m/s). The Balaenopteridae are the fastest for the mysticetes (Appendix B). These comparatively higher speeds may be a function of the highly streamlined body contour of the Balaenopteridae (figure 5; Williamson, 1972; Fish, 1993a). Within the Odontoceti, the highest speeds are attained by the Delphinidae whereas the Platanistidae are the slowest (Appendix B).

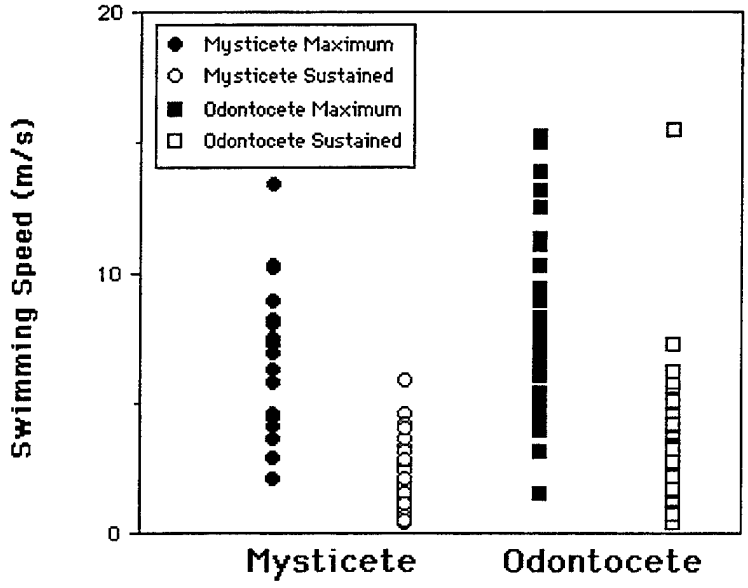

Figure 4. Plot of sustained and maximum swimming speeds for mysticete and odontocete cetaceans based on Appendix B.

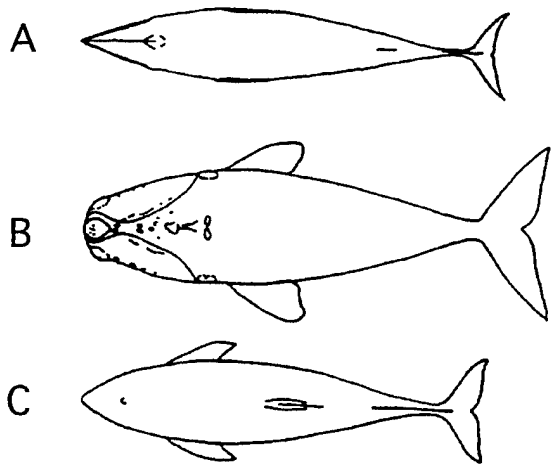

Figure 5. Body shape variation for a balaenopterid mysticete (A: *Balaenoptera acutorostrata*), a balaenid mysticete (B: *Eubalaena glacialis*), and an odontocete (C: *Phocoena phocoena*).

There are few systematic studies of maximum swimming speeds. Lang and Daybell (1963) measured a top speed of 7.7 m/s for a *Lagenorhynchus* swimming in a towing tank. In open-ocean tests with captive animals, maximum speeds of 11.1 m/s for *Stenella* (Lang and Pryor, 1966) and 8.3 m/s for *Tursiops* (Lang and Norris, 1966) were recorded. The latter study indicated that swimming speed is related to duration of activity. *Tursiops* can swim at 3.08 m/s indefinitely, 6.09 m/s for 50 s, 7.01 m/s for 10 s, and 8.3 m/s for 7.5 s (Lang, 1975). Speeds as high as 15 m/s were reported for burst swims by *Tursiops* (Lockyer and Morris, 1987) although this record was made from a cliff-top observation and was probably an overestimate (Fein, 1998; Fish, 1998a). Dependence of speed on the swimming duration was supported further from energetic models (Kozlov, 1981).

Rohr et al. (1998b) examined the variance of maximum swimming speeds from nearly 2000 swimming speed measurements that were obtained for both captive and free-ranging dolphins, including *Tursiops*, *Pseudorca*, and *Delphinus*. Measurements were made from (1) videotapes of trained dolphins swimming around a large pool, (2) videotapes of captured wild dolphins immediately after release, and (3) sequential aerial photographs of a school of free-ranging dolphins startled by a passing airplane. Maximum speeds for trained animals over a 0.7- to 2.8-s swim were 8.2 m/s for *Tursiops*, 8.0 m/s for *Delphinus*, and 8.0 m/s for *Pseudorca*. Average speeds were 20 to 24% lower than the maximum speeds attained. Wild *Tursiops* demonstrated a maximum speed over a 2.7-s interval of 5.7 m/s. Maximum swimming speed of free-ranging *Delphinus* responding to multiple passes by an airplane was 6.7 m/s although the average speed for the school was 4.8 m/s (figure 6). Newborn dolphins within the school may have lowered the average speed.

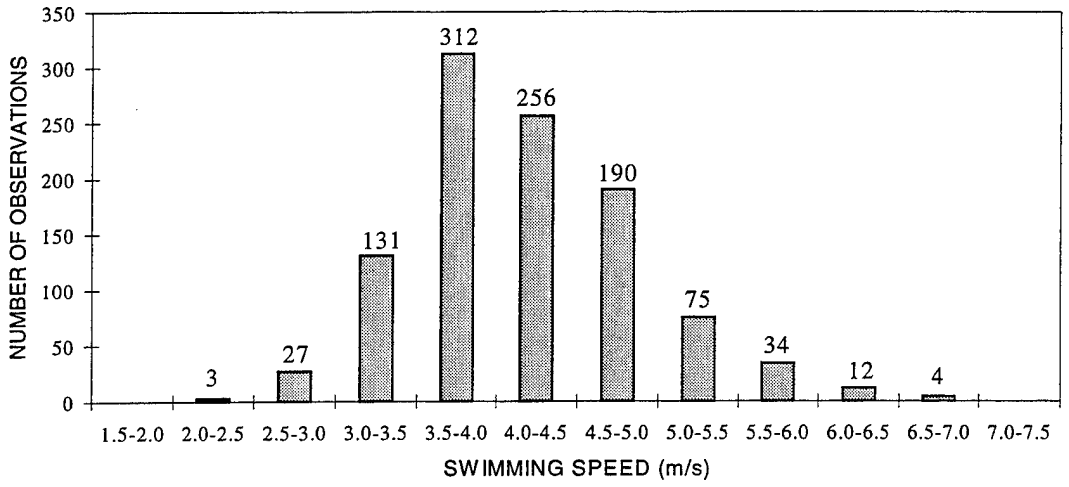

Figure 6. Total distribution of swimming speeds (m/s) obtained from five airplane passes over a school of long-beaked, common dolphins (*Delphinus capensis*); total number of observations equals 1044 (from Rohr et al., 1998b)

Although maximum swimming speeds overlap considerably despite taxonomic status, there is a marked dependence of length-specific speed on size (Webb, 1975). Large whales have low length-specific swimming speeds compared to smaller dolphins and porpoises. In ascending order of body mass, length-specific speeds for various dolphins were recorded at 6.0 *BL*/s (*Stenella attenuata*; 52.7 kg), 4.4 *BL*/s (*Delphinus delphis*; 104.8 kg), 4.3 *BL*/s (*Tursiops truncatus gilli*; 89 kg), 3.8 *BL*/s (*Tursiops truncatus*; 149.2 kg), 2.2 *BL*/s (*Pseudorca crassidens*; 461.8 kg), 1.5 *BL*/s (*Orcinus orca*; 1995.8 kg) (Lang and Pryor, 1966; Lang and Norris, 1966; Fish 1998a; Rohr et al., 1998b). A 27.4-m blue whale (*Balaenoptera musculus*) sprinting at 10.2 m/s (Tomilin, 1957) would have a length-specific speed of 0.37 *BL*/s. This trend is explained as a matter of scaling. Animals maintain the same proportion of muscle mass in the body independent of size, but smaller animals have relatively greater muscular power outputs per unit volume than larger animals (Hill, 1950; Pedley, 1977).

5. BODY MORPHOLOGY AND CONTROL SURFACE DESIGN

Fast-swimming animals display morphological characteristics associated with enhanced thrust production, high propulsive efficiency, and reduced drag (Weihs and Webb, 1983). For cetaceans, these morphological characteristics include a streamlined body, tight skin, a strongly compressed caudal peduncle, and high aspect ratio flukes and flippers with sweepback (Webb, 1975; Fish et al. 1988; Fish, 1993a, 1998a; Videler, 1993).

5.1 STREAMLINING

5.1.1 Fineness Ratio

Drag is minimized primarily by streamlining the shape of the body and appendages (i.e., flukes, flippers, dorsal fin) (Fish, 1993a). Streamlining minimizes drag by reducing the magnitude of the pressure gradient over the body and allowing water to flow over the surface without separation (Vogel, 1994). The streamlined profile is characterized by a fusiform shape emulating an elongate teardrop with a rounded leading edge extending to a maximum thickness and a slowly tapering tail. This fusiform shape is displayed by all cetaceans (figures 2 and 5), but is not axisymmetrical, as the caudal peduncle exhibits extreme narrow-necking in the plane of oscillation (Lighthill, 1969, 1970; Fish and Hui, 1991). Necking in the caudal region reduces virtual mass effects and unstable movements (Aleyev, 1977; Webb, 1975: Blake, 1983b).

An indicator of the degree of streamlining is the fineness ratio (*FR* = body length/maximum diameter). The *FR* value of 4.5 gives the least drag and surface area for the maximum volume (figure 7; von Mises, 1945; Hertel, 1966; Webb, 1975) although only a 10% increase in drag is realized in the *FR* range of 3 through 7. Since Gray (1936), there has been an active search for special mechanisms to reduce drag in dolphins (Fish and Hui, 1991). Despite the various mechanisms hypothesized (see section 7, DRAG-REDUCTION MECHANISMS), the body shape is the major determinant of drag (figure 7). A stream- lined body with *FR* = 4.5 will have a 75% reduction in pressure drag coefficient from that for a sphere of equal volume (von Mises, 1945).

The *FR* range for the various cetacean families spans a significant portion of optimal range for reduced drag (figure 7; Fish, 1993a). The greatest range of *FR* (4 through 11) is found in the cetacean family Delphinidae from Dall's porpoise (*Phocoenoides dalli*) to the northern right whale dolphin (*Lissodelphis borealis*) (Fish, 1993a). The exaggerated length of the latter species has given it the name "snake porpoise." Despite the difference in body design as expressed by *FR*, these two species are considered among the fastest dolphins, with maximum speeds exceeding 8 m/s (Winn and Olla, 1979).

5.1.2 Comparison with Engineered Designs

When compared with modern submarines, the *FR* range for most cetaceans is lower (figure 7). *FR* for submarines falls outside the optimal range. This may be because of overriding constraints of construction costs, and systems and personnel requirements.

FR is a crude indicator of body streamlining because it does not provide information on changes in body contour. As a better indicator of body shape, dolphin profiles were compared to standard two-dimensional airfoils classified by the National Advisory Committee for Aeronautics (NACA). The dolphin body form is similar in outline with the NACA 66-018 foil (Hertel, 1966) whereas the killer whale is similar to NACA 66-026 (Pershin, 1983). These foils are designated as laminar profiles. The

position of their maximum thickness (*SP*), known as the shoulder, is located at a position 45% of length from the leading edge. The rearward displacement of the shoulder can maintain laminar flow over a large portion of the body because the maximum thickness is where transition to turbulent flow and boundary layer separation are likely to develop (Walters, 1962; Lang, 1963; Webb, 1975, Blake, 1983b). *SP* of dolphins is 34 to 45% of the body length (Fish and Hui, 1991).

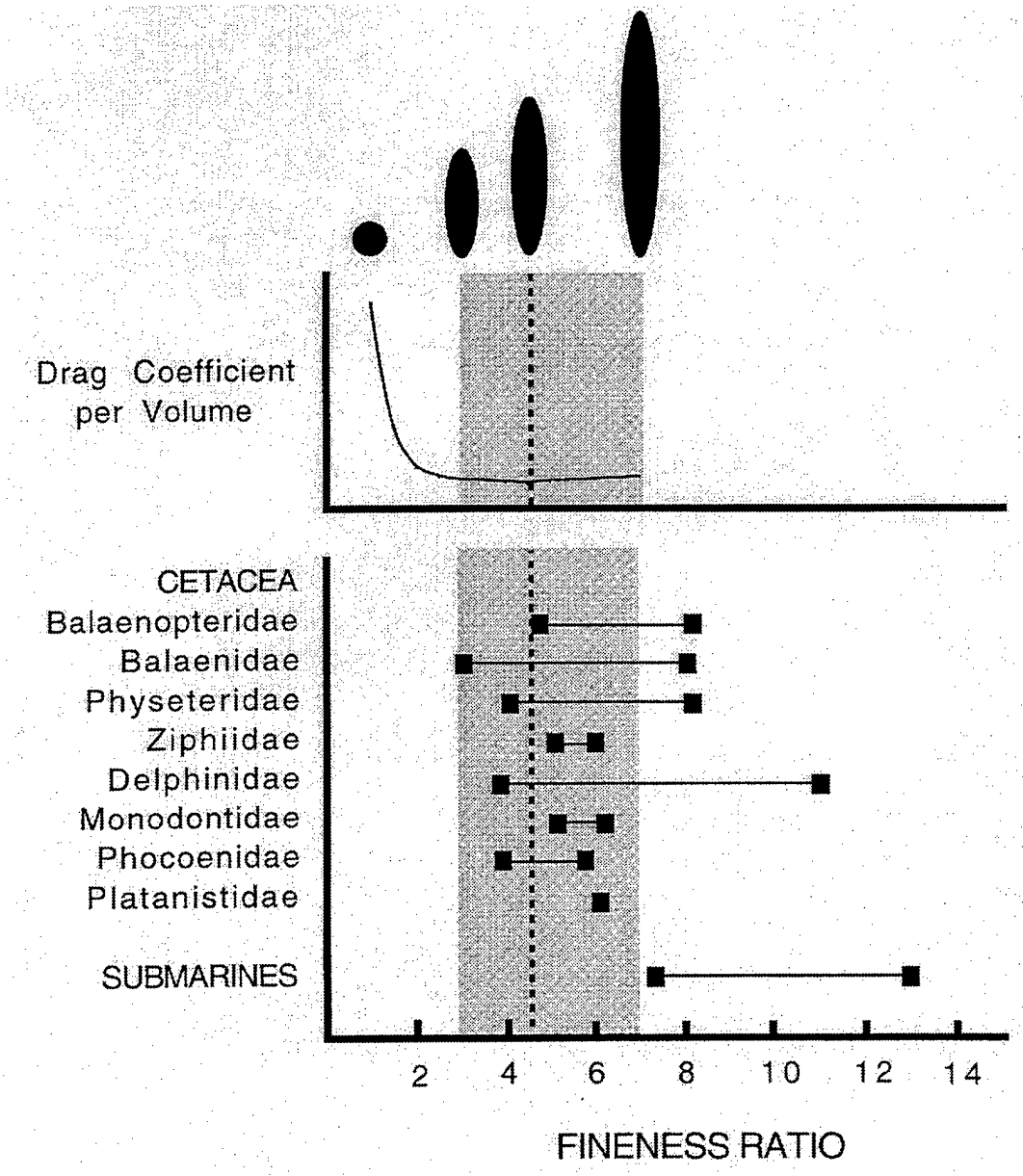

Figure 7. Fineness ratio (*FR*) in relation to drag per volume (adapted from von Mises, 1945) and *FR* for cetacean families (adapted from Fish, 1993a). Comparisons are made with modern submarine hulls. Silhouettes show the difference in shape in reference to *FR* from a circular shape (*FR* = 1) to an elongate form (*FR* = 7). The dashed line indicates the optimal *FR* of 4.5 whereby a body has the lowest drag for the maximum volume. The shaded area represents the *FR* range (3 through 7) in which drag increases by 10% above the minimum value.

Airfoil analogies are limited because of the animal's three-dimensional configuration and its deviation from the smooth fusiform shape. In particular, the rostrum of cetaceans is highly variable as its design is associated with feeding and echolocation. The concave and convex profile of the head may induce stepwise, gradual pressure changes that can reduce skin friction (Bandyopadhyay, 1989, 1993; Bannasch, 1995). In addition, differences in dolphin head shape may influence boundary layer crossflows caused by pitching movements that would affect drag (Lighthill, 1993).

5.2 FLUKES

5.2.1 Planform

The flukes are lateral extensions of the distal tail. Biomechanically, the flukes act like a pair of wings (Vogel, 1994). However, unlike the static wings of airplanes and jets, the flukes oscillate to generate a lift-derived thrust. As winglike structures, the flukes can be analyzed like engineered air- and hydro-foils to determine their effectiveness in lift generation. Fluke shape influences the energy requirements for swimming. The combination of moderate aspect ratio, sweep, cross-sectional design, and fluke flexibility furnishes a morphology that generates high lift with low drag performance.

Fluke planforms have a swept-back tapered design. The hydrodynamic parameters (Appendix C; figures 8 and 9) vary between different species. From the fluke planform, measurements can be made on the span (*S*: tip-to-tip distance), root chord (*RC*: distance from base of fluke to trailing edge), sweep (Λ: angle between a perpendicular to *RC* and one-quarter chord position), and planform area (*A*) (figure 10).

S and A are directly related to increasing body length for odontocetes (figure 11). This trend is expected because the fluke span and area determine the mass of water that is affected for thrust generation. Larger A would generate more thrust. Because thrust developed by the flukes is necessary to counter the drag incurred by the body as determined by its surface area (Bose et al., 1990), S and A are associated with body length (BL) where S is proportional to BL and A is proportional to BL^2. Fluke span displays a slight positive ($1.128 > 1.000$) allometry according to the relationship, $S = 0.111\ BL^{1.128}$ whereas fluke projected area displayed a slight negative ($1.946 < 2.000$) allometry according to the relationship, $A = 0.017\ BL^{1.946}$ (Fish, 1998b). Large whales would have a relatively larger S with a smaller A than smaller dolphins (from Fish, 1998b).

When the relationships between *S*, *A*, and *BL* are compared between life history stages within a species, differences between juveniles and adults are evident that affect performance (Amano and Miyazaki, 1993; Curren *et al.*, 1993). In neonates and prepubescent dolphins, the increase in *S* with respect to *BL* is not as rapid as observed for adults (Perrin, 1975; Amano and Miyazaki, 1993). Therefore, young animals may be at a disadvantage when swimming, thus requiring the use of free-riding behaviors to maintain speed with the parent (Lang, 1966b; see section 10.4.2, Drafting).

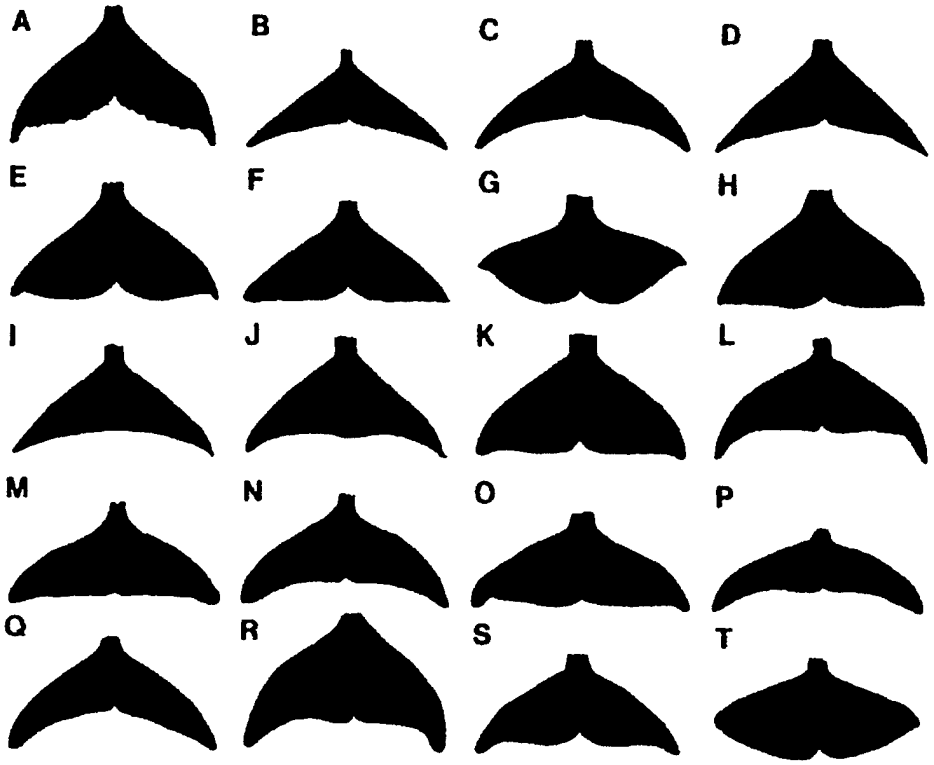

Figure 8. Planforms of flukes from representative cetacean species including: A. Humpback whale (*Megaptera novaeangliae*); B. Blue whale (*Balaenoptera musculus*); C. Minke whale (*Balaenoptera acutorostrata*); D. Right whale (*Eubalaena glacialis*); E. Gray whale (*Eschrichtius robustus*); F. Sperm whale (*Physeter macrocephalus*); G. Narwhal (*Monodon monoceros*); H. Beluga (*Delphinapterus leucas*); I. Sowerby's beaked whale (*Mesoplodon bidens*); J. Northern bottlenose whale (*Hyperoodon ampullatus*); K. Amazon river dolphin (*Inia geoffrensis*); L. Long-finned pilot whale (*Globicephala melaena*); M. Bottlenose dolphin (*Tursiops truncatus*); N. Pacific white-sided dolphin *Lagenorhynchus obliquidens*); O. Killer whale (*Orcinus orca*); P. False killer whale (*Pseudorca crassidens*); Q. Heavyside's dolphin (*Cephalorhynchus heavisidii*); R. Northern right whale dolphin (*Lissodelphis borealis*); S. Harbor porpoise (*Phocoena phocoena*); T. Dall's porpoise (*Phocoenoides dalli*) (from Fish, 1998b).

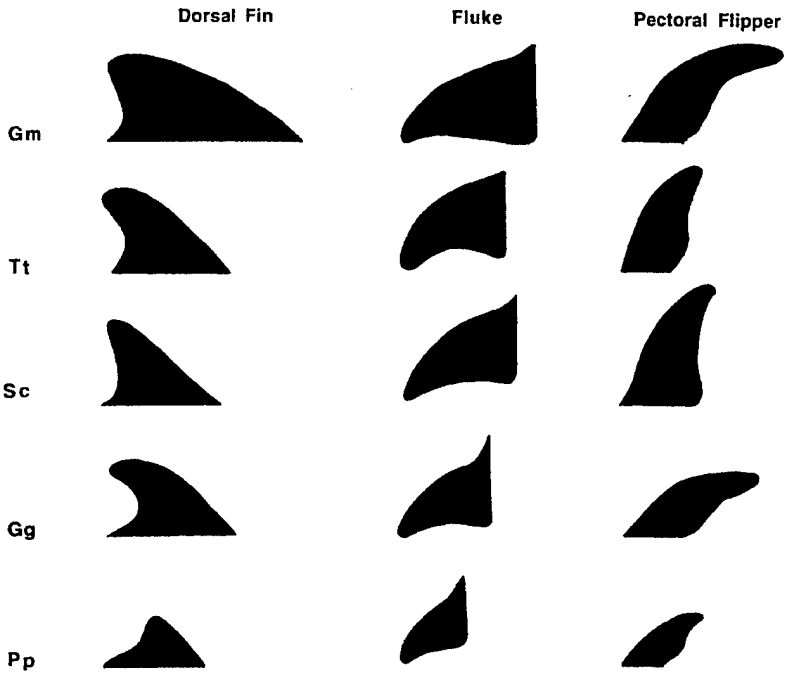

Figure 9. Comparative planforms for the dorsal fin, fluke, and flipper of *Globicephala melaena* (Gm), *Tursiops truncatus* (Tt), *Stenella coeruleoalba* (Sc), *Grampus griseus* (Gg), and *Phocoena phocoena* (Pp).

5.2.2 Cross-sectional Design

Structurally, the flukes are composed of a cutaneous layer, a subcutaneous blubber layer, a ligamentous layer, and a core of dense fibrous tissue which constitutes the bulk of the fluke (Felts, 1966). Both the cutaneous and subcutaneous layers are continuations of their respective layers covering the rest of the body.

Fluke sections along the longitudinal axis display a conventional streamlined foil profile with a rounded leading edge and long tapering trailing edge. The sharp trailing edge and rounded leading edge are crucial for generating lift and minimizing drag (Lighthill, 1970; Vogel, 1994). The flukes are symmetrical about the chord (Lang, 1966a; Pershin, 1975; Bose *et al.*, 1990). In examining the flukes of the common dolphin (*Delphinus bairdi*), Lang (1966a) reported that some warpage was evident. This may explain the contradictory results of Purves (1969) who noted an asymmetry in the fluke cross sections. While an asymmetry would have supported optimal thrust production through only half of the stroke cycle of the dolphin, the symmetrical fluke design indicates that optimal thrust is generated on both up- and down-strokes (see section 8.2, UP AND DOWN PHASES).

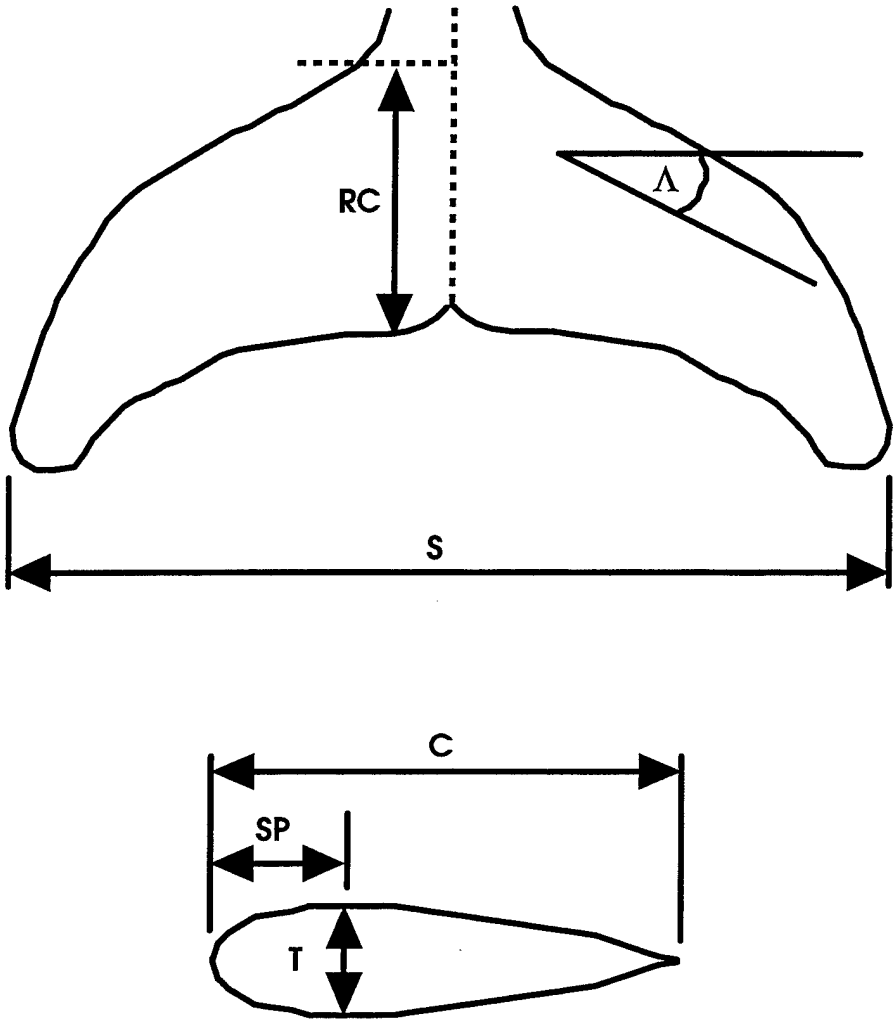

Figure 10. Fluke dimensions of planform (above) and cross-section profile (below). Explanation of dimensions is given in text.

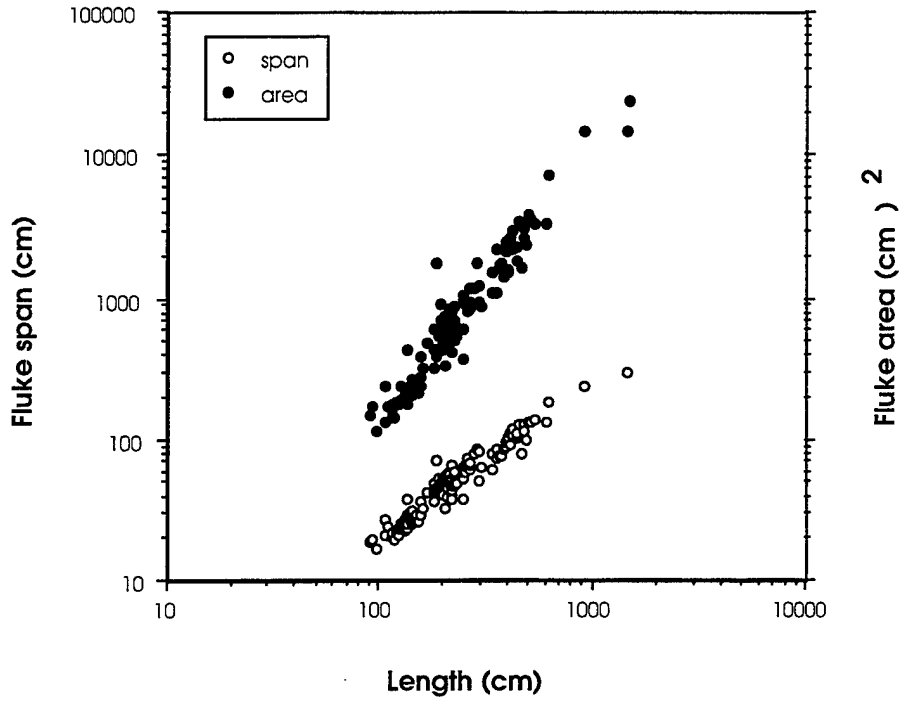

Figure 11. Relationship of planar surface area and fluke span with body length (from Fish, 1998b).

For any section through the fluke in the parasagittal plane, measurements can be made on the chord (*C*), maximum thickness (*T*), and shoulder position (*SP*: distance of *T* from leading edge expressed as a percentage of *C*) (figure 10). *SP* and the thickness ratio (*TR* = *T*/*C*) indicate hydrodynamic performance relating to the generation of foil section lift and drag (von Mises, 1945; Hoerner, 1965). Flukes range from 25 to 40% for *SP* and between 0.16 and 0.25% for *TR* (Lang, 1966a; Shpet, 1975; Bose *et al.*, 1990). Researchers believe that the more posterior *SP* is associated with faster swimming whales (Shpet, 1975). The NACA 63_4-021 foil (Abbott and von Doenhoff, 1959) provides a reasonable facsimile of the fluke sections. The symmetrical profile of the NACA 0018 was also used to describe the cross-sectional fluke design of *Tursiops truncatus* (Kayan, 1979).

5.2.3 Aspect Ratio

The interaction between *S* and *A* as related to hydrofoil design effectiveness is expressed as the aspect ratio (*AR*). *AR* is calculated as S^2/A (Webb, 1975; Vogel, 1994). High *AR* indicates long, narrow flukes whereas low *AR* indicates broad flukes with a short *S*. High *AR* hydrofoils are characteristic of relatively fast swimmers. High AR hydrofoils have high lift-to-drag ratios.

AR varies from 2.0 for the Amazon river dolphin (*Inia geoffrensis*) to high values of 6.1 and 6.2 for the fin whale (*Balaenoptera physalus*) and false killer whale (*Pseudorca crassidens*), respectively (Appendix C; Bose and Lien, 1989; Fish, 1998b). These values correspond to the swimming performance in these species whereby high *AR* species swim faster than species with low *AR* flukes (Appendix B; Fish, 1998a, b).

Well-designed flukes maximize the ratio of lift (L) to drag (D) generated by their action (Webb, 1975; Weihs, 1989). An increase in the maximum L/D with increasing size is achieved by increasing *S* more rapidly than the square-root of *A*, thereby increasing *AR* (von Mises, 1945; Lighthill, 1977; van Dam, 1987). The lift for flukes of a given area and motion would be greatest when *AR* is highest (Bose *et al.*, 1990; Daniel *et al.*, 1992). The longer trailing edge of a high *AR* fluke increases the mass of water deflected posteriorly, augmenting the thrust component. However, *AR* above 8 to 10 provides little further advantage and may be structurally limited because of the lack of rigidity from skeletal elements in the flukes (Felts, 1966; Webb, 1975).

Drag incurred by the flukes is inversely dependent on *AR* primarily because of the induced drag component (Webb, 1975). Induced drag is produced as a consequence of the lift generated by the flukes. As the flukes are canted at an angle to the water flow, lift is produced by deflection of the water and pressure difference between the dorsal and ventral surfaces of the flukes (Webb, 1975; Blake, 1983b; Fish, 1993b, 1998a). The pressure difference produces spanwise cross flows that go around the fluke tips, forming spiraling vortical flow. The flow is shed from the fluke tip as longitudinal tip vortices. The energy dissipated by the vortices represents the induced drag. High *AR* and tapering of the flukes reduce tip vorticity and induced drag (Webb, 1975; Rayner, 1985; Webb and Buffrénil, 1990; Daniel *et al.*, 1992).

Induced drag is also limited by the sweep (Λ) of the flukes. Research by van Dam (1987) showed that a tapered wing with sweptback or crescent design could reduce the induced drag by 8.8% compared to a wing with an elliptical planform. Minimal induced drag is fostered by a swept wing planform with a root chord greater than the chord at the tips giving a triangular shape (Küchermann, 1953; Ashenberg and Weihs, 1984). This optimal shape approximates the planform of cetacean flukes (figure 8 8; Pershin, 1983; Fish, 1998b). Flukes have sweep angles ranging from lows in killer whale (*Orcinus orca*) and Dall's porpoise (*Phocoenoides dalli*) of 4.4 and 5.4°, respectively, to a maximum value of 47.4° for white-sided dolphin (*Lagenorhynchus acutus*) (Appendix C; Bose *et al.*, 1990; Fish, 1998b).

Sweep of the fluke together with taper concentrates the surface area towards the trailing edge. This effectively shifts the lift distribution posterior of the center of gravity affecting pitching equilibrium (von Mises, 1945; Webb, 1975). Lighthill (1970) and Wu (1971b) suggested that a minimum in wasted energy would be realized when the pitching axis was moved to the 0.75 chord position. Proximity of the pitch axis close to the trailing edge was supported by Chopra (1975).

An inverse relationship is evident between Λ and the *AR* of the flukes of various cetaceans (Fish 1998b; figure 12). The combination of low Λ with high *AR* allows for highly efficient, rapid swimming (Azuma, 1983). High Λ may compensate for the reduced lift production of low *AR* flukes. Highly swept-back, low *AR* wings produce maximum lift when operating at large angles of attack. Low Λ, high *AR* designs would fail under these conditions (Hurt, 1965). However, the maximum lift is reduced with increasing sweep angle for a given *AR* whereas efficiency increases (Liu and Bose, 1993). Mathematical analysis by Chopra and Kambe (1977), however, found that Λ exceeding about 30° leads to a reduction in efficiency. The relationship between Λ and *AR* also indicates a structural limitation to the strength and stiffness of the flukes (van Dam, 1987; Bose *et al.*, 1990). The ability to sustain certain loads without breaking is considered a major constraint on increasing span and *AR* (Daniel, 1988). Because the fibrous composition not only strengthens the flukes but increases flexibility, an extreme increase in span with increased *AR*, although potentially generating higher lift, would exaggerate the bending of the appendage in an oscillatory mode and reduce performance.

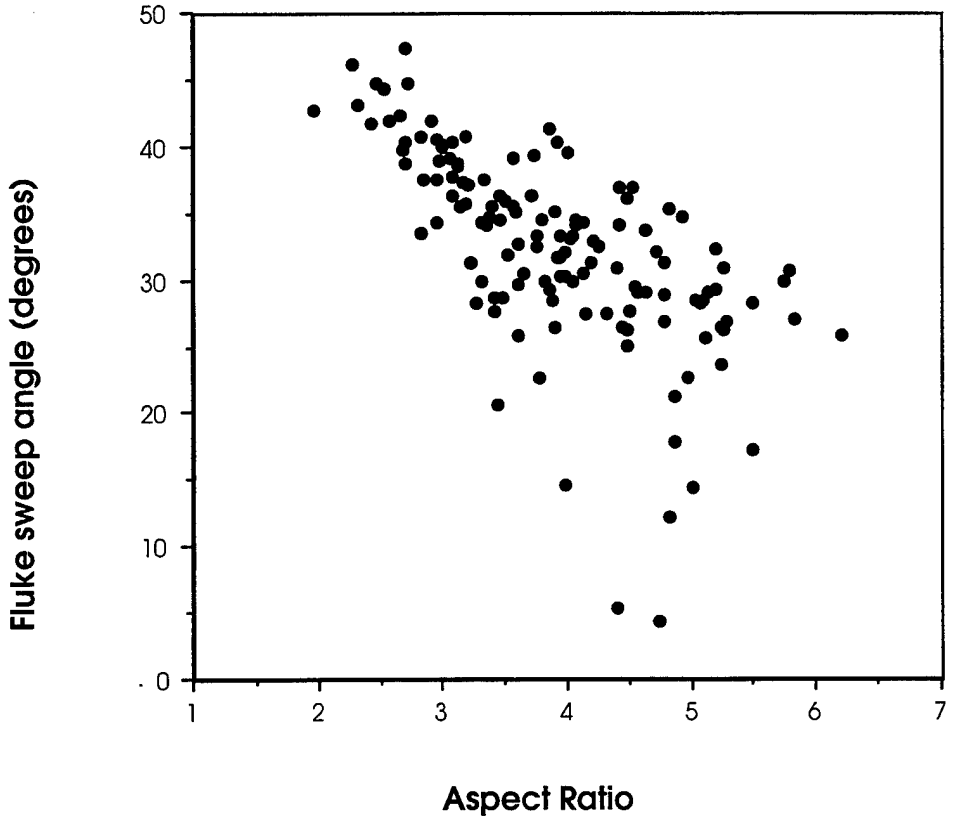

Figure 12. Relationship between fluke sweep angle (Λ) and aspect ratio (AR) for various cetaceans (Fish, 1998b).

Flukes, however, do show some degree of both spanwise and chordwise flexibility. The center of the flukes is more rigid than the tips. During the up-stroke, fluke tips are bent down slightly from the plane of the fluke and lag behind the center whereas bending in the opposite direction occurs during the down-stroke. Bose *et al.* (1990) suggested that the phase difference caused by this spanwise flexibility would prevent the total loss of thrust at the end of the stroke. While the tips would be ending the stroke and effectively generating no thrust, the center would have started the next stroke and have begun thrust generation. Chordwise flexibility at the trailing edge of the flukes could potentially increase fluke efficiency by up to 20% with only a moderate decrease in the overall thrust (Katz and Weihs, 1978).

Rigid control surfaces are significant noise sources and increase the size of the turbulent wake (Cincotta and Nadolink, 1992). Bending the flukes would surpress disruption of the flow caused by hydrodynamic effects over the fluke surface. Thrust producted without excessive noise would benefit dolphins in preying on fish possessing arrays of vibration sensors.

5.3 FLIPPERS AND DORSAL FIN

5.3.1 Planform

Aside from the flukes, which are largely responsible for the generation of thrust, the other control surfaces on cetaceans are the pectoral flippers, dorsal fin, and caudal peduncle. For odontocetes, the relative proportions of the control surfaces vary substantially between the different species. The percentage of total control surface area ranges from 14 to 42% for the flippers, 0 to 18% for the dorsal fin, 16 to 48% for the peduncle, and 22 to 37% for the flukes (Fish, 1997).

Flipper planforms vary from elongate wing-like forms in the humpback whale (*Megaptera novaeangliae* ; figure 13) to rounded paddle-like forms in the killer whale (*Orcinus orca*) and beluga (*Delphinapterus leucas*). The humpback whale has the longest flipper of any cetacean (True, 1983), with a length that varies from 25 to 33% of body length (Tomilin, 1957; Winn and Winn, 1985; Edel and Winn, 1978). The flippers of other cetaceans are no longer than 0.14 body length (Edel and Winn, 1978). For odontocetes, flipper length directly increases with increasing body length (figure 14).

When present, dorsal fins are shaped as falcate, triangular, or rounded (Minasian et al., 1984). Dorsal fin height is directly related to body length (figure 14). The largest dorsal fin (1.8 m high) is found in male killer whales (*Orcinus orca*) and is a distinct sexual dimorphic characteristic in this species. No association between swimming speed and dorsal fin design is apparent. Finless whales, such as *Lissodelphis*, are considered rapid swimmers (Winn and Olla, 1979) whereas the beluga (*Delphinapterus leucas*) is reportedly a slow swimmer (Fish, 1998a).

5.3.2 Cross-sectional Design

The cross-sectional design of flippers and the dorsal fin displays the characteristic fusiform design (figure 13, 15; Felts, 1966; Lang, 1966a; Pershin, 1988). Because of the addition of skeletal elements in the flippers, these appendages are relatively thick compared to flukes and the dorsal fin. Sections from the elongate flipper of *Megaptera* range in *TR* (*TR* = *T*/*C*; see figure 10) from 0.20 to 0.28 (Fish and Battle, 1995). *SP* for the humpback flipper is 49% at the tip, but decreases to 19% at the mid-span. Dorsal fin sections measured for *Lagenorhynchus obliquidens* and *Phocoenoides dalli* have *TR* values of 0.19 and 0.15, and *SP* values of 33 and 36%, respectively (Lang, 1966a). The fin shape induces a fairly even pressure distribution in the chordwise direction (Lang, 1966a).

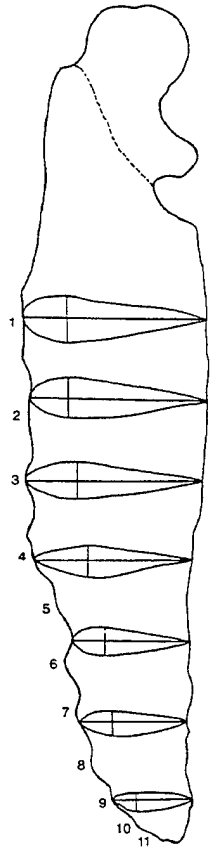

Figure 13. Flipper planform for *Megaptera novaeangliae*. Flipper planform showing representative cross-sections. Flipper is oriented with its distal tip pointed down. Horizontal lines through each cross-section represent the chord length (*C*) and vertical lines represent the maximum thickness (*T*). Distance from the leading edge (left side) to *T* represents the position of maximum thickness (*SP*). Numbers located along the leading edge indicate the center for each of the tubercles (from Fish and Battle, 1995).

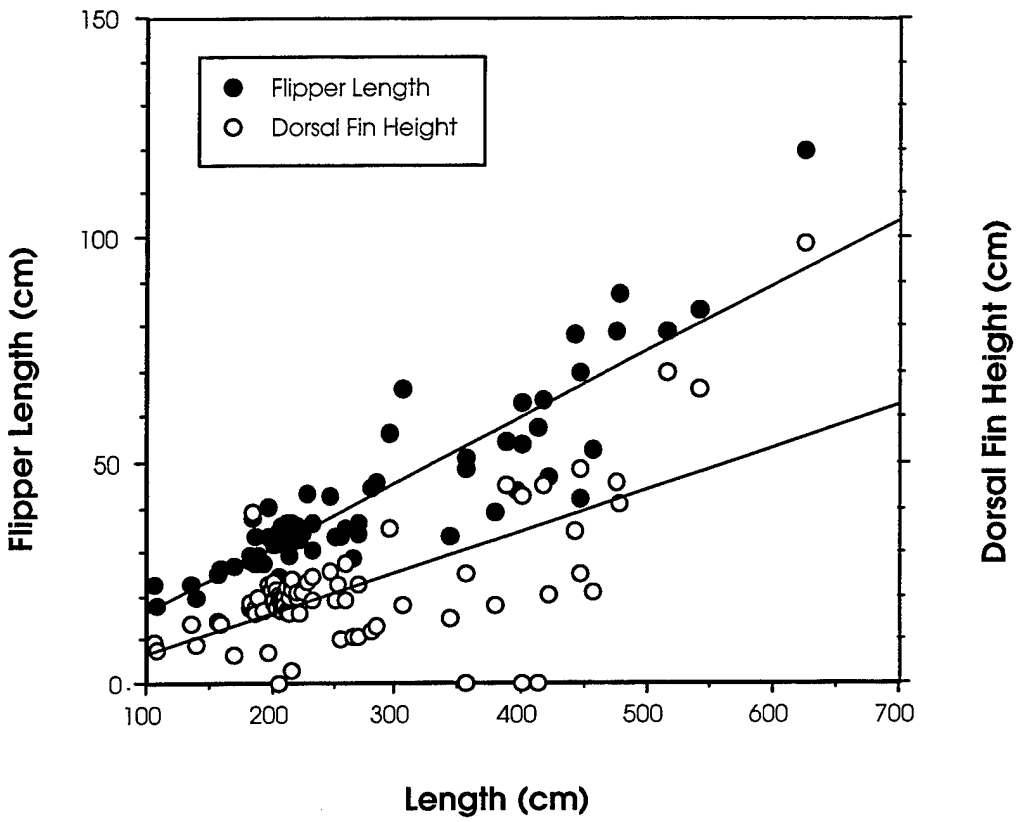

Figure 14. Relationships between flipper length and dorsal fin height with respect to body length for odontocete whales. A total of 81 individuals were examined from 26 species. Flipper length (*FL*) increased with increasing body length (*BL*) according to the equation $FL = 1.80 + 0.15\ BL$ ($r = 0.89$); dorsal fin height (*DF*) increased directly with *BL* according to the equation $DF = -2.93 + 0.09\ BL$ ($r = 0.65$).

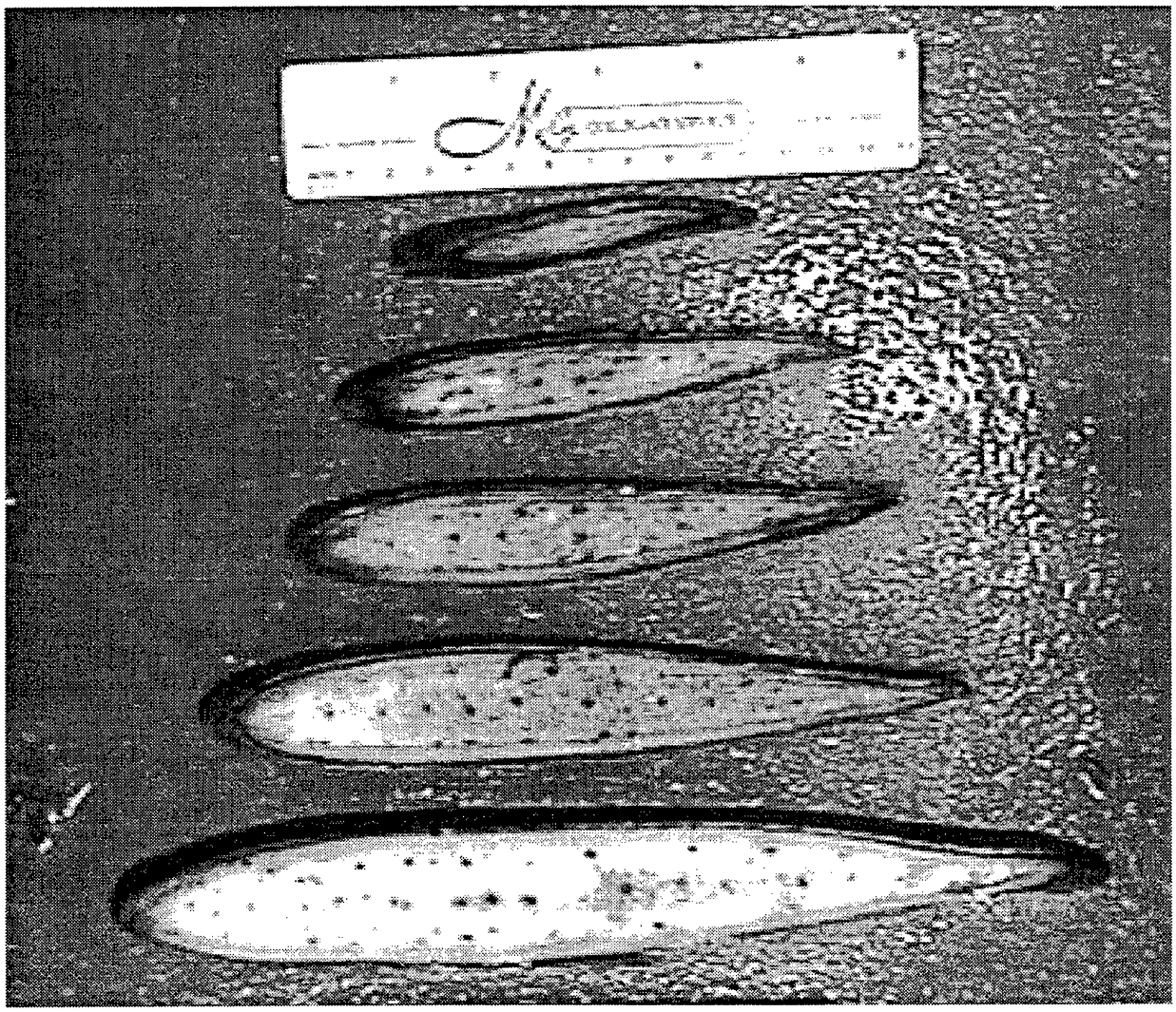

Figure 15. Sections of dorsal fin from *Tursiops truncatus*.

5.3.3 Aspect Ratio

Flipper *AR* is most pronounced for mysticetes in *Megaptera* (*AR* = 6.1; Fish and Battle, 1995). For odontocete flippers (Appendix C), *AR* values range from 1.9 for *Orcinus orca* to 7.7 for *Globicephala melaena* . Dorsal fin *AR* is significantly smaller than the flipper *AR*. The largest dorsal fin *AR* of 2.4 is found for a male *Orcinus orca*. For cetaceans that possess a dorsal fin, the smallest *AR* is displayed for the triangular fin of *Inia geoffrensis*. Dorsal fin Λ is inversely related to *AR* (figure 16) so that animals with high Λ have low *AR* and vice versa.

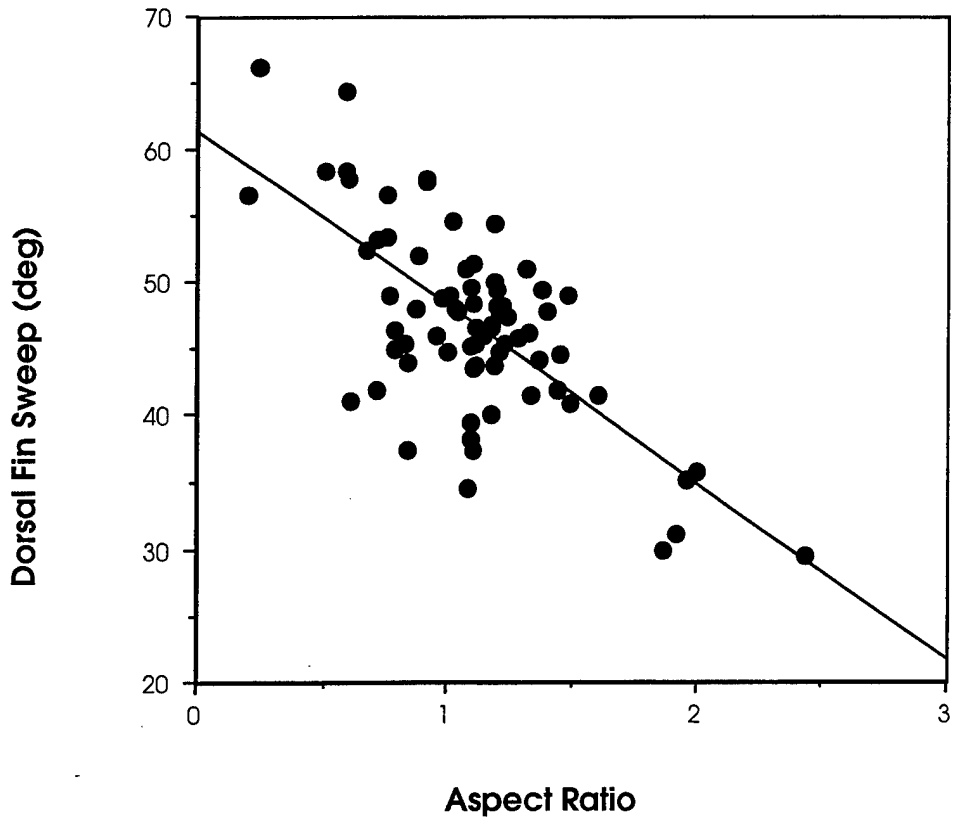

Figure 16. Relationship of dorsal fin sweep (Λ) to aspect ratio (*AR* from data listed in Appendix C). The regression line is described by the equation $\Lambda = 61.29 - 13.16\ AR$ ($r = 0.70$).

5.3.4 Flipper and Fin Mobility

The flippers of cetaceans function as hydrofoils to control moments that produce pitch, yaw, and roll. Control of these moments is important in maintenance of stability and in maneuvering. Reduced motion of the flippers of fast swimming dolphins is necessary to enhance stability (Fish, 1997). The mobility of the flippers of fast swimmers appears to be more constrained when compared to the flippers of slow-swimming, highly maneuverable animals (Howell, 1930; Vasilevskaya, 1974; Pilleri et al., 1976; Edel and Winn, 1978; Klima et al., 1987; Fish, 1997). The shoulder muscular of *Inia geoffrensis* is highly differentiated in contrast to the faster swimming *Lagenorhynchus*, *Phocoena*, and *Tursiops* (Klima et al, 1987). *Inia* turns with a radius that is 10% of its body length (Fish, 1997). This degree of maneuverability is necessary to operate in the complex environment of a shallow river habitat. Similarly, *Megaptera* uses its mobile, high *AR* flippers to maneuver in coastal waters for prey (Edel and Winn, 1978; Jurasz and Jurasz, 1979; Fish and Battle, 1995).

Dorsal fins are not mobile. The position of the dorsal fin aft of the center of gravity is important for stability (Parry, 1949b; Maslov, 1970; Fish, 1987). The fin resists yawing and rolling motion and acts to prevent side-slip during turning maneuvers.

6. DRAG ESTIMATES

6.1 METHODS

Early studies of dolphin swimming energetics and hydrodynamics used drag estimates based on rigid body models. These models assumed that the thrust generated by swimming dolphins was equal to drag estimates from gliding dolphins (Lang and Daybell, 1963; Lang and Pryor, 1966; Kayan, 1974), towed reproductions of dolphins (Purves et al, 1975; Aleyev, 1977), or a hydrodynamic flat plate formulae (Gray, 1936; Kayan and Pyatetskiy, 1978; Hui, 1987).

Total body drag as estimated from gliding is determined by the deceleration of a live dolphin after it has terminated active swimming. The deceleration is measured by motion analysis using data collected from film or video records. For a glide of time (t), the average deceleration (a) is determined from the equation:

$$a = (U_i - U_f)/t, \tag{1}$$

where U_i and U_f are initial and final velocities, respectively (Lang and Daybell, 1963; Bilo and Nachtigall, 1980; Williams, 1987). The drag is equal to

$$\text{Drag} = m_V\, a, \tag{2}$$

where m_V is the virtual body mass. The virtual mass is the mass of the dolphin and added mass of water entrained with the body (Webb, 1975; Vogel 1994). For a 4:1 spheroid, the added mass is equal to the body mass times 0.082 (Vogel, 1994). Williams (1987) argued that this method was superior to the use of rigid models or carcasses because it (1) accounts for surface characteristics, (2) occurs within the normal range of swimming speeds, and (3) uses the routine animal behaviors. Williams (1987) also noted that this technique could underestimate the average glide velocity, producing a lower deceleration estimate. In addition, small changes in body posture or appendage orientation could increase drag.

Towing experiments involve drag measurements on rigid models or preserved and frozen carcasses suspended by a force balance in a water flume or wind tunnel (Webb, 1975; Aleyev, 1977; Blake, 1983b; Williams, 1987). An advantage of this method is that measurements can be made at a controlled velocity without deceleration effects. In addition, the appendages can be removed to measure the proportion of drag caused by these structures. The major disadvantage to towing experiments is that the flow may be turbulent, which could augment the drag. Corrections must be made for mounting struts that could influence the flow over the body.

Estimates of drag assuming equivalence to a flat plate are made by using the equation:

$$\text{Drag} = 1/2\, \rho\, C_D\, S_w\, U^2, \tag{3}$$

where ρ is the density of the medium, C_D is the nondimensional drag coefficient, S_w is the wetted body surface area, and U is the velocity. Equating the drag on a flat plate with the drag on the body of a dolphin assumes that the drag is totally frictional, arising from the boundary layer (Webb, 1975). For a flat plate, the total (both sides) C_D can be related to Re for a laminar boundary layer,

$$C_D\,(\text{laminar}) = 1.33\, \text{Re}^{-0.5}, \tag{4}$$

and for a turbulent boundary layer,

$$C_D \text{ (turbulent)} = 0.072\ \mathrm{Re}^{-0.2}. \quad (5)$$

Experimentally, transition from laminar to turbulent flow occurred at Re between 5×10^5 and 10^6. Equations (4) and (5) apply to Re between 10^5 and 10^7 for turbulent flow, and Re greater than 10^2 for laminar flow (White, 1974). Biologists have traditionally used these equations, however, there are other empirical flat plate, skin-frictional formulae for turbulent flow over different Re ranges (White, 1974). Although cetaceans swim at speeds that put them in the Re range where turbulent boundary conditions are expected, the choice of a C_D for laminar flow best satisfy the power estimates used by Gray (1936). The arbitrary assignment of boundary conditions and assumption that the drag pressure component is unimportant can produce large errors associated with drag estimates using this simple hydrodynamic model (Gray, 1936; Kermack, 1948; Webb, 1975; Fish and Hui, 1991).

A dolphin, however, does not swim as a rigid body, but oscillates its tail and flukes in large amplitude motions for propulsion (Joh, 1925; Slijper, 1961; Lang and Daybell, 1963; Pyatetskiy and Kayan, 1975; Kayan, 1979; Videler and Kamermans, 1985; Fish, 1993b, 1998a). Most hydromechanical models (based on kinematics) provided values of power outputs for actively swimming animals, which exceeded equivalent rigid bodies by three to seven times (Lighthill, 1971; Kayan, 1974; Webb, 1975; Kayan and Pyatetskiy, 1978; Fish et al., 1988; Fish, 1998a). Consequently, drag estimates based on rigid-body analogies and gliding bodies were generally thought to underestimate the energy expenditure of a dolphin swimming. However, there are recent studies suggesting that the drag on an undulating robotic fish may be more than 50% less than that on the same body when passively dragged (Anderson and Kerrebrock, 1997).

Hydromechanical models based on swimming kinematics are considered the only method with sufficient predictive value to calculate power output and the drag associated with active swimming (Webb, 1975). Dolphins are good models for this type of analysis because their swimming mode (subcarangiform with a lunate-tail) effectively separates the structures associated with thrust production from drag production (Lighthill, 1969; Webb, 1975; Fish et al., 1988). Thrust estimates based on fluke motion can independently assess the drag caused by body form and swimming motions. Many studies have used kinematic data (Norris and Prescott, 1961; Lang and Daybell, 1963) to help develop hydromechanical models based on oscillating plates or hydrofoils (Parry, 1949a; Lighthill, 1970; Wu, 1971b; Chopra and Kambe, 1977; Yates, 1983). However, application of these models has relied on data from a single swimming speed for a single dolphin. Estimates of swimming energetics and hydrodynamics have come mainly from examinations of maximal swimming effort (Lang, 1975; Goforth, 1990) and have ignored submaximal swimming by dolphins. In the wild, dolphins swim over a wide range of speeds (Norris and Prescott, 1961; Würsig and Würsig, 1979; Au and Perryman, 1982; Lockyer and Morris, 1987). Studies by Fish (1993b; 1998a) have examined different species locomoting over a full range of speeds to present a more complete picture of dolphin swimming energetics and hydrodynamics.

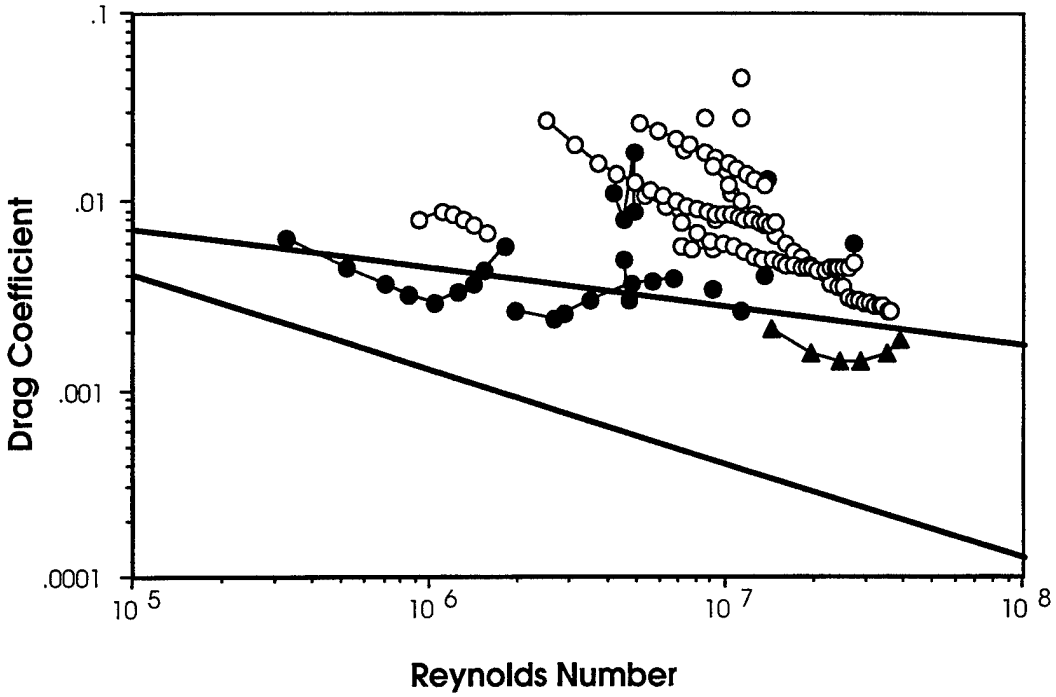

Figure 17. Drag coefficient plotted against Reynolds number for cetaceans. Data were obtained from experiments on rigid models, towed bodies, and gliding animals (closed circles), and from hydrodynamic models based on swimming kinematics (open circles). The upper line represents the drag coefficient for a flat plate with turbulent boundary layer flow; the lower line is for a flat plate with laminar boundary flow. The solid triangles are drag coefficients for a rigid "dolphin" model with the shape of a solid of revolution of the NACA 66 series. Data are from Lang and Daybell, 1963; Lang and Pryor, 1966; Aleyev and Kurbatov, 1974; Kayan, 1974; Purves et al., 1975; Webb, 1975; Aleyev, 1977; Chopra and Kambe, 1977; Yates, 1983; Videler and Kamermans, 1985; Fish, 1998a.

6.2 COMPARATIVE DATA

Dolphin drag coefficients based on hydrodynamic models are, in general, higher than values from towing or gliding experiments. They are also higher than theoretical frictional drag coefficients with turbulent boundary conditions (figure 17). Studies using towed models and gliding dolphins gave mixed results, with some values of C_D below fully turbulent conditions. However, some C_D values fall in the Re region where transition between laminar and turbulent flow occurs (Kayan, 1974). Indeed, as Re increased, the C_D climbed into the turbulent regime (figure 17).

The shape and movements of dolphins dictate high C_D values compared to the theoretical values for a flat plate with a laminar boundary layer. Both factors influence the streamlining of the dolphin and the drag pressure and frictional components. Fish (1998b) found that the beluga (*Delphinapterus leucas*) with its bulbous head and skin folds along its flanks had higher C_D than dolphins with tighter skin and a smoother body contour. The bulbous head would increase the high-pressure area and increase the drag. In addition, the beluga is reported to have an entirely turbulent boundary layer

(Pershin, 1988). At high *Re*, *Orcinus orca* displayed the lowest C_D. This species has a *FR* close to the optimum of 4.5 for minimum drag with maximum body volume (Webb, 1975; Fish, 1998a). Minimum C_D for fast-swimming species occurs close to the maximum speeds (Fish, 1998a). Reduced drag at high speeds facilitates burst swimming, particularly during foraging. *Delphinapterus* can tolerate a higher C_D because this cetacean feeds on slower moving prey, including crustaceans and annelids (Brodie, 1989).

Idealized streamlined bodies such as a solid of revolution with the NACA 66 series design can promote a mostly laminar boundary layer and have a lower drag than a dolphin body (figure 17; Kayan, 1974; Parsons et al., 1974; Hansen and Hoyt, 1984). Indeed, the cetacean body design is not optimal to minimize drag by maintenance of laminar flow. There may be a simple reason for this. A laminar boundary layer presents a higher risk of increased drag because of boundary layer separation. In contrast, a turbulent boundary layer can flow farther against an adverse pressure gradient before separating, thus reducing pressure drag. Cetacean FR of 5.5 to 7 (figure 7) is optimal for minimum turbulent flow resistance, and reduces the chances of boundary layer separation (Romanenko, 1995). Also, sensitivity to roughness and particles in the water may limit the practicality of low-drag laminar shapes to restricted conditions (Hansen and Hoyt, 1984). Moreover, low-drag foils do not perform well in situations necessitating maneuverability. The shape of the dolphin, therefore, represents a compromise between drag reduction and the biological role of the organism.

Adding appendages increases drag. The body of the harbor porpoise (*Phocoena phocoena*) makes a disproportionate contribution to the total drag in that the body is 87.6% of the total surface area, but only 64.3% of the drag (Yasui, 1980). The dorsal fin, pectoral flippers, and flukes comprised only 2.6, 4.2, and 5.6% of the total surface area of the harbor porpoise, respectively; however, these appendages are responsible for 35.7% of the total drag (4.3, 18.0, 13.4%, respectively). The drag added by the appendages of *Stenella* was estimated as 28% of the total drag (Lang and Pryor, 1966). The skin friction, interference, and induced drag associated with the appendages cause increased drag. Interference drag occurs as the appendages distort flow over the body. Induced drag from the appendages results from the differential pressure associated with lift. It is manifested as tip vortices generated at the flukes and flippers during propulsive strokes and the dorsal fin during maneuvers (Hoerner, 1965; Webb, 1975; Fish, 1993a; 1998b, c; Vogel, 1994). The induced drag is highly dependent on *AR*, with high drag associated with low *AR*, untapered hydrofoils.

For actively swimming animals, higher C_D is expected because the oscillating motions of the flukes and body will produce "boundary layer thinning" (Lighthill, 1971). The increased drag corresponds to a boundary layer that is thinner than that for a rigid body because of body movements perpendicular to the boundary flow. Lighthill (1971) estimated that skin friction could increase up to a factor of five. This effect was confirmed using computational fluid dynamics for undulatory swimming (Liu, 1997). In addition, the pressure component of drag will increase because the propulsive body motions will produce a deviation from a streamlined body (Williams and Kooyman, 1985; Fish et al., 1988; Fish, 1993b). The frontal area of an actively swimming dolphin will be larger compared to one passively gliding. The increased frontal area is caused by body oscillations around its center of gravity. Indeed, any gyrations will increase drag on the control surfaces. Unless the flippers can be manipulated in tune with the fluke oscillations to present the smallest frontal area, the result will be added drag. Increased drag would also occur as dolphins bend their bodies to maneuver (Fish, 1997). Dolphins swimming in small radius circles have higher calculated power outputs than for linear swimming (Hui, 1987).

Flukes incur increased drag-due-to-lift because of the dolphin's propulsive mode. As the flukes oscillate at an attack angle , they produce both lift for propulsion and increased drag. A fluke with a

cross-section similar to a NACA 63_4-021 will show increased drag in steady flow above an attack angle of 4°(Abbott and von Doenhoff, 1959). Between attack angles of 4° and 10°, the drag coefficient increases by 58%. This additional drag and drag from the increased frontal area and boundary layer thinning would effectively augment the total drag during active swimming compared to gliding.

6.3 BOUNDARY LAYER CHARACTERIZATION

6.3.1 Flow Visualization

Resolution of arguments regarding the character of the boundary layer was attempted by direct visualization of the boundary layer. Rosen undertook the first investigation of flow visualization on dolphins in 1958. He photographed the pattern of flow lines from water entrained to a body of a *Lagenorhynchus* leaping into the air (Rosen, 1959, 1962). The flow pattern visualized a series of elliptical vortices extending from the dorsal fin and flukes, which Rosen concluded were associated with thrust production (figure 18).

Later, Rosen (1962, 1963) initiated a series of flow visualization experiments on another *Lagenorhynchus* involving dye, air bubbles, and a "particle curtain." The fluorescence-sodium dye was applied to the dolphin's melon and illuminated under ultraviolet light. The flow over the dolphin was laminar over the anterior 32% of the dolphin. Transition began before the dorsal fin with turbulence aft of the fin. Boundary flow separation occurred smoothly near the base of the flukes. These results were supported by pressure measurements on live dolphins (Romanenko, 1981). Tests with paint on a rigid model of *Tursiops truncatus* indicated that boundary flow separation occurred behind the dorsal fin, which is posterior of the shoulder (Purves et al., 1975). Using a curtain of particles raining down on a dolphin, Rosen (1963) showed an array of vortices in the outer flow produced from the animal's swimming motions.

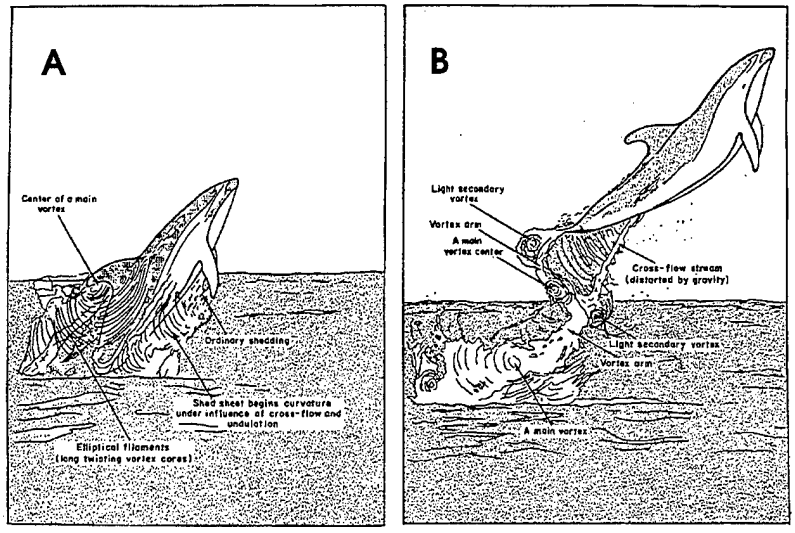

Figure 18. Drawings of water flow lines extending from the body surface of a Pacific white-sided dolphin (*Lagenorhynchus obliquidens*) based on photographs taken by Rosen (1959). A. Dolphin emerging from water showing the flow lines entrained to the body and distorted by elliptical vortex. B. Vortices produced by fluke oscillation.

Bioluminescence as a mechanism for visualizing flow has been well known from observations on the wakes of fish, divers, seals, torpedoes, and surface ships (Bityukov, 1971; Staples, 1966; Lythgoe, 1972; Steven, 1950; Harvey, 1952, Stefanick, 1988). The last U-boat sunk during World War I was detected by its bioluminescent wake (Herring, 1998).

Flow visualization using bioluminescence within the dolphin boundary layer was exploited by Rohr and Latz with their colleagues (Latz et al., 1995; Rohr et al., 1998a). Unicellular plankton called dinoflagellates produces the bioluminescence. The bioluminescence response of the dinoflagellates was calibrated to a hydrodynamic induced shear stress (Latz et al., 1995). Stimulation of bioluminescence occurred above a shear stress of approximately 1 dynes/cm^2 in both laminar and turbulent flows. A gliding dolphin moving through water with the dinoflagellates stimulated bioluminescence over its body (figure 19**a**; Rohr et al., 1998a). There was a conspicuous lack of bioluminescence around the melon and leading edges of the flippers and dorsal fin. Here, shear stresses were predicted to be high, but the boundary layer was exceedingly thin. Flow separation was apparent only when the dolphin executed a turning maneuver (Rohr et al., 1998a). During rectilinear glides, the boundary layer remained attached up to the fluke base and provided no indication of major flow separation. On some frames a conspicuous increase in bioluminescence beginning behind the blowhole suggested laminar to turbulent transition occurred there (figure 19b). Bioluminescent "footprints" of the wakes of 6- to 12-cm fish have also been recorded (figure 19c). There are anecdotal accounts of fishermen discriminating between different species of fish by their bioluminescent trails (Roithmayr, 1970). It has also been suggested that these trails are used by nocturnal marine predators to stalk their prey (Hobsen, 1966). In summary, although the presence of high shear stress along the body indicated by bioluminescence was not conclusively shown to differentiate laminar from turbulent flow (Rohr et al., 1998a), the presence of bioluminescence clearly showed that the boundary layer remained attached over most of the animal.

When actively swimming, flow separation appears restricted to the tips of the lifting surfaces (i.e., flukes, flippers, and dorsal fin). Bioluminescent "contrails" have been reported frequently (Steven , 1950; Wood, 1973; Fitzgerald, 1991). These contrails are the tip vortices generated from the differential pressures along the two surfaces of a lifting surface. Similar observations were made on seals swimming through bioluminescence (Williams and Kooyman, 1985).

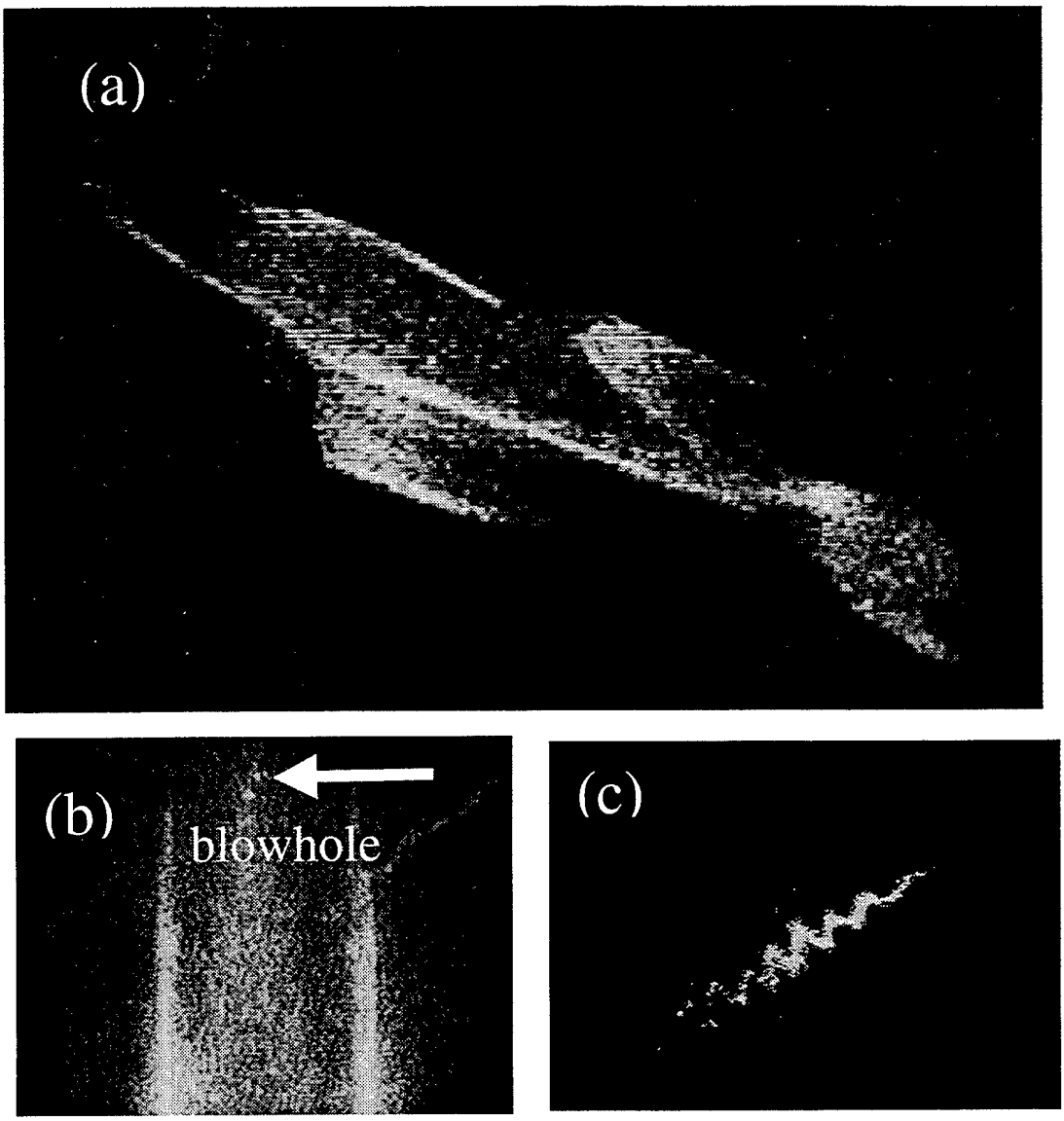

Figure 19. (a) Bioluminescence image of a gliding dolphin (*Tursiops truncatus*); (b) increase of bioluminescence around blowhole; (c) bioluminescence "footprint" of small fish (swimming from left to right).

6.3.2 Velocity and Pressure Measurements

As indicated from flow visualization experiments on dolphins, differences in boundary layer flow occur between actively swimming and gliding animals. Examination of flow with a hot-wire anemometer on a dolphin model showed a transition from laminar to turbulent flow that occurred sooner than on a theoretical laminar profile (Pyatetskiy and Shakalo, 1975). Experiments using remote pressure sensors in the boundary layer of an actively swimming dolphin indicated that although agitated the boundary layer did not become completely turbulent (Kozlov and Shakalo, 1973; Romanenko and Yanov, 1973; Romanenko, 1976, 1981). The inferred transition was anterior to the dorsal fin and corresponded with a local Re of about 3×10^6 (Aleyev, 1977). This transition in boundary flow differs from a gliding dolphin where the boundary layer is considered to be fully turbulent (Sokolov and Yablokov, 1978).

The dynamic pressure variation over a dolphin body was modeled from the bending oscillations (Romanenko, 1995). Maximum pressure occurred between 0.2 and 0.4 *BL*, and pressures rapidly fell between 0.6 and 0.8 *BL*. Romanenko (1995) considered that the turbulence in the boundary layer began in the middle part of the body where the pressure gradient is small and perhaps positive. However, the reduction in pressure over the tail would promote a laminar or near laminar flow. Observations of *Lagenorhynchus* swimming through bioluminescence with brightly illuminated mid-bodies (Wood, 1973) was believed to support this contention.

Although the degree of turbulence and the pressure were determined to decrease over the posterior portion of the body of the actively swimming dolphin, these results may not be associated with viscous dampening as has been hypothesized (Pershin, 1988; Romanenko, 1981). Indeed there is no direct evidence to suggest that viscous dampening of the skin should be any more likely when the animal is oscillating its flukes as opposed to gliding (Fish and Hui, 1991).

The important point is that regardless of the flow conditions the boundary layer of the dolphin remains attached. Premature separation of the boundary layer produces a substantial increase in pressure drag (Webb, 1975; Vogel, 1994). A laminar boundary layer is more prone to separation than a turbulent boundary layer. A dolphin may pay a higher energetic cost in frictional drag by allowing the development of a turbulent boundary layer, but the pressure and total drags will be substantially lower than if laminar flow with separation transpires. This is because a turbulent boundary layer has higher stability and resistance to separation (Webb, 1975). The increased momentum of the turbulent layer allows it to penetrate farther aft into the region of increasing pressure along the body. When separation does occur into the wake, the size of the wake is reduced as is the total drag. The textbook example of this phenomenon is the design of golf balls with dimples to promote boundary layer transition for reduced drag and increased flight distance (Shapiro, 1961).

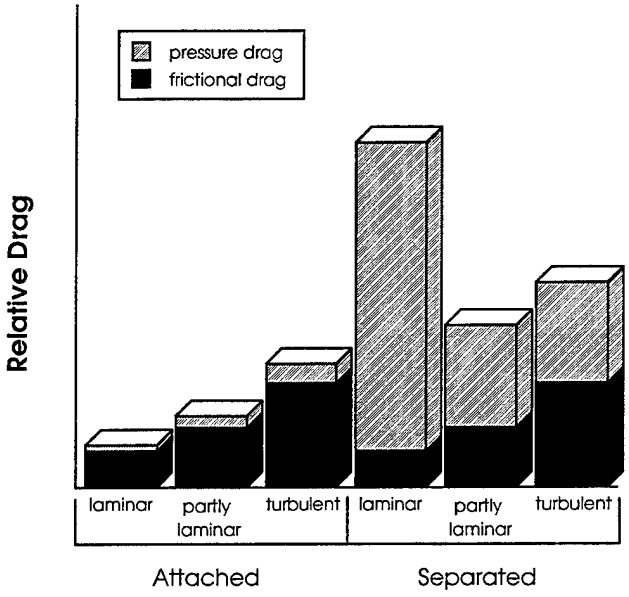

Figure 20. Relative drags for attached and separated flow with laminar, partly laminar, and turbulent boundary layer flow (modified with permission from Webb 1975).

7. DRAG-REDUCTION MECHANISMS

7.1 VISCOUS DAMPENING

The idea of viscous dampening as a mechanism for drag reduction by dolphins was developed by Kramer in the early 1960s (1960a, 1960b, 1965; section 3.3, KRAMER). Kramer (1960b) argued that through the interaction of the flow and the compliant dolphin skin, transition from laminar to turbulent flow in the boundary layer on the dolphin could be delayed. Based on the structure of the dolphin's epidermis and dermis, Kramer attempted to produce an artificial skin that had this transition-delaying property. One mechanism proposed to delay transition was through passively dampening the incipient boundary layer perturbations of the Tollmien–Schlichting wave type, which lead to transition (Pershin, 1988). However, to observe the Tollmein–Schlichting waves, background turbulence levels must be lower than what might normally be expected in the marine environment (Kramer, 1965). In general, replication of Kramer's experiments using a compliant surface modeled after the dolphin's skin were not successful although some limited success in reducing skin friction has been possible with other compliant coatings (Landahl, 1962; Blick and Walters, 1968; Carpenter, 1990; Gad-el-Hak, 1987, 1998; Carpenter, 1990, 1998; Henricks and Ladd, 1991).

It has also been suggested that a compliant coating, rather than delaying transition, would reduce drag by effecting turbulence in the boundary layer (Riley et al., 1988: Carpenter, 1998). As part of the Compliant Coating Drag Reduction Program effort sponsored by the Office of Naval Research, 44 specimens of compliant material were tested between 1980 and 1985 for drag-reducing properties in fully turbulent flow (Rathsam and Borkat, 1987). Many types of materials were represented including: polyvinyl chloride (PVC) plastisols, natural rubber, neoprene rubber, silicone rubber, urethane rubber, foamed blends of PVC and nitrile rubber, and hydrophilic and hydrophobic coatings. Some of the materials were tested with and without thin cover films, and some were made from more than one material. Drag data were calculated from velocity-profile measurements obtained in the boundary layer using laser Doppler velocimetry. The principle conclusion of these series of tests (Ratham and Borkat, 1987) was: "none of the compliant materials or chemical coatings was found to have less drag than its appropriate reference specimen, and no information was discovered to indicate which types or designs of compliant materials are most promising for future studies".

The structure of the dolphin skin and blubber layer is highly organized and complex (Parry, 1949c; Sokolov, 1960; Aleyev, 1977; Haun et al., 1983; Pershin, 1988; Toedt et al., 1997; Hamilton et al., 1998). Thus, the analogy with the compliant skin proposed by Kramer may be only superficial and have little functional similarity. The elasticity of the dolphin's skin is caused by large amounts of organized collagen and elastic fibers (Pershin, 1988; Toedt et al., 1997; Hamilton et al., 1998). Kramer (1965) reported a modulus of elasticity (E) of 1×10^8 N/m^2 for a dolphin skin sample, but this high modulus was considered an artifact of testing-preserved tissue (Babenko, 1979). E may vary with species, position on the body, degree of training, and physical condition (Babenko et al., 1982; Toedt et al., 1997). E of 1.7×10^4 N/m^2 was lower in the middle of the white-sided dolphin compared to more anterior and posterior sections of the body (Babenko, 1979). For recently captured *Tursiops*, E was 4.5×10^5 N/m^2 in the middle of the body. After training, when the animal was calm, E decreased to 2.4×10^2 N/m^2. The higher value of E was viewed as corresponding to the condition of high-speed swimming (Babenko et al., 1982). The elastic properties of the integument are dependent particularly on the deeper layer of thick blubber. The blubber layer is highly resilient with E similar to biological rubbers (Pabst et al., 1995a).

Babenko (1998) reported a maximum 95% absorption of perturbation energy for energies representative of turbulent pulsations in the boundary layer. This value was determined by bouncing a ball on the integument. Madigosky et al. (1986) examined the velocity and absorption of acoustic surfaces on live dolphins and concluded that the lower hypodermis with its associated blubber played an important role in determining the compliant response to hydrodynamic disturbances.

It has been argued that most of the experimental investigations on compliant coating drag reduction failed because the surface was not properly characterized through measurements of the dynamic complex shear compliance (Fitzgerald et al. 1998). Shear compliance of blubber is intermediate between soft-compliant coatings that increase drag and harder compliant coatings that have no effect on drag (Fitzgerald et al., 1995). If the shear impedance of a developing turbulent boundary layer is matched to the blubber, it is hypothesized that the incipient turbulent energy will be reduced by energy flow into the compliant layer where it will be dissipated as heat (Fitzgerald et al., 1995, 1998). *In situ* surface shear impedance measurements on live dolphins could provide improved values of their viscoelastic properties, thereby increasing the possibility of fabricating materials with increased drag reduction (Fitzgerald et al. 1998).

Passive changes in compliance were envisioned by regulating blood pressure within the blood vessels of the dermal papillae (Babenko et al, 1982; Kozlov and Pershin, 1983). For a rapidly swimming dolphin, the reduction in hydrodynamic pressure over the maximum thickness of the body would foster increased peripheral capillary profusion, causing distention of the skin surface (Babenko et al., 1982). Experiments demonstrating changes in capillary profusion with varying atmospheric pressure were performed on humans with a thinner integument than dolphins. Evidence against this mechanism for control of boundary layer turbulence is supplied by pressure measurements on swimming dolphins where turbulence is shown to occur at the position where pressure is reduced (Romanenko, 1995).

Active regulation of the skin was also considered to explain the low turbulence on swimming dolphins over a range of velocities (Kozlov and Shakalo, 1973; Pershin, 1988). An active mechanism of turbulence dampening through a muscular mechanism was hypothesized *via* microvibrations (Haider and Lindsley, 1964; Babenko et al, 1982; Haun et al., 1983, 1984; Kozlov and Pershin, 1983; Ridgway and Carder, 1993). This mechanism relies upon a sensory input of pressure pulsations from the richly innervated skin. Microvibrations are small tremor-like vibrations (1 to 5 μm; 7 to 13 Hz) that occur at all times over the entire body of warm-blooded animals (Haider and Lindsley, 1964; Ridgway and Carder, 1993). The microvibrations, as with the grosser tremors of shivering, are associated with thermoregulation (Haider and Lindsley, 1964). Dolphin skin generates microvibrations with amplitudes three to four times higher than for humans. Ridgway and Carder (1993) suggested that the dolphin skin could move or vibrate to improve hydrodynamic performance.

Active deformation of the skin is under the control of the *musculus cutaneous*. This muscle can move the skin and is noted as the "flyshaker" in horses (Ridgway and Carder, 1993). The *musculus cutaneous* is found in dolphins as a sheet lying between the outer blubber layer (hypodermis) and inner blubber layer of subcutaneous fat. The muscle is well-developed, with fibers arranged obliquely to the long axis of the body (Purves and Pilleri, 1978). In *Tursiops,* the *musculus cutaneous* is located 2 to 4 cm below the skin surface (Ridgway and Carder, 1993). *Tursiops* initiated microvibrations in the 25- to 40-Hz range, which were considered to lend support to active compliance as a drag reducer (Haun et al., 1984). However, Aleyev (1974) argued that the function of the *musculus cutaneous* was not to generate deformation waves in the skin, but to do the opposite and maintain a smooth contour to the body. It is conceivable that if the skin was sensitive enough to detect turbulence, and responsive enough to actively flex to cancel pressure waves along the surface, drag could be reduced.

Through active control of laminar instability waves on an axisymmetric body, via a suction/blowing slot, significant decreases in drag (55% reduction in shear stress) have been demonstrated in the laboratory (Ladd, 1990). However, it has been noted that the time scales of the coherent structures in the flow, which the skin would have to dampen to achieve drag reduction, may be several orders of magnitude less than the minimum response time of the dolphin's skin (Lisi, 1999).

The control of electrical potentials along the skin surface also was hypothesized to improve boundary layer conditions and reduce drag (Babenko and Yaremchuk, 1998). Surface electric field intensity can be as high as 1 mV/mm in areas of increased hydrodynamic resistance. The electric field is considered to influence the pattern of water molecules within the boundary layer and subsequently reduce the drag. However, this mechanism has not been tested on dolphins where the flow is presumably too rapid to make this a viable mechanism of turbulence suppression. This hypothesis should not be confused with magnetohydrodynamic (MHD) control of electrically conducting fluid flows. For fluids (i.e., seawater) that are weakly conductive, MHD flow control can be achieved only by application of both electric and magnetic fields (Bushnell and Hefner, 1990).

The presumption of both active and passive compliance appears inconsistent with dolphin swimming patterns in association with boundary flow. The results of live dolphin studies indicate a turbulent boundary layer flow when gliding, but an incomplete turbulent layer when swimming (Romanenko and Yanov, 1973; Romanenko, 1981; Kozlov and Shakalo, 1973; see section 6.3.2, Velocity and Pressure Measurements). Drag minimization would be equally important for gliding and active swimming. There is no reason to expect that either passive or active mechanisms are switched on or off depending on the activity state. Both mechanisms entreat skin properties that are uncoupled from activation of the propulsive musculature. Gliding is performed during surfacing for respiratory exchange (Amundin, 1974) and as an energy-conserving strategy to reduce the cost of swimming (Weihs and Webb, 1983). For active swimming, metabolically powered muscular effort for continuous boundary layer damping would incur increased energy expenditure compared to passive mechanisms, thus reducing swimming efficiency.

7.2 DERMAL RIDGES

Cetacean skin is generally described as smooth (Shoemaker and Ridgway, 1991). However, cutaneous ridges are present at the skin surface in many dolphins. The ridges are formed from the dermal crests and papillae (Sokolov, 1960; Purves, 1963, 1969; Purves et al., 1975; Aleyev, 1977; Haun et al., 1983; Pershin, 1988). A survey of ridges in seven species of cetaceans showed that the ridges were spaced 0.41 to 2.35 mm apart and were 7 to 114 μm in height (Shoemaker and Ridgway, 1991).

The literature presents a contradictory picture of the orientation of the cutaneous ridges. As summarized by Aleyev (1977), Sokolov and his colleagues noted a streamwise arrangement for dolphins. Purves (1963) and Pilleri (1976) described the ridge direction as oblique, not lengthwise, to the longitudinal axis. Finally, Shoemaker and Ridgway (1991) made skin impressions and histological sections, noting that the ridges were oriented perpendicular to the longitudinal axis of the body. The ridges ran circumferentially around the body from the eye to the base of the dorsal fin (figure 21; Ridgway and Carder, 1993). Posterior of the dorsal fin, the ridges ran obliquely.

The orientation and profile of the ridges has been thought to be crucial for drag reduction. Riblets are streamwise microgrooves with sharp peaks that act as fences to break up spanwise vortices and reduce the surface shear stress and momentum loss from the boundary layer (Yurchenko and Babenko, 1980; Walsh, 1990). A 7 to 9% drag reduction has been demonstrated repeatedly with

riblets (Reidy, 1987; Walsh, 1990; Rohr et al., 1992). Some of the early riblet studies were stimulated by the dermal denticles of fast-swimming sharks who have scales with finely spaced ridges that are essentially aligned with the local flow (Walsh, 1990).

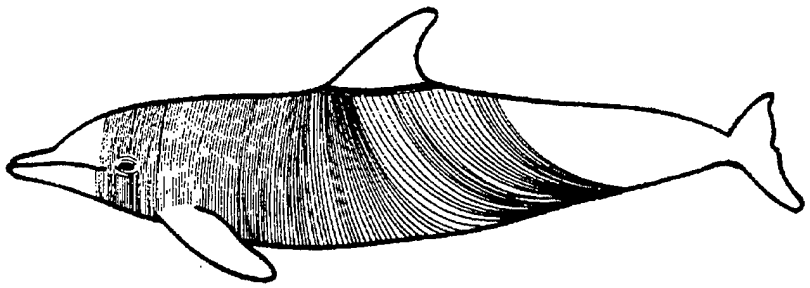

Figure 21. Sketch showing orientation of cutaneous ridges on a bottlenose dolphin (with permission from Ridgway and Carder, 1993).

The ridge orientation and profile described by Shoemaker and Ridgway (1991) could not function for drag reduction like riblets (Fish and Hui, 1991). Indeed, their effects for drag reduction for dolphins have never been experimentally demonstrated. However, the size, shape, and distribution of the cutaneous ridges for *Tursiops truncatus* is theoretically found to be optimally configured to affect the dynamics of the vortex filaments. By altering the dynamics of the vortex filaments, dolphin skin could reduce the rate of energy transport, resulting in a net reduction in skin friction. Maximal surface drag reductions up to 8% are predicted for swimming speeds consistent with observation (Lisi, 1999).

The dense packing of dermal papillae associated with the cutaneous ridges suggests a sensory function (Palmer and Weddell, 1964; Khomenko and Khadzhinskiy, 1974). The dermal papillae contain blood vessels and a rich supply of nerve bundles. The highly innervated skin has a threshold sensitivity of 10 to 40 mg/mm^2, which is close to the most sensitive skin areas (i.e., fingertips, lips, eyelids) of humans (Ridgway and Carder, 1993). Dolphins are sensitive to vibrations and small pressure changes. The skin, therefore, could function in the detection of flow velocities and flow disruptions. Sensory feedback would be more important in detecting boundary layer separation that would more severely impact drag rather than boundary layer transition.

7.3 SECRETIONS

The addition of dilute solutions of long-chain polymers into flow is well established as a means of drag reduction (Rosen and Cornford, 1971; Hoyt, 1975; Daniel, 1981). The addition of non-Newtonian drag-reduction additives can extend the viscous sublayer and reduce turbulent stresses near the wall (Baier et al., 1985; Hoyt, 1990). The epidermal cells of dolphins contain masses of tonofilaments and lipid droplets which, when concentrated, are similar to mucopolysaccharides (Harrison and Thurley, 1972). Epidermal cell production in *Tursiops truncatus* occurs at a rate 250 to 290 times that of humans (Palmer and Weddell, 1964). This high rate is associated with an extensive germinative layer (Brown et al., 1983) and increased skin sloughing. Cells shed from the epidermis were investigated as a mechanism to reduce drag, but had a negligible effect on hydrodynamic drag (Sokolov et al., 1969).

The surface chemical/physical properties of the skin and its high sloughing rate may help to maintain low drag characteristics by preventing fouling by encrusting organisms on the dolphin's surface (Gucinski and Baier, 1983). Biofouling consisting of slime and barnacles can cause a four-fold increase in resistance (Swain, 1998). Dolphin skin has similarities to the oral mucosa, which is self-cleaning and resists fouling (Baier et al., 1985).

Secretions from the dolphin eye are highly viscous complexes of proteins and polysaccharides (Uskova et al., 1983). Their molecular weight is between about 700,000 and 2 million, which is high enough to have drag-reducing properties (Haun et al, 1984). Uskova et al. (1983) demonstrated that the eye secretions could reduce turbulent skin friction and concluded that the secretions had a hydrodynamic function.) However, Sokolov et al. (1969) found these secretions to have no effect of drag characteristics. Although the secretions may fill in any disruptions in skin contour from the eyes, the area covered by the secretions is generally too small to aid in any significant drag reduction for the body. Recent research involving the use of polymer drag reduction for underwater vehicles is briefly described in Appendix E.

7.4 BOUNDARY LAYER HEATING

Increasing the temperature of water will decrease its viscosity, thereby reducing viscous forces at the surface (Vogel, 1994). Warm-bodied cetaceans as with other marine animals (i.e., scombrid fishes, laminid sharks, phocid seals, otariid seals) can use heat conducted from the body surface to decrease water viscosity (Lang, 1966b; Fish and Hui, 1991). The surface temperatures of *Stenella longirostris* and *Tursiops truncatus gilli* were reported to be higher than water temperature by as much as 9°C (McGinnis et al., 1972: Hampton and Whittow, 1976). However, in water at 27°C, a reduction in viscosity of only 11% would be realized (Fish and Hui, 1991). Furthermore, the decrease in viscosity would result in drag reduction only if the water was instantaneously heated. The animal's swimming speed precludes sufficient contact between the skin and the water for effective heating. In addition, heat from the body is convected to the water through thermal windows via the extensive circulatory network in the appendages (Scholander and Schevill, 1955; Pershin et al., 1979; Pabst et al., 1995). Consequently, the effectiveness of heating as a drag-reduction mechanism is considered limited (Lang and Daybell, 1963; Lang, 1966b) or insignificant (Webb, 1975).

7.5 SKIN FOLDS

Mobile skin folds have been observed on accelerating dolphins (Essapian, 1955; Backhouse, 1960; Pershin, 1988). These folds are believed to result from vorticity along the body surface, creating pressure differences that could deform the flexible skin (Backhouse, 1960; Aleyev, 1977) or from active control by muscles (Sokolov et al., 1969). Wrinkles in the skin were observed at the point of flexure of the tail during active swimming, but these irregularities were not believed to be caused by hydrodynamic effects (Fejer and Backus, 1960). Hydrodynamically generated folds move in a wave-like manner perpendicular to the direction of the dolphin's movement and along the body in an anterior to posterior direction (Essapian, 1955). It was hypothesized that the folds were a mechanism to dampen turbulence (Sokolov et al., 1969; Babenko and Surkina, 1969).

To test the hypotheses of active generation of the folds and dampening ability, a model test analogous to the dolphin's skin was examined. The prerequisites of the system were a smooth skin with a layer of subcutaneous adipose tissue and with no active control. This system was represented by naked women aged between 17 and 30 years who were towed through water at speeds of 2 to 4 m/s (Aleyev, 1977). Skin folds similar to those observed on dolphins developed passively from the interaction of the dynamic water pressure and skin elasticity. The speed of the posterior movement of the

folds was 10% lower than the towing speed. The folds increased the drag on the body. When subjects were tested while wearing a swimsuit to suppress the formation of skin folds, the drag was decreased 6.1% compared to nude subjects (Aleyev, 1977).

Although the skin folds exhibited by dolphins and naked women were similar, the composition and mechanical properties of cetacean blubber and human adipose tissue are different. Skin folds caused by flexion of the dolphin body during swimming probably are minimized by the crossed helically wound layer of collagen fibers within and underlying the blubber (Wainwright et al., 1985; Pabst, 1996a, b, 1988; Toedt et al., 1997; Hamilton et al., 1998).

7.6 INDUCED TURBULENT BOUNDARY LAYER

No difference in drag was apparent when tripping rings were carried by a dolphin during gliding experiments (Lang and Daybell, 1963), indicating the presence of a turbulent boundary layer that is less likely to separate. Separation will produce a higher drag caused by an increase in pressure or form drag (figure 20; Webb, 1975). An anteriorly located structure that promotes transition of the boundary layer would be advantageous in stabilizing the flow over the body. On the swordfish (*Xiphias gladius*), an elongate rostrum with a rough surface is present that could promote transition and delay separation (Aleyev, 1977; Videler, 1993). The rostrum of dolphins is generally smooth although the shape is variable. No study has examined the influence of rostrum design on flow over the cetacean body.

The position and number of tubercles on the flipper of the humpback whale, *Megaptera novaeangliae* (figure 13), suggest analogues with specialized leading-edge control devices associated with improvements in hydrodynamic performance (Fish and Battle, 1995). Bushnell and Moore (1991) suggested that humpback tubercles could reduce the drag caused by lift on the flipper. The tubercles of the humpback whale flipper would function to generate vortices by unsteady excitation of flow to maintain lift and prevent stall at high attack angles (Hoerner and Borst, 1975; Shevell, 1986; Rao, 1991; Wu et al., 1991; Barnard and Philpott, 1995; Erickson, 1995).

Vortex generation along the leading edge is particularly effective for unswept wings of high aspect ratio that have abrupt stall characteristics (Rao, 1991). Stall is postponed because the vortices exchange momentum within the boundary layer to keep it attached over the wing surface. The lift curve is modified by this mechanism so that it plateaus with a highly reduced negative slope above the maximum lift coefficient of the wing (Hoerner and Borst, 1975; Rao, 1991). Vortex generation improves lift capabilities without significant drag penalty (Rao, 1991). Vortices shed from leading-edge discontinuities such as notches are used to control stall on wings of commercial and military aircraft (Erikson, 1995). The induced vortices extends the lift generation and delays stall at higher attack angles (Shevell, 1986; Rao, 1991; Erickson, 1995). An increased attack angle is necessary during turning maneuvers to generate the lift force for the turn (von Mises, 1945; Hurt, 1965; Weihs, 1993; Fish and Battle, 1995).

Although no direct evidence from humpback whales exists for vortex generation and water channeling by leading edge tubercles, the pattern of barnacle attachment indicates non-uniform flow patterns. The velocity gradient of water over a solid surface is a major determinate of the attachment success of barnacle larvae (Crisp, 1955). Whale barnacle larvae fail to attach themselves to areas of strong water flow (Crisp, 1955; Crisp and Stubbings, 1957; Lewis, 1978). At water velocities exceeding 1 to 2 m/s, attachment by larvae does not occur and attachment above 2 m/s would be possible in areas of surface irregularities forming local eddies with reduced velocity gradients (Crisp, 1955). Typically, barnacles are found on the upper leading edge of the humpback whale tubercles

(Edel and Winn, 1978; True, 1983; Winn and Reichley, 1985). The lack of barnacles between tubercles indirectly supports a hypothesis of flow modification by the tubercles where water is channeled at high speeds (Fish and Battle, 1995).

7.7 BOUNDARY LAYER ACCELERATION

As Gray (1936) originally proposed, acceleration of the boundary layer caused by propulsive fluke actions could re-laminarize the boundary layer to reduce the drag on a dolphin. Drag reduction by oscillating-foil production has been demonstrated for robotic tuna (Triantafyllou et al., 1996). Fluke oscillations generate unsteady velocity and pressure gradients by accelerating water over the body (Gray, 1936; Lang, 1963; Romanenko, 1995). Delay of transition is possible by injection of high-momentum fluid into the boundary layer (Webb, 1975). However, the high drag values reported above (see section 6, DRAG ESTIMATES) indicate turbulence within at least a significant portion of the boundary layer. A more important consideration in minimizing drag by a dolphin is prevention of separation (Webb, 1975; Fish, 1998b). Indeed, accelerated flow could prevent separation and explain the flow visualization and pressure study results (Steven, 1950; Rosen, 1962, 1963; Romanenko and Yanov, 1973; Wood, 1973; Purves et al., 1975; Romanenko, 1976, 1981). Suppression of boundary layer separation has been achieved under conditions of high oscillatory frequency and/or large chord lengths for flapping-foil propellers (Platzer et al., 1998).

Purves et al., 1975 noted boundary layer separation from just behind the dorsal fin for rigid dolphin models in a flow whereas actively swimming dolphins exhibited separation further downstream at the flukes (Steven, 1950; Rosen, 1962, 1963; Wood, 1973). For a model, an adverse pressure gradient fostering separation is expected to develop as the flow over the body decelerates posterior of the maximum thickness. Dynamic pressure measurements on dolphin models indicate steep negative pressure gradients that begin anterior of the maximum thickness (Aleyev, 1977).

Acceleration of boundary flow along with fluid accelerated by the flukes into the propulsive wake would delay separation by reducing the pressure gradient. From Bernoulli's theorem, the pressure in the wake will be slightly lower than pressure in the free stream as fluid is discharged into the wake at a velocity greater than the free stream (Webb, 1975). This action reduces the pressure gradient over the posterior portion of the body. Calculations of the dynamic pressure distribution over an actively swimming dolphin indicated the extension of a favorable pressure gradient over the total body, with a steep pressure reduction in the region of the peduncle and flukes (Romanenko, 1981, 1995).

8. SWIMMING KINEMATICS

The swimming kinematics of cetaceans are characteristic of the thunniform mode, also known as carangiform with lunate-tail (Lighthill, 1969, 1970; Webb, 1975; Lindsey, 1978; Fish et al., 1988). The thunniform mode is typical of some of the fastest marine vertebrates, including scombrid fishes, laminid sharks, and pinnipeds (Lighthill, 1969; Fish et al., 1988). The propulsive motions are not produced as a continuous traveling wave as found in most fish (Webb, 1975). The motions are characterized as an oscillation in which bending is restricted to particular points along the body (Webb, 1975; Fish et al., 1988; Yanov, 1990; Fish, 1993b; Long et al., 1997). As with the other thunniform swimmers, dolphins generate thrust exclusively with a high aspect ratio, caudal hydrofoil (Fish and Hui, 1991; Fish, 1993a).

The posterior one-third of the body is bent to effect dorsoventral movement of the flukes (figure 22; Parry 1949b; Slijper, 1961; Lang and Daybell, 1963; Videler and Kamermans, 1985; Yanov, 1991; Fish, 1993b). Although these heaving motions vertically displace the flukes through an arc, the flukes do not move as a simple pendulum. Superimposed on the motion, the flukes are pitched at a joint at their base. Pitching at the fluke base occurs because of the double hinge mechanism of the caudal vertebrae including the "ball" vertebrae (Watson and Fordyce, 1993). These heaving and pitching motions change attack angle and thrust generation throughout the stroke cycle (Lang and Daybell, 1963; Lighthill, 1969, 1970; Videler and Kamermans, 1985; Fish et al., 1988; Fish, 1993a, 1998a, b).

Thrust is derived from a combination of the horizontal component of the lift force and leading edge suction (Ahmadi and Widnall, 1986). Thrust from lift increases directly with increasing angle of attack. However, low angles of attack increase hydromechanical efficiency while reducing the probability of stalling and decreased thrust production (Chopra, 1976). Excessive leading-edge suction could also induce stalling caused by boundary layer separation, but the curved leading edge of the flukes (van Dam, 1987) should reduce leading-edge suction without a decrease in total thrust (Chopra and Kambe, 1977).

8.1 MECHANICAL LINKAGE

The propulsive musculature of cetaceans is composed of the longitudinal muscles associated with the vertebral column. The muscles are divided into dorsally positioned epaxial muscles (*multifidus, longissimus*) and ventrally located hypaxial muscles (*hypaxialis lumborum, intertransverarius caudae ventralis*) (Howell, 1930; Parry, 1949b; Agarkov and Lukhanin, 1970; Pilleri, 1976; Smith et al., 1976; Strickler, 1980; Bello et al., 1985; Pabst, 1990, 1993). The relative masses of the muscles differ with the epaxial muscles composing a larger portion of the propulsive musculature. The epaxial and hypaxial muscles could produce equivalent propulsive forces and movements, given the similar arrangement of the fasciculi, tendons, and muscle insertions (Arkowitz and Rommel, 1985). Equivalent numbers of slow oxidative and fast glycolytic muscle fibers in the epaxial and hypaxial muscles also indicate similar propulsive power distribution (Mankovskaya, 1975; Ponganis and Pierce, 1978; Bello et al., 1983, 1985; Suzuki et al., 1983). In addition, abdominal muscles may add large bending moments that help the hypaxial muscles depress the tail (Arkowitz and Rommel, 1985), although there have been some arguments against this concept (Purves and Pilleri, 1978).

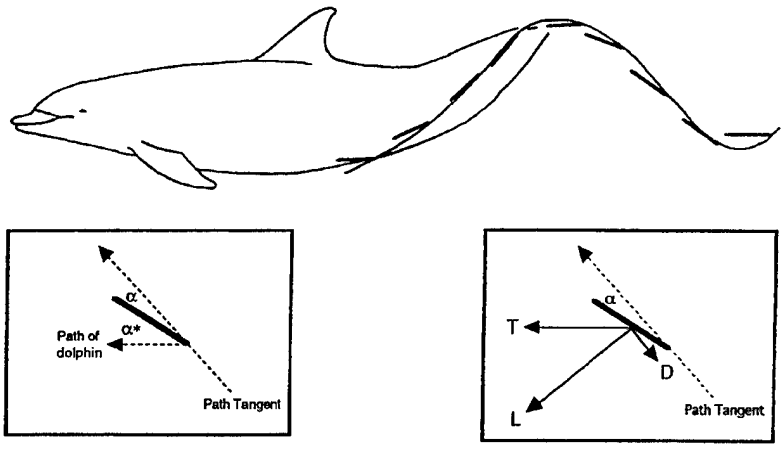

Figure 22. Path of oscillating dolphin flukes through a stroke cycle. Tips of flukes move along a sinusoidal path. Sequential fluke positions along path are illustrated as straight lines. Box on left shows relationship between tangent to fluke path with attack angle, α, and pitch angle, α^*. Attack angle is angle between tangent of fluke's path and axis of fluke's chord; pitch angle is angle between fluke axis and translational movement of animal. Box on right shows relationship between major forces produced by fluke motion. D is drag, L is lift, and T is thrust resolved from L (from Fish, 1993b).

The vertebral column design includes long spinous and transverse processes on the trunk vertebrae and chevron bones of the tail vertebrae for tendonous attachment of the muscles. These structures act as long lever arms to increase mechanical advantage (Slijper, 1961; Agarkov and Lukhanin, 1970; Smith et al, 1976; Pabst, 1990). These lever arms amplify the muscle force output compared to insertions closer to the central axis of the vertebral column (Fish and Hui, 1991). Pabst (1988) has suggested that the subdermal connective tissue sheath under the blubber acts as a force transmission system. The distal position of the sheath far from the vertebral column would provide a large mechanical advantage for flexing the spine and the peduncle.

It has been suggested that cetacean tendons function analogously to the elastic tendons of running mammals (Bello et al., 1985; Blickhan and Cheng, 1994; Pabst, 1996). Theoretically, collagen fibers would store elastic energy generated during the stroke (Wainwright et al., 1985; Pabst, 1996a; Pabst et al., 1997). Energy would subsequently be released to reaccelerate the flukes, reducing the metabolic energy input (see section 9.4, METABOLIC EFFICIENCY). A model proposed by Bennett et al. (1987) examined the relationship between ratios of strain energy to kinetic energy and hydrodynamic force to inertial force for the tendons of two dolphin species. The model predicted optimum compliance for the tendons necessary to minimize both muscular work and metabolic energy during swimming. However, tendon measurements indicated that their elastic compliance is above the optimum and may actually increase the energy cost of swimming (Bennett et al., 1987). In a re-evaluation of the data of Bennett et al (1987), Blickhan and Cheng (1994) used a different model for the hydrodynamic force acting on the flukes. The results of the re-evaluation indicated that the elastic elements in the body had the correct properties for near-maximum energy savings.

The properties of spring-like fibers may reside in locations other than in the tendons. Blubber is an elastic structure (Orton and Brodie, 1985; Pabst et al., 1995a). It is composed of compression-resistant adipose cells aligned in three dimensions by a weave of fibers. The blubber fibers of stiff

collagen and rubbery elastin are arranged in a crossed helical geometry (Pabst et al., 1995a; Pabst, 1996a, b; Toedt et al., 1997; Hamilton et al., 1998). The angle between the crossed fibers is greater than 60° (Pabst, 1996a, b). An angle of this magnitude is predicted to increase fiber strain during bending of the body (Alexander, 1987), returning the body to the stable straight position (Pabst, 1996a). There is variation in blubber compliance along the body that results from differences in the distribution and orientation of the structural fibers (Toedt et al., 1997). Fibers from the blubber of the peduncle attach directly to the vertebral column (Pabst et al., 1995a). Large strains near the anal region were measured for blubber from the peduncle, but low strains were recorded at the insertion of the flukes (Toedt et al., 1997).

Elastic elements occurring in isolated segments of the vertebral column of the dolphin, *Delphinus delphis*, exhibited resilience of 20 to 50% (Long et al., 1997). The region of greatest stiffness was at the tail base, the lumbo-caudal joint. Because of the high stiffness, the lumbo-caudal joint has the resistance to function as the insertion point for the powerful epaxial muscles. The joint at the fluke base is more flexible with lower stiffness, allowing control of attack angle with small muscular input throughout the stroke (Pabst, 1993; Long et al., 1997).

The posterior-most caudal vertebrae continue into the flukes and end immediately anterior to the fluke notch (Parry, 1949b; Rommel, 1990). Vertebrae anterior to the flukes are laterally compressed whereas vertebrae within the flukes are dorsoventrally compressed. The peduncle-fluke junction is characterized by relatively large intervertebral spacings (Rommel, 1990; Long et al., 1997). The intervertebral joint at the fluke base mechanically acts as a low-resistance hinge, acting as a center of rotation about the sagittal plane (Parry, 1949b; Long et al., 1997). In addition to the low stiffness of the joint, rotation is aided by the "ball" vertebrae (Watson and Fordyce, 1993). Located at the peduncle-fluke junction, the ball vertebrae have convex cranial and caudal surfaces. Fluke rotation is controlled by the epaxial *extensor caudae lateralis* muscle and the *hypaxial hypaxialis lumborum* muscle (Pabst, 1990).

Flukes are attached to the numerous, short caudal vertebrae and intervertebral discs by a thick core of collagen fibers (Felts, 1966). This attachment unites the caudal vertebrae associated with the flukes into a single resilient element. Within the fluke, the collagen fibers are arranged in horizontal, vertical, and oblique bundles (Felts, 1966; Purves, 1969). Horizontal fibers radiate out through the fluke. The fiber bundle pattern indicates an orientation appropriate for incurring high tensile stresses.

Overlying the fibrous core is a ligamentous layer in the flukes that is arranged to resist tension particularly at the trailing edge and tips (Felts, 1966). The ligamentous layer is thickest at the tips and inserts perpendicularly at the trailing edge. This architecture during the stroke cycle would limit bending that is variable between species. The harbor porpoise (*Phocoena phocoena*) displays almost no bending at either the fluke tips or the trailing edge whereas the white-sided dolphin (*Lagenorhynchus acutus*) with larger flukes shows 35 and 13% deflections across the chord (i.e., distance from leading to trailing edges) and tip-to-tip span, respectively (Curren *et al.*, 1994). Such differences in flexibility may reflect modification of the fibrous layers that could affect swimming performance. Flexibility across the chord can increase propulsive efficiency by 20% with a small decrease in thrust, compared to a rigid propulsor executing similar oscillations (Katz and Weihs, 1978).

8.2 UP AND DOWN PHASES

Whales use their axial muscles to propel themselves by vertical fluke oscillations (Parry, 1949a; Slijper, 1961; Strickler, 1980; Bello *et al.*, 1985). The fluke movement is exclusively up and down

with no indication of rotational or sculling actions (Parry, 1949a; Backhouse, 1960; Slijper, 1961). An exception is the blind river dolphin (*Platanista gangetica*) that swims on its side (Herald et al., 1969). Dolphins also were observed to side-swim when chasing fish in shallow water onto a beach*.

Flukes follow a sinusoidal pathway (figure 22) that is symmetrical about the longitudinal axis of the body and in time (Pyatetskiy and Kayan, 1975; Videler and Kamermans, 1985; Goforth, 1990; Fish, 1993b, 1998a). Previously, it was assumed that cetaceans swam with an asymmetrical propulsive stroke. This assumption was predicated on differences in the epaxial and hypaxial muscle masses (Parry, 1949b; Purves, 1963). Smith et al. (1976) found that the hypaxial muscles were smaller than the epaxial muscles in *Phocoena phocoena*, but the muscles were considered powerful enough to flex the tail during a downstroke. Parry (1949a) confirmed differences in stroke duration between upstroke and downstroke from counts of film frames of a dolphin swimming away from a camera (figure 23). Unfortunately, the film records of the swimming dolphin showed that the animal was giving birth at the time. This would have changed the normal swimming pattern. Subsequent reproductions of the swimming sequence excluded the tail flukes of the neonate (Slijper, 1961; Hertel, 1966).

Videler and Kamermans (1985) analyzed the swimming kinematics of dolphins swimming in an aquarium. Despite equal time periods for both upstrokes and downstrokes, they found that the downstroke generates more thrust than the upstroke and that drag increases during the upstroke. This may have been an artifact of the low swimming speeds ($\leq$ 3.17 m/s) exhibited. Fluke control does permit variable movements during upstrokes and downstrokes, so a stroke cycle can be divided into power and recovery phases and the animal can decelerate (Purves, 1963; Niiler and White, 1969). In addition, asymmetrical fluke motions can be observed during accelerations (figure 24).

Vertical oscillations have been depicted as confined to the posterior one-third of the body (Backhouse, 1960). However, the large moment generated about the center of gravity by the flukes produces a pitching moment in the anterior end (Lang and Daybell, 1963; Videler and Kamermans, 1985). The pitching oscillations of the rostrum are 1 to 7% of body length as measured from maximum and minimum vertical displacements (Peacock and Fish, unpublished data). Rostrum oscillations are small compared to fluke movements, despite the distance of the rostrum from the center of gravity (0.42 *BL*) being only slightly shorter than the distance from the center of gravity to the flukes (0.58 *BL*). The body does not act as a rigid beam. Control is exerted by the rigid skeletal framework in the body anterior and by muscular coordination. The pitching oscillations are nearly in phase so that the rostrum and flukes are pitched downward or upward simultaneously (Fish, unpubl. data). Oscillation control in the dolphin anterior reduces drag by maintaining a more streamlined profile with reduced frontal surface area. In addition, limiting oscillatory movements in the anterior end helps stabilize the sensory organs in the head. The coordination of movements at the head and tail indicate that the oscillatory swimming mode of dolphins was evolutionarily derived from spinal flexion associated with the rapid asymmetrical gaits (i.e., gallop, bound) used by terrestrial ancestors (Fish, 1996, 1998b; Thewissen and Fish, 1997).

* Fish, personal observation; C. Grubbins, personal communication.

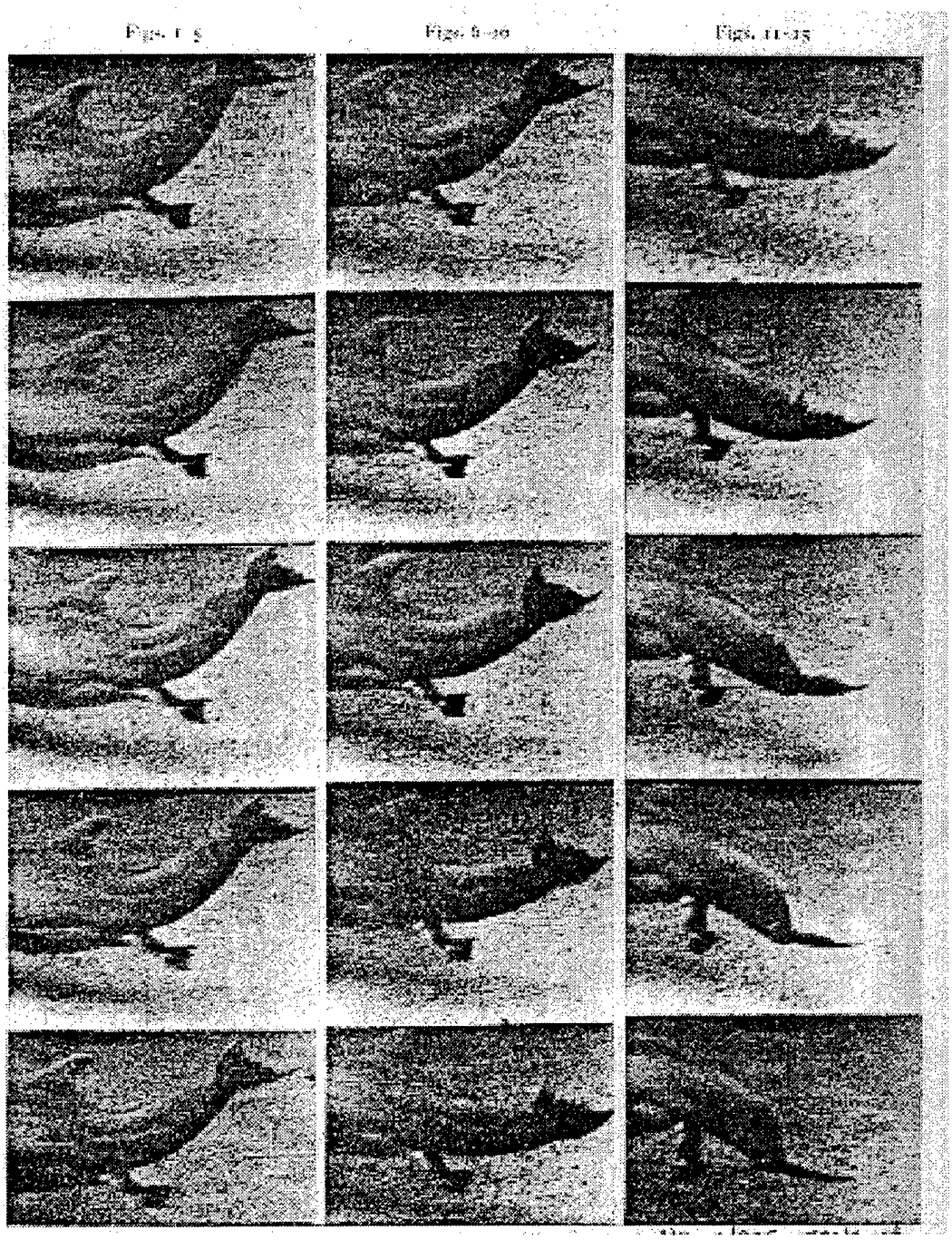

Figure 23. Cine' sequence of dolphin tail fluke motions from Parry (1949a); Company of Biologists Limited). Pictures are spaced evenly in time.

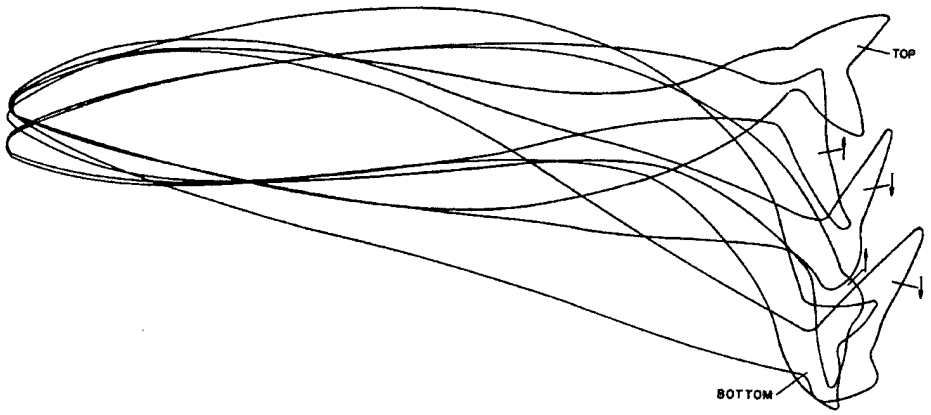

Figure 24. Dolphin movements during acceleration. Outlines are superimposed with horizontal position of rostrum fixed. Time intervals between pictures are not equal (from Lang and Daybell, 1963).

8.3 KINEMATIC PARAMETERS AND RELATION TO VELOCITY

8.3.1 FREQUENCY

The stroke frequency varies directly with swimming speed (figure 25; Pyatetskiy and Kayan, 1975; Kayan and Pyatetskiy, 1977; Kayan et al., 1978; Fish, 1993b, 1998a; Rohr et al., 1998b). Maximum frequency corresponds to tail beat frequency at maximum voluntary muscular effort for dolphins (Goforth, 1990). Maximum tail beat frequencies of approximately 3 Hz were exhibited by *Tursiops* and *Pseudorca* (Goforth, 1990; Fish, 1998a; Rohr et al., 1998b). Woodstock (1948) reported a lower tail beat frequency of 1.9 Hz at 5.15 m/s for dolphins swimming along the side of a ship. Differences in slope of tail beat frequency versus speed are dependent on body size (figure 25). For the linear relationship between tail beat frequency and length-specific swimming speed (*BL*/s), slope decreased with increasing body size (Fish, 1998a).

The positive linear relationship of frequency with swimming speed for cetaceans is consistent with observations of other marine mammals and fish that used hydrofoil propulsion (Webb, 1975; Feldkamp, 1987; Fish *et al.*, 1988). Frequency modulation with constant amplitude would prevent excessive body distortion, which would increase overall drag and decrease locomotor efficiency. This trend differs from semiaquatic paddlers that modulate amplitude and maintain a constant frequency to achieve higher swimming speeds (Fish, 1993a, 1996).

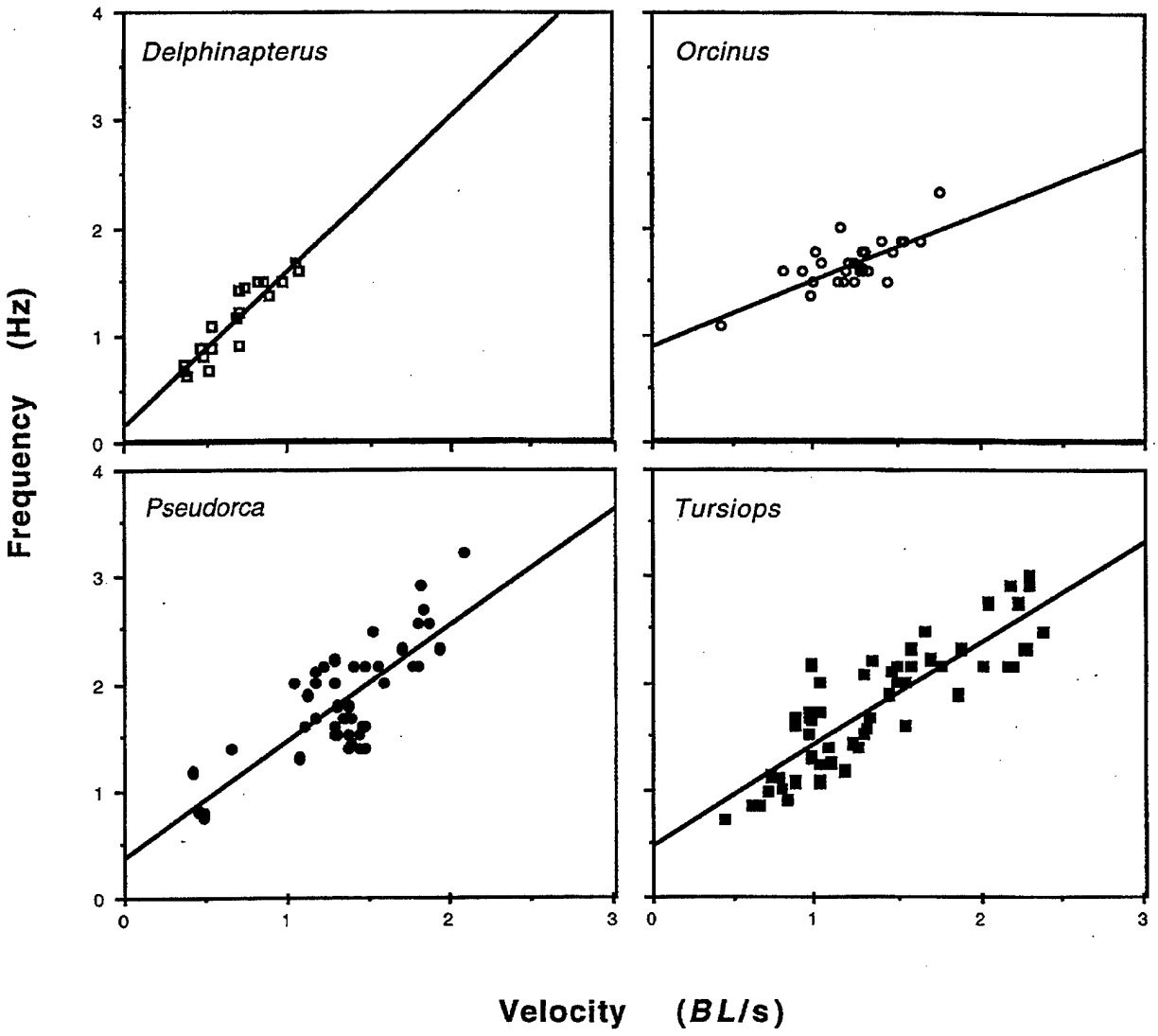

Figure 25. Tail-beat frequency, f (Hz) , as a function of length-specific swimming velocity (*BL*/s) for four species of odontocete cetaceans swimming steadily. Lines indicate statistically significant regressions (from Fish, 1998a).

8.3.2 Amplitude

Maximum heaving amplitude occurs at the fluke tips. At low swimming speeds (< 2.2 m/s for *Lagenorhynchus*), heave amplitude appears to increase with speed (Curren *et al.*, 1994). Heave amplitude (h), however, is independent of swimming speed at routine and sprint speeds (figure 26; Kayan and Pyatetskiy, 1977; Fish, 1993b; 1998a; Rohr et al., 1998b). Maximum peak-to-peak amplitude ($2h$) measured over a complete tail beat cycle remains a constant proportion of body length (approximately 20%). The exception is *Delphinapterus,* in which amplitude decreases with swimming speed.

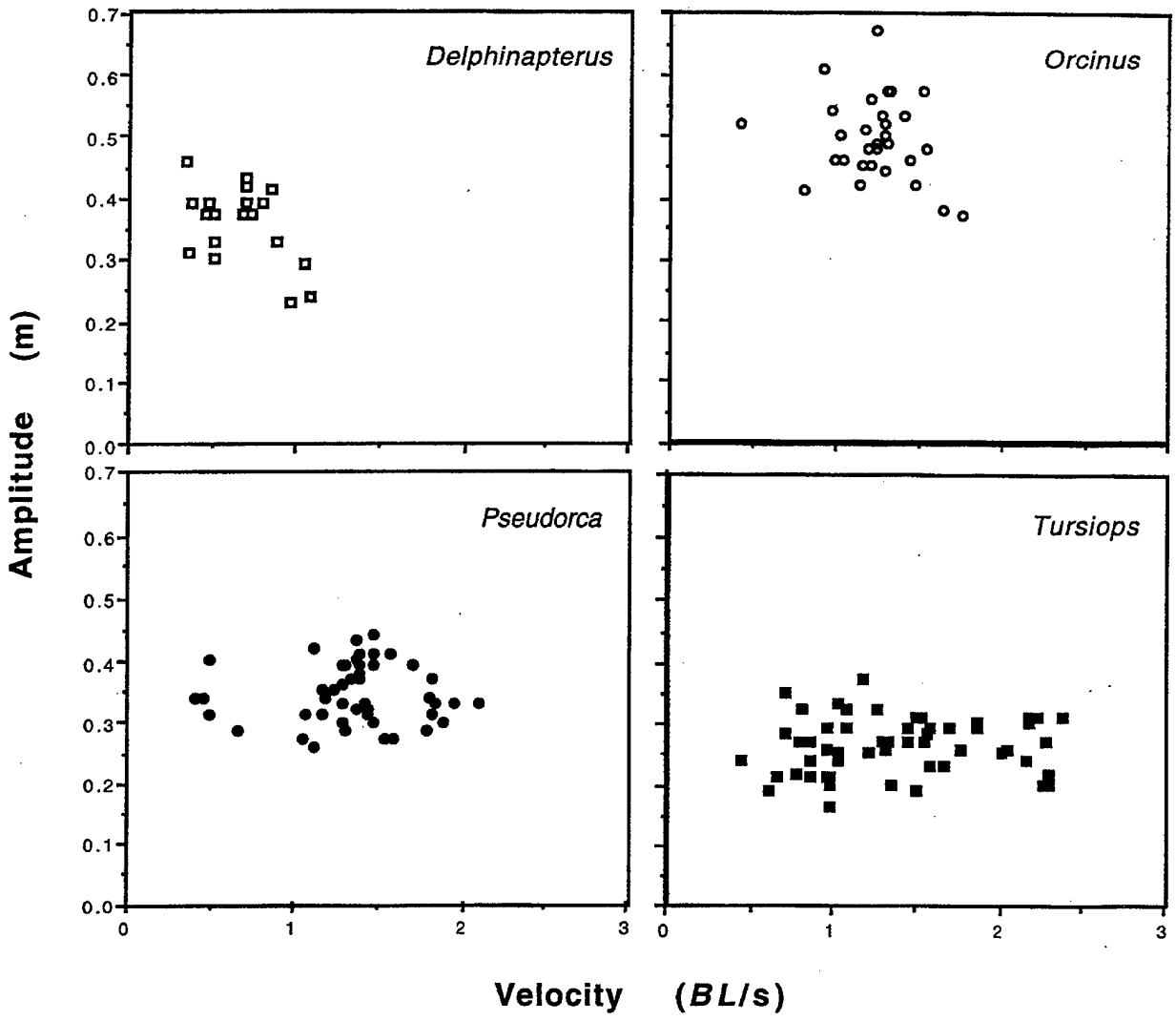

Figure 26. Relationship between the amplitude of heave, *h* (m), and length-specific swimming velocity (*BL*/s) (from Fish, 1998a).

8.3.3 PITCH AND ATTACK ANGLES

The fluke heaving and pitching motions result in a varying angle (pitch angle, α^*) between the flukes and the horizontal plane (figures 22 and 27). At its maximum vertical displacement, the flukes have a pitch angle of zero so that the axis of the fluke chord is parallel to the axis of progression (i.e., horizontal when the animal is swimming at constant depth). This orientation effectively minimizes the fluke drag, but generates no thrust. As the flukes are swept downward, the pitch angle increases by flexion at the peduncle-fluke junction. Through the middle of the downward stroke excursion, the pitch angle is at a maximum (figure 27). The end of the stroke is accompanied by a decrease in the pitch angle, with the flukes again oriented parallel to the direction of forward progression.

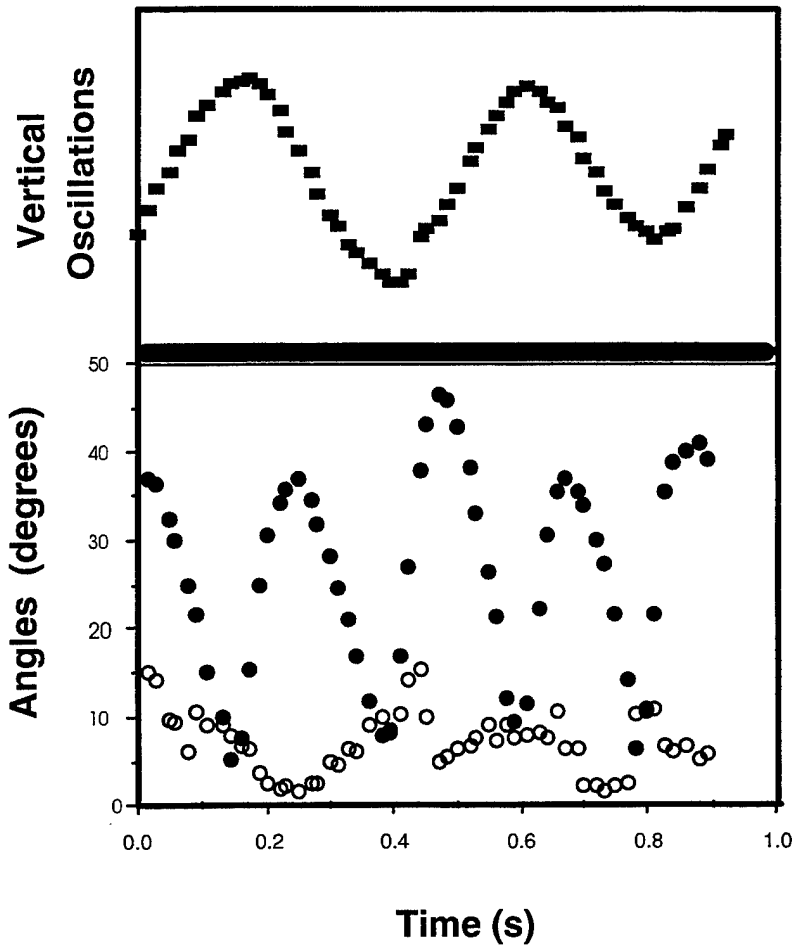

Figure 27. Relationship between heaving motions at fluke tips (filled squares), pitch angle (filled circles), and attack angle (open circles) for a *Tursiops truncatus* swimming at 4 m/s.

Pitch angle showed a linear decrease with increasing length-specific velocity for *Delphinapterus*, *Orcinus*, *Pseudorca*, and *Tursiops* (figure 28; Fish, 1998a). *Delphinapterus* exhibited the most rapid decrease in pitch angle whereas *Tursiops* showed the shallowest decrease. Maximum pitch angles ranged from 33 to 40°. The average pitch angle for the harbor porpoise (*Phocoena phocoena*) and white-sided dolphin (*Lagenorhynchus acutus*) was 34 and 33°, respectively (Curren *et al.*, 1994).

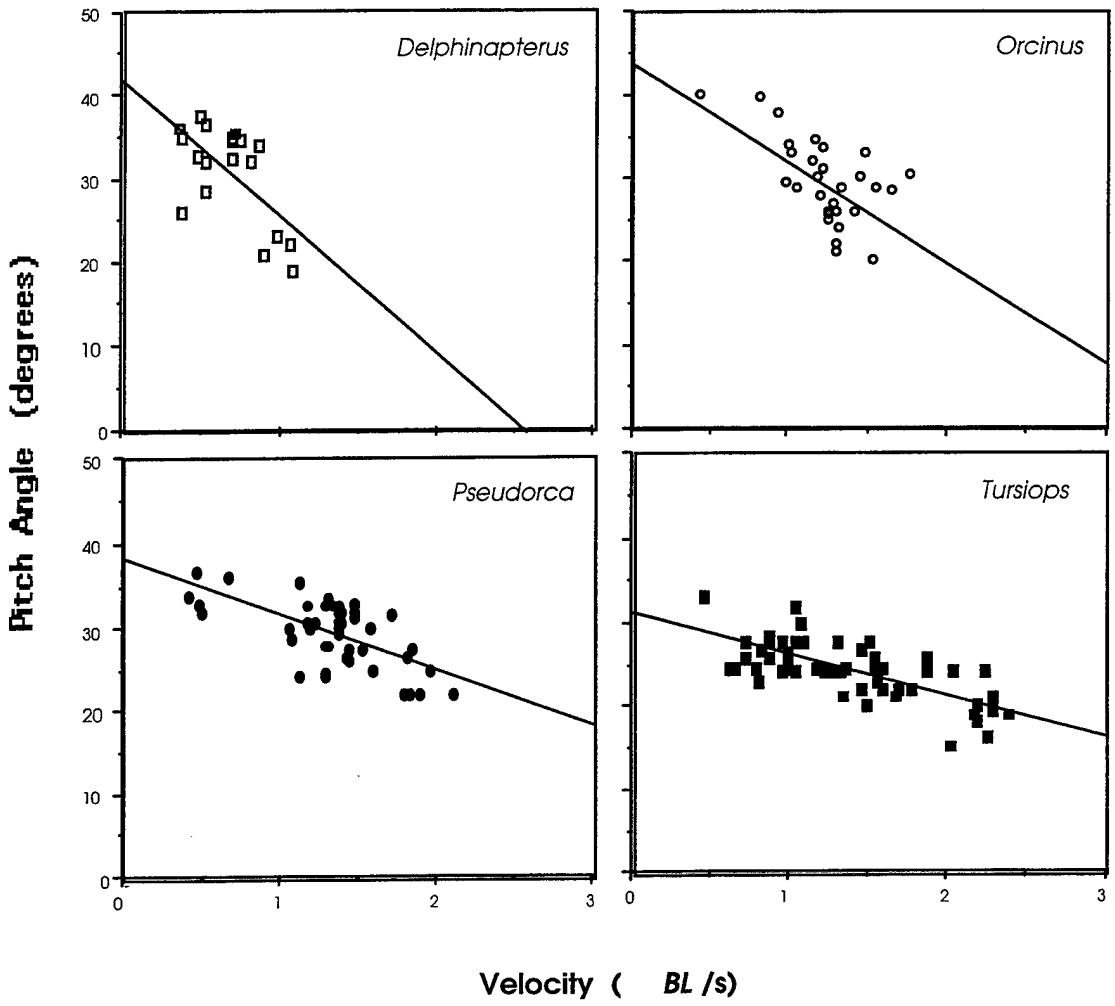

Figure 28. Relationship between maximum pitch angle and length-specific swimming velocity. Lines indicate statistically significant regressions (from Fish, 1998a).

The ability to rotate the flukes about a pitching axis allows for attack angle control. An attack angle is defined as the angle between the tangent of the fluke's path and the axis of the fluke's chord (figure 22; Fierstine and Walters, 1968; Fish, 1993b). Maintenance of a positive attack angle ensures thrust generation throughout most of the stroke cycle (Lang and Daybell, 1963; Lighthill, 1969, 1970; Videler and Kamermans, 1985; Goforth, 1990).

The magnitude of the attack angle will affect the propulsive efficiency and the thrust generated in lift-based swimming (Webb, 1975). As attack angle is increased for a hydrofoil, there is increase in both lift and drag. Lift will increase faster than the drag with increasing attack angle up to a critical level. Further increase of attack angle leads to an increase in drag and precipitous loss of lift in a condition called stall. Stall is caused by separation of the flow from the foil surface, which is unavoidable above the critical attack angle.

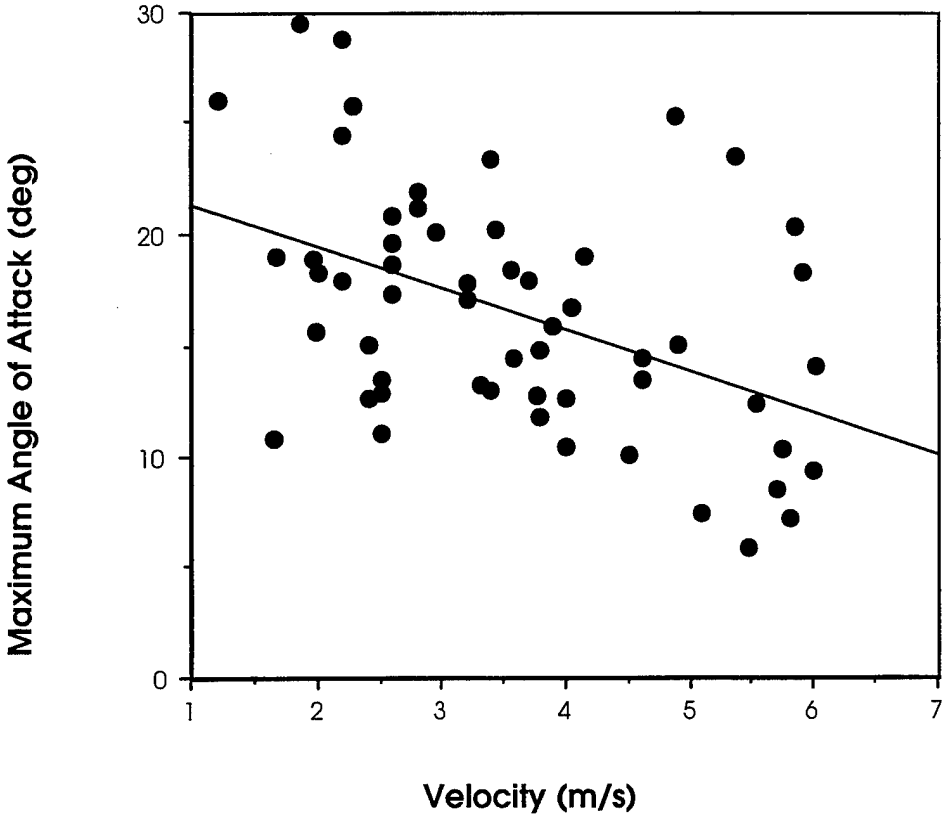

Figure 29. Plot of relationship between maximum attack angle and swimming velocity for *Tursiops truncatus*. The line indicates a statistically significant regression (from Fish, 1993b).

The attack angle of oscillating dolphin flukes increases rapidly at the initiation of upstrokes and downstrokes, reaching a maximum within the first third of the stroke (figure 27; Fish, 1993b). Maximum angle of attack varies indirectly with swimming speed in *Tursiops truncatus* (figure 29; Fish, 1993b). Mean values range from 4.6 to 17.5° for *Tursiops*, although maximum values approach 30° at low velocities (Fish, 1993b). The maximum attack angle is 22.5 to 24° for *Lagenorhynchus* (Lang and Daybell, 1963).

The attack angles observed for dolphins are higher than would be expected compared to non-oscillating airfoils and hydrofoils. Conventional airfoils stall at low attack angles in steady flow (typically, around 15°). An oscillating hydrofoil appears to perform more efficiently at higher attack angles than non-oscillating hydrofoils (Fierstine and Walters, 1968; Maresca et al., 1979). At high reduced frequencies (see section 9.1, equation (7)), the coefficient of lift of an oscillating foil will increase with increased attack angle above the angle for static stall (Maresca et al., 1979). The attack angle between 15 and 25° provided optimal thrust production for a two-dimensional oscillating foil (Anderson et al., 1998). Hydrofoils similar to the dolphin flukes can sustain lift without stalling at an

attack angle of 30° (Triantafyllou and Triantafyllou, 1995). This value may represent an upper limit to attack angle for an oscillating system above which thrust and efficiency are reduced (Chopra, 1976).

An oscillating foil can function at high attack angles because of dynamic stall or delayed stall caused by unsteady effects (Maresca et al., 1979; Ellington et al., 1996; Anderson, et al., 1998). If attack angle is increased rapidly or if a foil is accelerated with a high attack angle, the foil can travel several chord lengths before the separation associated with stall develops (Ellington, 1995). Before the onset of stall, higher lift will be generated than for a foil in steady flow. High lift and high efficiency are associated with the formation of a leading-edge vortex (McCroskey, 1982; Ohmi et al., 1990; Triantafyllou et al., 1996; Anderson et al., 1998; Dickinson et al., 1999). The leading-edge vortex augments lift by enhancing the circulation around the foil. Circulation is the difference between velocities above and below the foil. Enhanced circulation produces an increased pressure difference between the surfaces of the foil resulting in increased lift and thrust. This mechanism is not without a cost as enhanced drag accompanies the increased lift (McCroskey, 1982).

Another unsteady mechanism for enhanced lift and thrust production is wake capture (Dickinson et al., 1999). In this case, the flukes would benefit from the shed vorticity of the previous stroke. The flow induced at the end of one stroke increases the water's velocity at the beginning of the next stroke, thereby increasing both lift and thrust that are directly proportional to the square of the velocity. Orientation of the force vectors is dependent on the the phase relationship between rotation and translation (Dickinson et al., 1999). The fluke rotation proceeding stroke reversal (figures 22 and 27) permits the flukes to intercept their wake to generate positive lift. In addition, fluke rotation can augment the circulation to generate lift (Dickinson et al., 1999).

Vortical flow control by the dynamic stall mechanism may increase thrust production for dolphin flukes. Within the range of reduced frequencies for dolphins (Fish, 1993b, 1998a), the average lift caused by unsteady effects is 2 to 3.2 times higher than steady lift (Maresca et al., 1979). The high angles of attack achieved by dolphins would promote the formation of a leading-edge vortex, particularly at the initiation of a stroke.

9. THRUST PRODUCTION AND EFFICIENCY

9.1 HYDROMECHANICAL MODELS

Gray (1936) modeled the swimming dolphin as a flat plate according to the equation for drag (equation (3); see section 6.1, METHODS). This simple model grossly underestimated the dolphin thrust production of the dolphin, because (1) laminar boundary conditions were assumed, lowering C_D by 88% compared to turbulent conditions, (2) the contours and three-dimensional design of the dolphin were not considered, and (3) no consideration was given to increased drag from waves, propulsive motions, and flow modifications.

Following the resistance model used by Gray (1936), Kermack (1948) estimated the power output for the blue whale (*Balaenoptera musculus*) and the fin whale (*Balaenoptera physalus).* Assuming a swimming speed of 12.9 m/s (25 kts) with laminar and turbulent flows, thrust was calculated as 206 kN and 3864 kN for the fin whale and 259 kN and 5285 kN for the blue whale, respectively.

Because the flukes are connected to the body by a narrow attachment, the caudal peduncle, which oscillates in the direction of its minimum resistance, the flukes are essentially separated from the body (Lighthill, 1969, 1970; Fish et al., 1988; Fish and Hui, 1991; Fish, 1993b, 1998a). This allows for analysis of thrust production by the flukes to be made separate of the body and its actions, and the drag produced.

Parry (1949a) developed a quasi-static resistance model based on fluke motion. He showed schematically how thrust was generated as a resultant of a hydrodynamically derived force (figure 30). Parry (1949a) applied the theory of quasi-static flow around an oscillating aerofoil from von Holse and Kuchemann (1942). Parry developed a general equation to calculate the thrust generated by a dolphin as:

$$\text{Thrust} = 0.0175\, BL^2\, U^2\, [\, (0.38\, BL\, f/U) - 0.047\,], \qquad (6)$$

where BL is body length in cm, U is velocity in cm/s, and f is tail-beat frequency in Hz, and thrust is in units of erg/s.

Kayan (1979) used a quasi-steady approach based on the lift and drag characteristics of isolated flukes for *Tursiops*. Based on a swept wing planform with a NACA 0018 profile, the lift and drag coefficients were determined for various attack angles. These coefficients were applied to force calculations and correlated with the motion and position of the flukes at discrete times and integrated over the entire stroke cycle. Results indicate low thrust production so that drag coefficients were in the intermediate range between values of laminar and turbulent boundary flow.

Although Kayan (1979) considered the values from his model to represent maxima, the results may be underestimates caused by the assumptions of the quasi-steady approach. This approach assumes that the forces acting on the flukes at any instant are the same as those acting under equivalent steady-state conditions of velocity and attack angle (Webb, 1975). Quasi-steady estimates are not directly translated to thrust production because of the unsteady oscillatory fluke motions. Videler and Kamermans (1985) were unable to reconcile inertial forces, necessary to accelerate the body and entrained fluid, that were five-fold larger than the propulsive forces calculated with a quasi-steady model. In cases where $Re > 10^3$, there are large inertial effects (Lighthill, 1970; Webb, 1975). Acceleration reactions, associated with imparting momentum to the water, become more important and

increase power output (Daniel, 1984; Daniel et al., 1992). Unsteady effects may contribute to thrust production by increasing the relative velocity and, thus, the lift (Daniel *et al.*, 1992).

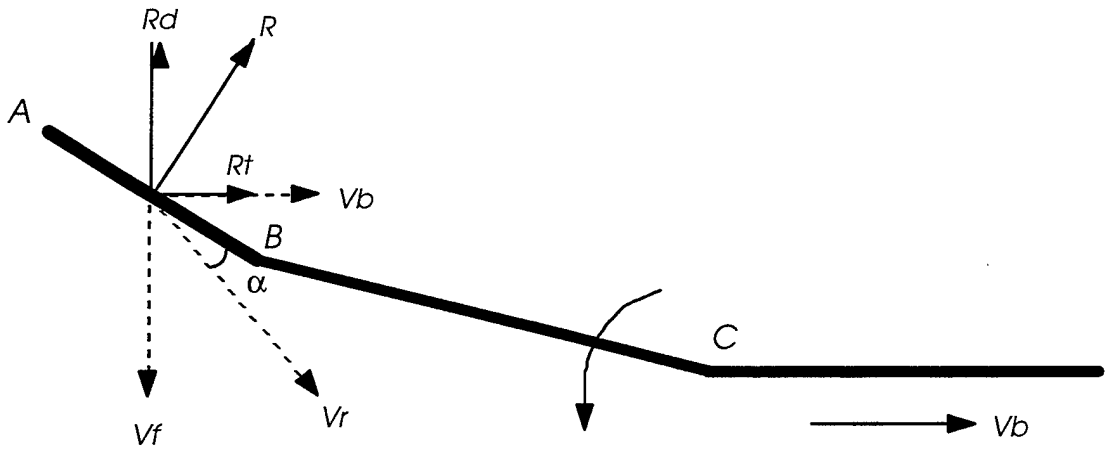

Figure 30. Schematic of velocities and forces associated with motion of dolphin flukes redrawn from Parry (1949a). Body segments are indicated as AB for the flukes and BC for the tail, which is being swept downward. The whole system is moving forward with a velocity, *Vb*. As the flukes are moving downward with a velocity, *Vf*, the true velocity of the flukes is *Vr*. *R* is the resultant force of water on the fluke, which is resolved into fluke drag, *Rd*, and dolphin thrust, *Rt*. Angle of attack is indicated by α.

An additional limitation of the quasi-steady approach is its reliance on the lift characteristics of conventional foil sections in steady flows. Foils similar to whale flukes under steady flow conditions stall at attack angles over 20° (Abbott and von Doenhoff, 1959). However, an oscillating high aspect ratio fin can continue to generate lift, and thus, thrust, up to an attack angle of 30° (Triantafyllou and Triantafyllou, 1995). Therefore, measurements and calculations of lift and drag performance by static hydrofoils and wings permit only a rudimentary understanding of the development of thrust by oscillating flukes.

To comprehend the dynamic production of lift-based thrust from high aspect ratio lunate tails, Lighthill (1969, 1970) suggested the use of unsteady lifting-line theory. Subsequent unsteady hydromechanical models were developed that were based on differing assumptions and techniques (Wu, 1971b; Chopra, 1974, 1975, 1976; Chopra and Kambe, 1977; Lan, 1979; Yates, 1983; Cheng and Murillo, 1984; Rayner, 1985; Ahmadi and Widnall, 1986; Bose and Lien, 1989; Karpouzian et al., 1990; Triantafyllou et al., 1991; Liu and Bose, 1993; Blickhan and Cheng, 1994). Lighthill (1969, 1970), Wu (1971a, b), and Chopra (1976) used a two-dimensional approach that probably overestimates thrust production and efficiency because of higher energy losses to the wake for finite wings. Two-dimensional theory only accounts for energy of the cross-section of the wake vorticity (perpendicular to the direction of motion) and does not account for trailing vorticity parallel to the direction of motion (Lighthill, 1969, 1970; Blake, 1983b). Bose and Lien (1989) analyzed the propulsion of a fin whale (*Balaenoptera physalus*) with Lighthill's two-dimensional oscillating foil, but applied the results of Chopra (1976) and Chopra and Kambe (1977) on three-dimensional oscillating foils as a correction.

Numerical calculations of thrust and propulsive efficiency of oscillating rigid flat plates as a three-dimensional lunate-tail model were made by Chopra and Kambe (1977) for a series of swept planforms and by Lan (1979) and Liu and Bose (1993) using an quasi-vortex lattice method. The latter method was considered superior because it could be applied to arbitrary planforms and reliably predicted leading-edge suction (Liu and Bose, 1993). Lan (1979) found a 20% lower thrust than Chopra and Kambe (1977) although the predicted efficiency is in good agreement (Yates, 1983). Analysis by Ahmadi and Widnall (1986) examined various combinations of kinematic parameters to look for optimal solutions to maximize efficiency. Large amplitude motions of the propulsor were correlated with enhanced values of thrust and efficiency. The effects on thrust and efficiency caused by chordwise flexibility were treated by Katz and Weihs (1978).

The basis for thrust production is that, as the flukes oscillate, they are pitched at a positive attack angle to the oncoming flow (figure 22). The attack angle and fluke velocity are determined by the vertical velocity of the flukes and horizontal velocity of the body (figure 30). The streamlines of fluid are deflected above and below the flukes, imparting a higher velocity to the upper flow. By the Bernoulli theorem, a pressure difference results with a lower pressure on the dorsal aspect of the flukes. The net pressure produces a pressure force that is resolved into the drag tangent to the axis of the motion of the flukes, and a lift perpendicular to the axis of motion (figure 22; Webb, 1975). The center of lift is relatively near the leading edge at or anterior to the maximum thickness (Vogel, 1994). The pressure force is reversed on the upstroke relative to the downstroke.

The fluke orientation throughout the stroke produces lift directed forward and upward during the downstroke and forward and downward during the upstroke. The anteriorly directed component from the mean forward tilt of lift represents the thrust (Daniel *et al.*, 1992). Thrust from lift increases directly with increases in attack angle. However, low attack angles increase hydrodynamic efficiency while reducing the probability of stalling and decreasing thrust production (Chopra, 1976). Dolphins must then strike a balance between the competing trends of thrust and efficiency by regulating the various kinematic parameters to optimize swimming performance.

Lift also depends on the frequency of fluke oscillation. Thrust increases with frequency whereas efficiency decreases (Daniel, 1991). The reciprocating action of the flukes means that the flow pattern is reversed through the stroke, and since the water has inertia, the flow pattern will take time to redevelop, potentially affecting performance (Wu, 1971b; Daniel, 1991; Daniel *et al.*, 1992). The importance of the oscillatory motion to thrust generation and efficiency is determined by the reduced frequency parameter that is the ratio of oscillatory to forward motion (Daniel *et al.*, 1992). A dimensionless frequency, the reduced frequency, σ, is calculated as:

$$\sigma = \omega RC / U, \tag{7}$$

where ω is the radian frequency equal to $2\pi f$, RC is the root chord, and U is the velocity of the animal (Yates, 1983).

A reduced frequency less than 0.1 indicates nearly steady motion (Yates, 1983; Daniel, *et al.*, 1992). High values of reduced frequency indicate the dominance of unsteady effects that incur lower lift than steady motion (Lighthill, 1970). Reduced frequencies of 0.88 to 0.99 for *Delphinapterus*, 0.4 for *Lagenorhynchus*, 0.59 to 1.41 for *Orcinus*, 0.54 to 0.83 for *Pseudorca*, and 0.51 to 1.15 for *Tursiops* were reported by Fish (figure 31; 1993b, 1998a) and Webb (1975), indicating the dominance of unsteady effects.

As thrust from lift is produced, momentum is transferred from the flukes to the water. The momentum is proportional to the affected water mass and fluke velocity. The water is pushed back in

a direction opposite to the swimming direction with a net rate of change of momentum that according to Newton's third law is equal and opposite to the thrust (Wu, 1971a; Chopra, 1975; Videler, 1993). The thrust must balance the viscous and pressure drag of the body and flukes, and wave drag if the animal is near the surface.

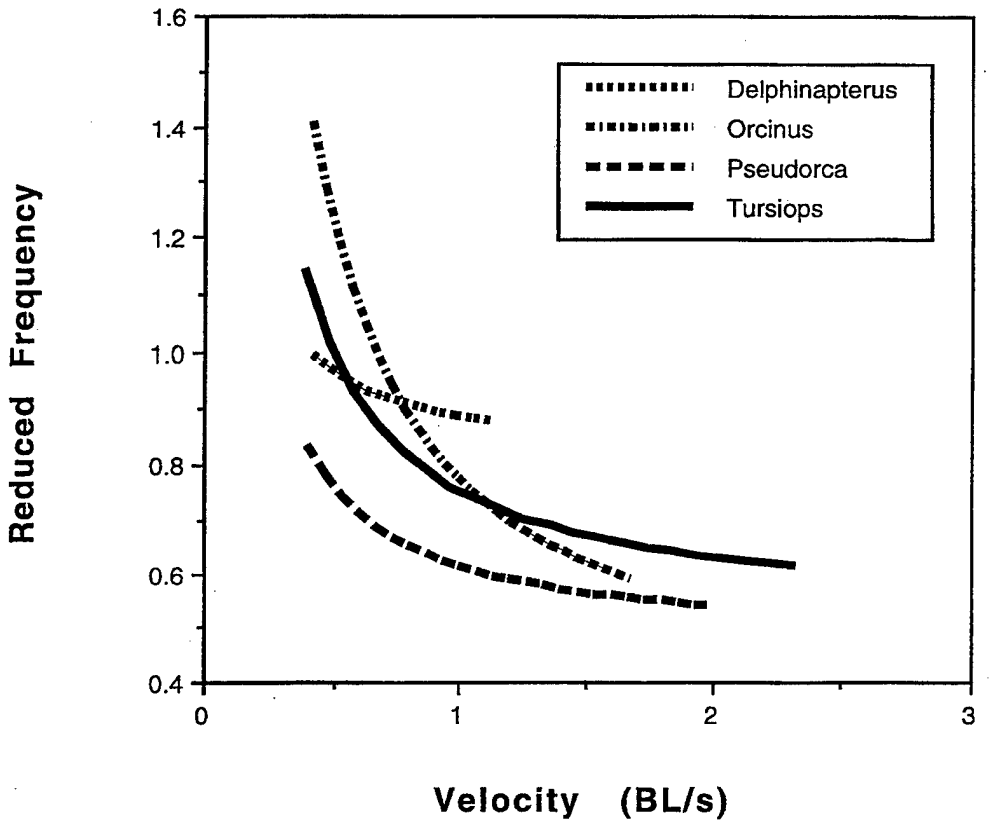

Figure 31. Reduced frequency, σ, plotted as a function of length-specific swimming velocity (*BL* /s) (from data presented in Fish,1998a).

The momentum imparted to the fluid is concentrated in a jet of fluid directed on average opposite to the swimming direction (Wu, 1971a; Rayner, 1985; Videler, 1993; Anderson et al., 1998). Thrust is derived from the reaction of the jet stream. The jet induces the resting water around it to generate a vortex wake. A wake is necessary to produce thrust. The wake is visualized as a trail of connected alternating clockwise and anti-clockwise vortex rings with the jet directed through the center of the rings (figure 32). The rotation of the vortices is opposite to the Karman street behind stationary objects in a flow that creates drag (Weihs, 1972). This vortex pattern is generated at the bottom and top of the stroke as vortices shed from the flukes with opposite circulation (Vogel, 1994). Tip vortices that roll off the fluke tips connect the shed vortices to form the ring.

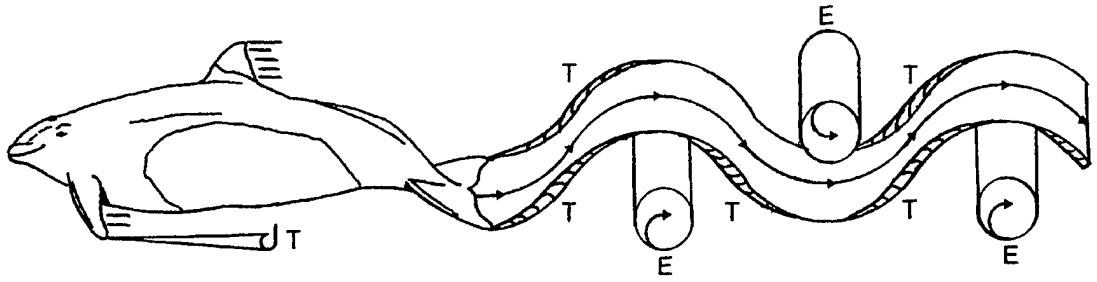

Figure 32. Pattern of vorticity shed in wake of a dolphin. Tip vortices (T) generated from flippers and flukes and trailing edge vortices (E) generated from flukes are shown (from Fish, 1993a).

If thrust is to be generated efficiently, the energy lost into the wake must be minimized (Blake, 1983b). The energy loss to the vortex wake can be minimized by partially feathering the flukes (Blake, 1983b). The proportional feathering parameter (θ) is the ratio of the maximum α^* (figure 22) to the maximum angle ($\omega h / U$) achieved by the trajectory of the pitching axis of the flukes (Yates, 1983) and is:

$$\theta = \alpha^* \ U \ / \ \omega h, \tag{8}$$

where ω is the radian frequency equal to $2\pi f$ (Yates, 1983). At $\theta = 1$, the motion of the flukes is pure heaving. In this case, the flukes are oriented parallel to the dolphin's direction of forward movement. At $\theta = 0$, the fluke is perfectly feathered and the fluke chord is tangential to the trajectory of the pitching axis so that attack angle is zero (Lighthill, 1969; Yates, 1983).

In a comparative study of cetacean kinematics (Fish, 1998a), values of θ increased with increasing swimming speed, reaching maxima between 0.7 and 1.4 *BL*/s before decreasing (figure 33). *Pseudorca* had the highest maximum θ of approximately 0.67 and *Tursiops* had the lowest value of 0.37.

In addition to lift, leading-edge suction contributes to thrust (Lighthill, 1970; Chopra and Kambe, 1977; Ahmadi and Widnall, 1986). A suction is created as the flow becomes highly accelerated as it moves around a sharp corner (Yates, 1983). The high acceleration locally decreases the pressure and produces the suction. At the trailing edge where vorticity is shed, flow around the edge is precluded because it would require infinite velocity that is physically impossible (Videler, 1993; Vogel, 1994). This represents the Kutta condition. The rounded leading edge promotes the suction force (Lighthill, 1970; Wu, 1971b). The effect of leading edge suction is to tilt the pressure force forward by an angle equal to the attack angle (Weihs, pers. comm.). The total lift force, which is typically normal to the fluke axis, is tilted perpendicular to the direction of fluke motion and, thus, increases the thrust component. However, excessive leading-edge suction could induce stalling caused by boundary layer separation and, thus, reduce thrust. The lunate configuration of the leading fluke edge reduces leading-edge suction without a decrease in total thrust (Chopra and Kambe, 1977; van Dam, 1987).

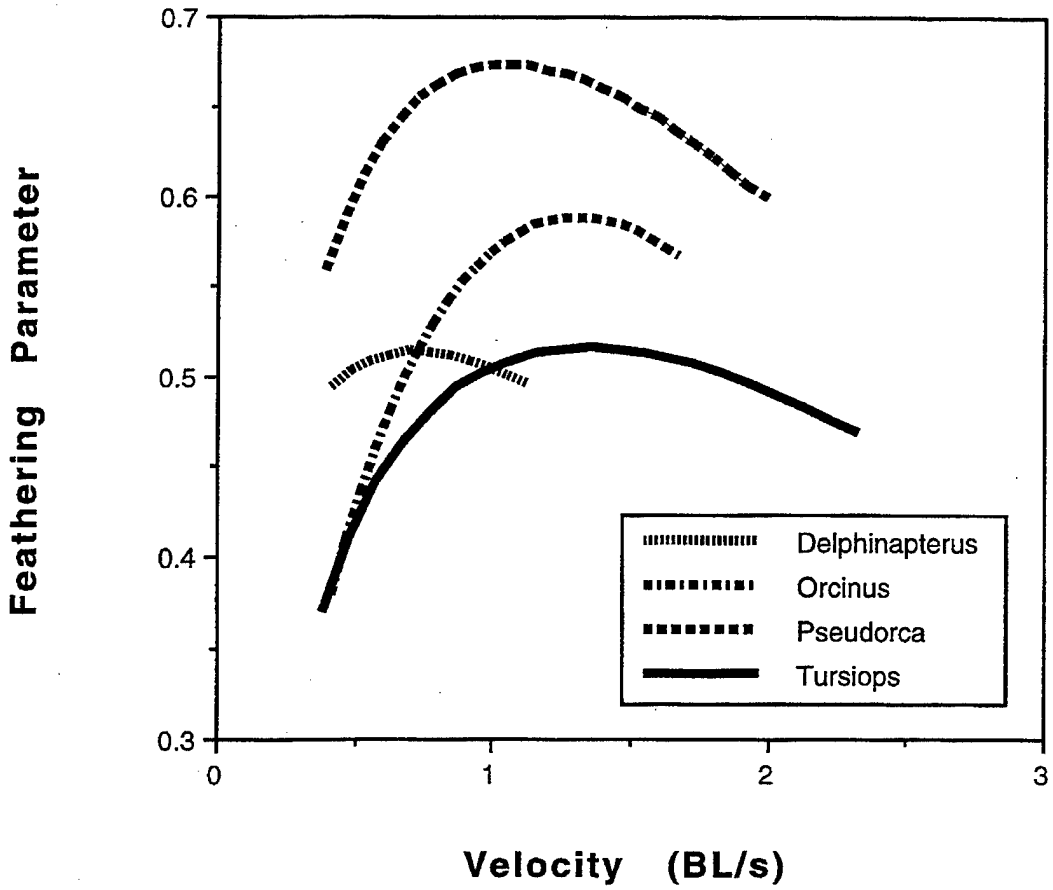

Figure 33. Feathering parameter, θ, plotted as a function of length-specific swimming velocity (*BL*/s) (from data presented in Fish,1998a).

When θ = 0, no water is accelerated posteriorly and all thrust is derived from leading-edge suction (Magnuson, 1978). In this case, the flukes have a high coefficient of thrust, but the hydrodynamic efficiency is low. Conditions that optimize combinations of lift, leading-edge suction, and efficiency occur with proportional feathering between 0.6 and 0.8 (Lighthill, 1969).

The hydromechanical model of lunate-tail propulsion based on three-dimensional unsteady wing theory with continuous loading (planform B2: Chopra and Kambe, 1977; Yates, 1983) has been used to calculate thrust power output (P_T) and Froude (propulsive) efficiency (η) for a variety of cetaceans (Fish, 1993b, 1998a). Froude efficiency, henceforth referred to as the efficiency, η, is defined as the mean rate of mechanical work derived from mean thrust divided by the mean rate of all work that the animal is performing while swimming (Chopra and Kambe, 1977). This model theory gives good accuracy for low aspect ratio ($AR < 6$) conditions (Yates, 1983; Liu and Bose, 1993). However, P_T may be an overestimate caused by possible interference effects of the peduncle (Chopra and Kambe, 1977).

In the model, the relationship between reduced frequency (σ) and proportional feathering parameter (θ) determines the coefficient of thrust (C_T) and η (Lighthill, 1969; Chopra and Kambe, 1977). The mean thrust power output (P_T) is given by:

$$P_T = 0.5\,\rho\,C_T\,U^3\,A\,(h/RC)^2 \qquad (9)$$

where ρ is the density of sea water and A is the fluke planform area. For a body moving at constant U, P_T is equal to the power output expended in overcoming drag, and the dimensionless drag coefficient (C_D) is calculated as:

$$C_D = P_T / 0.5\,\rho\, S_W U^2, \tag{10}$$

where S_W is the wetted surface area of the body.

9.2 THRUST AND POWER ESTIMATES

Table 3 summarizes estimates of thrust power based on different models for various species. To compensate for differences because of size, the thrust power was also divided by body mass. Particular errors are associated with each method based on the assumptions used. The drag-based model of Gray (1936) is highly dependent on the flow conditions of the boundary layer whereas unsteady lifting theory models consider the flukes to be stiff and possess an idealized planform. Swimming was assumed to be rectilinear with the exception of Hui (1987), who examined dolphins swimming in small circular pools. Hui (1987) introduced a correction factor of 4.77 to 5.24 for the added centripetal energy required for turning. Several estimates of dolphin thrust power were performed using kinematic data from Lang and Daybell (1963) for a single *Lagenorhynchus* (Webb, 1975; Chopra and Kambe, 1977; Yates, 1983). Results were determined from an acceleration model (Lang and Daybell., 1963), quasi-steady model (Parry, 1949a; Webb, 1975), and unsteady lifting wing model (Lighthill, 1969; Webb, 1975; Yates, 1983). The lack of consistency between results reflects differences in the models. However, there would have been potential errors in the calculation of thrust and efficiency caused by the unsteady nature of the swimming motions because the dolphin was accelerating in some instances.

Gray's (1936) original thrust power calculations (1939 W) for a dolphin with turbulent conditions provided a mass-specific thrust power of 21.4 W/kg. At the time, this value was believed to be too high for the dolphin based on muscle power output. However, data from table 3 show that the thrust power calculated by Gray (1936) agrees with studies using various approaches and models. Indeed, mass-specific power in humans for a 0.5-second period is 57.5 W/kg (Lang and Daybell, 1963). Even with a fully turbulent boundary layer, the dolphin can produce enough power to overcome the drag. Based on their model using unsteady lifting wing theory, Chopra and Kambe (1977) concluded the flow around the dolphin was like a turbulent flow over a smooth surface.

Table 3. Thrust power estimates.

Species	Mass (kg)	U (m/s)	Model*	Thrust Power (W)	Mass-Specific Thrust Power (W/kg)	Reference
Balaenoptera musculus	N/A	12.9	D	398949.5	NA	Kermack (1948)
Balaenoptera physalus	N/A	12.9	D	291568.7	NA	Kermack (1948)
Balaenoptera physalus	27000	12.0	US	208800	7.3	Bose and Lien (1989)

Table 3. Thrust power estimates. (continued)

Species	Mass (kg)	U (m/s)	Model*	Thrust Power (W)	Mass-Specific Thrust Power (W/kg)	Reference
Delphinus bairdi		4.3	QS	896	NA	Webb (1975)
Delphinus delphis	90.7	10.1	D	1938.8	21.4	Gray (1936)
Delphinus delphis	59.2	2.4	D	190.8	3.2	Hui (1987)
Delphinus delphis	54.7	2.1	D	122.1	2.2	Hui (1987)
Delphinapterus leucas	664.2	4.0	US	3436	5.2	Fish (1998a)
Lagenorhynchus obliquidens	91.0	4.6	A	1568.0	17.2	Lang and Daybell (1963)
Lagenorhynchus obliquidens	91.0	5.5	QS	6180	67.9	Webb (1975)
Lagenorhynchus obliquidens	91.0	5.5	US	4030	44.3	Webb (1975)
Lagenorhynchus obliquidens	91.0	5.2	US	1223.7	13.4	Yates (1983)
Phocoena sp.	24.0	7.6	D	447.4	18.6	Gray (1936)
Phocoenoides dalli		4.3	QS	1180	NA	Webb (1975)
Orcinus orca	1645.4	8.0	US	36259.6	22.0	Fish (1998a)
Pseudorca crassidens	535.8	7.5	US	12065.7	22.5	Fish (1998a)
Stenella attenuata	52.7	11.1	A	4517.8	85.7	Lang and Pryor (1966)
Sotalia guianensis	85	2.4	A	48.4	0.6	Videler and Kamermans (1985)
Tursiops truncatus	232.0	2.0	A	155.5	0.7	Videler and Kamermans (1985)
Tursiops truncatus	214.9	6.0	US	5090.9	23.7	Fish (1998a)

* Models: A - acceleration (Lang and Daybell, 1963); D - drag-based (Gray, 1936); QS - quasi-steady (Parry, 1949a); US - unsteady lifting surface (Lighthill, 1969; Chopra and Kambe, 1977); NA - Not available.

The quasi-steady model appears to give higher values of thrust power compared to other models over a similar range of swimming speeds (table 3). Webb (1975) applied the model developed by Parry (1949a; equation (6)) to data from Norris and Prescott (1961) and Lang and Daybell (1963) for *Delphinus bairdi*, *Phocoenoides dalli*, and *Lagenorhynchus obliquidens* swimming at 4.3, 4.3, and 5.54 m/s, respectively. By multiplying the thrust by U, the thrust power was determined. The thrust power developed was 896, 1800, and 6180 W for *Delphinus*, *Phocoenoides*, and *Lagenorhynchus*, respectively. When these values were compared to the theoretical frictional drag power based on a flat plate with turbulent boundary conditions, the thrust power of the cetaceans was 6.3 to 16.0 times greater. Webb (1975) considered that the high thrust power values could have resulted from increased drag from swimming near the water surface. Drag can increase by up to five times the frictional drag when swimming near the surface (Hertel, 1966; see section 10.1. PORPOISING).

Lang and Pryor (1966) explored maximal performance for an accelerating *Stenella attenuata*. At a maximum speed of 11.1 m/s, thrust power was 4517.8 W with a mass-specific thrust power of 85.7 W/kg. This high power output could only be maintained for a 1.5-s acceleration. Although the dolphin maintained speed, its power output decreased below the maximum power by 30% after the acceleration.

Fish (1998a) found that thrust power, P_T, was highly dependent on swimming velocity and size (figure 34). Based on unsteady lifting wing theory (Chopra and Kambe, 1977), the calculated P_T showed a curvilinear increase with increasing U/BL for the four species examined. P_T was found to be mass dependent. *Orcinus* had the highest P_T of 36.3 kW at U of 8 m/s. This represented a mass-specific power output of 22.0 W/kg. *Pseudorca* and *Tursiops* had maximum mass-specific power outputs of 22.5 and 23.7 W/kg, respectively. Although *Delphinapterus* had higher values of P_T compared to *Pseudorca* and *Tursiops* over equivalent swimming speeds, higher maximum P_T values were reached by the latter two species as they swam at higher speeds. Maximum P_T for *Delphinapterus* was 3.4 kW with a mass-specific power output of 5.2 W/kg.

Direct measurement of thrust for locomoting dolphins has not been accomplished. Goforth (1990) developed a technique in which dolphins (*Tursiops truncatus*) were trained to push against a load cell to measure the force generated by the animal's swimming actions. Because the water acting on by the flukes did not have an initial velocity during these static experiments, the force measured from the load cell could not be regarded equivalent to the thrust generated during forward progression. However, this type of experiment was used for physiological studies of maximum force production (Goforth, 1990) and metabolic correlates (i.e., oxygen consumption, heart rate, lactic acid production) with exercise (Williams et al., 1993a). Dolphins produce maximum forces during static swimming of 1.08 to 1.56 times body weight and forces of 0.3 to 0.6 times body weight at maximum oxygen consumption with minimum lactate production (Goforth, 1990; Williams et al., 1993a).

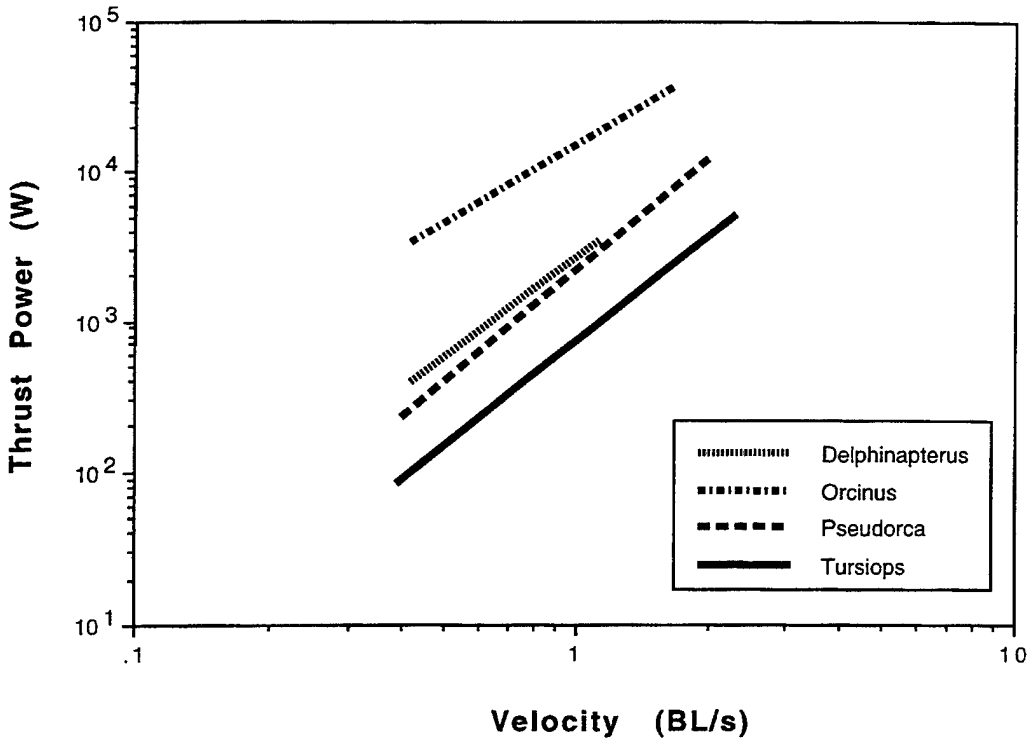

Figure 34. Thrust power, P_T, as a function of length-specific swimming velocity (BL/s).

As demonstrated in shows at theme parks and in the wild, dolphins are extremely acrobatic and can jump to remarkable heights (figure 35; Backhouse, 1960; Hester et al., 1963). Jump height (i.e., distance of the center of gravity above the water) was used as a way to calculate maximum velocity and power output (Gero, 1952; Lang and Daybell, 1963; Lang, 1966b; Rohr et al., 1998b).

Lang and Daybell (1963) proposed a relationship between underwater swimming speed and jump height for the vertical jumps of dolphins. This relationship was as follows:

$$m\,g\,H = 0.5\,m\,U_e^2 + m\,g\,h_e = P_{av}\,t_a, \tag{11}$$

where m is the mass, g is the gravitational acceleration (9.8 m/s^2), H is the maximum height of the dolphin's center of gravity from the water surface, U_e is the water exit velocity when the tail emerges, h_e is height of the center of gravity when the tail emerges, P_{av} is the average power expended during time t_a, and t_a is acceleration period. If the average velocity during the acceleration period underwater is $U_e/2$, then:

$$t_a = 2\,s/U_e, \tag{12}$$

where s equals the distance traveled during acceleration. Modifying equation (11) gives

$$P_{av} = m\,g\,H/t_a. \tag{13}$$

Lang and Daybell (1963) calculated a P_{av} of 6264 W for a 181-kg dolphin to leap 2.1 m with a U_e of 6.4 m/s. This power output corresponds to a total mass-specific output of 34.5 W/kg, which is comparable to power outputs for actively swimming dolphins provided above.

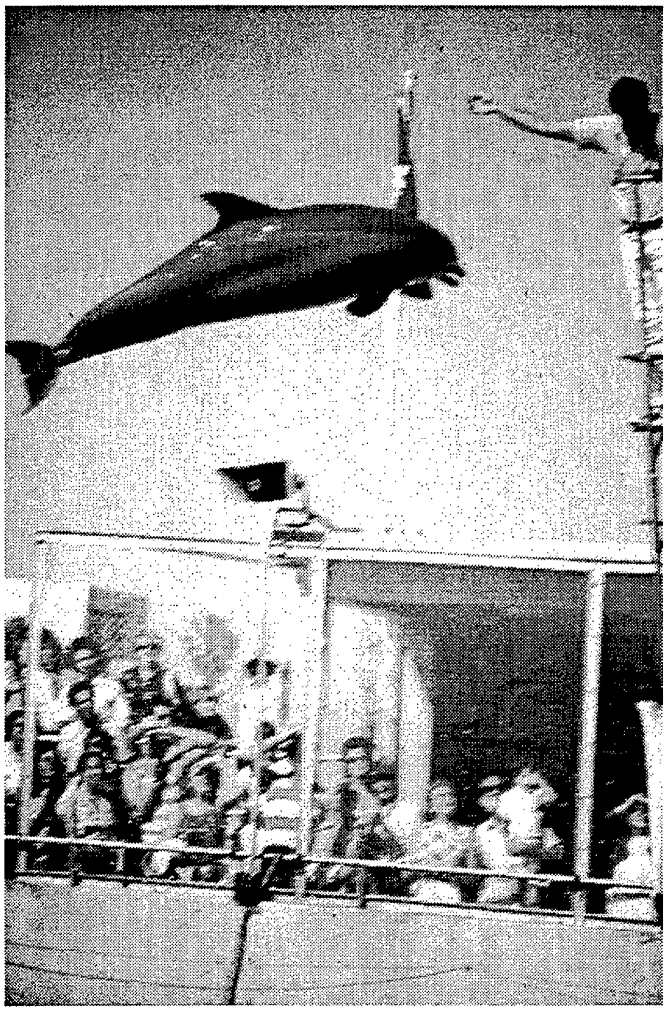

Figure 35. Aerial leap by trained *Tursiops truncatus.*

9.3 PROPULSIVE EFFICIENCY

Propulsive efficiency, η, is defined as the ratio of the mean thrust power required to overcome the drag on the animal divided by the mean rate at which the animal is doing work against the surrounding water (Lighthill, 1970). Efficient thrust production requires high lift production while minimizing energy loss into the wake (Blake, 1983b). Table 4 provides the maximum propulsive efficiency for various cetaceans.

Wu (1971b) estimated that the propulsive efficiency of a dolphin could be as high as 0.99 (table 4). This efficiency was assumed to be an over-estimate because Wu used a two-dimensional analysis that underestimated trailing vorticity and wake energy loss (Ahmadi and Widnall, 1986; Karpouzian et al., 1990). Competing three-dimensional models of lunate tail swimming predict dif-

ferent levels for efficiency. The quasi-vortex-lattice method developed by Lan (1979) and used by Liu and Bose (1993) produced higher values of η compared to values generated from the unsteady lifting theory model of Lighthill (1970) and Chopra and Kambe (1977) for some of the same species (Webb, 1975; Yates, 1983; Fish 1998a). The inviscid nature of different models means that the peak values of η will be reduced in practice by frictional forces (Liu and Bose, 1993). For comparison, efficiencies as high as 0.85 have been measured for torpedoes (Lang, 1966b). Experiments on an oscillating foil (NACA 0012) produced a maximum efficiency of 0.87 (Anderson et al., 1998).

Table 4. Maximum propulsive efficiency, η.

Species	U (m/s)	η	Reference
Balaenoptera physalus	8.0	0.87	Bose and Lien (1989)
Balaenoptera physalus	N/A	0.96	Liu and Bose (1993)
Delphinapterus leucas	N/A	0.90	Liu and Bose (1993)
Delphinapterus leucas	3.0	0.84	Fish (1998a)
Lagenorhynchus acutus	N/A	0.96	Liu and Bose (1993)
Lagenorhynchus obliquidens	5.2	0.99	Wu (1971b)*
Lagenorhynchus obliquidens	5.5	0.77	Webb (1975)*
Lagenorhynchus obliquidens	5.2	0.92	Yates (1983)*
Lagenorhynchus obliquidens	5.2	0.98	Blickhan and Cheng (1994)*
Orcinus orca	6.5	0.88	Fish (1998a)
Pseudorca crassidens	3.8	0.90	Fish (1998a)
Sotalia guianensis	2.4	0.83	Blickhan and Cheng (1994)#
Tursiops truncatus	2.4	0.78	Blickhan and Cheng (1994)#
Tursiops truncatus	3.8	0.86	Fish (1998a)

* Based on data from Lang and Daybell (1963)
# Based on data from Videler and Kamermans (1985)

However, efficiencies on actively swimming whales may be higher than predicted by all the models because the models assume that the hydrofoil is a rigid plate. Dolphin flukes exhibit both spanwise and chordwise flexibility (Joh, 1925; Felts, 1966; Purves, 1969; Curren, 1992). Katz and Weihs (1978) found chordwise flexibility of a foil to increase propulsive efficiency by 20% with only

a slight decrease in thrust compared to a rigid foil. In general, η is expected to be lower than 0.99 but above 0.7 at routine swimming speeds (Table 4; Chopra and Kambe, 1977; Yates, 1983; Bose and Lien, 1989; Karpouzian et al., 1990; Fish, 1993b, 1996, 1998a). Efficiencies in this range are considered good, because few engineered propellers achieve efficiencies higher than 0.7 (Larrabee, 1980; Liu and Bose, 1993).

The high efficiencies associated with swimming by cetaceans are dependent on a fluke design that enhances high thrust with reduced drag and on fluke oscillations that maintain continuous thrust production (Fish, 1992). The aspect ratio is the most important morphological parameter (Bose and Lien, 1989; Liu and Bose, 1993; Fish, 1998a, b). High aspect ratio reduces drag while maximizing thrust (Webb, 1975; Daniel et al., 1982). The fin whale (*Balaenoptera physalus*) with 6.1 aspect ratio flukes has a higher maximum η (0.96) than the beluga whale (*Delphinapterus leucas*) and white-sided dolphin (*Lagenorhynchus acutus*) with aspect ratios of 3.3 and 2.7, respectively (Liu and Bose, 1993). Fish (1998a) found a similar relationship whereby high η was associated with high aspect ratio.

The lift-based propulsion of cetaceans produces reduced η at low speeds (Webb, 1975; Fish, 1993a, 1996). Fish (1998a) showed minimum values of propulsive efficiency, η, at swimming speeds less than 0.5 *BL*/s (figure 36). With increasing velocity, η increased rapidly to a maximum, at which it remained or decreased slightly. The speeds associated with maximum η for *Delphinapterus*, *Pseudorca*, and *Tursiops* approximated their normal cruising speeds. Although maximum η for *Orcinus* occurred at 6.5 m/s, which was above the normal range of cruise speeds (Appendix B), there was a less than 1.6% reduction in η from maximum at the upper end of cruising speed range (5.1 m/s). When cruising, dolphins would be expected to power their movements using the slow oxidative muscles fibers. Alexander (1969) suggested that slow oxidative muscles operate at a contraction rate to promote efficiency whereas the faster contracting, less sustainable fast glycolytic muscle fibers produce maximum power output at the expense of efficiency. Fish and Hui (1991) considered that cetaceans should swim routinely at speeds that maintain the greatest efficiencies. Maximum η at cruising speeds would be beneficial in reducing energy costs during transit between widely dispersed feeding sites or during migration.

Through theoretical and experimental studies of the dynamics of the wake of an oscillating foil, Triantafyllou et al. (1991, 1993) concluded that optimal propulsive efficiency is achieved when the principal wake parameter, the Strouhal number, is between 0.25 and 0.35. The Strouhal number is a dimensionless number, representing the ratio of unsteady and steady motion. Strouhal number (*St*) is defined by the equation:

$$St = A_{p\text{-}p} f / U, \tag{14}$$

where $A_{p\text{-}p}$ is the tail-beat peak-to-peak amplitude (the distance from the peak of the tail fluke upstroke to the peak of the tail fluke downstroke; $A_{p\text{-}p} = 2\ h$). Similar combinations of these kinematic swimming parameters have previously characterized the swimming motion of fish (Rosen, 1959, 1963; Pyatetskiy, 1970; Webb, 1975), dolphins (Semonov et al., 1974; Kayan and Pyatetskiy, 1977), and athletes (Pershin, 1988), but not within a rigorous theoretical context for swimming efficiency.

Strouhal numbers for swimming fish and dolphins were between 0.25 and 0.35, as predicted by the theory described in Triantafyllou et al. (1993). The *St* calculation for the dolphin in this study consisted of two values obtained from Lang and Daybell (1963). One *St* value, 0.32, corresponded to

dolphin swimming while wearing a 1.91-cm-diameter drag collar. The remaining *St* value, 0.30, corresponded to swimming without the drag collar.

Rohr et al. (1998b) examined the distribution of *St* with respect to swimming speed for captive *Pseudorca* and *Tursiops* (figure 36). *St* derived from video recordings of swimming *Pseudorca* ranged from 0.21 to 0.37 with a mean of 0.29. Corresponding *St* for *Tursiops* ranged from 0.15 to 0.36 with a mean of 0.25. Comparison data sets for *Tursiops* showed a mean *St* of 0.25 (Kayan and Pyatetskiy, 1977) and 0.27 (Fish, 1993b). Although the mean *St* for each of the dolphin data sets was within the 0.25 to 0.35 range predicted by Triantafyllou et al. (1993), this range included only 56% of all the data compared to 89% of the data residing between *St* of 0.2 and 0.35 (Rohr et al., 1998b). Indeed, efficiency decreases only slightly at $St = 0.2$ from peak efficiency and is approximately the same as the efficiency at $St = 0.35$ (Triantafyllou et al., 1991).

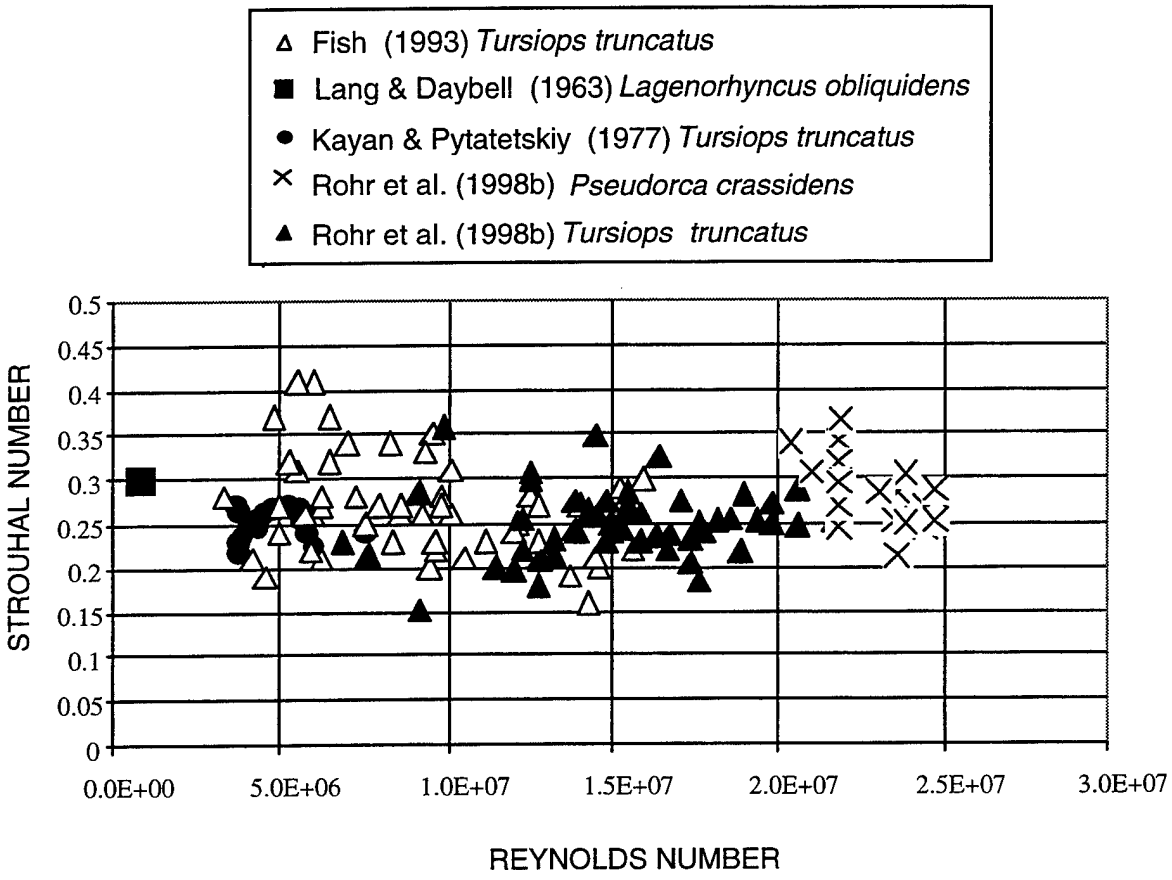

Figure 36. Dolphin Strouhal number plotted as a function of Reynolds number (from Rohr et al, 1998b).

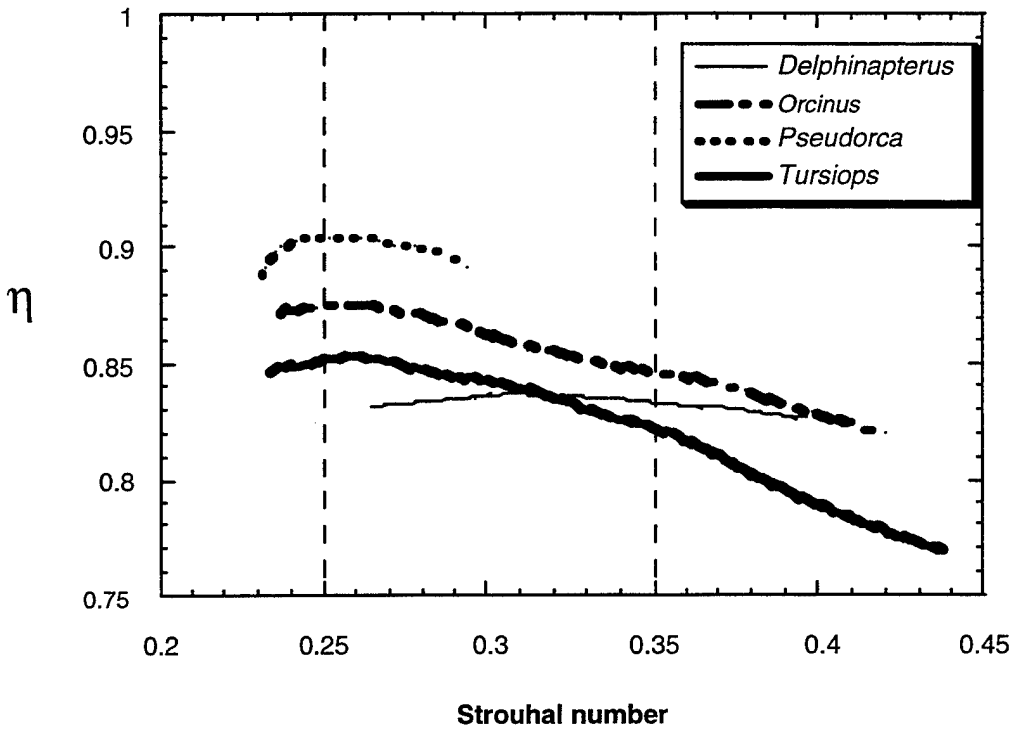

Figure 37. Relationship between Strouhal number, *St*, and propulsive efficiency, η, for four ceteacean species (based on data from Fish,1998a). Region between vertical dashed lines represents optimal range of *St* predicted by Triantafyllou et al. (1991, 1993) for maximum η.

Analysis of data from Fish (1998a) demonstrated the relationship between *St* and η for *Delphinapterus*, *Orcinus*, *Pseudorca*, and *Tursiops* (figure 37). Maximum η at *St* of 0.26 was found for *Orcinus*, *Pseudorca*, and *Tursiops*, but for *Delphinapterus* maximum η occurred at 0.31. Within the optimal *St* range (0.25 to 0.35), η remained above 0.83.

9.4 METABOLIC EFFICIENCY

Power input represents the rate of energy use that is potentially available to do work. In dolphins, the power input is limited proximally by metabolic capacities and ultimately by the availability of food resources (Hui, 1987). Power input for swimming dolphins can be determined from estimates of metabolic rate (M) and, therefore, is related to thrust and drag power outputs according to

$$M \eta_a = T U = D U, \quad (15)$$

where η_a is the aerobic efficiency, T is thrust, and D is drag (Fish, 1992). The η_a is determined by the efficiency of hydrolyzing ATP for work by muscles, work that moves water, and the fraction of work going into thrust (Daniel, 1991). Williams (1987) has reviewed the methodology for measuring swimming metabolism by oxygen consumption. Equation 15 assumes that the metabolism is fueled aerobically by steady-state consumption of oxygen with no significant anaerobic contribution. Because of their large size and rapid swimming, it has been difficult to directly measure oxygen consumption on cetaceans. A harbor porpoise was trained to breathe into a respirometer as it swam in

a pool (Worthy et al., 1987), although the speed of the animal was not regulated. Other methods have been employed to estimate the metabolic increase associated with particular swimming speeds, including correlation of heart rate and oxygen consumption (Williams et al., 1992, 1993a, 1993b), breathing rate (Sumich, 1983; Blix and Folkow, 1995), and hydrodynamic models (Schmidt-Nielsen, 1972; Kawamura, 1975; Yasui, 1980, Hui, 1987; Kshatriya and Blake, 1988; Edwards, 1992). The latter two approaches may not be accurate because of the assumptions that were adopted for the metabolic determination. Such inaccuracies are particularly prevalent when using hydrodynamic models because of optimistic estimates of drag reduction and muscle efficiency (Gray, 1936; Fish and Hui, 1991).

Hui (1987) computed the total power input for a dolphin of the *Stenella-Delphinus* morphology based on the assumptions of a rigid-body analogy and η_a equal to 0.10. His estimates of dolphin power input for routine and maximum swimming speeds were 1.0 to 3.4 and 13.4 times the resting metabolic rate, respectively. Furthermore, Hui (1987) estimated that an 11 m/s burst of less than 2 s by a dolphin represents a 166-fold increase of the metabolism over resting rates when including the anaerobic contributions.

The only estimate of η_a based on measurements of metabolic rate and thrust power was reported by Fish (1996). Using data from Williams et al. (1992) and Fish (1993b), a η_a of 0.25 was calculated. This value is consistent with η_a for other lift-based swimmers (e.g., seal and sea lions), which typically reaches 0.20 with a maximum of 0.30 (Fish, 1992, 1996).

Analysis of η_a has been limited because energetic studies of locomotion rarely examined both metabolic power input and mechanical power output. Examination of the oxygen consumption for calculation of the cost of transport (COT) represents an approach whereby locomotor energetics can be compared without consideration of power output (Videler, 1993). COT is defined as the metabolic energy required to transport a unit mass a unit distance and is calculated by dividing the mass-specific metabolic rate by the swimming velocity (Fish, 1992). COT is inversely proportional to the efficiency and represents the energetic cost to move a unit weight a unit distance (Tucker, 1970). COT is calculated as:

$$COT = M / m g U, \tag{16}$$

where M is the metabolic rate in J s^{-1}, m is body mass in kg, g is the gravitational acceleration of 9.8 m/s^2, and U is velocity in m/s (Videler and Nolet, 1990). The units of COT are J/N m, which makes COT dimensionless. For swimming, COT typically displays a U-shaped curve where it reaches a minimum value within the mid-range of velocities (Williams, 1987; Williams et al., 1993b).

The minimum COT (COT_{min}) is the most efficient and is considered to occur at the velocity (U_m) that the animal can cover the largest distance for the smallest energy cost. Williams et al. (1993b) defined a theoretical maximum range of speeds (U_{mr}) as $\pm$ 10% of U_m. The minimum cost of transport of captive *Tursiops* corresponded to routine swimming speeds measured from wild populations (Williams et al., 1993b). Similarly, gray whales *Eschrichtius robustus* and minke whales *Balaenoptera acutorostrata* cruise at the speed of the lowest cost of transport (Sumich, 1983; Blix and Folkow, 1995). Fish have the lowest COT_{min} for any vertebrate (Tucker, 1970, 1975; Schmidt-Nielsen, 1972; Videler, 1993); therefore, comparisons of COT_{min} values are made with salmonid fish of equivalent size (Williams, 1998), based on the equation from Brett (1964):

$$COT_{min} = 2.15\ m^{-0.25}/g \tag{17}$$

Table 5 provides data for COT_{min} and U_m, and figure 38 shows COT as a function of body mass. In certain cases, COT_{min} was determined from animals over a range of U (Williams et al., 1993a; Kreite, 1995; Yazdi et al., in press). However, some measurements were taken at a single speed chosen by the animal and assumed to represent U_m, at which COT_{min} occurred (Sumich, 1983; Worthy et al., 1987; Blix and Folkow, 1995). Gray whales, *Eschrichtius robustus*, migrate at the speed used in the estimation of the lowest cost of transport (Sumich, 1983). The decrease in COT_{min} with increasing body mass (figure 38) is believed to be primarily the result of higher optimum swimming speeds of large animals (Videler and Nolet, 1990).

The COT_{min} values of values for whales parallel the line for fish (figure 38). In addition, the similarity of cetacean locomotor cost with fish indicates that these mammalian specialists have reached an optimum in energetic performance (Williams, 1998). Except for the relatively low COT_{min} for *Balaenoptera* (0.9 x fish COT), the cetaceans have COT_{min} two to three times higher than a similarly sized fish. However, swimming by cetaceans is substantially more efficient than swimming by terrestrial and semiaquatic mammals, which have COT_{min} 10 to 25 times that of fish (Fish, 1992, 1993a, 1996; Williams, 1998).

Table 5. Cost of transport (COT_{min}) and swimming speed (U_m) of cetaceans

Species	Mass (kg)	COT_{min} (J/Nm)	x fish COT*	Reference
Balaenoptera acutorostrata	4000	0.026	0.9	Blix and Flokow (1995)
Eschrichtius robustus	15000	0.043	2.2	Sumich (1983)
Orcinus orca	5153	0.077	3.0	Kriete (1995)
Orcinus orca	2738	0.085	2.8	Kriete (1995)
Phocoena phocoena	41.5	0.205	2.4	Worthy et al. (1987)
Tursiops truncatus	145	0.132	2.1	Williams et al. (1993a)
Tursiops truncatus	162	0.120	2.0	Yazdi et al. (In press)

*Multiples of cost of tranport for almonid fish based on data from Brett (1964)

Williams (1998) has asserted that the maintenance costs (i.e., energy expended for basal physiological processes and thermoregulatory costs) of aquatic mammals is higher than for their terrestrial counterparts. Examination of the resting and active metabolic rates of aquatic mammals showed that when maintenance costs were omitted (giving a net COT), aquatic mammals have similar locomotor costs with fish. Because fish and cetaceans use the same high-efficiency swimming modes, the implication is that cetaceans have a large component of their total locomotor budget devoted to endothermic maintenance. Extra energy expenditures are required during swimming to cope with thermoregulatory demands of working in an environment that is more thermal conductive than air.

The maintenance costs of dolphins is 57% of the active metabolic rate (Williams et al., 1993a; Williams, 1998). Recently, Alexander (1999) validated Williams' (1998) conclusions by analyzing the mechanical power for swimming. As the mechanical power of moving through water at a velocity, U, is proportional to U^3, the metabolic rate is $(MR + cU^3)$, where MR is the resting rate and c is a constant. The cost of locomotion is $(MR + cU^3)/U$ and the cost is minimal at $U = (MR/2c)^{0.33}$. A high MR would give a high U with an associated increased locomotor cost (Alexander, 1999).

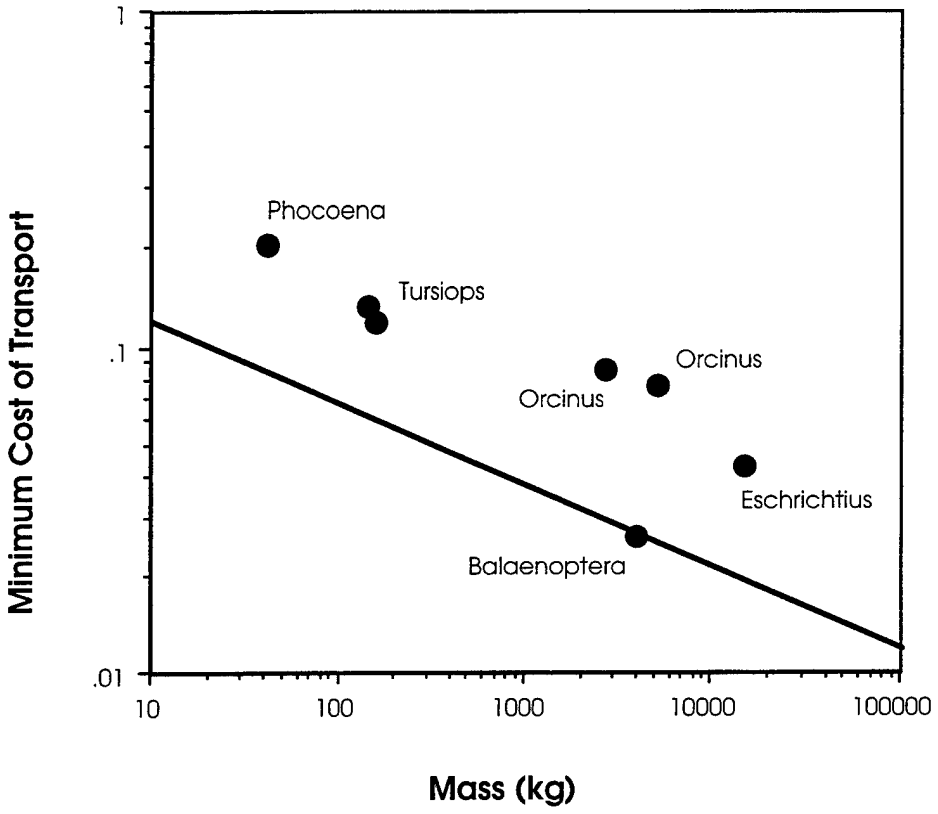

Figure 38. Cost of transport for cetaceans (table 5) as a function of body mass. Line represents minimum cost of transport for salmonid fish (from Brett, 1964).

A proposed mechanism to increase metabolic efficiency by swimming dolphins involves the assertion that dolphins use springs to swim. If elastic components of the body act as tuned springs, elastic strain energy, which is generated during bending of the tail, could be used to replace muscular efforts to decelerate or re-accelerate the flukes (Pabst, 1996). Indeed, the blubber, tendons, and ligaments have elastic properties (Wainwright et al., 1985; Pabst, 1996a, b, 1988; Pabst et al., 1995a; Long et al., 1997; Toedt et al., 1997; Hamilton et al., 1998). Such a mechanism could reduce metabolic costs by 55% if optimally applied (Blickhan and Cheng, 1994). A computational model for oscillating-foil propulsion where springs transmit force to the foil from actuators predicted a reduction in energy cost of 33% (Harper et al., 1998).

Williams et al. (1993a) demonstrated that dolphins swimming at speeds up to 2.1 m/s showed no significant increase in aerobic or anaerobic metabolism despite increasing drag. Above 2.1 m/s, both oxygen consumption and lactate production increased. This trend is similar to the metabolic response observed in kangaroos, which store elastic energy in tendons to maintain a constant metabolic rate with increasing hopping speed (Baudinette, 1994). Williams et al. (1993a) found that dolphins pushing against a static load cell maintained a constant respiratory rate and rate of oxygen consumption with increasing load, although lactate production increased. Pershin (1970) has argued that swimming dolphins show resonance at an oscillatory frequency of 1.5 to 1.9 Hz. For *Tursiops*, this frequency range corresponds to 2.8 to 4.0 m/s (Fish, 1993b, 1998a). This range is at the swimming speeds at which dolphins increase metabolism (Williams et al., 1993a). The use of resonating springs in aquatic animals may be limited because there is substantial dampening by the highly dense and viscous medium as opposed to air where such mechanisms are employed (Alexander, 1988; Clark and Fish, 1994). However, elastic energy storage mechanisms have been used by various invertebrate swimmers that locomote by jet propulsion (Alexander, 1966; Gosline and Shadwick, 1983; DeMont and Gosline, 1988a, 1988b, 1988c; DeMont, 1990).

10. BEHAVIORAL STRATEGIES FOR ENERGY ECONOMY

10.1 SUBMERGED SWIMMING

The need to breathe gaseous oxygen to fulfill metabolic demands incurs a potentially high drag and associated energy demand for cetaceans. Respiratory exchange can only take place at the water surface (Scholander, 1959a). When swimming near or at the surface, the animal experiences increased resistance from production of surface waves. Kinetic energy from the animal's motion is lost as it is changed into potential energy in the formation of waves (Denny, 1993; Vogel, 1994). This energy exchange results in increased drag at or near the surface compared to the drag when the body is submerged without the formation of waves (Lang and Daybell, 1963; Hoerner, 1965; Hertel 1966; Williams and Kooyman 1985; Fish, 1992, 1993a).

Wave drag estimates (based on towed bodies: Hertel, 1966) suggest that when the animal is within a few body widths of the surface, wave drag becomes important and, in fact, exceeds frictional drag. Theoretical attempts (Lang and Daybell, 1963; Hoerner, 1965) have indicated that wave drag will peak at a Froude number of 0.45. The Froude number (F) is the dimensionless ratio of inertial forces to gravitational forces experienced by a body moving at or close to a fluid/air interface. F is calculated as:

$$F = U / (g L_W)^{½}, \quad (18)$$

where L_W is the water line length along the longitudinal axis of the body protruding through the water surface. Because waves can be produced when the body does not pierce the surface, *BL* can substitute for L_W to compute F for submerged bodies. The occurrence of maximum wave drag at F=0.45 is supported by empirical results from streamlined bodies and boats (Hoerner, 1965; Hertel 1966, 1969; Marchaj, 1991). As submergence depth increases, wave drag is reduced (Lang and Daybell, 1963; Hertel 1966). Estimates of wave drag on a *Lagenorhynchus* were made by J. A. Poore and presented as an appendix in Lang and Daybell (1963). Below a depth of two body diameters, the wave drag was determined to be essentially zero at U of 6.1 to 9.1 m/s (Lang and Daybell, 1963).

An additional reduction in wave drag was associated with increasing speed (F >0.45), which effects the wave system generating the drag (Lang and Daybell, 1963). While moving at the water surface, the body of an animal will act as a displacement hull of a ship and will produce two distinct wave systems: a bow wave system and a stern wave system (Taylor, 1933). These systems are comprised of diverging and transverse waves, with each contributing half of the wave drag (Hoerner, 1965). The diverging waves from bow and stern cannot interfere with one another; however, the transverse bow waves can be superimposed on the transverse stern waves because wavelength is variable and dependent on body speed (Marchaj, 1964; Hoerner, 1965). With increasing speed, the wavelength of the bow wave system increases and interacts with the waves generated at the stern (Taylor, 1933; Marchaj, 1964). Depending on the phase relationship, the bow and stern waves can produce a positive or negative interference. Thus, the drag on a body is exaggerated when wave crests constructively interfere and can be reduced when a wave crest and trough destructively interfere. Maximum wave drag occurs at the critical value of F = 0.45, when the wavelength of the bow wave matches the *BL* and the second bow wave constructively interferes with the first stern wave. Above the critical F, the second wave of the bow wave falls astern of the stern wave and no further reinforcing of the wave system occurs. Therefore, wave drag will decline when above the critical F (Taylor, 1933; Lang and Daybell, 1963; Hoerner, 1965).

Empirical data regarding wave drag and submergence depth were generated from towing experiments on a dolphin-shaped body of revolution (NACA 60-018 profile) in a water tank (Hertel, 1966, 1969). Wave drag was found to reach a maximum of five times frictional drag (Hertel 1966). Au and Weihs (1980a) considered the maximum drag augmentation factor for a dolphin to be 4.5 because the dolphin is not an exact body of revolution. The maximum wave drag occurs when half of the body is submerged so that the relative depth is 0.5 of maximum body diameter. Wave drag decreases with increasing and decreasing submergence depths and becomes unimportant at depths greater than three times body diameter or when the animal becomes airborne (Hertel 1966).

The locomotor strategy of submerged swimming can result in increased efficiency by drag reduction (Williams, 1989). Energy saved by swimming away from the surface would offset increased energy expended in coming to the surface to breathe. Aquatic mammals are adapted for using this strategy during high-speed travel by swimming for prolonged periods below the surface. Hui (1989) postulated that dolphins could gain large energy benefits by swimming for long distances between breaths as long as the dolphins swam at depths greater than one-half of one body length. Furthermore, to prevent increased energy cost when coming to the surface to breathe, these animals limit such times, and quickly ventilate the lungs before submerging. Free-ranging dolphins (*Delphinus delphis*) ventilate in 0.38 s (Hui, 1989). Spinner dolphins could breathe in and out in as little as 0.5 to 0.6 s, although the average time is 0.77 s (Norris and Johnson, 1994a). To facilitate ventilation, the velocity of exhaled air can be as high as 65 m/s (Kooyman and Cornell, 1981). Dall's porpoise (*Phocoenoides dalli*) surface briefly and rapidly, exhaling explosively before descending to resume subsurface swimming (Law and Blake, 1994). Blowhole exposure is also correlated to the propulsive movements of the body and tail (Amundin, 1974), which maintains momentum and reduces time at the surface. An alternate approach to prolong ventilation time while reducing drag is by porpoising (Au and Weihs, 1980a, b; Hui, 1987, 1989; Williams, 1987; Fish and Hui, 1991).

10.2 PORPOISING

Porpoising has been hypothesized as a strategy for energy economy. This behavior is performed by the fastest mammalian swimmers (Williams 1987; Fish and Hui 1991) and consists of rhythmic, serial leaping (Fish and Hui 1991).

Au and Weihs (1980a, 1980b) and Blake (1983a) proposed models that showed that the energy to swim a given distance increases with swimming speed faster than the energy to leap that distance. Therefore, above a critical swimming speed, U_C, where the energies converge, there is an energetic advantage to swimming by porpoising (figure 39). Using reasonable hydrodynamic assumptions, these models had similar predictions (figure 40); however, differences were apparent when the drag augmentation factor caused by swimming motion (k) was considered in Blake's model. At k = 4, in which the drag increased because of swimming motions (Lighthill, 1970), the crossover speed is lower than k = 1, where the dolphin is modeled as a rigid body (figure 40). Thus, the higher drag caused by swimming motions makes it more economical to porpoise at a lower speed whereas no advantage by porpoising would be attained if the dolphin exhibited low drag while in the water. The estimated U_C from the model by Au and Weihs (1980a) for a 2.69 m long dolphin was 6.18 m/s, and from the model by Blake (1983a), was 3.03 m/s (k = 4) and 6.03 m/s (k = 1). Data from Fish (1998a) can be applied to Au and Weihs' model for a *Tursiops* of similar size with a drag coefficient of 0.007, where the increased drag from body motions was included. U_C of 3.9 m/s is computed indicating k = 3.

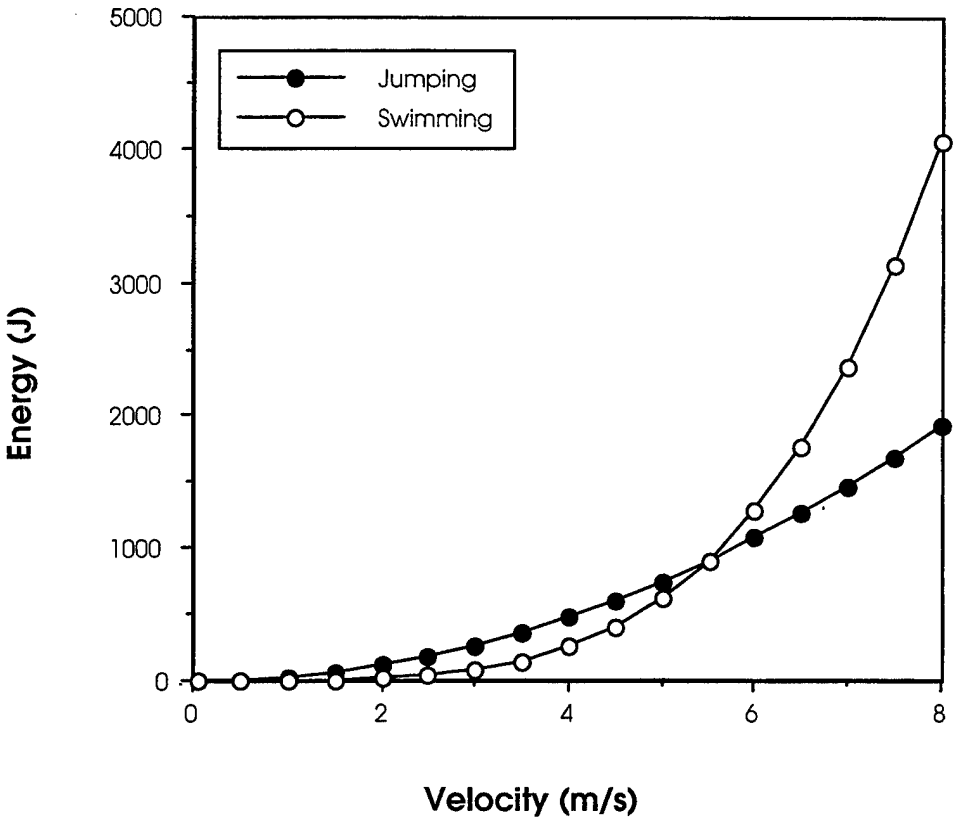

Figure 39. Energies required for swimming close to water surface and for jumping according to model (proposed by Au and Weihs, 1980a). Dolphin was assumed to be neutrally buoyant with a volume of 0.1 m^3, drag coefficient of 0.02 and drag augmentation factor of 4.5. Crossover velocity (i.e., where it becomes more economical to jump a given distance than to swim) was at approximately 5.5 m/s.

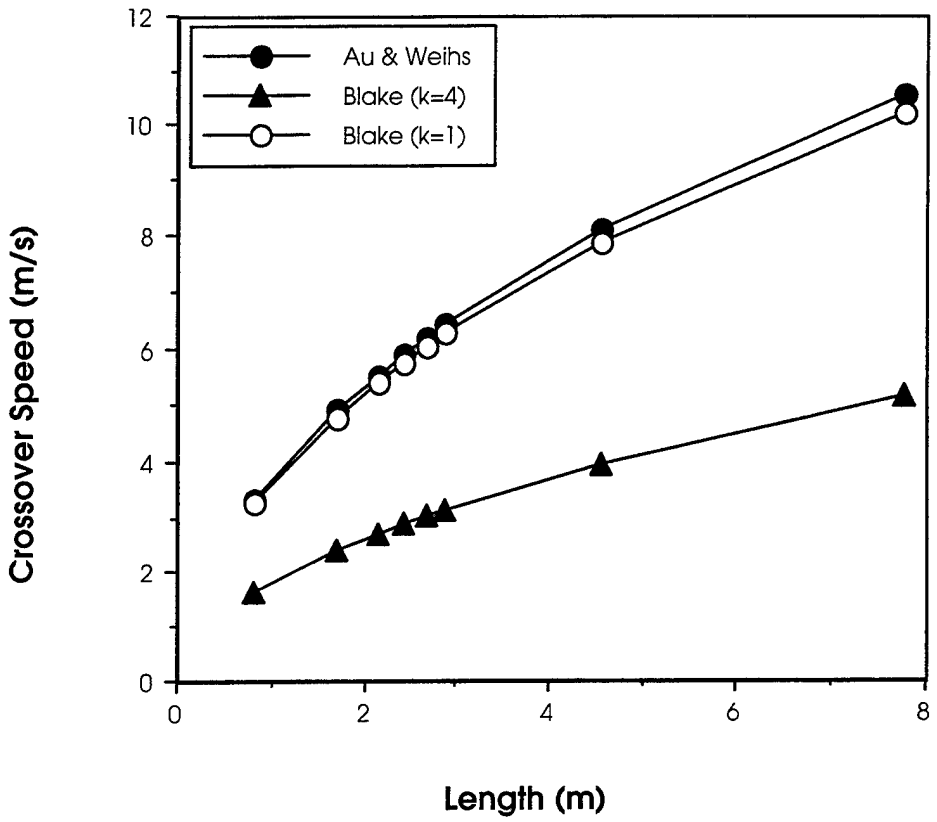

Figure 40. Comparison of predicted crossover speeds for porpoising (from models by Au and Weihs, 1980a, and Blake, 1983a) for dolphins of different body length. Value k is a drag augmentation factor. The value, k = 4, corresponds to dolphin swimming by tail oscillation. The value, k = 1, corresponds to dolphin moving as a rigid body.

Gordon (1980) argued that the correction factor for the added mass (i.e., mass of water entrained with dolphin) in the calculation of jumping energy was an overestimation by a factor of 3. Au and Weihs (1980a) used an added mass correction factor of 0.2 whereas Gordon (1980) suggested a value of 0.066 for a fusiform dolphin. This change in correction factor would result only in a 5% increase in U_c (Au and Weihs, 1980b). Another consideration by Gordon (1980) is that fast-swimming animals should try to maintain their forward speed by using an emergence angle of 30°, the compromise between maximum distance and maximum forward speed of a leap. Au and Weihs (1980a) assumed that the animals would maximize leap distance by employing an 45° emergence angle.

Fish and Hui (1991) questioned the concept of U_c based on field data. Porpoising *Stenella* spp. swim twice the distance they leap whereas the assumption of U_c predict that dolphins would spend more time leaping than swimming at greater than U_c (Au et al., 1988). Video data of free-ranging dolphins (*Delphinus delphis* and *Stenella attenuata*) indicate a graded transition from minimal blowhole exposure at the surface at the low swimming speeds, to quasi-leaps in which the dolphin is never

completely out of the water at any instant at the medium swimming speeds, and to complete porpoising leaps at the highest swimming speeds (Hui, 1989). Lang (personal communication) observed that the natural inclination of dolphins that were trained to swim fast was to porpoise. These observations are consistent with maintaining a minimum blowhole exposure time for respiratory inhalation while swimming. Emergence angles of leaps by dolphins were widely distributed between a 30° angle for maximum speed and a 45° angle predicted for maximum leap distance (Au and Weihs 1980a; Gordon, 1980; Hui 1989). Porpoising may be an energy conservation behavior that is directed more to economical breathing than as an energetically cheap method of swimming (Hui, 1989; Fish and Hui, 1991). The greater energetic demands of rapid swimming necessitate the ability to prolong ventilation without potential interference from waves.

10.3 GLIDING

A substantial amount of time during swimming may be occupied by gliding when low drag would be beneficial (Lighthill, 1970; Weihs and Webb, 1983; Williams et al, 1996). During deep dives, dolphins can reduce energy costs by approximately 20% when transiting to the bottom by using intermittent swimming behaviors (Williams et al., 1996). Diving dolphins use gliding to reduce locomotor energy costs when they are negatively buoyant during descent and positively buoyant during ascent (Skrovan et al., In press). When diving deeply (> 20 m), lung collapse reduces the net buoyant force causing the animal to sink (Ridgway et al., 1969; Ridgway and Howard, 1979; Kooyman and Ponganis, 1998). The dolphin can descend using its negative buoyancy to glide, thus saving energy over active swimming. During ascent, the reverse occurs, and the dolphin accelerates by actively swimming until its lung re-inflate sufficiently to provide positive buoyancy (Skrovan et al., In press). By allowing the body to be neutrally or slightly negatively buoyant, an animal foraging on the bottom can conserve its oxygen reserves and increase its dive time.

Sperm whales (*Physeter macrocephalus*) are the deepest diving of the Cetacea. Diving is facilitated by density changes of the spermaceti organ located in the head (Clarke, 1970, 1978a, 1978b, 1978c, 1979). The spermaceti organ is filled with an oil that becomes denser when cooled below 31°C (Clarke, 1978b, 1978c, 1979). When diving, the oil could be cooled by heat exchange mechanisms associated with the circulatory system and by flooding the nasal passage with seawater (Clarke, 1978a, 1978c, 1979). Increased density on descent and decreasing density on ascent would reduce the effort of swimming from depths over 3000 m. Estimates of density change with decreasing temperature and depth indicate that a 91.5-kg change in buoyancy is possible (Clarke, 1970). The maximum descent rate (12.7 m/s) reported for sperm whales was higher than maximum burst speed (Lockyer, 1977; Papastavrou et al., 1989). The increased speed was probably caused by increased swimming effort and increased density (Lockyer, 1977). This explanation was criticized as the changes in buoyancy were considered insignificant to account for a 23% increase in the speed of the whale (Papastavrou et al., 1989).

10.4 FREE RIDING

Dolphins have probably been riding the bow waves of boats since shortly after the invention of the sail. Rather than increasing energy demands as in wave drag, wave energy from external sources can be used to reduce swimming effort. Kinetic energy from the environment is used by the animal to effect locomotion. The greatest economy for swimming will occur by means of free-riding behavior. In this behavior, an animal takes advantage of the thrust produced by another body by swimming in the hydrodynamically favorable area arising from the interaction of the pressure fields (figure 41; Lang, 1966b).

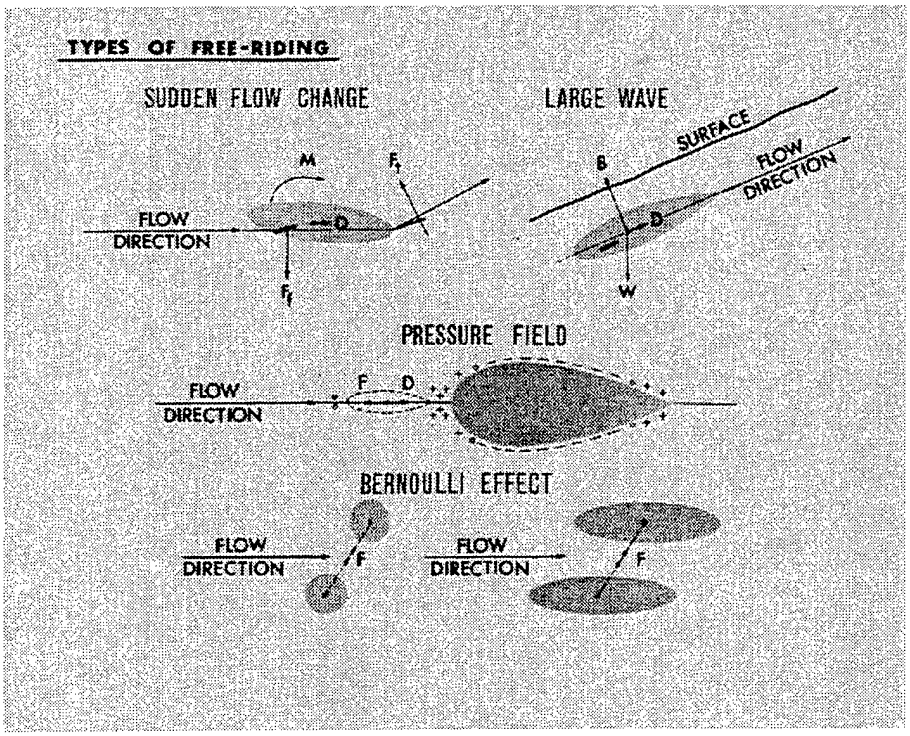

Figure 41. Types of free-riding (from Lang, 1966b).

10.4.1 Wave Riding

It is well-known that dolphins ride the pressure waves of ships and large whales (Woodcock, 1948; Caldwell and Fields, 1959; Fejer and Backus 1960; Norris and Prescott 1961; Hertel, 1969; Leatherwood, 1974; Herman and Tavolga, 1980; Fish and Hui, 1991; Johnson and Norris, 1994). This behavior will occur from minutes to hours (Williams et al., 1992). Dolphins judge whether the bow wave is suitable. Upon approaching a ship, dolphins will swim from side to side of the bow, testing the pressure field (Yuen, 1961).

The first careful description of the behavior of bow-wave riding by dolphins (Woodcock, 1948) was used to develop models of the mechanics of the behavior (Woodcock and McBride, 1951; Hayes, 1953, 1959; Scholander, 1959a, b). These models were all shown to be inadequate due partly to their common requirement that the behavior could occur only when the dolphin was in a specific location holding a specific pose. Scholander (1959a) experimentally tested a foil section in the bow wave and found that the optimal position to derive thrust was with the foil pitched down at 28°. Tail flukes of bow-riding animals were observed with the opposite orientation with an angle of 30° (Norris and Prescott, 1961; Yuen, 1961). Although it is unclear whether Scholander performed tests through an entire 180° rotation of his foil, it is possible that either orientation may provide maximum thrust (Norris and Prescott, 1961).

This behavior is complex with any energy savings to the dolphin related to bow design, swimming depth, body orientation, and distance from the ship (figure 42; Fish and Hui 1991). Dolphins also readily change positions (Fejer and Backus, 1960; Norris and Prescott, 1961) and their flukes are not maintained in any specific orientation (Yuen, 1961). These observations were explained by a model

based on the pressure wave in front of the bow (Fejer and Backus, 1960). The pattern of the pressure distribution relative to boat length and to dolphin drag coefficient prescribes an optimum distance for bow riding, depending on various hydrodynamic characteristics of the animal and the sea state (figure 43).

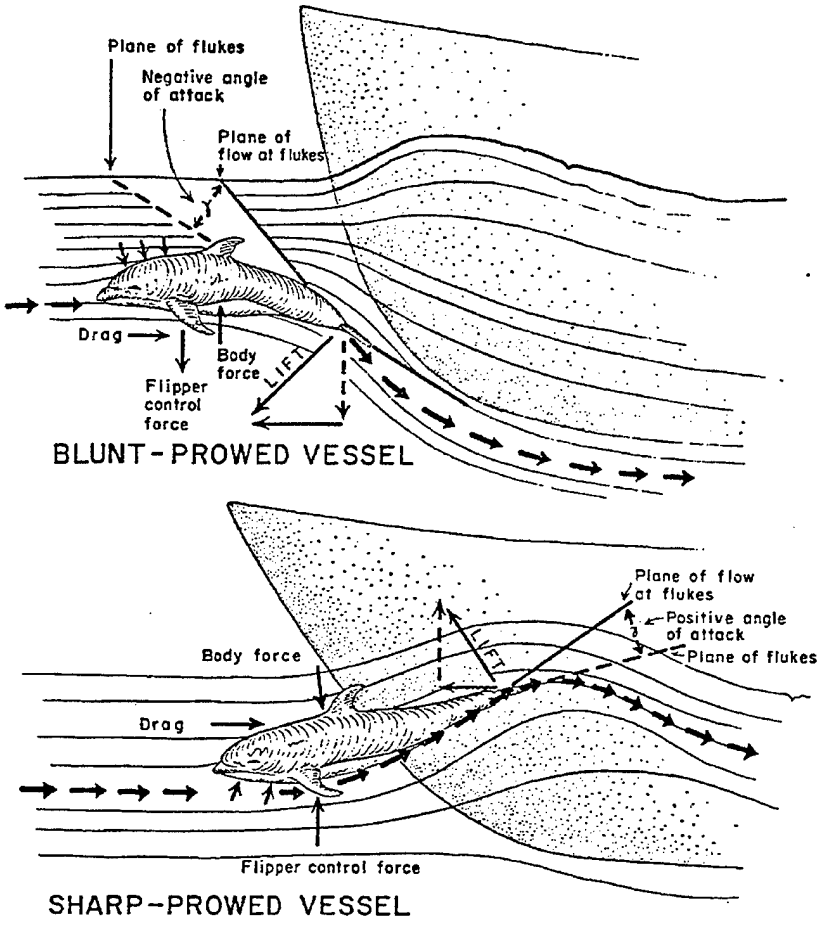

Figure 42. Bow wave riding dolphins. Forces and orientation of animals are different depending on the bow design (from Norris and Prescott, 1961; The Regents of the University of California, Univeristy of California Press).

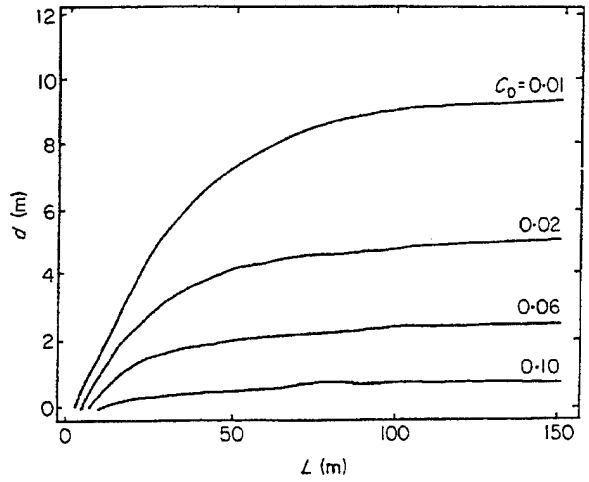

Figure 43. Distance (*d*) between bow of vessel and tail of bow-riding dolphin relative to length of vessel (*L*) and drag coefficient (C_D) of dolphin. The dolphin's posture affects its C_D. Sea state, ship motion, distance from the surface, and bow shape influence pressure field. Therefore, myriad combinations of postures and locations are possible for bow-riding dolphins (from Fish and Hui, 1991).

Newman (1975) numerically modeled wave riding as swimming in a non-uniform flow by applying slender-body theory (Lighthill, 1960). The dolphin body experiences a thrust equal to the buoyant forces times the longitudinal pressure gradient of the flow (Newman and Wu, 1974). The longitudinal pressure gradient in the bow wave is created by the steady flow past the ship. A dolphin near the surface is in equilibrium with the bow wave at 6 m/s with a wave slope of 7° (Newman, 1975). This wave slope is below the maximal slope of 30°, but slope decreases exponentially with depth. The model also predicts that to travel in the same direction of the ship the dolphin must be directly in front of the bow. The movement of the bow wave laterally occurs at an acute angle. Because of an additional lateral force in both horizontal and vertical directions from the diverging wave system, a wave riding dolphin positioned off the bow is expected to swim on its side with its flukes in the vertical plane (Newman and Wu, 1974; Newman, 1975). Fejer and Backus (1960) have reported dolphins to bow ride on their sides. When shifting from between port and starboard sides of the front of a bow wave, dolphins will roll from side to side (Yuen, 1961; Hertel, 1969). However, this orientation requires that dolphins periodically roll 90° to surface and breathe.

The ability to use ship-generated waves to free-ride is largely responsible for many of the misconceptions and erroneous conclusions regarding dolphin swimming speeds and hydrodynamics. Williams et al. (1992) found that wave-riding dolphins could swim at a higher speed while reducing or maintaining metabolic rate, heart rate, lactate production, and respiratory rate (figure 44).

Wind-wave riding and surf-wave riding can also reduce the energy of surface swimming (Caldwell and Fields, 1959). These wave-riding behaviors differ from bow-wave riding because they use the interaction of the dolphin's weight and slope of the wave front to effect movement analogous to human surfers (Hayes, 1953; Fejer and Backus, 1960; Perry et al., 1961). Dolphins have been

observed riding on breakers or breaking wind waves (Norris and Prescott, 1961). Dolphins can ride waves with a forward slope of 10 to 18° at velocities of 5 to 6 m/s (Hertel, 1969).

Extraction of energy from the waves by oscillating a hydrofoil has been hypothesized as a mechanism to reduce energy expenditure for propulsion (Wu, 1972; Grue et al., 1988). Such a mechanism has been proposed in watercraft design (Lai et al., 1993). Wind-generated ocean waves were considered to provide a large whale with up to 25% of its propulsive power in head seas and 33% in following seas (Bose and Lien 1990). By synchronizing the motion of the wave with the motion of the flukes, large whales could theoretically increase the relative velocity experienced by the flukes and thereby increase the lift and thrust generated. Small whales, however, do not appear to be able to take advantage of this phenomenon (Curren, 1992).

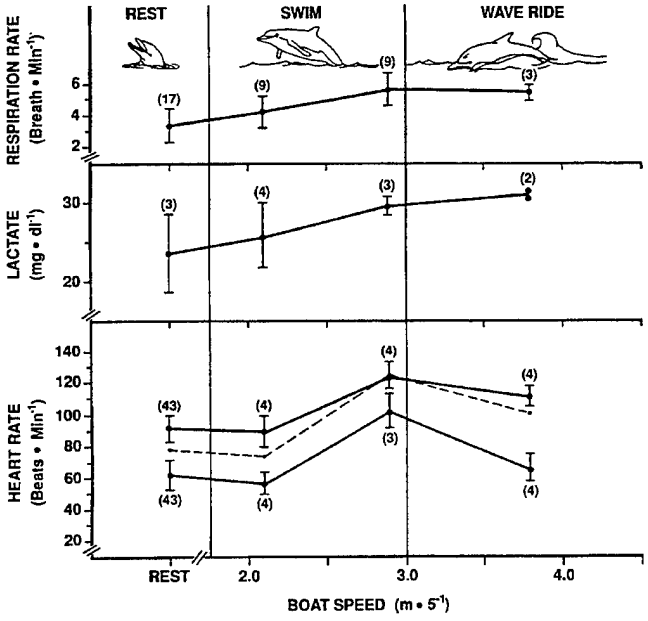

Figure 44. Respiratory rate, blood lactate, and heart rate measured for resting and active (swimming, wave riding) dolphins (with permission from Williams et al., 1992). Mean values are indicated ± one standard deviation with values in parentheses denoting sample size. Upper and lower lines for heart rate show levels of bradycardia and tachycardia, respectively. Heart rate was correlated with oxygen consumption from load cell experiments. When wave riding, heart rate and metabolism decreased compared to active swimming levels despite an increase in speed.

10.4.2 Drafting

Highly organized formations by cetaceans has been suggested as an adaptation for energy economy (Kelly, 1959; Lang, 1966b; Brodie, 1977; Norris and Johnson, 1994b). Formation swimmers

influence water flow around adjacent individuals, resulting in decreased drag with a concomitant decrease in the overall energy cost of locomotion (Weihs, 1973).

Large groups of dolphins were observed in side-by-side and echelon formations (Norris and Prescott, 1961; Leatherwood and Walker, 1979; Johnson and Norris, 1994; Norris and Johnson, 1994b). Small whales often position themselves beside (figure 45) and slightly behind the maximum diameter of a larger animal (Tavolga and Essapian, 1957; Norris and Prescott, 1961; Dohl et al., 1974; Reid et al., 1995; Marino and Stowe, 1997). While the larger whale will experience increased drag, the smaller gains an energetic benefit (Kelly, 1959; Lang, 1966b). This effect is beneficial, particularly for young whales to maintain speed with their mothers. Throughout the first year, up to 75% of the observations showed that calves swim next to the mid-section or near the genital region of the mother (Gubbins et al., 1999). Both positions would increase energy saving by drafting.

In *Platanista*, the young are said to bite on the flipper of the mother and be dragged along (Pilleri and Peixun, 1979). The finless porpoise (*Neophocaena*) carry their young out of the water on their backs (Pilleri and Peixun, 1979). The young porpoise is carried at a position on the mother's back where the skin is not smooth, but covered with small wart-like excrescences.

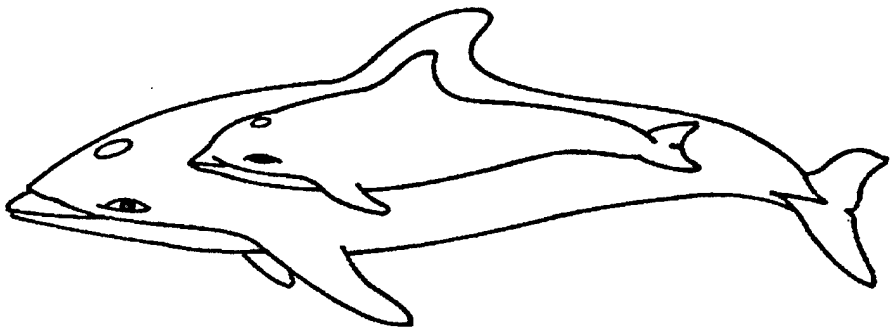

Figure 45. Drafting position maintained by juvenile dolphin (redrawn from Norris and Prescott, 1961; The Regents of the University of California, University of California Press).

11. MANEUVERABILITY

11.1 THEORY

Animals rarely move continuously in straight lines. This is especially true in instances where potential prey must out-maneuver a predator, or the reverse for a predator to turn fast enough to catch its prey (Howland, 1974; Webb, 1983). In addition, the search patterns employed by animals use continuous turning maneuvers. Within the three-dimensional realm of water, maneuvering can be effected in six degrees of freedom from translation in the three spatial dimensions and from rotation around three orthogonal axes. Dolphins can turn and also perform complex barrel-roll maneuvers (Marino, 1997). Even the largest of all animals, whales, display considerable proficiency in their maneuverability (Fish and Battle, 1995).

Various morphologies within animal lineages have evolved that foster maneuverability (Aleyev, 1977; Weihs, 1993). Within the marine mammals, there are divergent body designs that suggest differences in turning performance. Of the fastest swimming marine mammals, the pinnipeds and cetaceans display considerable variation in both their morphology and propulsive mode, which could affect maneuverability (Fish, 1996, 1997). In addition, control of buoyancy allows most fish and sirenians to swim in reverse by using highly mobile pectoral appendages (Hartman, 1979; Blake, 1983; Webb, 1984; Domning and De Buffrenil, 1991) whereas cetaceans must reverse direction by executing turns.

To understand how variation in the morphology of marine mammals can affect maneuverability, consideration should be given to parameters associated with stability (Fish, 1997; Webb, 1997). In cruising, perturbations are arrested as an animal moves forward in a rectilinear manner and maintains static stability (Weihs, 1993). Maneuverability represents the inverse of stability, that is, an instability where a disturbance will cause a change in orientation, speed, or center of mass trajectory within a small time-scale. However, a maneuver must be a controlled instability to be effective. Control for such a system requires energy, sensors that compare the existing state to the desired one, and neural networks that determine the actions (Weihs, 1993). The opposing nature of stability and instability requires that the body and control surface morphology will differ between organisms adapted for stable motion or high maneuverability. This results in an organism that is adapted to continuous high-speed swimming for long distances being less maneuverable than a creature with a design for rapid turning and vice versa.

For marine mammals, maneuverability has had limited study. Accelerations were examined at the beginning of the U.S. Navy's research on dolphins (Lang and Daybell, 1963; Lang and Pryor, 1966). The results of those studies have been discussed above (see section 3.4, NAVAL RESEARCH). Recently, turning maneuvers have been investigated with respect to morphological variation (Fish, 1997). Turning is effected by dynamic forces. These forces include unsteady non-inertial forces such as body internal dynamics (i.e., redistribution of body mass) and fluid inertial reaction (i.e., pulsed jet), and include steady non-inertial forces such as lift and drag.

In aquatic maneuvering systems, the non-inertial forces dominate. Animals can use an asymmetrically applied drag to rotate around and turn. Appendages modified as paddles can produce this effect, which works well in conditions dictated by low velocity and precise control. However, drag-based turning is less effective in conditions of rapid movement with high velocity. The consequences of using drag-based turning is a dramatic reduction in velocity because appendages used for propulsion become braking devices without producing thrust. The energy cost will be high, even

under conditions where thrust is maintained by other appendages as non-propulsive appendages generate the drag for turning.

Lift-based maneuvering systems have the advantage of producing a centripetal force to effect turning without incurring a large decelerating drag (Watts, 1961). This is the primary system used by ships, fish, and marine mammals (Manning , 1930; Howland, 1974; Hoerner and Borst, 1975; Weihs, 1981; Webb, 1983, 1997; Marchaj, 1988; Fish and Battle, 1995; Fish, 1997). The control surface works best with a high aspect ratio, wing-like morphology. The effectiveness of lift-based mechanisms varies with speed (Marchaj, 1988). Lift used by the control surfaces to create destabilizing moments varies in proportions to U^2. However, the mass to be moved by the destabilizing moments is proportional to body mass and independent of speed (Webb, 1997). As speed decreases, the lift also decreases relative to the required force necessary to turn so that maneuvering is more difficult at low U.

Morphologies adapted to increased turning maneuverability become evident when compared to designs for increased stability. Analysis of aerodynamics can be used to elucidate parameters associated with stability for a moving object (Wegener, 1991; Smith, 1992; Weihs, 1993; Fish, 1997), which include:

1. Control surfaces located far from the center of gravity
2. Concentration of control surface area posterior of center of gravity
3. Anterior placement of center of gravity
4. Dihedral of control surfaces
5. Sweep of control surfaces
6. Reduced motion of control surfaces
7. Reduced flexibility of body

The possession of morphological characteristics that deviate from these design parameters is expected to enhance turning performance. Comparing the placement and design of control surfaces on sea lions and cetaceans (figure 46), there are marked differences between the two groups. The control surfaces of sea lions are represented by fore- and hindflippers with the larger foreflippers (65% of total control surface area) near the center of gravity. Because of the high mobility of the foreflippers, both the sweep and the flipper dihedral are variable. For the cetaceans, the flippers, flukes, dorsal fin, and caudal peduncle are the control surfaces, with the more mobile surfaces distant from the center of gravity (Slijper, 1961; Aleyev, 1977; Edel and Winn, 1978; Klima et al., 1987; Fish and Battle, 1995; Fish, 1997). The flippers, flukes, and dorsal fin, when present, can be highly swept, particularly in the faster species. Sweepback results in a backward shift for the center of lift for increase stability (Weihs, 1993). Flexibility in the body of cetaceans is generally constrained (Long et al., 1997). The highly compressed cervical vertebrae and fusiform body restrict movement in the neck, although some species (e.g., *Delphinapterus*, *Inia*) have mobile necks. In comparison, pinnipeds display significant axial flexibility (Gal, 1993). Comparison of the morphology between pinnipeds and cetaceans suggests that whales and dolphins have a more stable design than marine mammals such as sea lions, which will be more highly maneuverable.

Comparisons in turning performance between animals have been measured (Fish, 1997) by examining turning radius, r, turning rate in deg/s, and centripetal acceleration, a_{cg}, in gs (9.8 m/s^2). Centripetal acceleration is computed according to:

$$a_{cg} = U^2/(r\,9.8), \tag{19}$$

where U and r are measured in m/s and m, respectively.

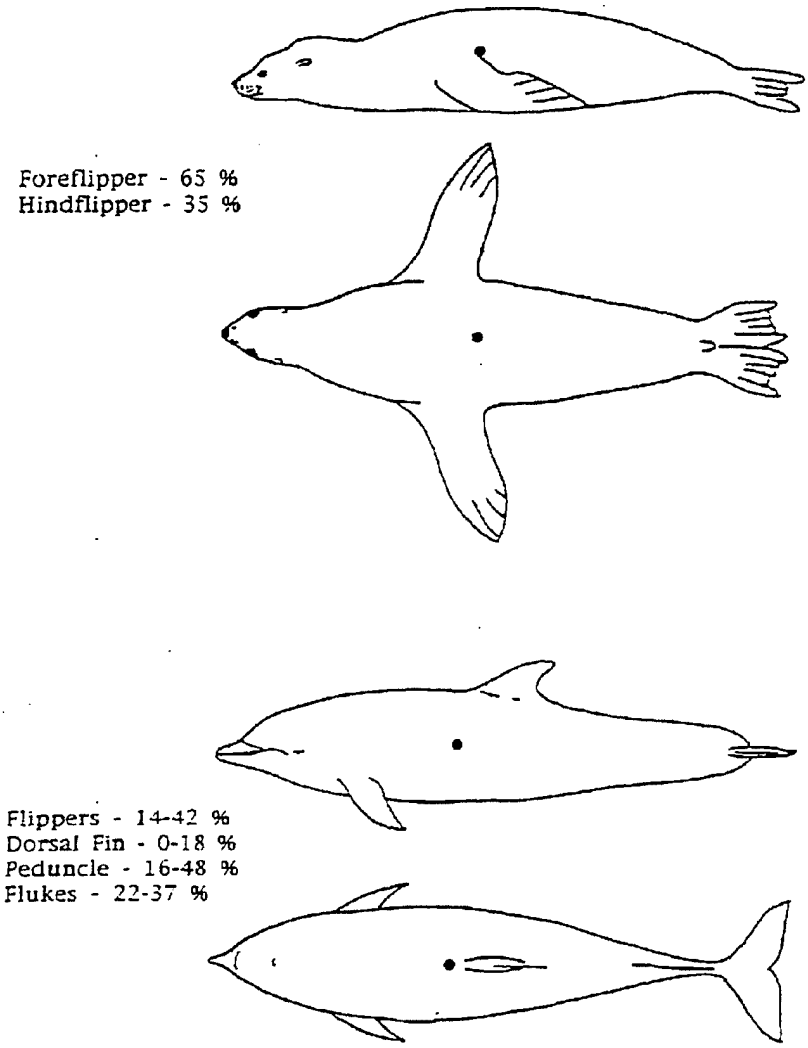

Figure 46. Position of center of gravity (filled circle) and distribution of control surface area for dolphin and sea lion (from Fish, 1987).

11.2 DOLPHINS

A dimensionless maneuverability index was used by Maslov (1970) to compare the turning performance of dolphins with submarines. The index was a compilation of variables including length, mass, turning velocity, time to execute the turn, power output, and turning radius. The results of the comparison showed that dolphins were more maneuverable than submarines (USS *Albacore*, USS *Skipjack*). Maslov (1970) considered that dolphins turned most effectively in the vertical plane because of the orientation of the flippers and flukes. Within the horizontal plane, dolphins were considered more stable.

Fish (1997) examined the horizontal turning performance of various cetaceans, including the bottlenose dolphin (*Tursiops truncatus*), killer whale (*Orcinus orca*), Commerson's dolphin (*Cephalorhynchus commersonii*), Pacific white-sided dolphin (*Lagenorhynchus obliquidens*), false killer whale (*Pseudorca crassidens*), beluga (*Delphinapterus leucas*), and Amazon river dolphin (*Inia geoffrensis*). *Orcinus* was the largest cetacean with one individual of 4536 kg whereas the smallest at 29 kg was *Cephalorhynchus*. *Pseudorca* and *Lagenorhynchus* were regarded generally as fast swimmers whereas, *Delphinapterus* and *Inia* are considered slow swimmers. *Delphinapterus* and *Inia* are different from the other cetaceans by possessing mobile necks and flippers. *Inia* has a notable degree of lateral flexion. In addition, the dorsal fin is reduced in *Inia* and absent in *Delphinapterus*.

Observations of the cetaceans were made as the animals executed turns with the longitudinal axis of the body remaining within the horizontal plane. The cetaceans showed two turning patterns: powered and unpowered (Fish, 1997). Powered turns were defined as turns in which the animal was continuously propelling itself by the dorso-ventral oscillations of the flukes, whereas in unpowered turns, the animal glided through the turn without apparent use of the caudal propulsor. Turns were initiated from the animal's anterior, with lateral flexion of the head and rotation of the flippers into the turn. The flippers also were adducted. During unpowered turns, substantial lateral flexion of the peduncle was observed in addition to twisting at the base of the flukes. The twisting action depressed the inner fluke tip. Some inward banking was observed during unpowered turns. Oscillation around the longitudinal axis occurred during powered turns that were associated with the propulsive fluke motions and produced a rolling movement. Both *Inia* and *Delphinapterus* proved to be exceptions to the general cetacean turning pattern. *Inia* showed no tendency to bank during turns, instead using its flexible body to produce the turn. *Delphinapterus*, without a dorsal fin, would bank 90° with its ventral surface facing into the turn. *Delphinapterus* also demonstrated the unusual swim style of paddling with both of its pectoral flippers to accelerate when coming out of a turn.

The force necessary to maintain a curved trajectory of a given radius is directly related to the square of the velocity and the mass of the body (Howland, 1974; Weihs, 1981). Indeed, minimum turning radius plotted for individuals was associated with body mass (figure 47). Unpowered turns for cetaceans had smaller minimum radii than powered turns for the same individuals. When scaled to body length, cetaceans generally demonstrated minimum unpowered turning radii of $< 50\%$ of body length (figure 48). Minimum radii within each species ranged from 11 to 17% of body length. In one instance, a 5 m long *Orcinus* turned within 4% of its body length (figure 49). However, the animal did not maintain its longitudinal axis within the horizontal plane. The turn was performed by depressing the posterior half of the body and rotating around the vertically oriented tail. Although the turning radius was small, the speed was low (0.93 m/s) because of the extra drag produced from the body orientation. The results for cetaceans are comparable to maneuvers by fish, penguins, and sea lions (Webb, 1983; Hui, 1985; Domenici and Blake, 1991; Bandyopadhyay et al., 1997; Fish, 1997).

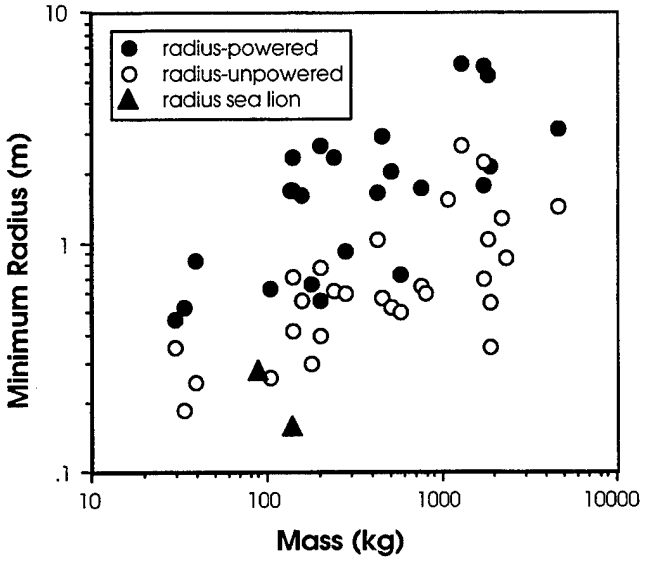

Figure 47. Minimum turning radius plotted against body mass for individuals (from Fish, 1997). Circles represent cetaceans for powered (solid) and unpowered (open) turns and triangles represent unpowered turns by sea lions (*Zalophus californianus*).

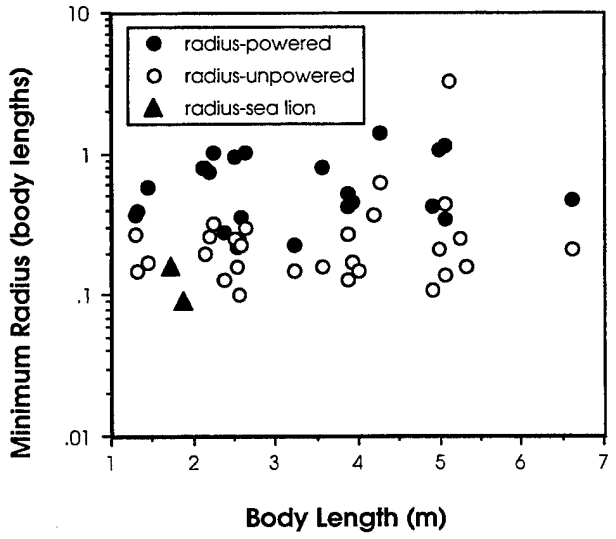

Figure 48. Minimum length-specific turning radius plotted against body length for individuals (from Fish, 1997). Circles represent cetaceans for powered (solid) and unpowered (open) turns, and triangles represent unpowered turns by sea lions.

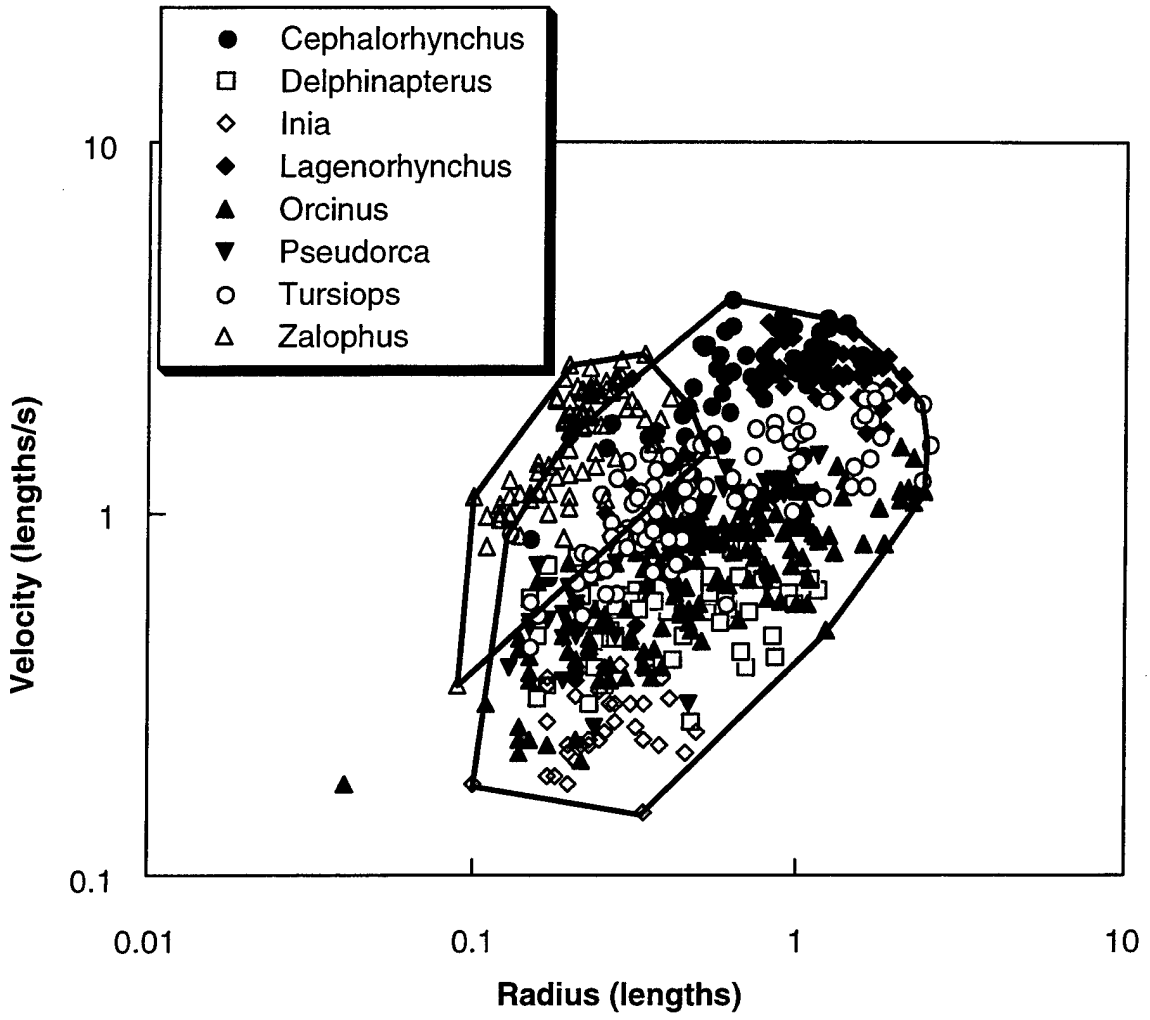

Figure 49. Average length-specific velocity in relation to length-specific turning radius. Polygons are drawn around data for cetaceans and around data for *Zalophus*. The single point outside the cetacean polygon represents a 1725.2-kg, 5.05-m *Orcinus*, which produced a turn radius of 4% of body length by ventrally flexing the posterior half of the body. The flukes pivoted the animal around its longitudinal axis.

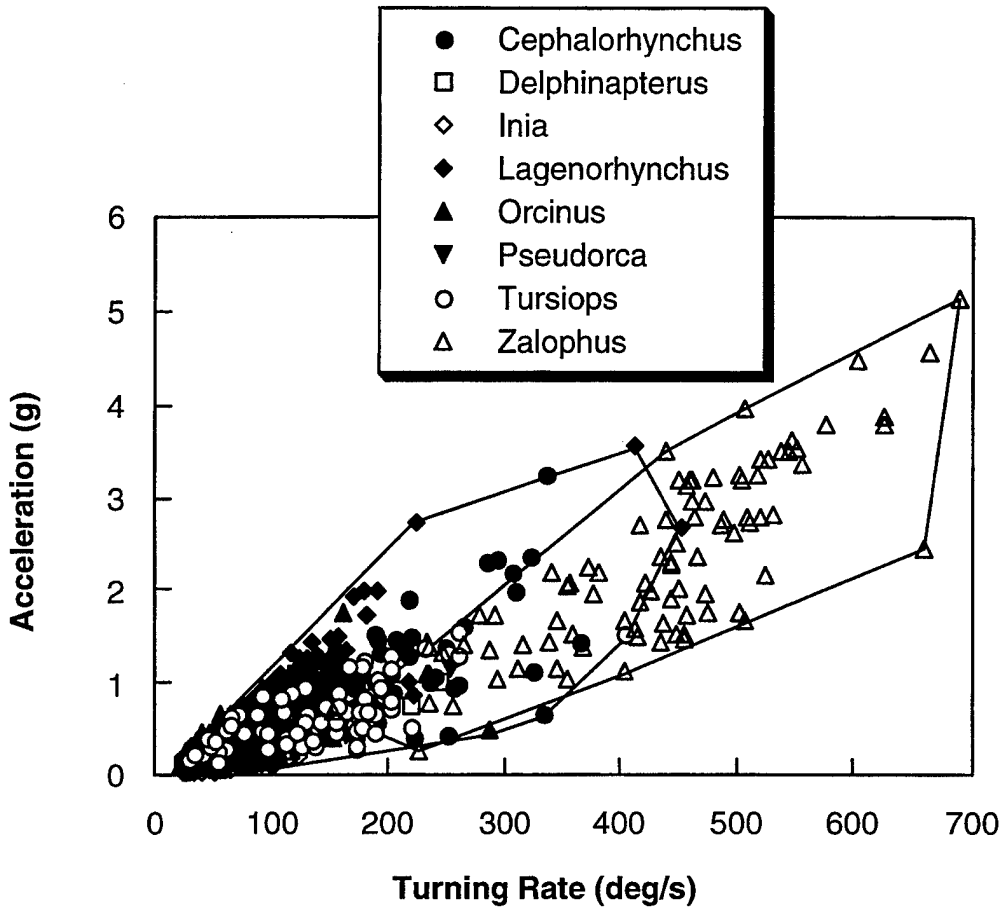

Figure 50. Relationship between centripetal acceleration and turning rate. Polygons are drawn around data for cetaceans and around data for *Zalophus*.

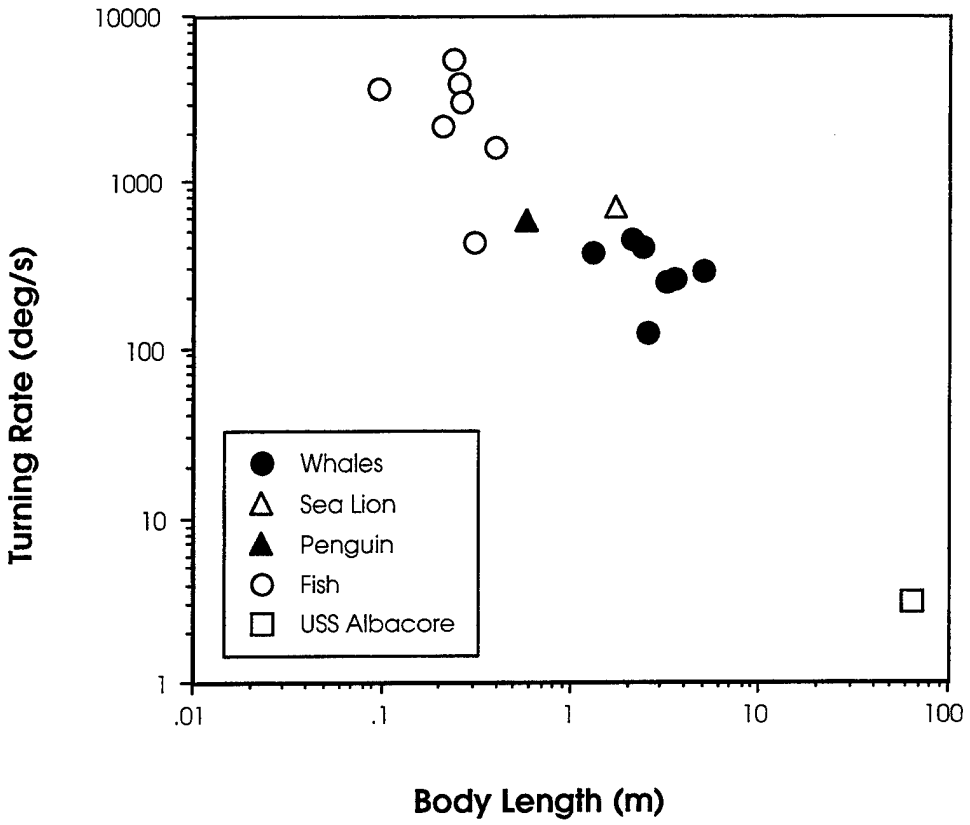

Figure 51. Turning rate as a function of body length. Data from Webb (1976, 1983), Hui (1985), Miller (1991), Blake et al. (1995), and Fish (1997).

Different levels of performance between species were indicated when all the data for turning radius were plotted as a function of velocity (figure 49). *Inia* and *Delphinapterus* produced low-speed, small radius turns. Faster speed but larger radius turns were performed by *Lagenorhynchus* and *Cephalorhynchus* and intermediate performance was displayed by *Orcinus*, *Pseudorca* and *Tursiops*.

In figure 50, a plot of centripetal acceleration and turning rate illustrates turning rate performance. Most data for cetaceans is clustered at accelerations < 1.5 *g*, with turning rates < 200 deg/s. Individuals of *Cephalorhynchus, Lagenorhynchus,* and *Tursiops* exceeded these lower values for cetaceans, with *Lagenorhynchus* displaying the maximum performance with an acceleration of 3.6 *g* and turning rate of 453 deg/s during unpowered turns. Other cetaceans exhibited generally lower performance. The lowest centripetal accelerations occurred in *Inia,* followed by *Delphinapterus;* both swam slowly during testing. Although higher than underwater vehicles (figure 51; Maslov, 1970; Bandyopadhyay et al., 1997), turning rates were lower than exhibited by fish, penguins, and sea lions.

11.3 SEA LIONS

Along with analysis of cetacean maneuverability, the California sea lion (*Zalophus californianus*) was examined (Fish, 1997). This animal swims by oscillations of the paired foreflippers (Fish, 1996). Analysis of turning performance was previously restricted to descriptions of gross body and appendage movements during turning (English, 1976; Godfrey, 1985), but no data were collected on performance capabilities.

Zalophus use only unpowered turns (Fish, 1997). As previously described (Godfrey, 1985), the animal's anterior end initiates the turn as the sea lion rolls 90° so that the ventral (abdominal) surface faces the outside of the turn. The body is flexed dorsally. The fore- and hindflippers are abducted and held in the vertical plane. This maneuver brings the full area of the flippers into use. In addition, the position of the foreflippers is set to execute a power stroke and accelerate the sea lion as it comes out of the turn.

Zalophus made small radius turns while at high speed (up to 4.5 m/s). Minimum unpowered turn radii for two individuals of *Zalophus* were 0.16 and 0.28 m, representing 9 and 16% of body length, respectively. While the length-specific radii were small, they were not substantially different from similar values for cetaceans (figures 47, 48, and 49). However, *Zalophus* typically demonstrated smaller turn radii at higher speeds than cetaceans (figure 47). In addition, turning rates were higher for *Zalophus*, exceeding the maximal performances of cetaceans (figures 50 and 51). One animal executed a 5.13-*g* turn at 690 deg/s. This performance exceeds the acceleration experienced during lift-off on the space shuttle (Fish, 1997).

11.4 MANEUVERABILITY CORRELATES

Marine mammals generally show a high level of performance with regard to turning. This performance, however, varies between species and between major taxonomic groups relating to the ecology and the morphology of the animals. Maneuverability by marine mammals is dependent on body size, body stiffness, and use of control surfaces. The body stiffness and the position and size of the control surface, in particular, determine the animal's stability when swimming. The sea lion, *Zalophus*, exhibits few adaptations for stability and executes tighter turns at higher rates than cetaceans. The highly flexible body and mobile control surfaces (e.g., fore- and hindflippers) aid in rapidly producing instability for turning. In addition, the large area of the flippers aid during the turn by preventing side-slip (Godfrey, 1985).

Conversely, cetaceans have a morphology that enhances stability, thereby constraining turning performance. Cetaceans with flexible bodies and mobile flippers (e.g., *Inia, Delphinapterus*) sacrifice speed for maneuverability whereas species with more restricted morphologies (e.g., *Lagenorhynchus, Cephalorhynchus*) produce faster, but wider turns. The dual function of the caudal appendages for both turning and propulsion presents a restriction to simultaneously maintain high speed during tight turns. To produce a small turn radius, cetaceans must use unpowered maneuvers by uncoupling the control surfaces from thrust production, which limits speed and acceleration after the turn. During unpowered turns, the peduncle and flukes are diverted from their propulsive orientation and used like a rudder.

The enhanced maneuverability of sea lions thus allows them to operate in restricted, in-shore waters with complex environments whereas the more stable design of cetaceans

limits these animals to swimming and foraging in more pelagic habitats. In addition, the limitations of the cetacean design may be a causative reason for the use of cooperative foraging behaviors by whales and dolphins that prey on smaller and, thus, more maneuverable organisms (Smith et al., 1981; Bel'kovich, 1991; Similä and Ugarte, 1993; Fish, 1997).

11.5 MANEUVERABILITY OF LARGE WHALES

The humpback whale (*Megaptera novaeangliae*) is the most acrobatic of the baleen whales. Its elongate wing-like flippers are important in its ability to maneuver. Observations of swimming performance by humpback whales show them as highly maneuverable (Tomilin, 1957; Nishiwaki, 1972), using their extremely mobile flippers for banking and turning (Edel and Winn, 1978; Madsen and Herman, 1980). This maneuverability is associated particularly with the feeding behavior of humpback whales. These whales feed on patches of plankton or fish schools, including euphausiids, herring, and capelin (Jurasz and Jurasz, 1979; Winn and Reichley, 1985; Dolphin, 1988). Turning is widely used in feeding employed with lunging and bubbling behaviors (Hain et al., 1982).

In lunge feeding, whales rush (approximately 2.6 m/s) toward their prey from below while swimming up to the water surface at a 30° to 90° angle (Jurasz and Jurasz, 1979; Hain et al., 1982). In "inside loop" behavior, the whale swims away rapidly from the prey aggregate with its flippers abducted and protracted (Edel and Winn, 1978), then rolls 180° making a sharp U-turn ("inside loop"), and lunges toward the prey (Hain et al., 1982). The entire "inside loop" maneuver is executed in 1.5 to 2 body lengths of the whale. Rapid turning maneuvers are also required for "flick feeding," which is performed in approximately 3 s (Jurasz and Jurasz, 1979). In this feeding behavior, the whale dives until the fluke base is at the water surface and the tail is flicked forward, producing a wave. The whale surfaces with its mouth open into the wave.

In "bubbling" behaviors, underwater exhalations from the blowhole produce bubble clouds or columns that concentrate the prey (Winn and Reichley, 1985; Sharpe and Dill, 1997). Columns of bubbles arranged as rows, semicircles, and complete circles form "bubble nets" (Jurasz and Jurasz, 1979; Hain et al., 1982). Bubble nets are produced as the whale swims toward the surface in a circular pattern from a depth of 3 to 5 m. At completion of the bubble net, the whale pivots with its flippers and then banks to the inside as it turns sharply into and through the center of the net (Ingebrigtsen, 1929; Hain et al., 1982). Bubble net size varies from a minimum diameter of 1.5 m for corralling euphausiids to a maximum diameter of 50 m to capture herring (Jurasz and Jurasz, 1979).

The turning radius (r) due to the humpback whale flippers alone can be found by setting the centripetal force (F_c) acting on the whale equal to the lift force (L) generated by the flippers (Howland, 1974; Weihs, 1981) so that

$$F_C = \mathrm{L}, \tag{20}$$

$$F_c = m_v a_c = m_v U^2 / r, \tag{21}$$

$$\mathrm{L} = 0.5\, \rho\, A_f C_L\, U^2 \sin \phi, \tag{22}$$

where m_v is the virtual mass of the whale (body mass + water entrained to whale), U is the velocity of the whale, ρ is the density of sea water, A_f is the total projected area of flippers, C_L is the lift

coefficient, and ϕ is the bank angle (Alexander, 1983). Turning radius is speed-independent because both centripetal and lift forces scale with the square of speed. Thus,

$$r = m_v / (0.5\, \rho\, A_f C_L \sin \phi). \tag{23}$$

Assuming neutral buoyancy, the virtual mass (m_v) is

$$m_v = m + m\, \lambda \tag{24}$$

where m_v equals the sum of the whale's mass, m, and m times an added mass coefficient, λ (0.082 for a 4:1 spheroid).

Fish and Battle (1995) computed the turning radius for a 9-m humpback whale. The whale's minimum turning radius equaled 7.4 m when ϕ equals 90° (figure 52). The calculated minimum turning radius falls within the minimum and maximum radii for turns during bubbling behaviors (Jurasz and Jurasz, 1979). Maximum bubble net radius (25 m) may be achieved by the humpback whale with ϕ of 17°. Considering that other surfaces of the whale (e.g., flukes, peduncle, body) are employed in turns (Edel and Winn, 1978), the actual minimum turning radius is assumed smaller. Fluke span is 27 to 38% of total body length (True, 1983; Tomilin, 1957). The relatively large size of the flukes would contribute to maneuverability by increasing the lift force. However, the restricted range of motion of the flukes and body and their use in thrust production limit their effectiveness to control maneuverability during powered swimming.

The feeding behavior of humpbacks is considered more energetically demanding than the skim feeding of bowhead whales (*Balaena mysticetus*) (Dolphin, 1987). However, Whitehead and Carlson (1988) suggested that faster swimming and individual foraging by finback whales (*Balaenoptera physalus*) was less advantageous for feeding success than maneuverability by groups of humpback whales.

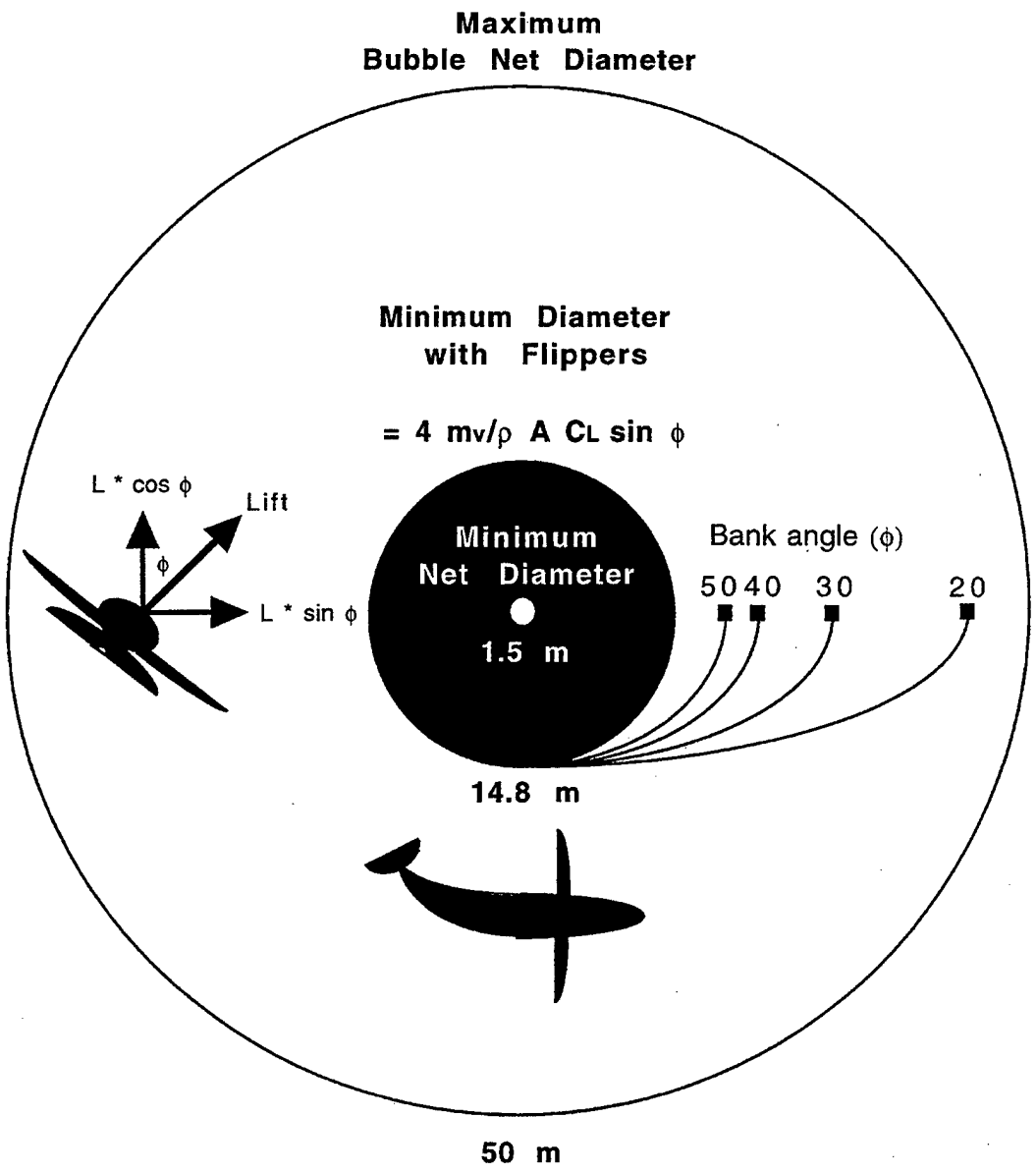

Figure 52. Calculated and observed turning performance of humpback whale (*Megaptera novaeangliae*). Calculated minimum turning diameter (14.8 m) for a 9-m whale is shown by outer black circle margin based on the equation shown. Turn margins for various bank angles are shown by curved lines. Minimum and maximum diameters of bubble nets are shown by central white circle and outer white circle margins, respectively. Inset illustrates lift (L) vectors with respect to bank angle. Silhouette indicates whale dimensions.

12. ASSESSMENT

With his simple calculations of dolphin swimming energetics, Gray (1936) inadvertently propelled the dolphin to an almost mythical status. Either the dolphin's muscles as compared to other animals were extraordinary powerful, or the drag force associated with dolphin swimming was about an order of magnitude less than that achieved in the laboratory. The biological ramification of marine mammal muscles being an order of magnitude more powerful than terrestrial mammal muscles are severe. Since the paradox could be "neatly" solved if the flow over the dolphin body was laminar, the notion of an unknown method of flow control was inviting. Thus, dolphins not only were affected by flow, but were perceived to control flow better than man-made devices.

In the early 60s, the reports of Kramer (1960a, 1960b) on the drag reducing properties of dolphin skin further stimulated interest in dolphin hydrodynamics. If the dolphin did possess some hydrodynamic "secret" through which it could maintain laminar flow at high speeds, this would be of particular interest to the Navy, as it might be applicable to the development of torpedoes and submarines (Shaw, 1959; Lang, 1975). Besides speed, other dolphin attributes that have interested the Navy are stealth, maneuverability, endurance, wakelessness, and mechanical efficiency. Much of the research on dolphin swimming performance has been guided by the investigation of these properties. Most recently, the application of the performance features of dolphins and other marine life has been expanded to the area of robotics in the development of autonomous underwater vehicles (figure 53; Triantafyllou and Triantafyllou, 1995; Triantafyllou et al., 1996; Bandyopadhyay* et al., 1997; Anderson and 2Kerrebrock, 1997; Anderson, 1998; Kumph and Triantafyllou, 1998; Wolfgang et al., 1998; Nakashima and Ono, 1999; Appendix D).

The work reported here was a review of the available literature concerning the hydrodynamic performance of swimming cetaceans. As is evident from the review, all the literature is not in agreement. In many instances, hypotheses predicting drag reduction have been presented with only circumstantial evidence and have never been rigorously tested. Often, investigators who were willing to believe in spectacular but erroneous levels of performance deferred to the default conclusion that flow had to be laminar. The overall effect was to generate a profusion of competing mechanisms based on a conclusion that was not verified nor critically examined. However, it is our opinion that the following major points can be stated regarding dolphin and whale hydrodynamics:

1. Gray's paradox is based on erroneous assumptions of muscle power outputs and boundary layer flow conditions. The paradox is reconciled when appropriate estimates of muscle power output for short-duration activity are used and when the boundary layer over the dolphin is considered to be partly laminar.

2. Currently, the most accurate high-speed measurements, albeit using captive dolphins, recorded swim speeds between 8 and 11 m/s. If one considers the single dolphin species, *Tursiops truncatus*, maximum captive dolphins swimming speeds are remarkably consistent between 7.8 and 8.3 m/s. These high swimming speeds were recorded for durations of the order of 10 seconds or less. For longer duration, *Tursiops truncatus* normally swim at low speeds around 2 m/s.

---

* An overview of some of the recent research on autonomous underwater vehicles conducted by Promode Bandyopadhyay and his colleagues at the Naval Undersea Warfare Center can be found in Appendix F.

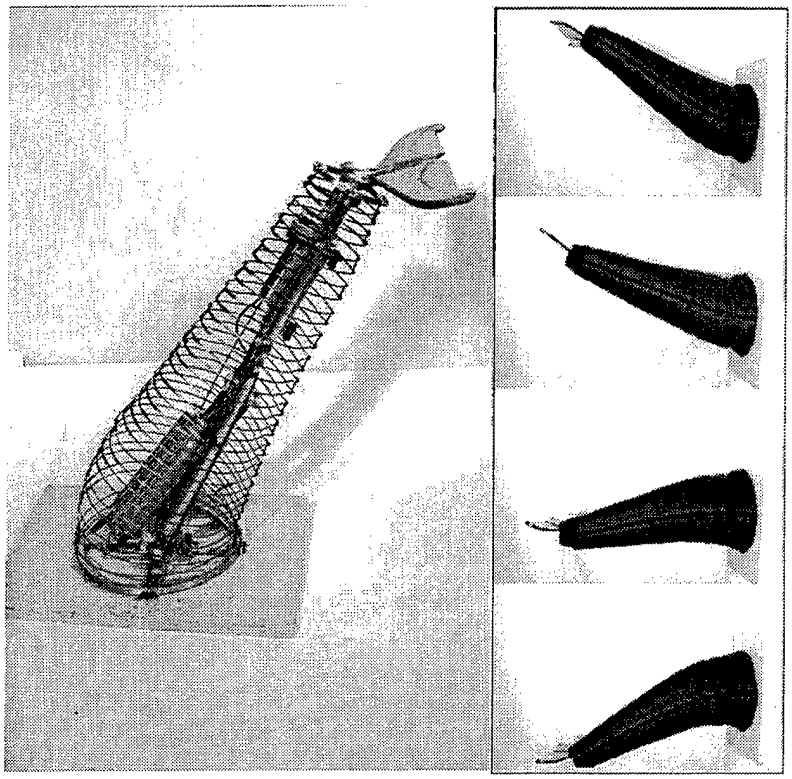

Figure 53. Robotic dolphin tail produced at the Australian Centre of Field Robotics of the University of Sydney. Courtesy of Hugh Durrant-Whyte.

3. Drag reduction is primarily caused by streamlining of the body and appendages. The fusiform or spindle-shaped body and control surfaces are similar to many engineered designs.

4. Drag is relatively low for a gliding dolphin although the present hydrodynamic models show swimming motions incur increased drag compared to rigid bodies.

5. The character of the boundary layer is still unresolved. However, flow visualization and pressure measurement experiments indicate that turbulence does occur and the boundary layer remains attached.

6. Despite the effectiveness of engineered mechanisms for drag reduction, there is no direct supporting evidence for special drag reduction mechanisms (i.e., maintenance of laminar flow) associated with the dolphin skin. Forced laminar to turbulent transition by leading-edge devices and boundary layer acceleration by propulsive motions could limit drag by preventing boundary layer separation.

7. The propulsive mechanism relies on symmetrical dorsoventral oscillations of a caudal hydrofoil (e.g., flukes) with controlled pitch. Oscillation frequency increases nearly linearly with velocity whereas peak-to-peak amplitude remains constant at approximately 20% of body length.

8. Hydromechanical models provide reasonable results of thrust power. Maximum propulsive efficiency is computed as 0.75 to 0.90. These efficiencies occur within the

predicted optimal range of Strouhal numbers. Vorticity control is an important mechanism in the generation of thrust at high propulsive efficiency.

9. Metabolic data show cetaceans to be highly efficient swimmers although a substantial amount of energy is necessary to maintain homeothermy.

10. The energetic cost of swimming can be minimized by various behavioral strategies including submerged swimming, porpoising, intermittent locomotion, bow and wave riding, and drafting.

11. Dolphins produce high-speed (453 deg/s), small-radius (10 to 17% of body length) turns. Performance, however, is constrained by morphology, with flexibility of the body and mobility of the control surfaces determining the performance level.

While studies of dolphins have elucidated much concerning their hydrodynamics and swimming performance since Gray's (1936) initial investigation, a fully comprehensive treatment of the subject has been limited. Previously, the restricted availability of whales and dolphins, their size, difficulties of working in an aquatic medium, restrictions on working with protected species, and the cumbersome and expensive apparatus necessary to research them meant that many studies only grossly described swimming motions and flow surrounding the animals. In addition, application of sophisticated hydromechanical models has been constrained by assumptions that do not adequately consider the full complexity of locomotor kinematics. This has resulted in a patchy and incomplete understanding of the swimming dynamics. Indeed, some of the questions posed by Shaw in 1959 have never been addressed. For example: How does flow noise effect echo ranging of swimming dolphins? Where does laminar to turbulent transition occur on the dolphin? Can we effectively apply principles found to be essential to sea-animal locomotion to underwater vehicles?

With the advent of new technologies and computational methods, future work on dolphin hydrodynamics can resolve some of the problems indicated in this review. Future work on dolphin swimming should be more considerate of variation between species, routine performance levels, and the complexity of biological systems. The following list of points can serve to direct this work. The authors consider this listing by no means comprehensive. The order of the points is not a reflection of their importance.

- Recent studies of robotic fish suggest lower C_D values when the fish is oscillating rather than drag. These results must be further corroborated. If proven true, hydrodynamic models that predict higher C_D values for oscillation must be re-evaluated.

- Researchers must continue to obtain reproducible observations of maximum dolphin swimming speeds. A possible method with captive dolphins is to train the animals to make maximal vertical leaps, and through underwater recordings measure the swimming speed of the animal just before it reaches the water surface.

- Swimming dolphins in an adequately large flume or water tunnel would allow for a rigorous experimental investigation of flow characteristics and energetics. This approach has substantial advantages over swimming trials in open ocean and pool environments, or pushing against stationary devices. Swimming speed, depth, and duration can be controlled for more precise physiological and mechanical testing.

- Because the dolphin is swimming against a constant flow, there is an animal-centered frame of reference that is optimal for high-speed videography, kinematic analysis, and use of remote sensors. In addition, swimming in a flume allows flow visualization with such techniques as digital particle image velocimetry (DPIV) to resolve flow conditions in the boundary layer and outer flow.

- Although controlled laboratory studies do allow for measurements of precise swimming speed, these data may not reflect ecologically relevant performance levels. The future use of microprocessors carried by free swimming cetaceans should provide accurate swimming speeds as well as information on diving performance.

- Only a small percentage of the species composing the Cetacea have been examined for swimming performance. The considerable variability existing within these groups indicate differing performance levels for speed and maneuverability. Is there a compromise between these two variables? Is there an optimal morphology that simultaneously enhances speed and maneuverability? Further examination of a wide range of species with divergent morphological designs is necessary to address these questions.

- Dolphins are creatures of the air–water interface, periodically coming to the surface to breathe. Consequently, most observations of dolphins swimming are when the animals are near the surface. How does swimming speed vary with depth? Despite the possibility of a significant increase in drag caused by waves and turbulence at the surface, the hydrodynamics of swimming at or near the surface has only been cursorily explored. The design and swimming motion of the dolphin may be important in reducing surface wave drag and turbulence for stealth.

- Variation in the design of the cetacean head suggests that it may have hydrodynamic function that could reduce drag and flow noise. The projected rostrum of certain species alludes to a structure similar to bulbous bows. Bulbous bows are important in reducing wave-making resistance. The streamline contour of the rostrum with the head of dolphins could prevent the occurrence of cavitation and associated noise that results in high-speed ships with bulbs (Comstock, 1967). The head design should be analyzed by computational fluid dynamics (CFD), DPIV, and model testing of head shapes attached to bodies of known hydrodynamic performance.

- Studies of the effect of swimming speed on echolocation have been lacking. Dolphins clearly must be able to use their acoustic abilities when swimming at high speed. How do dolphins prevent or function with turbulence developing in acoustically sensitive regions (i.e., melon, ear, lower jaw)?

- Questions concerning the stealth capabilities of the propulsive system of dolphins has never been adequately addressed. Prevention of premature separation from the body would effectively reduce noise production. The flexible nature of the flukes could suppress noise as is generated by rigid control surfaces and propellers. It should be relatively straightforward to obtain acoustic signatures of different species of captive delphinids at various speeds and turning radii.

- Maneuverability has only been examined with respect to turning in the horizontal plane. The placement and orientation of control surfaces for dolphins indicate enhanced agility by maneuvers in the vertical plane. This capability has not been previously examined. The development of autonomous underwater vehicles with maneuvering capabilities has focused on models based on fish which are highly limited with respect to turns within the vertical plane. The

dolphin with pectoral flippers and horizontal orientation of its flukes is expected to show enhanced performance for maneuvers in the vertical plane

- No data currently exist regarding the thrust, lift, and drag performance for the various planforms and cross-sectional designs of cetacean control and propulsive appendages. A survey of these designs can be accomplished from examination of dead, stranded animals. Both models and fresh specimens could be examined in flow tanks.
- The structural design of the spinal column and associated muscles and connective tissue is complex. As a result, there have been few studies regarding the integration of these structural components relating to transmission of force for propulsion. As an initial approach, detailed dissection and histochemistry of the transmission complex is necessary. Based on such information, mechanical models can be developed to elucidate how force is transmitted. Non-invasive methods need to be developed to look inside a living dolphin to study the dynamics of the musculoskeletal system.
- Emphasis should be placed on detailing the material properties of various parts of the dolphin (i.e., integument, blubber, tendons, ligaments). Composition of such components suggests spring-like properties that may be important in energy economy of the propulsive system. The advantages of flexible control surfaces over rigid structures has not been addressed. Much of the work on autonomous underwater vehicles using the biomimetic approach has been performed on a tuna model with a rigid oscillating tail. Flexibility as exhibited by the dolphin flukes may provide an alternate or superior solution to propulsion involving control of vorticity.
- Cetaceans demonstrate many novel designs for engineering applications. Structures such as the leading edge tubercles of humpback whales could be used to develop wing and control surfaces with low stall capabilities.
- Computation fluid dynamics (CFD) should be applied to the morphology and propulsive system of dolphins. Using x-ray computed tomography to create three-dimensional models, predictions of wave and form drag as a function of speed and depth could be calculated for gliding animals.
- Unsteady mechanisms may function in the oscillating fluke system to enhance thrust production. Numerical models and physical models should be examined to determine the role of leading-edge vortices, rotational circulation, and wake capture for increasing propulsive force.
- Of all the various mechanisms that have been hypothesized for drag reduction by dolphins, accelerated flow to laminarize or stabilize the boundary layer as originally proposed by Gray (1936) has received the least attention. Examination of this concept should be a priority. This examination could be accomplished on live dolphins in a flow tank using varied flow visualization methods and by engineered model systems.
- Buoyancy control is an important attribute of the deep-diving ability of dolphins. Although there is photographic evidence of lung collapse at depth, there is no study that has examined how buoyancy is controlled along with trim. Dolphins can orient and hold their bodies in the vertical nose-down position, vertical nose-up position, and horizontally with no regulating movements of the body and control surfaces. A detailed analysis of trim control is necessary to understand how dolphins can maintain static equilibrium in various body postures.
- Integration of the fields of morphology, physiology, and behavior are required to examine the dolphin's performance envelope. Although the bounds of the envelope represent maximal performance with respect to at least one functional parameter, consideration must be given to performance relating to preferred activities that may be submaximal. In focusing on maximal

speed, there has been a skewed opinion as to the capabilities of dolphins that have lead to erroneous conclusions. The dolphin's morphology and physiology may be defined more by routine swimming rather than maximal effort.

Progress in technologies concerned with aquatic locomotion comes from discovery and refinement of new designs. Imposition of the aquatic medium on both machines and animals requires that they contend with the same physical laws that regulate their design and performance (Fish, 1998c). It is no accident that modern submarines and dolphins possess similar shapes for drag reduction although evolved independently. Animal mechanisms often have been recognized only after an engineered solution was developed. In comparison to engineers who can limit variables in their systems, the problem for biologists has been that the systems they study are complex. These systems are composed of structural elements for which the physical characteristics have not been fully described. In addition, the biological systems are multitasking, thus limiting optimal solutions. However, nature retains a store of untouched knowledge that would be beneficial to engineers (Saunders, 1951).

As matters of energy economy and greater locomotor performance are desired in engineered systems, imaginative solutions from nature may serve as the inspiration for new technologies (Fish, 1998c). Dolphins, as well as other marine life, have existed in an environment that they mastered for millions of years. A complete understanding of how dolphins swim will aid in a technology transfer to engineered designs with increased performance. Insight into the various attributes of dolphins, including propulsive efficiency, stealth, high maneuverability, trim control, drag reduction, and flow control, could also aid the development of high-performance autonomous underwater vehicles and other watercraft.

Having said this, it should also be mentioned that there are a few occasions where "copying" nature has actually proved useful (Vogel, 1998; Fish 1998c). This is not to suggest that there is not an impressive, albeit smaller than what one might expect, record for success. These successes would include such well-worn examples as: Velcro and cockleburs, paper and wasps, bird wings and cambered airfoils, silkworms and artificial fabrics, and eardrums and telephone transducers (Vogel, 1998). A particular success most relevant to hydrodynamic applications is Sir George Cayley's use of dolphin and trout profiles to achieve a streamlined shape (Gibbs-Smith, 1962). Ironically, Cayley's attempt at applying this streamlined shape was unsuccessful. This was because he applied it to the hull of a surface vessel, where most of the resistance results from wave and not form drag (Vogel, 1998). To end on a positive note, as modern technology (which will provide more flexible materials and increased miniaturization) and naval requirements (such as increased maneuverability and stealth) converge on capabilities more characteristic of nature, it is more likely she will become an increasingly useful teacher. However, as stated by Shaw (1959) some 40 years ago, this will necessitate a strong collaboration between biologists and engineers.

> *"Finally, the writer would like to put in a plea for more mutual respect and collaboration between biologists and engineers. While their disciplines differ widely and their approaches are remote, as others have suggested, there is much to be gained by a marriage."*
>
> Shaw, 1959

predicted optimal range of Strouhal numbers. Vorticity control is an important mechanism in the generation of thrust at high propulsive efficiency.

9. Metabolic data show cetaceans to be highly efficient swimmers although a substantial amount of energy is necessary to maintain homeothermy.

10. The energetic cost of swimming can be minimized by various behavioral strategies including submerged swimming, porpoising, intermittent locomotion, bow and wave riding, and drafting.

11. Dolphins produce high-speed (453 deg/s), small-radius (10 to 17% of body length) turns. Performance, however, is constrained by morphology, with flexibility of the body and mobility of the control surfaces determining the performance level.

While studies of dolphins have elucidated much concerning their hydrodynamics and swimming performance since Gray's (1936) initial investigation, a fully comprehensive treatment of the subject has been limited. Previously, the restricted availability of whales and dolphins, their size, difficulties of working in an aquatic medium, restrictions on working with protected species, and the cumbersome and expensive apparatus necessary to research them meant that many studies only grossly described swimming motions and flow surrounding the animals. In addition, application of sophisticated hydromechanical models has been constrained by assumptions that do not adequately consider the full complexity of locomotor kinematics. This has resulted in a patchy and incomplete understanding of the swimming dynamics. Indeed, some of the questions posed by Shaw in 1959 have never been addressed. For example: How does flow noise effect echo ranging of swimming dolphins? Where does laminar to turbulent transition occur on the dolphin? Can we effectively apply principles found to be essential to sea-animal locomotion to underwater vehicles?

With the advent of new technologies and computational methods, future work on dolphin hydrodynamics can resolve some of the problems indicated in this review. Future work on dolphin swimming should be more considerate of variation between species, routine performance levels, and the complexity of biological systems. The following list of points can serve to direct this work. The authors consider this listing by no means comprehensive. The order of the points is not a reflection of their importance.

- Recent studies of robotic fish suggest lower C_D values when the fish is oscillating rather than drag. These results must be further corroborated. If proven true, hydrodynamic models that predict higher C_D values for oscillation must be re-evaluated.

- Researchers must continue to obtain reproducible observations of maximum dolphin swimming speeds. A possible method with captive dolphins is to train the animals to make maximal vertical leaps, and through underwater recordings measure the swimming speed of the animal just before it reaches the water surface.

- Swimming dolphins in an adequately large flume or water tunnel would allow for a rigorous experimental investigation of flow characteristics and energetics. This approach has substantial advantages over swimming trials in open ocean and pool environments, or pushing against stationary devices. Swimming speed, depth, and duration can be controlled for more precise physiological and mechanical testing.

- Because the dolphin is swimming against a constant flow, there is an animal-centered frame of reference that is optimal for high-speed videography, kinematic analysis, and use of remote sensors. In addition, swimming in a flume allows flow visualization with such techniques as digital particle image velocimetry (DPIV) to resolve flow conditions in the boundary layer and outer flow.

- Although controlled laboratory studies do allow for measurements of precise swimming speed, these data may not reflect ecologically relevant performance levels. The future use of microprocessors carried by free swimming cetaceans should provide accurate swimming speeds as well as information on diving performance.

- Only a small percentage of the species composing the Cetacea have been examined for swimming performance. The considerable variability existing within these groups indicate differing performance levels for speed and maneuverability. Is there a compromise between these two variables? Is there an optimal morphology that simultaneously enhances speed and maneuverability? Further examination of a wide range of species with divergent morphological designs is necessary to address these questions.

- Dolphins are creatures of the air–water interface, periodically coming to the surface to breathe. Consequently, most observations of dolphins swimming are when the animals are near the surface. How does swimming speed vary with depth? Despite the possibility of a significant increase in drag caused by waves and turbulence at the surface, the hydrodynamics of swimming at or near the surface has only been cursorily explored. The design and swimming motion of the dolphin may be important in reducing surface wave drag and turbulence for stealth.

- Variation in the design of the cetacean head suggests that it may have hydrodynamic function that could reduce drag and flow noise. The projected rostrum of certain species alludes to a structure similar to bulbous bows. Bulbous bows are important in reducing wave-making resistance. The streamline contour of the rostrum with the head of dolphins could prevent the occurrence of cavitation and associated noise that results in high-speed ships with bulbs (Comstock, 1967). The head design should be analyzed by computational fluid dynamics (CFD), DPIV, and model testing of head shapes attached to bodies of known hydrodynamic performance.

- Studies of the effect of swimming speed on echolocation have been lacking. Dolphins clearly must be able to use their acoustic abilities when swimming at high speed. How do dolphins prevent or function with turbulence developing in acoustically sensitive regions (i.e., melon, ear, lower jaw)?

- Questions concerning the stealth capabilities of the propulsive system of dolphins has never been adequately addressed. Prevention of premature separation from the body would effectively reduce noise production. The flexible nature of the flukes could suppress noise as is generated by rigid control surfaces and propellers. It should be relatively straightforward to obtain acoustic signatures of different species of captive delphinids at various speeds and turning radii.

- Maneuverability has only been examined with respect to turning in the horizontal plane. The placement and orientation of control surfaces for dolphins indicate enhanced agility by maneuvers in the vertical plane. This capability has not been previously examined. The development of autonomous underwater vehicles with maneuvering capabilities has focused on models based on fish which are highly limited with respect to turns within the vertical plane. The

dolphin with pectoral flippers and horizontal orientation of its flukes is expected to show enhanced performance for maneuvers in the vertical plane

- No data currently exist regarding the thrust, lift, and drag performance for the various planforms and cross-sectional designs of cetacean control and propulsive appendages. A survey of these designs can be accomplished from examination of dead, stranded animals. Both models and fresh specimens could be examined in flow tanks.
- The structural design of the spinal column and associated muscles and connective tissue is complex. As a result, there have been few studies regarding the integration of these structural components relating to transmission of force for propulsion. As an initial approach, detailed dissection and histochemistry of the transmission complex is necessary. Based on such information, mechanical models can be developed to elucidate how force is transmitted. Non-invasive methods need to be developed to look inside a living dolphin to study the dynamics of the musculoskeletal system.
- Emphasis should be placed on detailing the material properties of various parts of the dolphin (i.e., integument, blubber, tendons, ligaments). Composition of such components suggests spring-like properties that may be important in energy economy of the propulsive system. The advantages of flexible control surfaces over rigid structures has not been addressed. Much of the work on autonomous underwater vehicles using the biomimetic approach has been performed on a tuna model with a rigid oscillating tail. Flexibility as exhibited by the dolphin flukes may provide an alternate or superior solution to propulsion involving control of vorticity.
- Cetaceans demonstrate many novel designs for engineering applications. Structures such as the leading edge tubercles of humpback whales could be used to develop wing and control surfaces with low stall capabilities.
- Computation fluid dynamics (CFD) should be applied to the morphology and propulsive system of dolphins. Using x-ray computed tomography to create three-dimensional models, predictions of wave and form drag as a function of speed and depth could be calculated for gliding animals.
- Unsteady mechanisms may function in the oscillating fluke system to enhance thrust production. Numerical models and physical models should be examined to determine the role of leading-edge vortices, rotational circulation, and wake capture for increasing propulsive force.
- Of all the various mechanisms that have been hypothesized for drag reduction by dolphins, accelerated flow to laminarize or stabilize the boundary layer as originally proposed by Gray (1936) has received the least attention. Examination of this concept should be a priority. This examination could be accomplished on live dolphins in a flow tank using varied flow visualization methods and by engineered model systems.
- Buoyancy control is an important attribute of the deep-diving ability of dolphins. Although there is photographic evidence of lung collapse at depth, there is no study that has examined how buoyancy is controlled along with trim. Dolphins can orient and hold their bodies in the vertical nose-down position, vertical nose-up position, and horizontally with no regulating movements of the body and control surfaces. A detailed analysis of trim control is necessary to understand how dolphins can maintain static equilibrium in various body postures.
- Integration of the fields of morphology, physiology, and behavior are required to examine the dolphin's performance envelope. Although the bounds of the envelope represent maximal performance with respect to at least one functional parameter, consideration must be given to performance relating to preferred activities that may be submaximal. In focusing on maximal

speed, there has been a skewed opinion as to the capabilities of dolphins that have lead to erroneous conclusions. The dolphin's morphology and physiology may be defined more by routine swimming rather than maximal effort.

Progress in technologies concerned with aquatic locomotion comes from discovery and refinement of new designs. Imposition of the aquatic medium on both machines and animals requires that they contend with the same physical laws that regulate their design and performance (Fish, 1998c). It is no accident that modern submarines and dolphins possess similar shapes for drag reduction although evolved independently. Animal mechanisms often have been recognized only after an engineered solution was developed. In comparison to engineers who can limit variables in their systems, the problem for biologists has been that the systems they study are complex. These systems are composed of structural elements for which the physical characteristics have not been fully described. In addition, the biological systems are multitasking, thus limiting optimal solutions. However, nature retains a store of untouched knowledge that would be beneficial to engineers (Saunders, 1951).

As matters of energy economy and greater locomotor performance are desired in engineered systems, imaginative solutions from nature may serve as the inspiration for new technologies (Fish, 1998c). Dolphins, as well as other marine life, have existed in an environment that they mastered for millions of years. A complete understanding of how dolphins swim will aid in a technology transfer to engineered designs with increased performance. Insight into the various attributes of dolphins, including propulsive efficiency, stealth, high maneuverability, trim control, drag reduction, and flow control, could also aid the development of high-performance autonomous underwater vehicles and other watercraft.

Having said this, it should also be mentioned that there are a few occasions where "copying" nature has actually proved useful (Vogel, 1998; Fish 1998c). This is not to suggest that there is not an impressive, albeit smaller than what one might expect, record for success. These successes would include such well-worn examples as: Velcro and cockleburs, paper and wasps, bird wings and cambered airfoils, silkworms and artificial fabrics, and eardrums and telephone transducers (Vogel, 1998). A particular success most relevant to hydrodynamic applications is Sir George Cayley's use of dolphin and trout profiles to achieve a streamlined shape (Gibbs-Smith, 1962). Ironically, Cayley's attempt at applying this streamlined shape was unsuccessful. This was because he applied it to the hull of a surface vessel, where most of the resistance results from wave and not form drag (Vogel, 1998). To end on a positive note, as modern technology (which will provide more flexible materials and increased miniaturization) and naval requirements (such as increased maneuverability and stealth) converge on capabilities more characteristic of nature, it is more likely she will become an increasingly useful teacher. However, as stated by Shaw (1959) some 40 years ago, this will necessitate a strong collaboration between biologists and engineers.

> *"Finally, the writer would like to put in a plea for more mutual respect and collaboration between biologists and engineers. While their disciplines differ widely and their approaches are remote, as others have suggested, there is much to be gained by a marriage."*
>
> Shaw, 1959

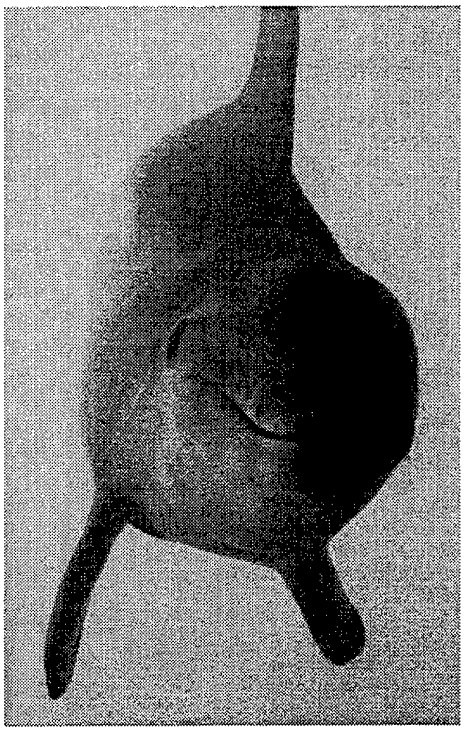

"When playing around in the ocean, dolphins are pleasing to the eye no end, but let it only add to your thrill that these rascals are a graveyard to our wits. For is not finding out infinitely more exciting than knowing the answer?"

Scholander, 1959

13. REFERENCES

Abbott, I. H. and von Doenhoff, A. E. 1959. *Theory of Wing Sections*. Dover, NY.

Agarkov, G. B. and V. Ya. Lukhanin. 1970. "Propulsive Tail Musculature of the Atlantic Common Dolphin," *Bionika* 4:61–64 (translated from Russian).

Ahmadi, A. R. and S. E. Widnall. 1986. "Energetics and Optimum Motion of Oscillating Lifting Surfaces of Finite Span," *J. Fluid Mech.* 162:261–282.

Alexander, R. McN. 1966. "Rubber-like Properties of the Inner Hinge-ligament of Pectinidae,"*J. Exp. Biol.* 44:119–130.

Alexander, R. McN. 1969. "Orientation of Muscle Fibres in the Myomeres of Fishes," *J. Mar. Biol. Assoc. UK* 49:263–290.

Alexander, R. McN. 1983. *Animal Mechanics*. Blackwell Scientific Publications, Oxford, U.K.

Alexander, R. McN. 1987. "Bending of Cylindrical Animals with Helical Fibres in their skin or Cuticle," *J. Theor. Biol.* 124:97–110.

Alexander, R. McN. 1988. *Elastic Mechanisms in Animal Movement*. Cambridge University Press, Cambridge, U.K..

Alexander, R. McN. 1999. "One Price to Run, Swim or Fly?," *Nature* 397:651–653.

Alexander, R. McN. and G. Goldspink. 1977. *Mechanics and Energetics of Animal Locomotion*. Chapman and Hall, London, U.K.

Aleyev, Y. G. 1974. "Hydrodynamic Resistance and Speed of Movement of Nekters," *Zool. Zh.* 53:493–507 (translated from Russian).

Aleyev, Y. G. 1977. *Nekton*. Junk, The Hague, Netherlands.

Aleyev, Y. G. and B. V. Kurbatov. 1974. "Hydrodynamic Drag of Living Fishes and Some Other Nekton in the Section of Inertial Movement," *Vopr. Ikhtiol.* 14:173–176 (translated from Russian).

Amano, M. and N. Miyazaki. 1993. "External Morphology of Dall's Porpoise (*Phocoenoides dalli*): Growth and Sexual Dimorphism," *Can. J. Zool.* 71:1124–1130.

Amundin, M. 1974. "Functional Analysis of the Surfacing Behavior in the Harbour Porpoise," *Phocoena phocoena*. Zeitschrift fur Saugetierkunde 39:313–318.

Anderson, J. M. and P.A. Kerrebrock. 1997. "The Vorticity Control Unmanned Undersea Vehicle— An Autonomous Vehicle Employing Fish Swimming Propulsion and Maneuvering." In *Tenth International Symposium on Unmanned Untethered Submersible Technology: Proceedings of the Special Session on Bio-Engineering Research Related to Autonomous Underwater Vehicles* (pp. 189-195). September 7-10, Autonomous Undersea Systems Institute, Durham, NH.

Anderson, J. M., K. Streitlien, D. S. Barrett, and M. S. Triantafyllou. 1998. "Oscillating Foils of High Propulsive Efficiency," *J. Fluid Mech.* 360:41–72.

Arkowitz, R and S. Rommel. 1985. "Force and Bending Moment of the Caudal Muscles in the Short Fin Pilot Whale," *Mar. Mamm. Sci.* 1:203–209.

Ashenberg, J. and D. Weihs. 1984. "Minimum Induced Drag of Wings with Curved Planform," *J. Aircraft* 21:89–91.

Askew, G. N. and R. L. Marsh. 1997. "The Effects of Length Trajectory on the Mechanical Power Output of Mouse Skeletal Muscles," *J. Exp. Biol.* 200:3119–3131.

Au, D. and W. Perryman. 1982. "Movement and Speed of Dolphin Schools Responding to an Approaching Ship," *Fish. Bull.* 80:371–379.

Au, D. and D. Weihs. 1980a. "At High Speeds Dolphins Save Energy by Leaping," *Nature* 284:548–550.

Au, D. and D. Weihs. 1980b. "Leaping Dolphins," *Nature* 287:759.

Au, D., M. D. Scott, and W. L. Perryman. 1988. "Leap-swim Behavior of "Porpoising" Dolphins," *Cetus*, 8:7–10.

Au, W. W. L. 1993. *The Sonar of Dolphins*. Springer-Verlag, New York, NY.

Azuma, A. 1983. "Biomechanical Aspects of Animal Flying and Swimming." In *Biomechanics VIII-A: International Series on Biomechanics,* 4A:35–53, H. Matsui and K. Kobayashi, Eds. Human Kinetics Publishers, Champaign, IL.

Babenko, V. V. 1979. "Investigating the Skin Elasticity of Live Dolphins," *Bionika* 13:43–52 (translated from Russian).

Babenko, V. V. 1998. "Hydrobionics Principles of Drag Reduction." In *Proceedings of the International Symposium on Seawater Drag Reduction* (pp. 453-455). July 22-23, J. C. S. Meng, Ed. Newport, RI.

Babenko, V. V. and R. M. Surkina. 1969. "Some Hydrodynamic Features of Dolphin Swimming," *Bionika* 3:19–26 (translated from Russian).

Babenko, V. V., L. F. Koslov, S. V. Pershin, V. Ye Sokolov, and A. G. Tomilin. 1982. "Self-adjustment of Skin Dampening in Cetaceans in Active Swimming," *Bionika* 16:3–10 (translated from Russian).

Babenko, V. V. and A. A. Yaremchuk. 1998. "On Biological Foundations of Dolphin's Control of Hydrodynamic Resistance Reduction." In *Proceedings of the International Symposium on Seawater Drag Reduction* (pp. 451-452). July 22-23, J. C. S. Meng, Ed. Newport, RI.

Backhouse, K. 1960. "Locomotion and Direction-Finding in Whales and Dolphins," *New Sci.* 7:26–28.

Baier, R. E., H. Gucinski, M. A. Meenaghan, J. Wirth, and P. -O. Glantz. 1985. "Biophysical Studies of Mucosal Surfaces. In *Oral Interfacial Reactions of Bone, Soft Tissue and Saliva*, pp. 83–95, P. O. Glantz, S. A. Leach, and T. Ericson, Eds. IRL Press, Oxford, U.K.

Baker, A. N. 1985. "Pygmy Right Whale *Caperea marginata* (Gray, 1846)." In *Handbook of Marine Mammals, Volume 3 The Sirenians and Baleen Whales*, pp. 345-354, S. H. Ridgeway and R. Harrison, Eds. Academic Press, London, U.K.

Balcomb, K. C. Jr. 1989. "Baird's Beaked Whale—*Berardius bairdii* Stejneger, 1883 Arnoux's Beaked Whale—*Berardius arnuxii* Duvernoy, 1851." In *Handbook of Marine Mammals, Volume 4 River Dolphins and the Larger Toothed Whales*, pp. 261-288, S. H. Ridgeway and R. Harrison, Eds. Academic Press, London, U. K.

Bandyopadhyay, P. R. 1989. "Viscous Drag Reduction of a Nose Body," *AIAA Journal*, 27:274–282.

Bandyopadhyay, P. R. and Ahmed, A. 1993. "Turbulent Boundary Layers Subjected to Multiple Curvatures and Pressure Gradients," *J. Fluid Mech.*, 246:503–527.

Bandyopadhyay, P. R, J. M. Castano, J. Q. Rice, R. B. Philips, W. H. Nedderman, and W. K. Macy. 1997. "Low-speed Maneuvering Hydrodynamics of Fish and Small Underwater Vehicles," *Trans. ASME* 119:136–144.

Bannasch, R. 1995. "Hydrodynamics of Penguins—An Experimental Approach." In *The Penguins: Ecology and Management*, pp. 141-176, P. Dann, I. Norman and P. Reilly, Eds. Surrey Beatty and Sons, Norton, NSW.

Barclay, C. J., J. K. Constable, and C. L. Gibbs. 1993. "Energetics of Fast-twitch and Slow-twitch Muscles of the Mouse," *J. Physiol.* 472:61–80.

Barnard, R. H. and D. R. Philpott. 1995. *Aircraft Flight*. Longman Scientific and Technical, Essex, U.K.

Barnes, L. G., D. P. Domning, and C. E. Ray. 1985. "Status of Studies on Fossil Marine Mammals," *Mar. Mamm. Sci.* 1:15–53.

Baudinette, R. V. 1994. "Locomotion in Macropodoid Marsupials: Gaits, Energetics and Heat Balance," *Aust. J. Zool.* 42:103–123.

Beddard, F. E. 1900. *A Book of Whales*. John Murray, London, U.K..

Bel'kovich, V. M. 1991. "Herd Structure, Hunting, and Play: Bottlenose Dolphins in the Black Sea." In *Dolphin Societies: Discoveries and Puzzles*, pp. 17-77, K. Pryor and K. Norris, Eds. University of California Press, Berkeley, CA.

Bello, M. A., R. R. Roy, I. Oxman, T. Martion, and V. R. Edgerton. 1983. "Fiber Type and Fiber Size Distributions in the Axial Musculature of the Dolphin (*Tursiops truncatus*)," *Physiologist* 26:A–26.

Bello, M. A., R. R. Roy, T. P. Martin, H. W. Goforth, Jr., and V. R. Edgerton. 1985. "Axial Musculature in the Dolphin (*Tursiops truncatus*): Some Architectural and Histochemical Characteristics," *Mar. Mamm. Sci.* 1:324–336.

Bennett, M. B., R. F. Ker, and R. McN. Alexander. 1987. "Elastic Properties of Structures in the Tails of Cetaceans (*Phocoena* and *Lagenorhynchus*) and Their Effect on the Energy Cost of Swimming," *J. Zool., Lond.* 211:177–192.

Berzin, A. A. 1972. *The Sperm Whale*. Israel Progr. Sci. Transl., Jerusalem, Israel.

Best, R. C. and V. m. F. da Silva. 1989. "Amazon River Dolphin, boto *Inia geoffrensis* (de Blainville, 1817)." In *Handbook of Marine Mammals, Volume 4 River Dolphins and the Larger Toothed Whales*, pp. 1-23, S. H. Ridgeway and R. Harrison, Eds. Academic Press, London, U.K..

Bilo, D. and W. Nachtigall. 1980. "A Simple Method to Determine Drag Coefficients in Aquatic Animals," *J. Exp. Biol.* 87:357–359.

Bityukov, E. P. 1971. "Bioluminescene in the Wake Current in the Atlantic Ocean and Mediterranean Sea," *Okean* 11:127–133.

Blake, R. W. 1983a. "Energetics of Leaping in Dolphins and Other Aquatic Animals," *J. Mar. Biol. Ass. U.K.* 63:61–70.

Blake, R. W. 1983b. *Fish Locomotion*. Cambridge University Press, Cambridge, U.K.

Blake, R. W., L. M. Chatters, and P. Domenici. 1995. "Turning Radius of Yellowfin Tuna (*Thunnus albacares*) in Unsteady Swimming Maneuvres. *J. Fish. Biol.* 46:536–538.

Blick, E. F. and R. R. Walters. 1968. "Turbulent Boundary-layer Characteristics of Compliant Surfaces," *J. Aircraft*, 5:11–16.

Blickhan, R. and J-Y Cheng. 1994. "Energy Storage by Elastic Mechanisms in the Tail of Large Swimmers—A Re-evaluation," *J. Theor. Biol.* 168:315–321.

Blix, A. S. and L. P. Folkow. 1995. "Daily Energy Expenditure in Free Living Minke Whales," *Acta Physiol. Scand.* 153:61–66.

Borelli, G. A. 1989. *On the Movement of Animals*. Springer-Verlag, Berlin, Germany.

Bose, N. and J. Lien. 1989. "Propulsion of a Fin Whale (*Balaenoptera physalus*): Why the Fin Whale is a Fast Swimmer," *Proc. R. Soc. Lond. B* 237:175–200.

Bose, N. and J. Lien. 1990. "Energy Absorption from Ocean Waves: A Free Ride for Cetaceans," *Proc. R. Soc. Lond. B* 240:591–605.

Bose, N., J. Lien, and J. Ahia. 1990. "Measurements of the Bodies and Flukes of Several Cetacean Species," *Proc. Roy. Soc. Lond. B* 242:163–173.

Braham, H. W., M. A. Fraker, and B. D. Krogman. 1980. "Spring Migration of the Western Arctic Population of Bowhead Whales," *Mar. Fish. Rev.* 42:36–46.

Brodie, P. F. 1977. "Cetacean Energetics, An Overview of Intraspecific Size Variation," *Ecology* 56:152–161.

Brodie, P. F. 1989. "The White Whale *Delphinapterus leucas* (Pallas, 1776)." In *Handbook of Marine Mammals,* Vol. 4 *River Dolphins and the Larger Toothed Whales*, pp. 119-144. S. H. Ridgeway, and R. Harrison, Eds. Academic Press, London, U. K.

Brown, W. R., J. R. Geraci, B. D. Hicks, D. J. St. Aubin, and J. P. Schroeder. 1983. "Epidermal Cell Proliferation in the Bottlenose Dolphin (*Tursiops truncatus*)," *Can. J. Zool.* 61:1587–1590.

Brett, J. R. 1964. "The Respiratory Metabolism and Swimming Performance of Young Sockeye Salmon," *J. Fish. Res. Bd. Can.* 21:1183–1226.

Bruyns, W. F. J. M. 1971. *Field Guide of Whales and Dolphins*. Uitgeverij tor/n.v. Uitgeverij v.h C. A. Mees, Amsterdam, Netherlands.

Bushnell, D. M. and K. J. Moore. 1991. "Drag Reduction in Nature," *Ann. Rev. Fluid Mech.* 23:65–79.

Caldwell, D. K. and H. M. Fields. 1959. "Surf-riding by Atlantic Bottle-nosed Dolphins," *J. Mamm.* 40:454–455.

Carpenter, P. W. 1990. "Status of Transition Delay Using Compliant Walls." In Viscous *Drag Reduction in Boundary Layers,* pp. 79–113. D. M. Bushnell and J. N. Heffner, Eds. AIAA, Washington DC.

Carpenter, P. W. 1998. "Recent Advances in the Use of Compliant Walls for Drag Reduction." In Proceedings *of the International Symposium on Seawater Drag Reduction,* pp. 185-188. J. C. S. Meng, Ed. Newport, RI.

Cheng, H. K. and L. E. Murillo. 1984. "Lunate-tail Swimming Propulsion as a Problem of Curved Lifting Line Unsteady Flow Part 1 Asymptotic Theory," *J. Fluid. Mech.* 143:327–350.

Cheng, J-Y, L-X Zhuang, and B. G. Tong. 1991. "Analysis of Swimming Three-Dimensional Waving Plates," *J. Fluid Mech.* 232:341–355.

Chittleborough, R. G. 1953. "Aerial Observations on the Humpback Whales, *Megaptera nodosa* (Bonnaterre), with Notes on other Species," *Aust. J. Mar. Freshwater Res.* 4:219–226.

Chopra, M. G. 1974. "Hydromechanics of Lunate-tail Swimming Propulsion," *J. Fluid Mech.* 64:375–391.

Chopra, M. G. 1975. "Lunate-tail Swimming Propulsion." In *Swimming and Flying in Nature*, 2:635–650. T. Y. Wu, C. J. Brokaw, and C. Brennen, Eds. Plenum Press, New York, NY.

Chopra, M. G. 1976. "Large Amplitude Lunate-tail Theory of Fish Locomotion," *J. Fluid Mech.* 74:161–182.

Chopra, M. G. and T. Kambe. 1977. "Hydrodynamics of Lunate-tail Swimming Propulsion," Part 2, *J. Fluid Mech.* 79:49–69.

Cincotta, M. and R. H. Nadolink. 1992. "Articulated Control Surface," *U.S. Patent* No. 5,114,104.

Clark, B. D. and F. E. Fish. 1994. "Scaling of the Locomotory Apparatus and Paddling Rhythm in Swimming Mallard Ducklings (*Anas platyrhynchos*): Test of a Resonance Model," *J. Exp. Zool.* 270:245–254.

Clarke, M. R. 1970. "Function of the Spermaceti Organ of the Sperm Whale," *Nature* 228:873–874.

Clarke, M. R. 1978a. "Structure and Proportions of the Spermaceti Organ in the Sperm Whale," *J. Mar. Biol. Ass. U.K.* 58:1–17.

Clarke, M. R. 1978b. "Physical properties of spermaceti oil in the sperm whale," *J. Mar. Biol. Ass. U.K.* 58: 19-26.

Clarke, M. R. 1978c. "Buoyancy Control as a Function of the Spermaceti Organ in the Sperm Whale," *J. Mar. Biol. Ass. U.K.* 58:27–71.

Clarke, M. R. 1979. "The Head of the Sperm Whale," *Sci. Amer.* 240:128–141.

Comstock, J. P. 1967. *Principles of Naval Architecture*. Society of Naval Architects and Marine Engineers, New York, NY.

Cranford, T. W., M. Amundin, and K. S. Norris. 1996. "Functional Morphology and Homology in the Odontocete Nasal Complex: Implications for Sound Generation," *J. Morph.* 228:223–285.

Crisp, D. J. 1955. "The Behaviour of Barnacle Cyprids in Relation to Water Movement Over a Surface," *J. Exp. Biol.* 32:569–590.

Crisp, D. J. and H. G. Stubbings. 1957. "The Orientation of Barnacles to Water Currents," *J. Animal Ecol.* 26:179–196.

Cruickshank, R. A. and S. G. Brown. 1981. "Recent Observations and Some Historical Records of Southern Right-Whale Dolphins, *Lissodelphis peronii," Fish. Bull. S. Afr.* 15:109–121.

Cummings, W. C., P. O. Thompson, and R. Cook. 1968. "Underwater Sounds of Migrating Gray Whales, *Eschrichtius glaucus* (Cope)," *J. Acoust. Soc. Am.* 44:1278–1281.

Curren, K. C. 1992. "Designs for Swimming: Morphometrics and Swimming Dynamics of Several Cetacean Species." M.S. Thesis. Memorial University of Newfoundland, St. John's, Newfoundland, Canada.

Curren, K. C., N. Bose, and J. Lien. 1993. "Morphological Variation in the Harbour Porpoise (*Phocoena phocoena*)," *Can. J. Zool.* 71:1067–1070.

Curren, K. C., N. Bose, and J. Lien. 1994. "Swimming Kinematics of a Harbor Porpoise (*Phocoena phocoena*) and an Atlantic White-sided Dolphin (*Lagenorhynchus acutus*)," *Mar. Mamm. Sci.* 10: 485–492.

van Dam, C. P. 1987. "Efficiency Characteristics of Crescent-shaped Wings and Caudal Fins," *Nature* 325:435–437.

Daniel, T. L. 1981. "Fish Mucus: In situ Measurements of Polymer Drag Reduction," *Biol. Bull.*, 160:376–382.

Daniel, T. L. 1984. "Unsteady Aspects of Aquatic Locomotion," *Am. Zool.* 24:121–134.

Daniel, T. 1988. "Forward Flapping Flight from Flexible Fins," *Can. J. Zool.* 66:630–638.

Daniel, T. 1991. "Efficiency in Aquatic Locomotion: Limitations from Single Cells to Animals."In *Efficiency and Economy in Animal Physiology*, pp. 83-95. R. W. Blake, Ed. Cambridge University Press, Cambridge, U.K.

Daniel, T., C. Jordan, and D. Grunbaum. 1992. "Hydromechanics of Swimming," In *Advances in Comparative & Environmental Physiology 11: Mechanics of Animal Locomotion*, pp. 17-49.
R. McN. Alexander, Ed. Springer-Verlag, Berlin, Germany.

Davis, R. W., G. A. J. Worthy, B. Würsig, and S. K. Lynn. 1996. "Diving Behavior and At-sea Movements of an Atlantic Spotted Dolphin in the Gulf of Mexico," *Mar. Mamm. Sci.* 12:569–581.

DeMont, M. E. 1990. "Tuned Oscillations in the Swimming Scallop *Pecten maximus," Can. J. Zool.* 68:786–791.

DeMont, M. E. and G. DeMont. 1988a. "Mechanics of Jet Propulsion in the Hydromeduan Jellyfish, *Polyorchis penicillatus*. I. Mechanical Properties of the Locomotor Structure," *J. Exp. Biol.* 134:313–332.

DeMont, M. E. and J. M. Gosline. 1988b. "Mechanics of Jet Propulsion in the Hydromeduan Jellyfish, *Polyorchis penicillatus*. II. Energetics of the Jet Cycle," *J. Exp. Biol.* 134:333–345.

DeMont, M. E. and J. M. Gosline. 1988c. "Mechanics of Jet Propulsion in the Hydromeduan Jellyfish, *Polyorchis penicillatus*. III. A Natural Resonating Bell; The Presence and Importance of a Resonant Phenomenon in the Locomotor Structure," *J. Exp. Biol.* 134:347-361.

Denny, M. W. 1993. *Air and water*. Princeton University Press, Princeton, NJ.

Dickinson, M. H., F-O. Lehmann, and S. P. Sane. 1999. "Wing Rotation and the Aerodynamic Basis of Insect Flight," *Science* 284:1954–1960.

Dolphin, W. F. 1987. "Ventilation and Dive Patterns of Humpback Whales, *Megaptera novaeangliae*, on their Alaskan Feeding Grounds," *Can. J. Zool.* 65:83–90.

Dolphin, W. F. 1988. "Foraging Dive Patterns of Humpback Whales, *Megaptera novaeangliae*, in Southeast Alaska: Cost-Benefit Analysis, *Can J. Zool.* 66:2432–2441.

Domenici, P. and R. W. Blake. 1991. "The Kinematics and Performance of the Escape Response in the Angelfish (*Pterophyllum eimekei*)," *J. Exp. Biol.* 156:187–205.

Domning, D. P. and V. De Buffrenil. 1991. "Hydrostasis in the Sirenia: Quantitative Data and Functional Interpretation," *Mar. Mamm. Sci.* 7:331–368.

Dohl, T. P., K. S. Norris, and I. Kang. 1974. "A Porpoise Hybrid: *Tursiops* x *Steno*," *J. Mamm.* 55:217-221.

Edel, R. K. and H. E. Winn. 1978. "Observations on Underwater Locomotion and Flipper Movement of the Humpback Whale *Megaptera novaeangliae*," *Mar. Biol.*, 48:279–287.

Edwards, E. F. 1992. "Evaluation of Energetics Models for Yellowfin Tuna (*Thunnus albacares*) and Spotted Dolphin (*Stenella attenuata*) in the Eastern Tropical Pacific Ocean," *SW Fish. Sci. Cen. Adm. Rept.* LJ-92-01.

Ellington, C. P. 1995. "Unsteady Aerodynamics of Insect Flight." In *Biological Fluid Dynamics*, pp. 109-129, C. P. Ellington and T. J. Pedley, Eds. The Company of Biologists, Cambridge, U.K.

Ellington, C. P., C. van den Berg, A. P. Willmott, and A. L. R. Thomas. 1996. "Leading-edge Vortices in Insect Flight," *Nature* 384:626–630.

English, A. W. 1976. "Limb movements and locomotor function in the California sea lion (*Zalophus californianus*)," *J. Zool., Lond.* 178: 341-364.

Erickson, G. E. 1995. "High Angle-of-Attack Aerodynamics," *Ann Rev. Fluid Mech.* 27: 45–88.

Essapian, F. S. 1955. "Speed-induced Skin Folds in the Bottle-nosed Porpoise," *Tursiops truncatus*. *Breviora Mus. Comp. Zool.* 43:1–4.

Fein, J. A. 1998. "Dolphin Drag Reduction: Myth or Magic." In Proceedings *of the International Symposium on Seawater Drag Reduction*, pp. 429–433, July 22-23, J. C. S. Meng, Ed. Newport, RI.

Fejer, A. A. and R. H. Backus. 1960. "Porpoises and the Bow-riding of Ships Under way," *Nature* 188:700–703.

Feldkamp, S. D. 1987. "Foreflipper Propulsion in the California Sea Lion, *Zalophus californianus*," *J. Zool., Lond.* 212:43–57.

Felts, W. J. L. 1966. "Some Functional and Structural Characteristics of Cetaceans Flippers and Flukes." In *Whales, Dolphins and Porpoises*, pp. 255–276, K. S. Norris, Ed. University of California Press, Berkeley, CA.

Fierstine, H. L. and V. Walters. 1968. "Studies of Locomotion and Anatomy of Scombrid Fishes," *Mem. S. Calif. Acad. Sci.* 6:1–31.

Fish, F. E. 1992. "Aquatic Locomotion." In *Mammalian Energetics: Interdisciplinary Views of Metabolism and Reproduction*, pp. 34–63, T. E. Tomasi and T. H. Horton, Eds. Cornell University Press, Ithaca, NY.

Fish, F. E. 1993a. "Influence of Hydrodynamic Design and Propulsive Mode on Mammalian Swimming Energetics," *Aust. J. Zool.* 42:79–101.

Fish, F. E. 1993b. "Power Output and Propulsive Efficiency of Swimming Bottlenose Dolphins (*Tursiops truncatus*)," *J. Exp. Biol.* 185:179–193.

Fish, F. E. 1996. "Transitions from Drag-based to Lift-based Propulsion in Mammalian Swimming," *Amer. Zool.* 36:628–641.

Fish. F. E. 1997. "Biological Designs for Enhanced Maneuverability: Analysis of Marine Mammal Performance." In *Tenth International Symposium on Unmanned Untethered Submersible Technology: Proceedings of the Special Session on Bio-Engineering Research Related to Autonomous Underwater Vehicles*, pp. 109–117, Autonomous Undersea Systems Institute, Lee, NH.

Fish, F. E. 1998a. "Comparative Kinematics and Hydrodynamics of Odontocete Cetaceans: Morphological and Ecological Correlates with Swimming Performance," *J. Exp. Biol.* 201:2867–2877.

Fish, F. E. 1998b. "Biomechanical Perspective on the Origin of Cetacean Flukes." In *The Emergence of Whales: Evolutionary Patterns in the Origin of Cetacea*, pp. 303-324, J. G. M. Thewissen, Ed. Plenum Press, New York, NY.

Fish, F. E. 1998c. "Imaginative Solutions by Marine Organisms for Drag Reduction." In *Proceedings of the International Symposium on Seawater Drag Reduction*, pp. 443-450, J. C. S. Meng, Ed. Newport, RI.

Fish, F. E., S. Innes, and K. Ronald. 1988. "Kinematics and Estimated Thrust Production of Swimming Harp and Ringed Seals," *J. Exp. Biol.* 137:157–173.

Fish, F. E. and C. A. Hui. 1991. "Dolphin Swimming—A Review," *Mamm. Rev.* 21:181–195.

Fish, F. E. and J. M. Battle. 1995. "Hydrodynamic Design of the Humpback Whale Flipper," *J. Morph.* 225:51–60.

Fitzgerald, J. W. 1991. "Artificial Dolphin Blubber Could Increase Sub Speed, Cut Noise," *Navy News Undersea Tech.* 9:1–2.

Fitzgerald, J. W., E. R. Fitzgerald, W. M. Carey, and W. A. von Winkle. 1995. "Blubber and Compliant Coatings for Drag Reduction in Water. II. Matched Shear Impedance for Compliant Layer Drag Reduction," *Mat. Sci. Eng.* C2:215–220.

Fitzgerald, J. W., J. E. Martin, and E. F. Modert. 1998. "Blubber and Compliant Coatings for Drag Reduction in Fluids: VI. Rotating Disc Apparatus for Drag Measurement on Compliant Layers." In Proceedings *of the International Symposium on Seawater Drag Reduction*, pp. 215-218, J. C. S. Meng, Ed. Newport, RI.

Flower, W. H. 1883. "On Whales, Past and Present, and their Probable Origin," *Nature* 28:226–230.

Gad-el-Hak, M. 1987. "Compliant Coatings Research: A Guide to the Experimentalist," *J. Fluid. Struct.*, 1:55–70.

Gad-el-Hak, M. 1998. "Compliant Coatings: The Simpler Alternative." In Proceedings *of the International Symposium on Seawater Drag Reduction*, pp. 197-204, J. C. S. Meng, Ed. Newport, RI.

Gal, J. M. 1993. "Mammalian Spinal Biomechanics. I. Static and Dynamic Mechanical Properties of Intact Intervertebral Joints," *J. Exp. Biol.* 174:247–280.

Gambell, R. 1985. "Fin Whale *Balaenoptera physalus* (Linnaeus, 1758)." In *Handbook of Marine Mammals, Volume 3 The Sirenians and Baleen Whales*, pp. 171-192, S. H. Ridgeway and R. Harrison, Eds. Academic Press, London, U.K.

Gaskin, D. E., P. W. Arnold, and B. A. Blair. 1974. "*Phocoena phocoena. Mamm,*" *Sp.* 42:1–8.

Gaskin, D. E., G. J. D. Smith, and A. P. Watson. 1975. "Preliminary Study of Movements of Harbour Porpoises (*Phocoena phocoena*) in the Bay of Fundy Using Radiotelemetry," *Can. J. Zool.* 53:1466-1471.

Gawn, R. W. L. 1948. "Aspects of the Locomotion of Whales," *Nature* 161:44–46.

Gero, D. R. 1952. "The Hydrodynamic Aspects of Fish Propulsion," *Am. Mus. Nov.* 1601:1–32.

Gibbs-Smith, C. H. 1962. *Sir George Cayley's Aeronautics 1796-1855*. Her Majesty's Stationery Office. London, U.K.

Gilmore, R. M. 1956. "The California Gray Whale," *Zoonooz* 29:4–6.

Godfrey, S. J. 1985. "Additional Observations of Subaqueous Locomotion in the California Sea Lion (*Zalophus californianus*)," *Aqu. Mamm.* 11:53–57.

Goforth, H. W. 1990. "Ergometry (exercise testing) of the Bottlenose Dolphin." In *The Bottlenose Dolphin*, pp. 559-574, S. Leatherwood, Ed. Academic Press, NY.

Gosline, J. M. and R. E. Shadwick, R. E. 1983. "The Role of Elastic Energy Storage Mechanisms in Swimming: An Analysis of Mantle Elasticity in Escape Jetting in the Squid, *Loligo opalescens*." *Can J. Zool.* 61:1421–1431.

Gordon, C. N. 1980. "Leaping Dolphins," *Nature* 287:759.

Gray, J. 1936. "Studies in Animal Locomotion VI. The Propulsive Powers of the Dolphin," *J. Exp. Biol.* 13: 192-199.

Gray, J. 1968. *Animal Locomotion.* Weidenfeld and Nicolson, London, U.K.

Grue, J., A. Mo, and E. Palm. 1988. "Propulsion of a Foil Moving in Water Waves," *J. Fluid Mech.* 186:393–417.

Gubbins, C., B. McCowan, L. K. Spencer, S. Hooper, and D. Reiss. 1999. "Mother-infant Spatial Relations in Captive Bottlenose Dolphins, *Tursiops truncatus*." *Mar. Mamm. Sci.* 15:751–765.

Gucinski, H. and R. E. Baier. 1983. "Surface Properties of Porpoise and Killer Whale Skin *in vivo*," *Amer. Zool.*, 23:959.

Haider, M. and D. B. Lindsley. 1964. "Microvibrations in Man and Dolphin," *Science* 146:1181–1183.

Hain, J. H. W., G. R. Carter, S. D. Kraus, C. A. Mayo, and H. E. Winn. 1982. "Feeding Behavior of the Humpback Whale, *Megaptera novaeangliae*, in the Western North Atlantic," *Fish. Bull.* 80:259–268.

Hamilton, J. L., W. A. McLellan, and D. A. Pabst. 1998. "Functional Morphology of Harbor Porpoise (*Phocoena phocoena*) Tailstock Blubber," *Amer. Zool.* 38:203A.

Hampton, I. F. G. and G. C. Whittow. 1976. "Body Temperature and Heat Exchange in the Hawaiian Spinner Dolphin, *Stenella longirostris*.," *Comp. Biochem. Physiol* 55A:195–197.

Hanson, M. T. and R. H. Defran. 1993. "The Behaviour and Feeding Ecology of the Pacific Coast Bottlenose Dolphin, *Tursiops truncatus*," *Aqu. Mamm.* 19.3:127–142.

Hansen, R.J. and J. G. Hoyt. (1984) "Laminar-to-turbulent Transition on a Body of Revolution With an Extended Favorable Pressure Gradient Forebody," Transactions of the ASME Vol. 106, June, 202-210.

Harper, K. A., M. D. Berkemeier, and S. Grace. 1998. "Modeling the Dynamics of Spring-driven Oscillating-foil Propulsion," *IEEE J. Ocean. Eng.* 23:285–296.

Harrison, R. J. and K. W. Thurley. 1972. "Fine Structural Features of Delphinid Epidermis," *J. Anat.*, 111:498–499.

Hartman, D. S. 1979. "Ecology and Behavior of the Manatee (*Trichechus manatus*) in Florida," *Sp. Publ. Amer. Soc. Mamm.* No. 5.

Harvey, E. N. 1952. *Bioluminescence.* Academic Press, New York, NY.

Haun, J. E., E. W. Hendricks, F. R. Borkat, R. W. Kataoka, D. A. Carder, and N. K. Chun. 1983. "Dolphin Hydrodynamics: Annual Report FY 82." NOSC* TR935. SSC San Diego, CA.

* Now SSC San Diego, CA.

Haun, J. E., E. W. Hendricks, F. R. Borkat,, R. W. Kataoka, D. A. Carder, C. A. Dooley, E. Lindner, and M. W. Stromberg. 1984. "Dolphin Hydrodynamics: FY83 and FY84 Report." NOSC* TR998. SSC San Diego, CA.

Haun , J. E. and E. W. Hendricks. 1988. "Dolphin Hydrodynamics," *Phys. Today* 41:S.39.

Hayes, W. D. 1953. "Wave Riding of Dolphins," *Nature* 172:1060.

Hayes, W. D. 1959. "Wave-riding of Dolphins," *Science* 130:1657–1658.

Hedrick, M. S. and D. A. Duffield. 1991. "Haematological and Rheological Characteristics of Blood in Seven Marine Mammal Species: Physiological Implications for Diving Behaviour," *J. Zool. Lond.* 225:273–283.

Henderson, Y. and H. W. Haggard. 1925. "The Maximum of Human Power and Its Fuel," *Amer. J. Physiol.* 72:264–282.

Henricks, E. W. and D. M. Ladd. 1991. "Skin Friction Measurements in Flows over Tethered Polymer Coatings." NOSC* TR1438. SSC San Diego, CA.

Herald, E. S., Brownell, R. L. Jr., W. E. Evans, and A. B. Scott. 1969. "Blind River Dolphin: First Side-swimming Cetacean," *Science* 166:1408–1410.

Herman, L. M. and W. N. Tavolga. 1980. "The Communication Systems of Cetaceans." In *Cetacean Behavior: Mechanisms and Functions*, pp. 149-209, L. M. Herman, Ed. Robert E. Krieger Publishing, Malabar, FL.

Herring, P. J. 1998. "Dolphins Glow with the Flow," *Nature* 393:731–733.

Hertel, H. 1966. *Structure, Form and Movement.* Rheinhold, New York, NY.

Hertel, H. 1969. "Hydrodynamics of Swimming and Wave-riding Dolphins." In *The Biology of Marine Mammals*, pp. 31-63, H. T. Andersen, Ed. Academic Press, New York, NY.

Hester, F. J., J. R. Hunter, and R. R. Whitney. 1963. "Jumping and Spinning Behavior in the Spinner Porpoise," *J. Mamm.* 44:586–588.

Hill, A. V. 1950. "The Dimensions of Animals and their Muscular Dynamics," *Sci. Prog.* 38:209–230.

Hobson, E. S. 1966. "Visual Orientation and Feeding in Seals and Sea Lions," Nature 214:326-327.

Hochachka, P. W. 1991. "Design of Energy Metabolism." In *Environmental and Metabolic Animal Physiology,* pp. 325-351, C. L. Prosser, Ed. Wiley-Liss, New York, NY.

Hoerner, S. F. 1965. *Fluid-Dynamic Drag.* Published by author, Brick Town, NJ.

Hoerner, S. F. and H. V. Borst. 1975. *Fluid-Dynamic Lift.* Published by the authors, Bricktown, NJ.

von Holste, E. and D. Kuchemann. 1942. "Biological and Aerodynamic Problems of Animal Flight," *J. Roy. Aero. Soc.* 46:44–54.

Howell, A. B. 1930. *Aquatic Mammals.* Charles C. Thomas, Springfield, IL.

Howland, H. C. 1974. "Optimal Strategies for Predator Avoidance: The Relative Importance of Speed and Manoeuvrability," *J. Theor. Biol.* 47:333–350.

Hoyt, J. W. 1975. "Hydrodynamic Drag Reduction due to Fish Slimes." In *Swimming and Flying in Nature,* pp. 653–672, T. Y. Wu, C. J. Brokaw, and C. Brennen, Eds. Plenum Press, New York, NY.

Hoyt, J. W. 1990. "Drag Reduction by Polymers and Surfactants." In *Viscous Drag Reduction in Boundary Layers.* D. M. Bushnell and J. N. Hefner, Eds. American Institute of Aeronautics and Astronautics, Inc., Washington, DC.

Hui, C. A. 1985. "Maneuverability of the Humboldt Penguin (*Spheniscus humboldti*) during Swimming," *Can. J. Zool.* 63:2165–2167.

Hui, C. 1987. "Power and Speed of Swimming Dolphins." *J. Mamm.* 68:126–132.

Hui, C. 1989. "Surfacing Behavior and Ventilation in Free-ranging Dolphins," *J. Mamm.* 70:833–835.

Hurt, H. H., Jr. 1965. *Aerodynamics for Naval Aviators.* U. S. Navy, NAVWEPS 00-80T-80.

Ingebrigtsen, A. 1929. "Whales Caught in the North Atlantic and Other Seas," *Rapp. P.-V. Reun. Cons. Int. Explor. Mer.* 56:1–26.

Jefferson, T. A. 1987. "A Study of the Behavior of Dall's Porpoise (*Phocoenoides dalli*) in Johnstone Strait, British Columbia," *Can J. Zool.* 65:736–744.

Joh, C. G. 1925. "The Motion of Whales during Swimming," *Nature* 116:327–329.

Johannessen, C. L. and J. A. Harder. 1960. "Sustained Swimming Speeds of Dolphins," *Science* 132:1550–1551.

Johnson, C. M. and K. S. Norris. 1994. "Social Behavior." In *The Hawaiian Spinner Dolphin*, pp. 243–286, K. S. Norris, B. Würsig, R. S. Wells, and M. Würsig, Eds. University of California Press, Berkeley, CA.

Jurasz, C. M. and V. P. Jurasz. 1979. "Feeding Modes of the Humpback Whale, *Megaptera novaeangliae*, in Southeast Alaska," Sci. *Rep. Whales Res. Inst.* 31:69–83.

Karpouzian, G., G. Spedding, and H. K. Cheng. 1990. "Lunate-tail Swimming Propulsion. Part 2. Performance Analysis," *J. Fluid Mech.* 210:329–351.

Katz, J. and D. Weihs. 1978. "Hydrodynamic Propulsion by Large Amplitude Oscillation of an Airfoil with Chordwise Flexibility," *J. Fluid Mech.*88:485–497.

Kawamura, A. 1975. "A Consideration on an Available Source of Energy and its Cost for Locomotion in Fin Whales with Special Reference to the Seasonal Migrations," *Sci. Rept. Whales Res. Inst.* 27:61–79.

Kayan, V. P. 1974. "Resistance Coefficient of the Dolphin," *Bionika* 8:31–35 (translated from Russian).

Kayan, V. P. 1979. "The Hydrodynamic Characteristics of the Caudal Fin of the Dolphin," *Bionika* 13:9–15 (translated from Russian).

Kayan, V. P. and V. Ye Pyatetskiy. 1977. "Kinematics of Bottlenosed Dolphins Swimming as Related to Acceleration Mode," *Bionika* 11:36–41 (translated from Russian).

Kayan, V. P. and V. Ye Pyatetskiy. 1978. "The Hydrodynamic Characteristics of the Black Sea Dolphin in Different Acceleration Modes." *Bionika* 12:48–55 (translated from Russian).

Kayan, V. P., L. F. Kozlov, and V. E. Pyatetskii. 1978. "Kinematic Characteristics of the Swimming of Certain Aquatic Animals," *Fluid Dynamics* 13:641–646 (translated from Russian).

Kellogg, R. 1928. "The History of Whales—Their Adaptation to Life in the Water," *Quart. Rev. Biol.* 3:29–76.

Kellogg, R. 1940. "Whales, Giants of the Sea," *Nat. Geo.* 67:35–90.

Kelly, H. R. 1959. "A Two -body Problem in the Echelon-formation Swimming of Porpoise," U.S. Nav. Ord. Test Sta. Tech. Note 40606-1, China Lake, CA.

Kermack, K. A. 1948. "The Propulsive Power of Blue and Fin Whales," *J. Exp. Biol.* 25:237–240.

Khomenko, B. G. and V. G. Khadzhinskiy. 1974. "Morphological and Functional Principles Underlying Cutaneous Reception in Dolphins," *Bionika* 8:106–113 (translated from Russian).

Klima, M., H. A. Oelschläger, and D. Wünsch. 1987. "Morphology of the Pectoral Girdle in the Amazon Dolphin Inia geoffrensis with Special Reference to the Shoulder Joint and the Movements of the Flippers," *Z. Saugertierkunde* 45:288–309.

Kooyman, G. L. 1989. *Diverse Divers:Physiology and Behavior.* Springer-Verlag, Berlin, Germany.

Kooyman, G. L. and L. H. Cornell. 1981. "Flow Properties of Expiration and Inspiration in a Trained Bottlenose Porpoise," *Physiol. Zool.*54:55–61.

Kooyman, G. L. and P. J. Ponganis. 1998. "The Physiological Basis of Diving to Depth: Birds and Mammals," *Ann. Rev. Physiol.* 60:19–32.

Kozlov, L. F. 1981. "Biological Power Engineering Method of Estimating the Hydrodynamic Resistance of Cetacea," *Bionika* 15:2–20 (translated from Russian).

Kozolv, L. F. and V. M. Shakalo. 1973. "Some Results of Measuring Velocity Pulsations in the Boundary Layer of Dolphins," *Bionika* 7:50–52 (translated from Russian).

Kozolv, L. F., V. M. Shakalo, L. D. Bur'yanova, and N. N. Vorob'yev. 1974. "Effect of Unsteadiness on Flow Conditions in the Boundary Layer of the Bottlenose Dolphin," *Bionika* 8:13–16 (translated from Russian).

Koslov, L. F. and S. V. Pershin. 1983. "Comprehensive Research on Hydrodynamic Drag Reduction in Dolphins by the Active Regulation of the Skin," *Bionika* 17:3–12 (translated from Russian).

Kramer, M. O. 1960a. "Boundary Layer Stabilization by Distributed Damping," *J. Amer. Soc. Nav. Eng.* 72:25–33.

Kramer, M. O. 1960b. "The Dolphins' Secret," *New Sci.*, 7:1118–1120.

Kramer, M. O. 1965. "Hydrodynamics of the Dolphin." In *Advances in Hydroscience*, Vol. 2, pp. 111–130, V. T. Chow, Ed. Academic Press, New York, NY.

Kriete, B. 1995. "Bioenergetics in the Killer Whale," *Orcinus orca*. Ph.D. Dissertation. University of British Columbia, Canada.

Kruse, S., D. K. Caldwell, and M. C. Caldwell. 1999. "Risso's Dolphin *Grampus griseus* (G. Cuvier, 1812)." In *Handbook of Marine Mammals*, Vol. 6, pp. 183–212, S. H. Ridgway and R. Harrison, Eds. Academic Press, San Diego, CA.

Kshatriya, M. and R. W. Blake. 1988. "Theoretical Model of Migration Energetics in the Blue Whale, *Balaenoptera musculus*," *J. Theor. Biol.* 133:479–498.

Küchermann, D. 1953. "The Distribution of Lift over the Surface of Swept Wings," *Aero. Quart.* 4:261–278.

Kükenthal, W. 1891. "On the Adaptation of Mammals to Aquatic Life," *Ann. Mag. Nat. Hist. Ser.*6 7:11–179.

Kumph, J. M. and M. S. Triantafyllou. 1998. "A Fast-starting and Maneuvering Vehicle, the ROBOPIKE." In *Proceedings of the International Symposium on Seawater Drag Reduction*, pp. 485–490, July 22-23, J. C. S. Meng, Ed. Newport, RI.

Lai, P. S. K., N. Bose, and R. C. McGregor. 1993. "Wave Propulsion from a Flexible-armed, Rigid-foil Propulsor," *Mar. Tech.* 30:30–38.

Lan, C. E. 1979. "The Unsteady Quasi-vortex-lattice Method with Applications to Animal Propulsion," *J. Fluid Mech.* 93:747–765.

Landahl, M. T. 1962. "On Stability of a Laminar Incompressible Boundary Layer over a Flexible Surface," *J. Fluid Mech.*, 13:609–632.

Lang, T. G. 1963. "Porpoise, Whale, and Fish: Comparison of Predicted and Observed Speeds," *Nav. Eng. J.* 75:437–441.

Lang, T. G. 1966a. "Hydrodynamic Analysis of Dolphin Fin Profiles," *Nature* 209:1110–1111.

Lang, T. G. 1966b. "Hydrodynamic Analysis of Cetacean Performance." In *Whales, Dolphins and Porpoises.*, pp. 410-432, K. S. Norris, Ed. University of California Press, Berkeley, CA.

Lang, T. G. 1975. "Speed, Power, and Drag Measurements of Dolphins and Porpoises." In *Swimming and Flying in Nature,* pp. 553–571, T. Y. Wu, C. J. Brokaw, and C. Brennen, Eds. Plenum Press, New York, NY.

Lang, T. G. and D. A. Daybell. 1963. "Porpoise Performance Tests in a Seawater Tank," Nav. Ord. Test Sta. Technical Report 3063, China Lake, CA.

Lang, T. G. and K. S. Norris. 1966. "Swimming Speed of a Pacific Bottlenose Porpoise," *Science* 151:588–590.

Lang, T. G. and Pryor, K. 1966. "Hydrodynamic Performance of Porpoises (*Stenella attenuata*)," *Science* 152: 531–533.

Larrabee, E. E. 1980. "The Screw Propeller," *Sci. Amer.* 243:134–148.

Latz, M. L., J. Rohr, and J. F. Case. 1995. "Description of a Novel Flow Visualization Technique Using Bioluminescent Marine Plankton," In *Flow Visualization*, Vol. VII, pp. 28-33, J. P. Crowder, Ed. Begell House, New York, NY.

Law, T. C. and R. W. Blake. 1994. "Swimming Behaviors and Speeds of Wild Dall's Porpoises (*Phocoenoides dalli*). *Mar. Mamm. Sci.* 10:208–213.

Leatherwood, S. 1974. "A Note on Gray Whale Behavioral Interactions with Other Marine Mammals," *Mar. Fish. Rev.* 26:50–51.

Leatherwood, S. and Ljungblad, D. K. 1979. "Nighttime Swimming and Diving Behavior of a Radio-Tagged Spotted Dolphin," *Stenella attenuata. Cetology* 34:1–6.

Leatherwood, S. and R. R. Reeves. 1986. "Porpoises and Dolphins." In *Marine Mammals of the Eastern North Pacific and Adjacent Arctic Waters*, pp. 110–131, D. Haley, Ed. Pacific Search Press, Seattle WA.

Leatherwood, S. and W. A. Walker. 1979. "The Northern Right Whale Dolphin *Lissodelphis borealis* Peale in the Eastern North Pacific." In *Behavior of Marine Animals*, vol. 3, pp. 85–141, H. E. Winn and B. L. Olla, Eds. Plenum Press, New York, NY.

Lewis, C. A. 1978. "A Review of Substratum Selection in Free-living and Symbiotic Cirripeds." In *Settlement and Metamorphosis of Marine Invertebrate Larvae*, pp. 207-218, F-S Chia and M. E. Rice, Eds. Elsevier, New York, NY.

Lighthill, J. 1960. "Note on the Swimming of Slender Fish," *J. Fluid Mech.* 4:397–430.

Lighthill, J. 1969. "Hydrodynamics of Aquatic Animal Propulsion—A Survey," *Ann. Rev. Fluid Mech.* 1:413–446.

Lighthill, J. 1970. "Aquatic Animal Propulsion of High Hydromechanical Efficiency," *J. Fluid Mech.* 44:265–301.

Lighthill, J. 1971. "Large-amplitude Elongate-body Theory of Fish Locomotion," *Proc. Roy. Soc.* B 179:125–138.

Lighthill, J. 1977. "Introduction to Scaling of Aerial Locomotion." In *Scale Effects in Animal Locomotion*, pp. 365–404, T. J. Pedley, Ed. Academic Press, London, U.K.

Lighthill, J. 1993. "Estimates of Pressure Differences Across the Head of a Swimming Clupeid Fish," *Phil. Trans. R. Soc. Lond. B* 341:129–140.

Lindsey, C. C. 1978. "Form, Function, and Locomotory Habits in Fish." In *Fish Physiology: Locomotion*, vol. 7, pp. 1-100, W. S. Hoar and D. J. Randall, Eds. Academic Press, New York NY.

Liu, P. and N. Bose. 1993. "Propulsive Performance of Three Naturally Occurring Oscillating Propeller Planforms," *Ocean Eng.* 20:57–75.

Lui, H., R. Wassersug, and E. Kawachi. 1997. "The Three-dimensional Hydrodynamics of Tadpole Locomotion," *J. Exp. Biol.* 200:2807–2819.

Lockyer, C. 1977. "Observations on the Diving Behavior of the Sperm Whale *Physeter catodon*." In *A Voyage of Discovery*, pp. 591–609, M. Angel, Ed. Pergamon Press, Oxford, U.K.

Lockyer, C. 1978. "The History and Behaviour of a Solitary Wild, but Sociable, Bottlenose Dolphin (*Tursiops truncatus*) on the West Coast of England and Wales," *J. Nat. Hist.* 12:513–528.

Lockyer, C. 1981. "Growth and Energy Budgets of Large Baleen Whales from the Southern Ocean." In *Mammals in the Sea*, vol. 3, pp. 379–487. FAO, Rome, Italy.

Lockyer, C. and R. Morris. 1987. "Observations on Diving Behaviour and Swimming Speeds in Wild Juvenile *Tursiops truncatus*," *Aqu. Mamm.* 13.1:31–35.

Long, J. H., Jr., D. A. Pabst, W. R. Shepherd, and W. A. McLellan. 1997. "Locomotor Design of Dolphin Vertebral Columns: Bending Mechanics and Morphology of *Delphinus delphis*," *J. Exp. Biol.* 200:65–81.

Lythgoe, J. N. 1972. "The Adaptation of Visual Pigments to the Photic Environment." In *Handbook of Sensory Physiology*, vol. VII. H. J. A. Dartnell, Ed.), pp. 566–603. Springer-Verlag, New York, NY.

Madigosky, W. M., G. F. Lee, J. Haun, F. Borkat, and R. Kataoka. 1986. "Acoustic Surface Wave Measurements on Live Bottlenose Dolphins," *J. Acoust. Soc. Am.* 79:153–159.

Madsen, C. J. and L. M. Herman. 1980. "Social and Ecological Correlates of Cetacean Vision and Visual Appearance." In *Cetacean Behavior:Mechanisms and Functions,* pp. 101–147, L. M. Herman, Ed. R. E. Krieger Publ., Malabar, FL.

Magnuson, J. J. 1978. "Locomotion by Scombrid Fishes: Hydrodynamics, Morphology and Behaviour." In *Fish Physiology*, vol. 7, pp. 239–313, W. S. Hoar and D. J. Randall, Eds. Academic Press, London, U.K.

Mankovskaya, I. N. 1975. "The Content and Distribution of Myoglobin in Muscle Tissue of Black Sea Dolphins," *Zh. Evol. Biokh. Fiziologii* 11:263–267.

Manning, G. C. 1930. *Manual of Naval Architecture*. van Nostrand, New York, NY.

Marchaj, C. A. 1964. *Sailing Theory and Practice*. Dodd, Mead and Co., New York, NY.

Marchaj, C. A. 1988. *Aero-Hydrodynamics of Sailing*. International Marine Publ., Camden, ME.

Maresca, C., D. Favier, and J. Rebont. 1979. "Experiments on an Aerofoil at High Angle of Incidence in Longitudinal Oscillations," *J. Fluid Mech.* 92:671–690.

Marino, L. and J. Stowe, 1997. "Lateralized Behavior in Two Captive Bottlenose Dolphins (Tursiops truncatus)," *Zoo Biol.* 16:173–177.

Martin, A. R., T. G. Smith, and O. P. Cox. 1993. "Studying the Behaviour and Movements of High Arctic Belugas with Satellite Telemetry," *Symp. Zool. Soc. Lond.* 66:195–210.

Maslov, N. K. 1970. "Maneuverability and Controllability of Dolphins," *Bionika* 4:46–50 (translated from Russian).

Mate, B. R. and Harvey, J. T. 1984. "Ocean Movements of Radio-tagged Gray Whales." In *The Gray Whale*, pp. 577–589, M. L. Jones, S. L. Swartz, and S. Leatherwood, Eds. Academic Press, Orlando, FL.

Mate, B. R., K. M. Stafford, R. Nawojchik, and J. L. Dunn. 1994. "Movements and Dive Behavior of a Satellite-monitored Atlantic White-sided Dolphin (*Lagenorhynchus acutus*) in the Gulf of Maine," *Mar. Mamm. Sci.* 10:116–121.

McCroskey, W. J. 1982. "Unsteady Airfoils," *Ann. Rev. Fluid Mech.* 14:285–311.

McGinnis, S. M., G. C Whittow, C. A Ohata, and H. Huber. 1972. "Body Heat Dissipation and Conservation in Two Species of Dolphins," *Comp. Biochem. Physiol.* 43A:417–423.

Miller, D. 1991. *Submarines of the World.* Orion Books, New York, NY.

Minasian, S. M., K. C. Balcomb III, and L. Foster, L. 1984. *The World's Whales.* Smithsonian Books, Washington, D. C.

von Mises, R. 1945. *Theory of flight.* Dover, New York, NY.

Mörzer Bruyns, W. F. J. 1971. *Field Guide to Whales and Dolphins.* Mees, Amsterdam, Netherlands.

Nakashima M. and K. Ono. 1999. "Experimental Study of Two-Joint Dolphin Robot." In *Eleventh International Symposium on Unmanned, Untethered Submersible Technology,* pp. 211–218, Autonomous Undersea Systems Institute. Lee, NH.

Newman, J. N. 1975. "Swimming of Slender Fish in a Non-uniform Velocity Field," *J. Austral. Math. Soc. B* 19:95–111.

Newman, J. N. and T. Y. Wu. 1974. "Hydromechanical Aspects of Fish Swimming." In *Swimming and Flying in Nature,* pp. 615–634, T. Y. Wu, C. J. Brokaw, and C. Brennen, Eds. Plenum Press, New York, NY.

Niiler, P. P. and H. J. White. 1969. "Note on the Swimming Deceleration of a Dolphin," *J. Fluid Mech.* 38:613–617.

Nishiwaki, M. 1972. "General Biology." In *Mammals of the Sea: Biology and Medicine*, pp. 3–204, S. H. Ridgway, Ed. C. C. Thomas, Springfield, IL.

Norris, K. S. and C. M. Johnson. 1994a. "Breathing at Sea." In *The Hawaiian Spinner Dolphin,*
pp. 206–215, K. S. Norris, B. Würsig, R. S. Wells, and M. Würsig, Eds. University of California Press, Berkeley, CA.

Norris, K. S. and C. M. Johnson. 1994b. "Schools and Schooling." In *The Hawaiian Spinner Dolphin*, pp. 232–242, K. S. Norris, B. Würsig, R. S. Wells, and M. Würsig, Eds. University of California Press, Berkeley, CA.

Norris, K. S., and J. H. Prescott. 1961. "Observations on Pacific Cetaceans of California and Mexican Waters," *Univ. Calif. Publ. Zool.* 63:291–402.

Norris, K. S., B. Würsig, R. S. Wells, M. Würsig, S. M. Brownlee, C. Johnson, and J. Solow. 1985. "The Behavior of the Hawaiian Spinner Dolphin," *Stenella longirostris. Southwest Fish. Center Admin. Rep.* LJ-85-06C.

Nowak, R. M. 1991. *Walker's Mammals of the World.* Johns Hopkins University Press, Baltimore, MD.

Ohmi, K., M. Coutanceau, T. P. Loc, and A. Dulieu. 1990. "Vortex Formation Around an Oscillating and Translating Airfoil at Large Incidences," *J. Fluid Mech.* 211:37–60.

van Oossanen, P. and M. W. C. Oosterveld. 1989. "Hydrodynamic Resistance Characteristics of humans, dolphins, and ship forms," *Schiffstechnik* 36:31–48.

Orton, L. S. and P. F. Brodie. 1985. "Whale Blubber Elasticity," *Amer. Zool.* 25:13A.

Pabst, D. A. 1988. "The Subdermal Connective Tissue Sheath in Dolphin is not a Typical Crossed Helical Fiber Array," *Amer. Zool.* 28:194A.

Pabst, D. A. 1990. "Axial Muscles and Connective Tissues of the Bottlenose Dolphin." In *The Bottlenose Dolphin*, pp. 51–67, S. Leatherwood and R. R. Reeves, Eds. Academic Press, San Diego, CA.

Pabst, D. A. 1993. "Intramuscular Morphology and Tendon Geometry of Epaxial Swimming Muscles of Dolphins," *J. Zool., Lond.* 230:159–176.

Pabst, D. A. 1996a. "Springs in Swimming Animals," *Amer. Zool.* 36:723–735.

Pabst, D. A. 1996b. "Morphology of the Subdermal Connective Tissue Sheath of Dolphins: a New Fibre-wound, Thin-walled, Pressurized Cylinder Model for Swimming Vertebrates," *J. Zool., Lond.* 238:35–52.

Pabst, D. A., W. A. McLellan, J. G. Gosline, and P. M. Piermarini. 1995a. "Morphology and Mechanics of Dolphin Blubber," *Amer. Zool.* 35:44A.

Pabst, D. A., S. A. Rommel, W. A. McLellan, T. M. Williams, and T. K. Rowles. 1995b. "Thermoregulation of the Intraabdominal Testes of the Bottlenose Dolphin (*Tursiops truncatus*) During Exercise," *J. Exp. Biol.* 198:221–226.

Pabst, D. A., W. A. McLellan, and J. H. Long, Jr. 1997. "Why Do Big Whales Swim Slowly?" *Amer. Zool.* 37:77A.

Palmer, E. and G. Weddel. 1964. "The Relationship Between Structure, Innervation and Function of the Skin of the Bottle Nose Dolphin (*Tursiops truncatus*)," *Proc. Zool. Soc. Lond.* 143:553–567.

Papastavrou, V., S. C. Smith, and H. Whitehead. 1989. "Diving Behaviour of the Sperm Whale, *Physeter macrocephalus*, Off the Galapagos Islands," *Can. J. Zool.* 67:839–846.

Parry, D. A. 1949a. "The Swimming of Whales and a Discussion of Gray's Paradox," *J. Exp. Biol.* 26:24–34.

Parry, D. A. 1949b. "Anatomical Basis of Swimming in Whales," *Proc. Zool. Soc. Lond.* 119:49–60.

Parry, D. A. 1949c. "The Structure of Whale Blubber, and a Discussion of its Thermal Properties," *Quart. J. Micro. Sci.* 90:13–25.

Parsons, J.S., R. E. Goodson, and F. R. Goldschmied. 1974. "Shaping of Axisymmetric Bodies for Minimum Drag in Incompressible Flow," J. Hydronautics, 8:100–107

Pedley, T. J. 1977. *Scale Effects in Animal Locomotion.* Academic Press. London, U.K.

Pelletier, C. and F. -X. Pelletier. 1980. "Rapport sur l'expedition delphinasia (Septembre 1977-Septembre 1978)," *Ann. Soc. Sci. Nat. Charente-Maritime* 6:647–679.

Perrin, W. F. 1975. "Variation of Spotted and Spinner Porpoise (genus *Stenella*) in Eastern Tropical Pacific and Hawaii," *Bull. Scripps Inst. Oceanogr,* no. 21.

Perrin, W. F., W. E. Evans, and D. B. Holts. 1979. "Movements of Pelagic Dolphins (*Stenella* spp.) in the Eastern Pacific as Indicated by Results of Tagging, with Summary of Tagging Operations, 1969-70," *NOAA Tech. Rept.* NMFS SSRF, 737:1–14.

Perrin, W. F., S. Leatherwood, and A. Collet. 1994. "Fraser's Dolphin *Lagenodelphis hosei* Fraser, 1956." In *Handbook of Marine Mammals*, Vol. 5: *The First Book of Dolphins*, pp. 225–240, S. H. Ridgway and R. Harrison, Eds. Academic Press: London,U.K.

Perry, B., A. J. Acosta, and T. Kiceniuk. 1961. "Simulated Wave-riding Dolphins," *Nature* 192:148–150.

Pershin, S. V. 1969. "The Hydrodynamic Characteristic of Cetaceans and Swimming Speeds of Dolphins Recorded in the Natural Environment and in Captivity," Bionika. 3. Izdvo Naukova, Kiev (translated from Russian).

Pershin, S. V. 1970. "Resonance Conditions in the Swimming of Dolphins," *Bionika* 4:31–36 (translated from Russian).

Pershin, S. V. 1975. "Hydrodynamic Analysis of Dolphin and Whale Fin Profiles," *Bionika* 9:26–32 (translated from Russian).

Pershin, S. V. 1983. "Hydrobionic Features for Optimizing the Exterior Forms of the Propeller System in cetaceans," *Bionika* 17:13–24 (translated from Russian).

Pershin, S. V. 1988. *Fundamentals of hydrobionics*. Sudostroyeniye Publ. Leningrad, Russia (translated from Russian).

Pershin, S. V., A. S. Sokolov, and A. G. Tomilin. 1979. "Regulated Hydroelastic Effect in the Fins of the Largest and Fastest Dolphin, the Killer Whale," *Bionika* 13:35–43 (translated from Russian).

Peterson, C. G. J. 1925. "The Motion of Whales During Swimming," *Nature* 116:327–329.

Pettigrew, J. B. 1893. *Animal Locomotion*. D. Appleton, New York, NY.

Pilleri, G. 1976. "Comparative Study of the Skin and General Myology of *Platanista indi* and *Delphinus delphis* in Relation to Hydrodynamics and Behaviour," *Invest. Cetacea* 6:89–127.

Pilleri, G. and J. Knuckey. 1969. "Behaviour Patterns of Some Delphinidae Observed in the Western Mediterranean," *Z. Tierpsychologie* 26:48–72.

Pilleri, G., M. Gihr, P. E. Purves, K. Zbinden, and C. Kraus. 1976. "On the Behaviour , Bioacoustics and Functional Morphology of the Indus River Dolphin (*Platanista indi* Blyth, 1859)," *Invest. Cetacea* 6:11–141.

Pilleri, G. and C. Peixun. 1979. "How the Finless Porpoise (*Neophocaena asiaeorientalis*) Carries its Calves on its Back, and the Function of the Denticulated Area of Skin, as Observed in the Changjiang River, China," *Invest. Cetacea* 10:105–110.

Pivorunas, A. 1979. "The Feeding Mechanisms of Baleen Whales," *Amer. Sci.* 67:432–440.

Platzer, M. F., J. C. S. Lai, and C. M. Dohring. 1998. "Flow Separation Control by Means of Flapping Foils." In *Proceedings of the International Symposium on Seawater Drag Reduction*, pp. 471–478, J. C. S. Meng, Ed. Newport, RI.

Ponganis, P. J. and R. W. Pierce. 1978. "Muscle Metabolic Profiles and Fiber-type Composition in Some Marine Mammals," *Comp. Biochem. Physiol.* 59B:99–102.

Purves, P. E. 1963. "Locomotion in Whales," *Nature* 197:334–337.

Purves, P. E. 1969. "The Structure of the Flukes in Relation to Laminar Flow in Cetaceans," *Z Saeugertierkd* 34:1–8.

Purves, P. E., W. H. Dudok van Heel, and A. Jonk. 1975. "Locomotion in Dolphins. Part I: Hydrodynamic Experiments on a Model of the Bottle-nosed Dolphin, *Tursiops truncatus*, (Mont.)," *Aqu. Mamm.* 3:5–31.

Purves, P. E. and G. Pilleri. 1978. "The Functional Anatomy and General Biology of *Pseudorca crassidens* (Owen) with a Review of the Hydrodynamics and Acoustics in Cetacea." In *Investigation on Cetacea*, vol. IX, pp. 68-227, G. Pilleri, Ed. Institute of Brain Anatomy, Bern, Switzerland.

Pyatetskiy, V. Ye. 1970. "Kinematics of Swimming Characteristics of Some Fast Marine Fish. *Bionika* 4:12–23 (translated from Russian).

Pyatetskiy, V. Ye. and V. M. Shakalo. 1975. "Flow Conditions in Boundary Layer of Dolphin Model," *Bionika* 9:46–50 (translated from Russian).

Pyatetskiy, V. Ye. and V. P. Kayan.1975. "On Kinematics of Swimming of Bottlenose Dolphin," *Bionika* 9:41-45 (translated from Russian).

Rao, D. M. 1991. "Vortex Control—Further Encounters," *AGARD-CP-494* Pap. No. 25.

Ray, G. C., E. D. Mitchell, D. Wartzok, V. M. Kozick, and R. Maiefsk. 1978. "Radiotracking of Fin Whale (*Balaenoptera physalus*)," *Science* 202:521–524.

Rayner, J. M. V. 1985. "Vorticity and Propulsion Mechanics in Swimming and Flying Animals," In *Konstruktionsprinzipen lebender und ausgestorbener Reptilien*, pp. 89–118, J. Riess and E. Frey, Eds. University of Tubingen, Tubingen, F.R.G.

Reeves, R. R. and S. Leatherwood. 1985. "Bowhead Whale *Balaena mysticetus* Linnaeus." 1758. In *Handbook of Marine Mammals*, Volume 3: *The Sirenians and Baleen Whales*, pp. 305-344, S. H. Ridgeway and R. Harrison, Eds. Academic Press, London, U.K.

Rehman, I. 1961. "Porpoise Aids Research," *Undersea Tech.* 2:36–39.

Reid, K., J. Mann, J. R. Weiner, and N. Hecker. 1995. "Infant Development in Two Aquarium Bottlenose Dolphins," *Zoo Biol.* 14:135–147.

Reidy, L. W. 1987. "Flat Plate Drag Reduction in a Water Tunnel Using Riblets," NOSC TD 1169 (May). Naval Ocean Systems Center*, San Diego, CA.

Renwick, D. M., R. Simmons, and S. C. Truver. 1997. "Marine Mammals are a Force Multiplier," *Nav. Inst. Proc.* 123:52–55.

---

* Now SSC San Diego.

Rice, D. W. 1989. "Sperm Whale *Physeter macrocephalus* Linnaeus." 1758. In *Handbook of Marine Mammals,* Vol. 4: *River Dolphins and the Larger Toothed Whales*," pp. 177-233, S. H. Ridgeway and R. Harrison, Eds. Academic Press, London, U.K.

Richardson, W. J. and C. Malme. 1993. "Man-made Noise and Behavioral Responses." In *The Bowhead Whale*, pp. 631–700, J. J. Burns, J. J. Montague, and C. J. Cowles, Eds. Sp. Pub. Soc. Mar. Mamm. No. 2.

Ridgway, S. H. and D. G. Johnston. 1966. "Blood Oxygen and Ecology of Porpoises of Three Genera," *Science* 151:456–457.

Ridgway, S. H., B. L. Scronce, and J. Kanwisher. 1969. "Respiration and Deep Diving in the Bottlenose Porpoise," *Science* 166:1651–1654.

Ridgway, S. H. and R. Howard. 1979. "Dolphin Lung Collapse and Intramuscular Circulation During Free Diving: Evidence From Nitrogen Washout," *Science* 206:1182–1183.

Ridgway, S. H., C. A. Bowers, D. Miller, M. L. Schultz, C. A. Jacobs, and C. A. Dooley. 1984. "Diving and Blood Oxygen in the White Whale," *Can. J. Zool.* 62:2349–2351.

Ridgway, S. H. and D. A. Carder. 1993. "Features of Dolphin Skin with Potential Hydrodynamic Importance," *IEEE Eng. Med. Biol.* 12:83–88.

Ridoux, V., C. Guinet, C. Liret, P. Creton, R. Steenstrup, and G. Beuplet. 1997. "A Video Sonar as a New Tool to Study Marine Mammals in the Wild: Measurements of Dolphin Swimming Speed," *Mar. Mamm. Sci.* 13:196–206.

Riley, J. J., M. Gad-el-Hak, and R. W. Metcalfe. 1988. "Compliant Coatings," *Ann. Rev. Fluid Mech.*, 20:393–420.

Rohr, J., G. W. Andersen, L. W. Reidy, and E. W. Hendricks. 1992. "A Comparsion of the Drag-Reducing Benefits of Riblets in Internal and External Flows," *Experiments in Fluids*, 13:361–368.

Rohr, J., M. I. Latz, S. Fallon, J. C. Nauen, and E. W. Hendricks. 1998a. "Experimental Approaches Towards Interpreting Dolphin-stimulated Bioluminescence," *J. Exp. Biol.* 201:1447–1460.

Rohr, J., E. Hendricks, L. Quigley, F. Fish, J. Gilpatrick, and J. Scardino-Ludwig. 1998b. "Observations of Dolphin Swimming Speed and Strouhal Number," TD 1769 (April). SSC San Diego, CA.

Romanenko, E. V. 1976. "Acoustics and Hydrodynamics of Certain Marine Animals," *Sov. Phys. Acoust.*, 22:357–358 (translated from Russian).

Romanenko, E. V. 1981. "Distribution of Dynamic Pressure Over the Body of an Actively Swimming Dolphin," *Sov. Phys. Dokl.* 26:1037–1038 (translated from Russian).

Romanenko, E. V. 1995. "Swimming of Dolphins: Experiments and Modelling." In *Biological Fluid Dynamics*, pp. 21-33, C. P. Ellington and T. J. Pedley, Eds. The Company of Biologists, Cambridge, U.K.

Romanenko, E. V. and V. G. Yanov. 1973. "Experimental Results of Studying the Hydrodynamics of Dolphins," *Bionika* 7:52–56 (translated from Russian).

Rommel, S. 1990. "Osteology of the Bottlenose Dolphin," In *The Bottlenose Dolphin*, pp. 29–49, S. Leatherwood and R. R. Reeves, Eds. Academic Press, San Diego, CA.

Rosen, M. W. 1959. "Water Flow About a Swimming Fish," NOTS TP 2298 (May). U. S. Naval Ordnance Test Station, China Lake, CA.

Rosen, M. W. 1962. "Experiments with Swimming Fish and Dolphins," *ASME Pap.* N. 61–WA–203.

Rosen, M. W. 1963. "Flow Visualization Experiments with a Dolphin," NOTS TP 3065 (April). U. S. Naval Ordnance Test Station, China Lake, CA.

Rosen, M. W. and N. E. Cornford. 1971. "Fluid Friction of Fish Slimes," *Nature*, 234:49–51.

Roithmayer, C. M. 1970. "Airborne Low-light Sensor Detects Luminescing Fish Schools at Night," Commercial Fisheries Review, Reprint No. 897, 32 (12):42–51.

Rugh, D. J. and J. C. Cubbage 1980. "Migration of Bowhead Whales Past Cape Lisburne," *Alaska. Mar. Fish. Rev.* 42:46–51.

Ryder, J. A. 1885. "On the Development of the Cetacea, Together with Consideration of the Probable Homologies of the Flukes of Cetaceans and Sirenians," *Bull. U.S. Fish Comm.* 5: 427–485.

Saayman, G. S. and C. K. Tayler. 1979. "The Socioecology of Humpback Dolphins (*Sousa* sp.)." In *Behavior of Marine Animals*, Vol. 3: *Cetaceans*, pp. 165-226, H. E. Winn and B. L. Olla, Eds. Plenum, New York, NY.

Saayman, G. S., D. Bower, and C. K. Tayler. 1972. "Observations on Inshore and Pelagic Dolphins on the South-eastern Cape Coast of South Africa," *Koedoe* 15:1–24.

Saunders, H. E. 1951. "Some Interesting Aspects of Fish Propulsion," *Soc. Nav. Arch. Mar. Eng., Ches. Sect.* (3 May).

Saunders, H. E. 1957. *Hydrodynamics in Ship Design.* Soc. Nav. Arch. Mar. Eng., New York, NY.

Scheffer, V. B. 1978. "False Killer Whale." In *Marine Mammals of Eastern North Pacific and Arctic Waters*, pp. 129-131, D. Haley, Ed. Pacific Search Press, Seattle, WA.

Schmidt-Nielsen, K. 1972. "Locomotion: Energy Cost of Swimming, Flying, and Running," *Science* 177: 222–228.

Scholander, P. F. 1959a. "Wave-riding Dolphins, How Do They Do It?," *Science* 129:1085–1087.

Scholander, P. F. 1959b. "Wave-riding Dolphins," *Science* 130:1658.

Scholander, P. F. and W. E. Schevill. 1955. "Counter-current Vascular Exchange in the Fins of Whales," *J. Appl. Physiol.* 8:279–282.

Semonov, N. P., V. V. Babenko, and V. P. Kayan, 1974. "Experimental Research on Some Features of Dolphin Swimming Hydrodynamics," *Bionika* 8: 23–31 (translated from Russian).

Shaffer, S. A., D. P. Costa, T. M. Williams, and S. H. Ridgway. 1997. "Diving and Swimming Performance of White Whales, *Delphinapterus leucas*: an Assessment of Plasma Lactate and Blood Gas Levels and Respiratory Rates," *J. exp. Biol.* 200:3091–3099.

Shapiro, A. H. 1961. *Shape and Flow: the Fluid Dynamics of Drag.* Doubleday and Company, Inc., New York, NY.

Sharpe, F. A. and L. M. Dill. 1997. "The Behavior of Pacific Herring Schools in Response to Artificial Humpback Whale Bubbles," *Can J. Zool.* 75:725–730.

Shaw, W. C. 1959. "Sea Animals and Torpedoes," NOTS TP 2299 (August). U. S. Naval Ordnance Test Station, China Lake, CA.

Shevell, R. S. 1986. "Aerodynamic Anomalies: Can CFD Prevent or Correct Them?" *J. Aircraft* 23:641–649.

Shoemaker, P. A. and S. H. Ridgway. 1991. "Cutaneous Ridges in Odontocetes," *Mar. Mamm. Sci.* 7:66–74.

Shpet, N. G. 1975. "Distinctions of Body Shape and Caudal Fin of Whales," *Bionika* 9:36–41.

Similä, T. and F. Ugarte. 1993. "Surface and Underwater Observations of Cooperatively Feeding Killer Whales in Northern Norway," *Can J. Zool.* 71:1494–1499.

Skrovan, R. C., T. M. Williams, P. S. Berry, P. W. Moore, and R. W. Davis. 1999. "The Diving Physiology of Bottlenose Dolphins (*Tursiops truncatus*) II: Biomechanics and Changes in Buoyancy at Depth," *J. Exp. Biol.* (In press).

Slijper, E. J. 1961. "Locomotion and Locomotory Organs in Whales and Dolphins (Cetacea)," *Symp. Zool. Soc. Lond.* 5:77–94.

Smith, G. J. D., K. W. Browne, and D. E. Gaskin. 1976. "Functional Myology of the Harbour Porpoise, *Phocoena phocoena* (L.)," *Can. J. Zool.* 54:716–729.

Smith, H. C. 1992. *Illustrated Guide to Aerodynamics.* McGraw-Hill, Blue Ridge Summit, PA.

Smith, T. G., D. B. Siniff, R., Reichle, and S. Stone. 1981. "Coordinated Behavior of Killer Whales, *Orcinus orca*, Hunting a Crabeater Seal, *Lobodon carcinophagus*," *Can J. Zool.* 59:1185–1189.

Sokolov, V., I. Bulina, and V. Rodionov. 1969. "Interaction of Dolphin Epidermis with Flow Boundary Layer," *Nature*, 222:267–268.

Sokolov, V. Ye. and A. V. Yablokov. 1978. *Advances in Cetacean and Pinniped Research.* Nauka, Moscow (translated from Russian).

Sokolov, W. 1960. "Some Similarities and Dissimilarities in the Structure of the Skin Among the Members of the Suborders Odontoceti and Mystacoceti (Cetacea)," *Nature* 185:745–747.

Staples, R. F. 1966. "The Distribution and Characteristics of Surface Bioluminescence in the Oceans." Technical Report 184, U.S. Naval Oceanographic Office, Stennis Space Center, MS

Stas, I. I. 1939a. "Recording on the Dolphin's Body Movement in the Sea," *Acad. Sci. USSR* 24:536–539.

Stas, I. I. 1939b. "Once More on the Recording on the Movements of the Dolphin in the Sea," *Acad. Sci. USSR* 25:668.

Stefanick, T. 1988. "The Nonacoustic Detection of Submarines," *Sci Amer.* 258:41–47.

Steven, G. A. 1950. "Swimming of Dolphins," *Sci. Prog.* 38:524–525.

Stone, N. L. 1980. "Dolphins, Submarines, Speed and Surprises," *Military Electronics/ Countermeasures* 6:46–51.

Strickler, T. L. 1980. "The Axial Musculature of *Pontoporia blainvillei*, with Comments on the Organization of this System and its Effect on Fluke-stroke Dynamics in the Cetacea," *Amer. J. Anat.* 157:49–59.

Sumich, J. L. 1983. "Swimming Velocities, Breathing Patterns, and Estimated Costs of Locomotion in Migrating Gray Whales," *Eschrichtius robustus. Can. J. Zool.* 61:647–652.

Suzuki, A., T. Tsuchiya, Y. Takahashi, and H. Tamate. 1983. Histochemical Properties of Myofibers in Longissimus Muscle of Common Dolphins (*Delphinus delphis*)," *Acta Histochem. Cytochem.* 16:223–231.

Swain, G. 1998. "Biofouling Control: A Critical Component of Drag Reduction." In *Proceedings of the International Symposium on Seawater Drag, Reduction*, pp. 155-161, J. C. S. Meng, Ed. Newport, RI.

Tanaka, S. 1987. "Satellite Radio Tracking of Bottlenose Dolphins *Tursiops truncatus*," *Nippon Suisan Gakkaishi* 53:1327–1338. (in Japanese)

Tavolga, M. C. and F. S. Essapian. 1957. "The Behavior of the Bottle-nosed Dolphin (*Tursiops truncatus*): Mating, Pregnancy, Parturition, and Mother-infant Behavior," *Zoologica* 42:11–31.

Taylor, D. W. 1933. *The Speed and Power of Ships*. Washington, D. C., Ransdell Inc.

Thewissen, J. G. M. 1998. *The Emergence of Whales*. Plenum, New York, NY.

Thewissen, J. G. M. and Fish, F. E. 1997. Locomotor Evolution in the Earliest Cetaceans: Functional Model, Modern Analogues, and Paleontological Evidence. *Paleobiology*, 23:482–490.

Toedt, M. E., L. E. Reuss, R. M. Dillaman, and D. A. Pabst. 1997. "Collagen and Elastin Arrangement in the Blubber of Common Dolphin (*Delphinus delphis*)," *Amer. Zool.* 37:56A.

Tomilin, A. G. 1957. *Mammals of the U.S.S.R. and Adjacent Countries*. Vol. IX, *Cetacea*. Izdatel'stvo Akademi Nauk SSSR, Moskva (translated from Russian).

Triantafyllou, M. S., G. S. Triantafyllou, and R. Gopalkrishnan. 1991. "Wake Mechanics for Thrust Generation in Oscillating Foils," *Phys. Fluids A* 3:2835–2837.

Triantafyllou, G. S., M. S. Triantafyllou, and M. A. Grosenbaugh. 1993. "Optimal Thrust Development in Oscillating Foils with Application to Fish Propulsion," *J. Fluids Struc.* 7:205–224.

Triantafyllou, M. S. and G. S. Triantafyllou. 1995. "An Efficient Swimming Machine," *Sci. Amer.* 272:64–69.

Triantafyllou, M. S., D. S. Battett, D. K. P. Yue, J. M. Anderson, M. A. Grosenbaugh, K. Streitien, and G. S. Triantafyllou. 1996. "A New Paradigm of Propulsion and Maneuvering for Marine Vehicles," *SNAME Trans.* 104:81–100.

True, F. W. 1983. *The Whalebone Whales of the Western North Atlantic.* Smithsonian Institution Press, Washington, D.C.

Tucker, V. A. 1970. "Energetic Cost of Locomotion in Animals," *Comp. Biochem. Physiol.* 34:841–846.

Tucker, V. A. 1975. "The Energetic Cost of Moving About," *Amer. Sci.* 63: 413–419.

Uskova, Ye. T., A. N. Shmyrev, V. S. Rayevskiy, L. N. Bogdanova, L. N., Momot, V. V. Belyayev, and I. A. Uskov. 1983. "The Nature and Hydrodynamic Activity of Dolphin Eye Secretions," *Bionika* 17:72–75 (translated from Russian).

Vasilevskaya, G. I. 1974. "Structural Features of the Delphinid Pectoral Flippers," *Bionika* 8:127–132 (translated from Russian)

Videler, J. 1993. *Fish Swimming.* Chapman and Hall, London, U.K.

Videler, J. and P. Kamermans. 1985. "Differences Between Upstroke and Downstroke in Swimming Dolphins," *J. Exp. Biol.* 119:265–274.

Videler, J. J. and B. A. Nolet. 1990. "Cost of Swimming Measured at Optimum Speed: Scale Effects, Differences Between Swimming Styles, Taxonomic Groups and Submerged and Surface Swimming," *Comp. Biochem. Physiol.* 97A:91–99.

Vincent, J. 1990. *Structural biomaterials.* Princeton University Press, Princeton, NJ.

Vogel, S. 1994. *Life in Moving Fluids.* Princeton University Press, Princeton, NJ.

Vogel, S. 1998. *Cat's Paws and Catapults.* W. W. Norton, New York, NY.

Wainwright, S. A., D. A. Pabst, and P. F. Brodie. 1985. "Form and Possible Function of the Collagen Layer Underlying Cetacean Blubber," *Amer. Zool.* 25:146A.

Walsh, M. J. 1990. "Riblets." In *Viscous Drag Reduction in Boundary Layers*, D. M. Bushnell and J. N. Hefner Eds. *Prog. Astro. Aero.*, 123:203–261.

Walters, V. 1962. "Body Form and Swimming Performance in Scombrid Fishes," *Am. Zool.*, 2:143–149.

Watkins, W. A., J. Sigurjónson, D. Wartzok, R. R. Maiefski, P. W. Howey, and M. A. Daher, 1996. "Fin Whale Tracked by Satellite Off Iceland," *Mar. Mamm. Sci.* 12:564–569.

Watson, A. G. and R. E. Fordyce. 1993. "Skeleton of Two Minke Whales, *Balaenoptera acutorostrata*, Stranded on the South-east Coast of New Zealand," *New Zealand Nat. Sci.* 20:1–14.

Watts, E. H. 1961. "The Relationship of fish locomotion to the design of ships. *Symp. Zool. Soc. Lond.* 5:37–41.

Webb, P. W. 1975. "Hydrodynamics and Energetics of Fish Propulsion," *Bull. Fish. Res. Bd. Can.* 190:1–158.

Webb, P. W. 1976. "The Effect of Size on the Fast-start Performance of Rainbow Trout, *Salmo gairdneri*, and a Consideration of Piscivorous Predator-prey Interactions," *J. Exp. Biol.* 65:157–177.

Webb, P. W. 1983. "Speed, Acceleration and Maneuverability of Two Teleost Fishes," *J. Exp. Biol.* 102:115–122.

Webb, P. W. 1984. "Form and Function in Fish Swimming," *Sci. Amer.* 251:72–82.

Webb, P. W. 1997. "Designs for Stability and Maneuverability in Aquatic Vertebrates: What can we learn?" In *Tenth International Symposium on Unmanned Untethered Submersible Technology: Proceedings of the Special Session on Bio-Engineering Research Related to Autonomous Underwater Vehicles* (pp. 86–103). Autonomous Undersea Systems Institute, Lee, NH.

Webb, P. W. and V. de. Buffrénil.1990. "Locomotion in the Biology of Large Aquatic Vertebrates," *Trans. Amer. Fish. Soc.* 119:629–641.

Wegner, P. P. 1991. *What Makes Airplanes Fly?* Springer-Verlag, New York, NY.

Weihs, D. 1972. "Semi-infinite Vortex Trails, and Their Relation to Oscillating Airfoils," *J. Fluid Mech.* 54:679–690.

Weihs, D. 1973. "Hydromechanics of Fish Schooling," *Nature* 241:290–291.

Weihs, D. 1981. "Effects of Swimming Path Curvature on the Energetics of Fish Motion," *Fish. Bull.* 79:171–176.

Weihs, D. 1989. "Design Features and Mechanics of Axial Locomotion in Fish," *Amer. Zool.* 29:151–160.

Weihs, D. 1993. "Stability of Aquatic Animal Locomotion," *Cont. Math.* 141:443–461.

Weihs, D. and P. W. Webb. 1983. "Optimization of Locomotion." In *Fish Biomechanics*, pp. 339-371, P. W. Webb and D. Weihs, Eds. Praeger, New York, NY.

Weis-Fogh, T. and R. McN. Alexander. 1977. "The Sustained Power Output from Striated Muscle." In *Scale Effects in Animal Locomotion*, pp. 511-525, T. J. Pedley, Ed. Academic Press, London, U.K.

White, F. M. 1979. *Fluid Mechanics*. McGraw-Hill, New York, NY.

Whitehead, H. and C. Carlson. 1988. "Social Behavior of Feeding Finback Whales Off Newfoundland: Comparison with the Sympatric Humpback Whale," *Can. J. Zool.* 217–221.

Williams, T. M. 1987. "Approaches for the Study of Exercise Physiology and Hydrodynamics in Marine Mammals." In *Approaches to Marine Mammal Energetics*, pp. 127-145, A. C. Huntley, D. P. Costa, G. A. J. Worthy, and M. A. Castellini, Eds. Spec. Publ. Soc. Mar. Mamm. No. 1.

Williams, T. M. 1989. "Swimming by Sea Otters: Adaptations for Low Energetic Cost Locomotion," *J. Comp. Physiol. A* 164:815–824.

Williams, T. M. 1998. "The Evolution of Cost Efficient Swimming in Marine Mammals: Limits to Energetic Optimization," *Phil. Trans. R. Soc. Lond. B* 353:1–9.

Williams, T. M. and G. L. Kooyman. 1985. "Swimming Performance and Hydrodynamic Characteristics of Harbor Seals," *Phoca vitulina. Physiol. Zool.* 58:576–589.

Williams, T. M., W. A. Friedl, M. L. Fong, R. M. Yamada, P. Sedivy, and J. E. Haun. 1992. "Travel at Low Energetic Cost by Swimming and Wave-riding Bottlenose Dolphins," *Nature* 355:821–823.

Williams, T. M., W. A. Friedl, and J. E. Haun. 1993a. "The Physiology of Bottlenose Dolphins (*Tursiops truncatus*): Heart Rate, Metabolic Rate and Plasma Lactate Concentration During Exercise," *J. Exp. Biol.* 179:31–46.

Williams, T. M., W. A. Friedl, J. E. Haun, and N. K. Chun. 1993b. "Balancing Power and Speed in Bottlenose Dolphins (*Tursiops truncatus*)," *Symp. Zool. Soc. Lond.* 66:383–394.

Williams, T. M., S. F. Shippee, and M. J. Rothe. 1996. "Strategies for Reducing Foraging Costs in Dolphins." In *Aquatic Predators and Their Prey*, pp. 4-9, S. P. R. Greenstreet and M. L. Tasker, Eds. Fishing News Books, Oxford, U.K.

Williamson, G. R. 1972. "The True Body Shape of Rorqual Whales," *J. Zool., Lond.* 167:277–286.

Wilson, A. D. 1999. "Using Marine Mammals When Technology Fails," *Sea Tech.* 40:61–63.

Winn, H. E. and B. L. Olla. 1979. *Behavior of Marine Animals*, Vol. 3. Plenum Press, NY.

Winn, H. E. and N. E. Reichley. 1985. "Humpback whale *Megaptera novaeangliae* (Borowski, 1981)." In *Handbook of Marine Mammals*, Vol. 4 *River Dolphins and the Larger Toothed Whales*, pp. 177-233, S. H. Ridgway and R. Harrison, Eds. Academic Press, London, U.K.

Winn, L. K. and H. E. Winn. 1985. *Wings in the Sea: The Humpback Whale*. University Press of New England, Hanover, MA.

Wolfgang, M. J., S. W. Tolkoff, A. H. Techet, D. S. Barrett, M. S. Triantafyllou, D. K. P. Yue, F. S. Hover, M. A. Grosenbaugh, and W. R. McGillis. 1998. "Drag Reduction and Turbulence Control in Swimming Fish-like Bodies." In *Proceedings of the International Symposium on Seawater Drag Reduction*, pp. 485-490, J. C. S. Meng, Ed. Newport, RI.

Wolman, A. A. 1985. "Gray whale *Eschrichtius robustus* (Lilljeborg, 1861)." In *Handbook of Marine Mammals,* Vol. 3 *The Sirenians and Baleen Whales*, pp. 67-90, S. H. Ridgeway and R. Harrison, Eds. Academic Press, London, U.K.

Wood, C. J. 1998. "Movement of Bottlenose Dolphins Around the South-west Coast of Britain," *J. Zool.* 246: 155–163.

Wood, F. G. 1973. *Marine Mammals and Man: The Navy's Porpoises and Sea Lions*. Robert B. Luce, Washington.

Woodcock, A. H. 1948. "The Swimming of Dolphins," *Nature* 161:602.

Woodcock, A. H. and A. F. McBride.1951. "Wave-riding Dolphins," *J. Exp. Biol.* 28:215–217.

Worthy, G. A. J., S. Innes, B. M. Braune, and R. E. A. Stewart. 1987. "Rapid Acclimation of Cetaceans to an Open-system Respirometer." In *Approaches to Marine Mammal Energetics*, pp. 115–126, A. C. Huntley, D. P. Costa, G. A. J. Worthy, and M. A. Castellini, Eds. Sp. Pub. Soc. Mar. Mamm. No. 1.

Wu, J. Z., A. D. Vakili, and J. M. Wu. 1991. "Review of the Physics of Enhancing Vortex Lift by Unsteady Excitation," *Prog. Aerospace Sci.* 28:73–131.

Wu, T. Y. 1971a. "Hydrodynamics of Swimming Propulsion. Part 1. Swimming of a Two-Dimensional Flexible Plate at Variable Forward Speeds in an Inviscid Fluid," *J. Fluid Mech.* 46:337–355.

Wu, T. Y. 1971b. "Hydrodynamics of Swimming Propulsion. Part 2. Some Optimum Shape Problems," *J. Fluid Mech.* 46:521–544.

Wu, T. Y. 1972. "Extraction of Flow Energy by a Wing Oscillating in Waves," *J. Ship Res.* 14:66–78.

Würsig, B. and M. Würsig. 1979. "Behavior and Ecology of the Bottlenose Dolphin, *Tursiops truncatus*, in the South Atlantic," *Fish. Bull.* 77: 399–412.

Würsig, B., F. Cipriano, and M. Würsig, 1991. "Dolphin Movement Patterns: Information from Radio and Theodolite Tracking Studies." In *Dolphin Societies:Discoveries and Puzzles*, pp. 79-111, K. Pryor and K. Norris, Eds. University of California Press, Berkeley, CA.

Würsig, M., B. Würsig, and J. F. Mermoz. 1977. "Desplazamientos, comportamiento general y un varamiento de la marsopa espinosa *Phocoena spinipinnis*, en el Golfo San Jose (Chubut, Argentina)," *Physis, Buenos Aires* 36:71–79.

Wyrick, R. F. 1954. "Observations on the Movements of the Pacific Gray Whale," *Eschrichtius glaucus* Cope. *J. Mamm.* 35:506–598.

Yanov, V. G. 1990. "Kinematics of Dolphins: New Experimental Results," *Sov. Phys. Dokl.* 35:921–923 (translated from Russian).

Yanov, V. G. 1991. "System-functional Organization of the Swim Kinematics of a Dolphin," *Dokl. Akad. Nauk SSSR* 317:1089–1093 (translated from Russian).

Yasui, W. Y. 1980. "Morphometrics, Hydrodynamics and Energetics of Locomotion for a Small Cetacean, *Phocoena phocoena* (L.)," Master of Science thesis, University of Guelph, Ontario, Canada.

Yazdi, P., A. Kilian, and B. Culik. 1999. "Energy Expenditure of Swimming Bottlenose Dolphins (*Tursiops truncatus*)," *Mar. Biol.* (In press).

Yates, G. T. 1983. "Hydromechanics of Body and Caudal Fin Propulsion." In *Fish Biomechanics*, pp. 177–213, P. W. Webb and D. Weihs, Eds. Praeger, New York, NY.

Yuen, H. S. H. 1961. "Bow Wave Riding of Dolphins," *Science* 134:1011–1012.

Yurchenko, N. F. and V. V. Babenko. 1980. "Stabilization of the Longitudinal Vortices by Skin Integuments of Dolphins," *Biophysics* 25:309–315.

Zeh, J. E., C. W. Clark, J. C. George, D. Withrow, G. M. Carroll, and W. R. Koshi. 1993. "Current Population Size and Dynamics." In *The Bowhead Whale*, pp. 409–489, J. J. Burns, J. J. Montague and C. J. Cowles, Eds. Sp. Pub. Soc. Mar. Mamm. No. 2.

APPENDIX A

BRIEF DESCRIPTION OF THE HYDRODYNAMIC TERMS USED THROUGHOUT THIS REPORT

Added mass coefficient is the ratio of the added mass to the mass of the displaced fluid. Added mass is an inertial force associated with the fluid that has to be moved around the accelerating body. An illustrative example of added mass is the increase of apparent inertia when moving an arm or paddle through water (Birkhoff, 1960; Childress, 1981). In contrast to drag, which will decrease acceleration and increase deceleration, added mass will reduce the rate of both acceleration and deceleration. The added mass coefficient depends on the density of the fluid and the shape of the body. Because the mass of the displaced fluid in air is much less than the mass of the body, added mass effects are much less important for flow around bodies in air than water. Nevertheless a pendulum clock with a spherical bob will run about 10 seconds slower per day in air than in a vacuum (Vogel, 1981). Added mass decreases the more streamlined the body is. For a sphere the added mass coefficient is (as computed for an ideal fluid) 0.5, 0.082 for a 4:1 spheroid and 0.067 for a fusiform dolphin (Gordon, 1980).

Angle of attack is the angle between the chord line and the flight direction. Inviscid airfoil theory predicts that the lift coefficient will increase linearly with angle of attack. Experiments with a NACA 0012 airfoil (commonly used on airplane tails and helicopter blades) show good agreement with theory until about 12° angle of attack, when flow separation occurs.

Aspect ratio is a geometric parameter of a wing defined as the square of the wingspan divided by the planform area of the wing. For a square lifting surface the aspect ratio is one. At constant angle of attack increasing the aspect ratio of a wing will generally increase the lift coefficient.

Bernoulli equation is a fundamental relation between kinetic ($1/2\ \rho\ U^2$) and potential ($\rho g h + p$) energy of a fluid particle moving along a constant energy stream. Here ρ, U, h are respectively the density, velocity and height (above some reference plane) of the fluid particle, g is the acceleration of gravity and p is the static pressure. A consequence of this equation is that in a nonviscous fluid deceleration of fluid particles along a streamline is accompanied by a rise in pressure. Conversely, in a nonviscous flow acceleration of fluid particles is accompanied by a fall in pressure along a streamline. Within the boundary layer the Bernoulli equation cannot be applied because of the importance of viscous forces near the boundary. However, when the boundary layer is thin the pressure will be the same as in the adjacent, essentially inviscid, outer flow where application of the Bernoulli equation is valid.

Boundary layer (δ) is the area of fluid adjacent to a body where the fluid velocity is effected by the presence of the body. At the body the fluid, because of molecular interactions, shares the same speed as the body. At some distance away body the fluid velocity is essentially the same as if the body was not there. There is of course no line where the presence of the body will have absolutely no effect on the flow. Often the boundary layer is arbitrarily taken as the region where the velocity differs by more than 1% than the freestream velocity. Note that the boundary layer is not a streamline.

Because of the thinness of the boundary layer and the difference in velocities between the body and the freestream fluid, large gradients in velocity can result. These large velocity gradients make viscous effects more pronounced (Note: There is no change in viscosity) so that viscous and inertial forces are of the same order. Boundary layers can be experienced at the sea shore, where they might be around 1 m thick, by standing in a strong wind and then stretching out on the beach, where much less wind would be felt (Nakayama and Boucher, 1999).

The boundary layer can also be defined as the region of appreciable vorticity. (The vorticity at a point can be thought as twice the instantaneous rate of spin of a small element of fluid centered at the point.) The generation of vorticity in the boundary layer is associated with pressure gradients. For an infinite flat plate

at zero angle of attack vorticity is generated at the tip of the plate and advected downstream. The thickness of this stream of advected vorticity grows along the plate as it diffuses outward. Except for where transition from laminar to turbulent flow occurs, at any downstream location the thickness of the boundary layer decreases with increasing (higher Reynolds number) flow. At some location downstream the boundary layer becomes unstable and small disturbances grow until the whole boundary layer is turbulent.

The thickness of a boundary layer on a flat plate, set up parallel to the free-stream for laminar flow grows like:

$$\delta(x) = x\ (4.99)\ (\nu/xU)^{1/2} = x\ (4.99)\ Re_x^{-1/2};$$

and for turbulent flow grows like:

$$\delta(x) = x\ (0.37)\ (\nu/xU)^{1/5} = x\ (0.37)\ Re_x^{-1/5}.$$

where ν is the kinematic viscosity of sea water (1.06×10^{-2} cm^2/s for seawater), x is the distance from the beginning of the plate, U is the free-stream velocity and Re is the Reynolds number.

Chord (C) is defined as the distance between the leading and trailing edges of a wing (or flipper).

Camber line for a cross section of a wing (or flipper) lies exactly between upper and lower wing surfaces. A cambered (curved) airfoil will produce more lift than a flat plat for the same angle of attack, and will also produce lift at zero angle of attack.

Circulation. Circulation within a closed contour in a body of fluid is defined as the integral around the contour of the component of the velocity vector, which is locally tangent to the contour (Currie, 1974).

Drag (D) is the resistance experienced by a moving object, a force in the direction opposite to its motion. Drag is equal to the rate of removal of momentum from a moving fluid by an immersed body. The drag on a swimming dolphin can be comprised of skin-friction, form, induced and wave drag components. All these resistive components arise from two types of forces, either normal or tangential to the body surface.

(1) Skin-friction drag is the resistance to motion, either laminar or turbulent, arising from shear stresses on the dolphin body.

(2) Form drag results from the pressure imbalance between the front and the back of the body. A large pressure imbalance can occur when the boundary layer separates from the surface of the body. The separated region is composed of low-energy, recirculating flow that exerts surface pressures on the aft end of a body that are less than if the flow was still attached.

(3) Induced drag is a by-product of lift as it is due to the pressure difference between the top and bottom surfaces of a wing (or fluke or fin). As the higher pressure, bottom surface fluid is pushed towards the lower pressure, upper surface region the flow tends to curl around the wing tip from bottom to top. This curling action superimposed on the main flow over the wing produces a vortex. These mini tornadoes disturb the flow near them, causing additional pressure drag (Anderson, 1998).

(4) Bodies at or near the air-water interface experience yet another type of resistance to motion when they make waves. The normal pressure field around a body moving at or near the water surface will produce elevations and depressions at the free surface since this must be a surface of constant pressure. Since these waves possess energy they represent a loss of energy from the body. At about three body widths beneath the surface, surface wave drag is negligible (Hertel, 1966).

Freestream velocity is the flow velocity relative to the body and far enough away from the body, so as not to be effected by its presence.

Froude Number (Fr) in the present context can is defined as the ratio of swimming speed to surface wave velocity. Froude numbers less than and greater than one are analogous for a compressible gas to subsonic and supersonic flow respectively.

Laminar flow is characterized by fluid particles that travel smoothly along a well-defined path. In laminar flow the speed at a fixed position is always the same and each fluid particle maintains its position between adjacent particles. Consequently when dye is injected into laminar flow a ribbon of dye is observed. The sole source of shear stress in laminar flow is due to viscosity. The viscous stresses developed in laminar flows of most fluids of interest (such as air, water and sea water) are found to be equal to the product of the kinematic viscosity and the local velocity gradient. This relationship was first proposed by Isaac Newton in 1687 (Cajori, 1946):

> "The resistance arising from want of lubricity in the parts of the fluid, is, other things being equal, proportional to the velocity with which the parts of the fluid are separated from one another."

Lift (L) is the rate of creation of a momentum, i.e. a force, normal to the flow of the undisturbed stream.

"no slip condition" refers to the thermodynamically imposed flow condition that the fluid at the boundary must, on average, move at the same velocity of the boundary (Rosenhead, 1963). At room temperature and pressure collisions between the molecules of the fluid and the surface over 1 second are of the order of 10^{-10}. Consequently, molecules adjacent to the boundary typically have the same velocity and temperature as the body. Note this does not necessitate that this layer is always composed of the same molecules.

Planform area (A) is the projected area of a body as seen from above (perpendicular to flow direction). Planform area is often used as the characteristic area in the definition of the drag coefficient for wide, flat bodies such as wings, fins and hydrofoils. (For more stubby bodies such as spheres cars and torpedoes the characteristic area is usually the projected area of the body as seen from the stream. For submerged bodies the total wetted area may be used.)

Reduced frequency (σ) is a nondimensional measure of the rate of change in oscillation with respect to the free stream velocity (Hoerner and Borst, 1985).

Reynolds number (Re) is a measure of the ratio of inertial forces acting on a small parcel of fluid to the force developed on the fluid parcel by viscous stresses. For large Reynolds numbers inertial forces predominate, for small Reynolds numbers viscous forces are most important. A person swims through water at a Re of about 10^6, through thick syrup at a Re of about 1. Although the Reynolds numbers associated with swimming dolphins are of the order of millions, within the boundary layer viscous forces can not be neglected. Reynolds numbers are always the product of a velocity (here the swimming speed) and a characteristic length (here the length of the person) divided by the kinematic viscosity (about 0.01 cm^2/sec for water). If inertial and viscous forces are the only important forces on a fluid particle, then at the same Reynolds number the flow around geometrically similar shapes will be similar

Separation is when the boundary layer separates from the body, resulting in a large increase in form drag . A fundamental feature of separation is the convection of vorticity away from the surface (and hence a much larger wake). Separation occurs when an external pressure increasing along the body, causes flow in the boundary layer to reverse direction. Streamlining the body can reduce external pressure gradients and thus decrease the chance of separation. A turbulent boundary layer is also less likely to separate because turbulent shear stresses provide momentum from the free stream that can push the boundary layer further downstream against an unfavorable pressure gradient.

Streamlines are curves whose direction at each point coincides with the direction of the velocity of the fluid. In a steady flow streamlines are also the paths along which fluid particles move. No fluid crosses a streamline. A shape is said to be streamlined if there is no boundary layer separation. Leonardo da Vinci (1452–1519) recognized the vortex formation behind bodies as the main source of its resistance and has been attributed with "inventing" streamlining as a method of drag reduction long before science justified it (von Kaman, 1942). The profile of a fish appears next to Leonardo's sketches of streamlined shapes (Anderson, 1998). At speeds less than the speed of sound it is far more important to streamline the back, rather than the front, of the body (Faber, 1995). A cylinder, fit with a fairing, at a Reynolds number of about 10^5 will experience a drag force reduction of about a factor of 50 (Faber, 1995).

Strouhal number (St) is used to scale oscillatory fluid phenomena, it can be thought as a dimensionless frequency. Historically the Strouhal number is considered as the proportionality constant between the frequency of vortex shedding and the free stream velocity divided by the body width. In the present context the body width is interpreted as double the amplitude of the tail excursion, the frequency is that of the tail oscillation, and the velocity is simply the swimming speed.

Turbulent flow is characterized by disordered fluid motions, is irreproducible in detail, performs efficient mixing and transport, and has vorticity irregularly distributed in three dimensions (Stewart, 1980). In turbulent flow there are two mechanisms, viscous and turbulent shear stresses, associated with momentum exchange. In fully developed (mean velocity profile not changing downstream) pipe flow the total shear stress, τ_{total} is:

$$\tau_{total} = \text{turbulent and laminar} = \rho\langle u'v'\rangle + \mu(dU/dr)$$

where $\langle u'v'\rangle$ represents the time-averaged product of the fluctuating velocities in the longitudinal and radial directions, du/dr is the cross-stream gradient of average velocity, and ρ and μ are respectively the density and kinematic viscosity of the water. Although individual turbulent velocity fluctuations are only a few per cent of average mean velocity, turbulent shear stresses except at the wall, constitute most of the total shear stress throughout the pipe.

Anderson, J. D. 1998. *A History of Aerodynamics.* Cambridge University Press, Cambridge, United Kingdom.

Birkhoff, G. *Hydrodynamics, a Study in Logic, Fact and Similitudel.* Princeton University Press, Princeton, New Jersey.

Cajori, F. 1946. *Sir Isaac Newton's Mathematical Principles.* Berkeley Press, Berkely, CA

Childress, S. 1981. *Mechanics of Swimming and Flying.* Cambridge University Press, Cambridge, United Kingdom.

Currie, I. G. 1974. *Fundamental Mechanics of Fluids.* McGraw-Hill, Inc. New York, NY.

Faber, T. E. 1995. *Fluid Dynamics for Physicists.* Cambridge University Press, Cambridge, United Kingdom.

Gordon, C. N. 1980. "Leaping Dolphins," *Nature* 287:759

Hertel, H. 1966. *Structure, Form and Movement.* Rheinhold. New York, NY.

Horner, S. F. and H. V. Borst. 1975. *Fluid-Dynamic Lift.* Published by author, Brick Town, NJ.

Nakayama Y. and R. F. Boucher. 1999. *Introduction to Fluid Mechanics.* Arnold Publishers, London, U.K.

Rosenhead, L. *Laminar Boundary Layers.* Dover Pub. Inc., New York, NY.

Stewart, R. W. 1980. "Turbulence." In *Illustrated Experiments in Fluid Mechanics*, pp 82-88. National Committee for Fluid Mechanics Films, The MIT Press, Cambridge, MA.

Vogel, S. 1981. *Life in Moving Fluids.* Princeton University Press, Princeton, NJ.

Von Karman Theodore 1942. "Isaac Newton and Aerodynamics," *Journal of Aeronautical Sciences*, 9:521–522.

APPENDIX B

REPORTED DOLPHIN SWIMMING SPEED MEASUREMENTS

Species	Speed (m/s)	Performance	Source
Balaena mysticetus	2.1	cruising	Tomilin, 1957
Balaena mysticetus	3.6-4.6	burst	Tomilin, 1957
Balaena mysticetus	0.5-1.0	lazing in feeding grounds	Williamson, 1972
Balaena mysticetus	1.5-2.1	migrating	Williamson, 1972
Balaena mysticetus	4.1	maximum (chased by catcher)	Williamson, 1972
Balaena mysticetus	0.9	migrating	Braham et al., 1980
Balaena mysticetus	1.3	migrating	Rugh and Cubbage, 1980
Balaena mysticetus	0.4-1.7	migrating	Reeves and Leatherwood, 1985
Balaena mysticetus	6.3	maximum	Reeves and Leatherwood, 1985
Balaena mysticetus	0.8-1.2	migrating	Zeh et al., 1993
Balaena mysticetus	2.1-2.9	fleeing	Richardson and Malme, 1993
Balaenoptera acutorstrata	0.5-1.5	lazing in feeding grounds	Williamson, 1972
Balaenoptera acutorstrata	1.5-2.6	migrating	Williamson, 1972
Balaenoptera acutorstrata	7.2	maximum (chased by catcher)	Williamson 1972
Balaenoptera acutorstrata	3.3	maximum cruising	Blix and Folkow, 1995
Balaenoptera borealis	13.4	maximum	Tomilin, 1957
Balaenoptera borealis	0.5-1.5	lazing in feeding grounds	Williamson, 1972
Balaenoptera borealis	1.5-3.1	migrating	Williamson, 1972
Balaenoptera borealis	8.2	maximum (chased by catcher)	Williamson, 1972
Balaenoptera borealis	<4.6	migrating	Lockyer, 1981
Balaenoptera borealis	8.2	maximum	Lockyer, 1981
Balaenoptera edeni	0.5-1.5	lazing in feeding grounds	Williamson, 1972
Balaenoptera edeni	1.5-3.1	migrating	Williamson, 1972

Species	Speed (m/s)	Performance	Source
Balaenoptera edeni	8.2	maximum (chased by catcher)	Williamson, 1972
Balaenoptera musculus	7.5	maximum (2 hr)	Gawn, 1948
Balaenoptera musculus	2.7-3.6	feeding	Tomilin, 1957
Balaenoptera musculus	8.0-8.9	burst	Tomilin, 1957
Balaenoptera musculus	10.2	maximum (10 min)	Tomilin, 1957
Balaenoptera musculus	0.5-1.5	lazing in feeding grounds	Williamson, 1972
Balaenoptera musculus	1.5-3.1	migrating	Williamson, 1972
Balaenoptera musculus	8.2	maximum (chased by catcher)	Williamson, 1972
Balaenoptera musculus	0.6-1.8	feeding	Lockyer, 1981
Balaenoptera physalus	1.3-1.8	feeding	Tomilin, 1957
Balaenoptera physalus	3.6-4.0	migrating	Tomilin, 1957
Balaenoptera physalus	6.9	maximum	Tomilin, 1957
Balaenoptera physalus	5.8-6.3	maximum (1 hr)	Tomilin, 1957
Balaenoptera physalus	0.5-1.5	lazing in feeding grounds	Williamson, 1972
Balaenoptera physalus	1.5-3.1	migrating	Williamson, 1972
Balaenoptera physalus	8.2	maximum (chased by catcher)	Williamson, 1972
Balaenoptera physalus	2.5	sustained	Ray et al., 1978
Balaenoptera physalus	>10.3	burst	Gambell, 1985
Balaenoptera physalus	1.5-2.6	routine	Whitehead and Carlson, 1988
Balaenoptera physalus	0.7-5.9	sustained	Watkins et al., 1996
Berardius sp.	0.8-1.1	routine	Balcomb, 1989
Caperea marginata	<2.6	routine	Baker, 1985
Dephinapterus leucas	1.3-2.2	cruising	Tomilin, 1957
Dephinapterus leucas	0.5	feeding	Tomilin, 1957
Dephinapterus leucas	3.1-4.0	migrating	Tomilin, 1957
Dephinapterus leucas	6.1	maximum (schooling)	Tomilin, 1957
Dephinapterus leucas	0.8-2.5	routine	Nowak, 1991
Dephinapterus leucas	6.1	maximum	Nowak, 1991

Species	Speed (m/s)	Performance	Source
Dephinapterus leucas	0.6-1.1	routine	Martin et al., 1993
Delphinus bairdi	1.5	maximum sustained	Norrris and Prescott, 1961
Delphinus capensis	6.7	maximum	Rohr et al., 1998b
*Delphinus delphis**	1.6	routine	Hui, 1987
Delphinus delphis	10.3	7 sec	Gray, 1936
Delphinus delphis	9.3	maximum	Kellogg, 1940
Delphinus delphis	12.5-13.9	maximum	Tomilin, 1957
Delphinus delphis	9.3	maximum	Johannessen and Harder, 1960
Delphinus delphis	13.2	maximum	Pershin, 1969
Delphinus delphis	2.8	routine	Nowak, 1991
*Delphinus delphis**	8.0	maximum	Rohr et al., 1998b
Eschrichtius robustus	2.4	migrating	Wyrick, 1954
Eschrichtius robustus	4.4	maximum	Gilmore, 1956
Eschrichtius robustus	3.6	chased	Tomilin, 1957
Eschrichtius robustus	2.8	migrating	Cummings et al., 1968
Eschrichtius robustus	0.5-1.0	lazing in feeding grounds	Williamson, 1972
Eschrichtius robustus	1.5-2.1	migrating	Williamson, 1972
Eschrichtius robustus	3.6	maximum (chased by catcher)	Williamson, 1972
Eschrichtius robustus	2.0	migrating	Sumich, 1983
Eschrichtius robustus	1.0-1.4	migrating	Mate and Harvey, 1984
Eschrichtius robustus	1.9-2.5	routine	Wolman, 1985
Eschrichtius robustus	0.9	feeding	Würsig et al., 1986
Eubalaena glacialis	1.8	cruising	Tomilin, 1957
Eubalaena glacialis	3.6	burst	Tomilin, 1957
Eubalaena glacialis	0.5-1.0	lazing in feeding grounds	Williamson, 1972
Eubalaena glacialis	1.5-2.1	migrating	Williamson, 1972
Eubalaena glacialis	4.1	maximum (chased by catcher)	Williamson, 1972
Globicephala sp.	11.3	maximum sustained	Johannessen and Harder, 1960

Species	Speed (m/s)	Performance	Source
Globicephala melaena	2.6-3.6	routine	Pilleri and Knuckey, 1969
Grampus griseus	1.7-1.9	routine	Kruse et al., 1999
Grampus griseus	7.8-8.9	maximum	Kruse et al., 1999
Inia geoffrensis	0.4-0.9	rountine	Best and da Silva, 1989
Inia geoffrensis	3.9	maximum	Best and da Silva, 1989
Kogia breviceps	1.5	routine	Morzer Bruyns, 1971
Lagenodelphis hosei	7.7	high speed schooling	Perrin et al., 1994
*Lagenorhynchus acutus**	1.4-3.4	routine	Curren et al., 1994
Lagenorhynchus acutus	3.95	sustained	Mate et al., 1994
*Lagenorhynchus obliquidens**	7.7	2 sec	Lang and Daybell, 1963
Lagenorhynchus obliquidens	7.2	burst	Ridgway and Johnston, 1966
Lagenorhynchus obscurus	1.7-5.8	routine	Würsig et al., 1991
Lissodelphis sp.	12.5	burst	Nowak, 1991
Lissodelphis borealis	9.4	maximum	Leatherwood and Walker, 1979
Lissodelphis peronii	6.1	maximum	Cruickshank and Brown, 1981
Megaptera novoangliae	1.1-4.0	migrating	Chittleborough, 1953
Megaptera novoangliae	1.1-4.0	cruising	Tomilin, 1957
Megaptera novoangliae	3.6-4.2	migrating	Tomilin, 1957
Megaptera novoangliae	7.5	burst (wounded)	Tomilin, 1957
Megaptera novoangliae	2.6-3.1	migrating	Dawbin, 1966
Megaptera novoangliae	0.5-1.0	lazing in feeding grounds	Williamson, 1972
Megaptera novoangliae	1.5-2.1	migrating	Williamson, 1972
Megaptera novoangliae	4.1	maximum (chased by catcher)	Williamson, 1972
Megaptera novoangliae	2.6	feeding	Jurasz and Jurasz, 1979
Megaptera novoangliae	0.44-0.66	migrating	Baker et al., 1985
Megaptera novoangliae	0.5-1.5	routine	Whitehead and Carlson, 1988

Species	Speed (m/s)	Performance	Source
Megaptera novoangliae	1.3	migrating	Gabriele et al., 1996
Mesoplodon stejnegeri	1.5-2.1	cruising	Bruyns, 1971
Mesoplodon stejnegeri	3.1	maximum	Bruyns, 1971
Monodon monoceros	0.8-2.3	migrating	Dietz and Heide-Jorgensen, 1995
Orcinus orca	10.3	maximum	Gawn, 1948
Orcinus orca	5.1	cruising (pack-12-13 abreast; 1 hr)	Tomilin, 1957
Orcinus orca	10.6	20 min	Johannessen and Harder, 1960
Orcinus orca	15.4	maximum	Johannessen and Harder, 1960
Orcinus orca	2.8-3.6	cruising	Nowak, 1991
Orcinus orca	12.5	maximum	Nowak, 1991
*Orcinus orca**	7.91	maximum	Fish, 1998a
Peponocephala sp.	5.6	unknown	Nowak, 1991
Phocoenoides dalli	5.6-5.8	cruising (following ship)	Tomilin, 1957
Phocoenoides dalli	8.9	burst	Ridgway and Johnston, 1966
Phocoenoides dalli	1.9	sustained	Gaskin et al., 1975
Phocoenoides dalli	15.3	burst	Leatherwood and Reeves, 1986
Phocoenoides dalli	1.4	average cruising	Jefferson, 1987
Phocoenoides dalli	6.0	maximum	Law and Blake, 1994
Phocoenoides dalli	1.6-3.4	routine	Law and Blake, 1994
Phocoena phocoena	4.6-6.2	maximum	Gaskin et al., 1974
*Phocoena phocoena**	2.0	routine	Worthy et al., 1987
Phocoena phocoena	6.1	maximum (pursued)	Nowak, 1991
Phocoena phocoena	2.8	migration	Bel'kovich et al., 1991
Phocoena phocoena	0.6-0.8	hunting	Bel'kovich et al., 1991
*Phocoena phocoena**	1.3-2.0	routine	Curren et al., 1994
Phocoena spinipinnis	1.0-1.25	surface swimming	Würsig et al., 1977
Physeter macrocephalus	1.3	cruising	Tomilin, 1957
Physeter macrocephalus	2.2-3.1	migrating	Tomilin, 1957

Species	Speed (m/s)	Performance	Source
Physeter macrocephalus	4.0-5.4	maximum (wounded)	Tomilin, 1957
Physeter macrocephalus	2.8	cruise	Berzin, 1972
Physeter macrocephalus	8.3	maximum	Berzin, 1972
Physeter macrocephalus	0.0-1.0	lazing in feeding grounds	Williamson, 1972
Physeter macrocephalus	1.5-2.1	migrating	Williamson, 1972
Physeter macrocephalus	4.1	maximum (chased by catcher)	Williamson, 1972
Physeter macrocephalus	12.7	maximum descent	Lockyer, 1977
Physeter macrocephalus	2.8	sustained	Papastavrou et al., 1989
Physeter macrocephalus	2.1	Routine	Rice, 1989
Physeter macrocephalus	8.3	burst	Rice, 1989
Physeter macrocephalus	0.68-0.82	surface swimming	Watkins et al., 1993
*Plantanista indi**	1.5	maximum (panic)	Pilleri et al., 1976
Plantanista sp.	7.5	maximum (in current)	Pelletier and Pelletier, 1980
Pseudorca crassidens	3.1	routine	Norris and Prescott, 1961
Pseudorca crassidens	6.2-7.2	routine	Scheffer, 1978
*Pseudorca crassidens**	7.46	maximum	Fish, 1998a
*Pseudorca crassidens**	8.0	maximum	Rohr et al., 1998b
*Sotalia guianensis**	2.4	routine	Videler and Kamermans, 1985
Sousa sp.	1.3	routine	Saayman and Tayler, 1979
Stenella sp.	0.4-1.9	16 hr	Perrin et al., 1979
Stenella sp.	7.3	burst	Au and Weihs, 1980a
Stenella sp.	6.7	burst	Au and Perryman, 1982
Stenella sp.	4.6	maximum cruise	Au and Perryman, 1982
Stenella sp.	8.2	maximum	Au et al., 1988
Stenella sp.	6.1-7.8	maximum	Nowak, 1991
*Stenella attenuata**	11.1	burst	Lang and Pryor, 1966
Stenella attenuata	6.2	burst	Leatherwood and Ljungblad, 1979
Stenella attenuata	3.3	average cruising	Leatherwood and Ljungblad, 1979

Species	Speed (m/s)	Performance	Source
Stenella longirostris	4.5	cruising	Au and Perryman, 1982
Stenella longirostris	4.8	pursued	Au and Perryman, 1982
Stenella longirostris	0.7-1.6	average cruising	Norris et al., 1985
Tursiops truncatus@*	8.3	7.5 sec	Lang and Norris, 1966; Lang, 1975
Tursiops truncatus@*	7.01	10 sec	Lang and Norris, 1966; Lang, 1975
Tursiops truncatus@*	6.09	50 sec	Lang and Norris, 1966; Lang, 1975
Tursiops truncatus@*	3.08	indefinitely	Lang and Norris, 1966; Lang, 1975
Tursiops truncatus	2.7	average cruising	Saayman et al., 1972
Tursiops truncatus	10.3	maximum sustained	Lockyer, 1978
Tursiops truncatus	1.7	average cruising	Würsig and Würsig, 1979
Tursiops truncatus	>8.3	burst	Würsig and Würsig, 1979
*Tursiops truncatus**	1.77-3.19	routine	Videler and Kamermans, 1985 *Tursiops*
Tursiops truncatus	15.0	burst	Lockyer and Morris, 1987
Tursiops truncatus	4.2	average cruising	Lockyer and Morris, 1987
Tursiops truncatus	2.1	maximum sustained	Tanaka, 1987
*Tursiops truncatus**	6.01	maximum	Fish, 1993b
Tursiops truncatus	8.15	burst	Henricks et al., 1994
Tursiops truncatus	2.2	routine	Ridoux et al., 1997
*Tursiops truncatus**	8.15	maximum	Rohr et al., 1998b
Tursiops truncatus	2.2	sustained	Wood, 1998
"dolphins"	7.2-9.3	maximum	Johannessen and Harder, 1960

* captive animals
@ *Tursiops truncatus* listed in source as *Tursiops gilli*

APPENDIX C

MORPHOLOGICAL MEASUREMENTS FOR ODONTOCETE CONTROL SURFACES

Species	Length (cm)	Fluke Span (cm)	Fluke AR	Fluke Sweep (deg)	Flipper Length (cm)	Flipper AR	Fin Height (cm)	Fin AR	Fin Sweep (deg)
Cephalorhynchus commersonii	136.5	38.2	3.3	37.5	22.8	4.0	14.0	0.7	41.8
Delphinapterus leucas	356.0	86.0	3.3	29.9	49.0	2.0	0.0	0.0	0.0
Delphinapterus leucas	399.0	102.0	4.0	14.6	54.0	2.2	0.0	0.0	0.0
Delphinapterus leucas	412.0	91.0	3.4	27.7	58.0	2.4	0.0	0.0	0.0
Delphinus delphis	182.0	36.0	4.0	33.1	28.2	5.5	17.4	1.1	46.1
Delphinus delphis	196.3	49.0	3.5	36.3	33.8	5.0	23.0	1.9	30.1
Delphinus delphis	199.0	45.3	3.9	31.7	32.9	5.2	21.6	1.2	47.5
Delphinus delphis	199.7	40.6	3.8	32.5	33.9	5.7	18.6	1.2	45.3
Delphinus delphis	200.0	50.0	4.1	34.1	31.9	4.7	23.3	1.3	46.2
Delphinus delphis	201.5	46.9	4.5	36.2	32.0	5.5	19.1	1.0	54.5
Delphinus delphis	203.1	49.9	4.9	34.7	32.4	5.1	21.6	1.3	50.9
Delphinus delphis	205.5	48.5	4.4	31.0	34.9	5.9	20.6	1.1	43.4
Delphinus delphis	214.5	49.3	4.2	32.9	33.7	5.2	23.1	1.3	45.7
Delphinus delphis	215.8	49.0	4.5	37.0	36.9	5.0	24.3	1.4	44.2
Delphinus delphis	219.7	46.0	4.1	34.6	34.6	5.2	19.7	1.1	48.3
Delphinus delphis	223.0	46.5	4.3	32.6	34.5	5.0	21.2	1.2	46.7
Delphinus delphis	231.5	51.3	4.1	34.4	36.6	5.8	24.5	1.4	47.8
Globicephala macrorhynchus	443.0	104.5	5.8	27.1	78.3	7.1	35.0	0.6	57.7
Globicephala macrorhynchus	476.0	126.5	5.2	29.3	79.0	5.8	46.0	0.7	52.2
Globicephala macrorhynchus	477.0	116.0	5.0	14.4	87.5	6.8	40.7	0.7	53.1
Grampus griseus	295.5	83.5	5.7	29.9	56.7	5.7	35.5	1.4	41.8
Globicephala melaena	304.8	63.3	4.6	33.7	66.0	7.7	18.2	0.6	58.3
Inia geoffrensis	196.0	42.0	2.0	42.8	40.3	2.5	7.0	0.2	66.2
Inia geoffrensis	256.0	49.7	2.6	38.9	45.8	3.6	8.1	0.2	56.5
Kogia breviceps	170.0	42.5	3.7	36.3	27.3	4.0	6.5	0.6	64.4
Kogia breviceps	281.0	78.1	5.1	25.8	44.5	4.3	11.8	0.5	58.3
Kogia breviceps	285.0	84.0	3.9	33.4	46.0	5.7	13.0	0.8	53.4
Lagenorhynchus acutus	209.0	48.0	3.9	41.3	32.0	6.3	20.0	0.8	46.4
Lagenorhynchus acutus	215.5	58.2	4.0	39.6	32.9	4.5	21.8	1.0	48.8
Lagenorhynchus acutus	216.0	57.6	3.9	40.5	32.5	4.8	3.3	1.2	48.2
Lagenorhynchus acutus	260.0	62.5	4.8	35.3	35.8	4.9	27.6	0.9	57.5

Species	Length (cm)	Fluke Span (cm)	Fluke AR	Fluke Sweep (deg)	Flipper Length (cm)	Flipper AR	Fin Height (cm)	Fin AR	Fin Sweep (deg)
Lagenorhynchus obliquidens	185.0	41.8	4.4	36.9	34.0	5.4	17.4	1.1	46.6
Lagenorhynchus obliquidens	212.0	56.1	4.8	29.0	36.6	4.7	16.7	0.8	56.5
Lagenorhynchus obliquidens	213.0	56.3	4.5	29.4	33.6	5.1	16.5	0.9	57.7
Lagenorhynchus obliquidens	220.0	53.3	4.7	32.1	36.3	5.1	20.8	1.2	50.0
Lipotes vexillifer	202.0	NA	3.1	40.4	NA	2.7	NA	0.6	41.2
Lissodelphis borealis	203.9	32.2	3.1	38.6	24.9	7.5	0.0	0.0	0.0
Mesoplodon densirostris	420.0	106.0	5.1	28.2	47.0	4.0	20.3	1.0	48.7
Mesoplodon europaeus	265.0	64.1	4.8	26.9	29.1	4.6	10.8	0.8	37.5
Mesoplodon europaeus	344.0	79.0	4.1	33.3	34.0	3.7	15.0	1.1	34.8
Mesoplodon europaeus	380.0	87.0	5.3	26.9	39.3	5.0	18.1	1.1	37.4
Mesoplodon europaeus	447.0	108.7	5.1	28.5	41.9	5.4	25.0	1.1	38.2
Mesoplodon mirus	456.0	129.0	4.8	31.4	53.0	4.4	21.0	1.1	39.5
Orcinus orca	416.0	110.0	4.5	27.7	64.0	2.4	45.0	1.5	40.8
Orcinus orca	446.0	105.0	4.9	17.8	70.0	2.9	49.0	2.0	35.9
Orcinus orca	516.0	133.0	5.0	22.8	79.0	2.5	70.0	2.0	35.4
Orcinus orca	540.0	136.0	5.5	17.3	84.0	2.3	66.0	1.9	31.2
Orcinus orca	624.8	185.0	4.7	4.4	120.0	1.9	99.0	2.4	29.7
Peponocephala electra	246.0	52.2	4.4	34.2	42.5	5.5	26.0	1.1	45.2
Phocoenoides dalli	202.9	49.3	4.4	5.4	19.3	2.6	17.7	1.0	45.9
Phocoenoides dalli	208.0	50.0	4.8	12.3	21.4	3.4	17.0	0.8	45.3
Pseudorca crassidens	355.0	74.0	5.0	28.5	51.0	4.8	25.0	1.1	49.5
Pseudorca crassidens	388.0	84.0	4.6	29.1	55.0	5.1	45.0	1.2	43.6
Pseudorca crassidens	399.0	98.0	6.2	26.0	63.0	4.2	43.0	1.2	54.3
Phocoena phocoena	109.2	24.6	3.5	32.0	17.9	5.8	7.7	0.8	45.0
Phocoena phocoena	139.0	30.5	3.9	35.2	20.0	3.7	9.0	0.8	48.9
Steno bredanensi	228.1	59.4	4.0	30.0	43.3	4.4	23.7	1.3	41.4
Stenella clymene	186.0	46.0	5.2	23.6	27.5	5.5	16.0	1.2	46.6
Stenella coeruleoalba	214.0	54.0	5.2	26.4	29.8	6.2	20.0	1.2	49.3
Stenella coeruleoalba	222.5	46.7	5.2	32.3	33.4	5.3	16.0	1.1	51.2
Stenella coeruleoalba	232.0	49.0	4.4	26.6	31.0	5.8	19.0	1.1	45.9
Stenella plagiodon	215.0	55.7	4.6	29.2	36.2	5.1	24.2	1.5	48.9
Stenella plagiodon	182.3	43.0	4.3	27.5	29.7	5.5	18.8	1.4	49.2
Stenella plagiodon	183.0	49.0	4.0	32.1	38.0	5.8	39.0	1.1	51.0
Stenella plagiodon	189.0	53.0	5.3	26.3	29.3	5.2	20.0	1.5	44.5
Stenella plagiodon	205.0	50.0	4.0	30.3	33.0	5.3	19.0	1.1	45.3
Stenella plagiodon	211.0	45.0	4.1	30.4	32.0	5.5	22.0	0.9	48.0

Species	Length (cm)	Fluke Span (cm)	Fluke AR	Fluke Sweep (deg)	Flipper Length (cm)	Flipper AR	Fin Height (cm)	Fin AR	Fin Sweep (deg)
Stenella plagiodon	191.5	44.0	4.5	25.0	28.0	4.6	17.0	1.0	47.7
Tursiops truncatus	251.0	63.0	3.8	34.5	34.0	4.8	19.1	1.0	44.7
Tursiops truncatus	270.0	65.0	3.6	25.8	37.0	4.4	23.0	1.2	48.1
Tursiops truncatus	106.0	26.8	3.0	34.4	23.0	4.6	9.9	0.9	51.9
Tursiops truncatus	157.6	29.5	3.1	38.8	25.0	5.2	14.6	1.6	41.4
Tursiops truncatus	158.8	36.4	3.4	34.8	26.8	3.8	14.1	1.1	43.8
Tursiops truncatus	206.0	55.6	4.1	27.6	36.2	3.5	19.8	1.2	44.7
Tursiops truncatus	208.5	39.4	3.0	37.6	32.3	5.4	20.2	1.2	47.3
Tursiops truncatus	210.0	48.1	4.1	34.4	33.5	4.8	18.0	1.0	47.9
Ziphius cavirostris	256.0	59.5	3.8	30.0	34.0	5.0	10.0	0.8	43.9
Ziphius cavirostris	269.0	61.0	3.9	31.7	34.5	4.1	11.0	1.2	40.1
Ziphius cavirostris	395.0	96.0	3.7	39.3	44.0	3.4	NA	NA	NA*

* Not available

APPENDIX D

A BRIEF HISTORY OF THE U.S. NAVY MARINE MAMMAL PROGRAM

by Tom LaPuzza, SSC San Diego

The U.S. Navy's Marine Mammal Program had its origin in the acquisition, in 1960, of a Pacific white-sided dolphin for hydrodynamic studies. Navy scientists designing torpedos had heard accounts of the hydrodynamic efficiency of dolphins, and were interested in determining whether dolphins did in fact have special characteristics that might be applied to the design of the underwater missiles. Work with the white-sided dolphin indicated that she possessed no unusual physiological or hydrodynamic capabilities, but it was suspected that limitations of the physical facilities and the measurement capabilities at the time might have affected the study data. Under a new program, research on dolphin hydrodynamics has been resumed with the same goal to determine if the dolphin does indeed possess a highly evolved drag reducing system. The capabilities for undertaking this work are now greatly improved and include instrumentation for measurements that previously could not be made. Among the possible drag-reducing mechanisms being studied are skin compliance, biopolymers, and boundary layer heating, which may or may not work synergistically.

Early Navy marine mammal work centered around Pt. Mugu, California, where a modest facility for research and exploratory development gradually evolved on a sand spit between Mugu Lagoon and the ocean. The program got underway in 1963. The primary interests were in the study of the marine mammals' specially developed senses and capabilities (such as sonar and deep diving physiology) and also how dolphins and sea lions might be used to perform useful tasks. A major accomplishment was the demonstration that trained dolphins and sea lions could be worked untethered in the open sea with great reliability. In 1965, a Navy dolphin named Tuffy participated in the Sealab II project off La Jolla, California, carrying tools and messages between the surface and aquanauts operating out of the habitat 200 feet below.

In 1967, the Point Mugu facility and its personnel were relocated to San Diego and placed under a newly formed organization which has since undergone a number of name changes, including Naval Undersea Center (NUC); Naval Ocean Systems Center (NOSC); Naval Command, Control and Ocean Surveillance Center Research, Development, Test and Evaluation Division (NRaD); and, currently, Space and Naval Warfare Systems Center San Diego (SSC San Diego). Shortly after the headquarters move to San Diego, a laboratory was established in Hawaii at the Marine Corps Air Station on Kaneohe Bay. Some of the personnel and animals at Point Mugu transferred to the Hawaii Laboratory, and later the rest of the operation moved to a new facility on Point Loma in San Diego.

Here the research and development program begun at Point Mugu has continued. This has included further studies of the capabilities of marine mammals; development of improved techniques for diagnosis and treatment of health problems; neurophysiological studies, using behavioral and other non-invasive techniques, to gain a better understanding of how the large dolphin brain functions; development of instrumentation for determining, by brain wave activity, the hearing range of a cetacean; and investigation of how dolphins produce the sounds they make.

Marine mammal work at the Hawaii Laboratory was concerned with behavior studies, reproductive physiology, further research on the dolphin echolocation system and investigation of the potential of marine mammals for performing useful tasks more efficiently, safely and cost effectively than is possible using human divers or deep submersibles.

In 1993, as the result of Base Closure and Realignment Commission action, the Hawaii Lab was closed, and the majority of the animals moved to San Diego. A small group of animals remained, participating in joint research with the University of Hawaii Institute of Marine Biology.

In its operational systems, the Navy employs dolphins and sea lions to perform underwater surveillance for object detection, location, marking and recovery, working under the close supervision of their Navy handlers. On cue from its handler, an animal searches a specific area using its sensitive underwater directional hearing (sea lions) or its biological sonar (dolphins). The animal reports to its trainer when the target object is detected. The trainer then makes a determination based on the situation what action to take: whether to send the animal to mark or recover the object, or employ human divers to make a recovery.

The Navy uses dolphins in operational programs for swimmer defense--to detect swimmers, divers and swimmer delivery vehicles, and, if the handler determines the situation warrants, to mark them; and mine countermeasures--to detect bottom mines and moored mines. Dolphins are used for these tasks because their extraordinary natural biological sonar capabilities enable them to find objects in waters where hardware sonars do not work well due to poor acoustic environmental conditions. The swimmer defense system was deployed to Vietnam in 1970-71 and to the Persian Gulf in 1987-88.

An operational system developed in Hawaii employs California sea lions to locate and attach recovery hardware to unarmed instrumented test ordnance, which is fired or dropped into the ocean and then must be recovered. Traditional recovery involved human divers, who are handicapped by brief working times on the bottom, poor visibility, currents and the requirement for medical personnel, a recompression chamber and other surface support. The sea lion recovery system, which eliminates this complex and potentially dangerous recovery approach, consists simply of a small rubber boat, a sea lion and two or three handlers. When the boat arrives at the recovery site, the sea lion is sent over the side. Trained to detect the ordnance by an acoustic beacon placed in the object before the test, the sea lion indicates if he hears the beacon and accepts a bite plate to which an attachment device is mounted. A strong line tied to this device is payed out from the boat as the sea lion swims down to the object and attaches the device. The sea lion then releases the bite plate and returns to the boat for a well-deserved reward of fish while a crane is used to pull the object off the bottom. The system, which has a recovery capability to a depth of 650 feet, became operational in 1975 and has been in service use since that time.

In a similar project, called Deep Ops, a pilot whale and two killer whales demonstrated their ability to recover objects from greater depths. The recovery device the whales attached to the target object, a dummy torpedo containing an acoustic beacon, incorporated a hydrazine gas generator which was activated upon attachment of the device to the torpedo. The generated gas filled a large lift bag which raised the torpedo to the surface. Using this device, the pilot whale successfully recovered the torpedo from a depth of 1,654 feet. Although much was learned from the Deep Ops project, work with pilot and killer whales, the largest of the dolphins, has not been continued.

The capabilities of belugas, or white whales, have been investigated at the SSC San Diego and Hawaii facilities, San Clemente Island, and torpedo test ranges in Seattle and Canada. Although belugas are inshore and estuarine animals which enter rivers for calving and feeding, they were found capable of

diving to at least 2100 feet. In studies to determine their ability to recover inert experimental torpedoes at a test range, the belugas attached the recovery device to a dummy torpedo at 1300 feet, the maximum depth available.

All Navy marine mammal training is performed using positive reinforcement with food reward, that is, the animals are rewarded with fish for performing their tasks correctly but they are not punished for failure to perform them. As the result of allegations of animal abuse within the Navy's mammal program, the Assistant Secretary of the Navy invited two in-depth reviews by the presidentially appointed Marine Mammal Commission. The reviews in 1988 and 1990 resulted in satisfactory to outstanding ratings for all aspects of the Navy program. Additionally, the National Marine Fisheries Service, which maintains oversight responsibility for all marine mammals in the care of people in the U.S., reported findings in the scientific literature that showed the Navy's dolphin survival rate is the highest among all organizations holding large numbers of marine mammals. This was attributed by the researchers conducting the study to "superior husbandry." Dolphin survival rate in the wild is reported in the scientific literature as 92-95 percent; the Navy's dolphin survival rate for the past 10 years has been 95-97 percent, and during one recent period the Navy maintained an unprecedented 100 percent survival rate for its 140 marine mammals for more than a year and a half.

Navy dolphins are maintained in their natural environment—bays and harbors of the Pacific and Atlantic Oceans--in open-mesh enclosures that provide a normal echolocation environment and ample socialization opportunities except during medical procedures and actual training periods. Navy dolphins are trained untethered in the open ocean on an almost daily basis, and yet in the course of 30 years of such training and many thousands of these open-ocean sessions only seven of the Navy's dolphins have failed to return to their enclosures.

The Navy's marine mammal systems are subject to the same rigorous test and evaluation process required of any Navy system prior to fleet acceptance. Systems failing to meet acceptable standards of effectiveness and reliability are rejected by the Navy. The Navy's operational marine mammal systems are efficient, reliable and cost-effective.

For further information, please contact Tom LaPuzza, SSC San Diego Public Affairs Officer, at (619) 553-2724.

APPENDIX E

THE POTENTIAL OF MARINE BIONICS

K. J. Moore
Cortana Corporation
520 N. Washington St., Falls Church, VA 22046

Recent demonstrations in the Flow Management Program have shown that multiple slots and stratified ejection of additives can be much more effective than traditional techniques for ejecting drag-reducing additives. The approach was physics-based and engineered to provide a favorable viscosity gradient in the near-wall region of the boundary layer. Once understood and demonstrated, the suggestion of the unique gill structure of a high-speed shark stimulated an examination of shark gill morphology which determined that nature had exploited the same physics millennia before our recent achievement.

This situation is not unique. Marine biologists are rarely interested in or equipped to explain the hydrodynamic function of the biological systems they investigate. Further, even in a multidisciplinary team, naval architects or marine engineers are often unaware of the physical implication of biological complexes, such as gill rakers. It can be a "Catch 22" situation in which the investigator does not recognize the elegance of the bionic model because he doesn't understand the physics. It is necessary for all but the most imaginative investigations to understand the physics in order to recognize all the functions. Successful biological systems are efficient, and efficient often means multifunctional. The shark's gill complex is a good example. We now believe it provides oxygen, cools the blood, ejects fluid in the boundary layer to energize the boundary layer and avoid separation of the flow during maneuvers, ejects mucin to produce the Toms Effect (friction reduction), and ejects water at the correct stratum to produce a favorable viscosity gradient. The ejecta also reduce interference drag at the base of the pectoral fins.

It was shark denticles that stimulated the research at NASA Langley into surface riblets to reduce skin friction. Only recently have we recognized that the denticles are not rigid, but act as smart roughness elements and are one of nature's close analogues to the concept of micro-adaptive surfaces.

Bionics research is not straightforward. Some of the most prominent scientists had previously published that fish mucin increased rather than reduced drag. This conclusion was based on the evaluation of mucin as a drag-reducing agent after it had been scraped off an animal and left for extended periods in laboratory test tubes before testing. Many marine investigators had little understanding of live systems and their chemical degradation, when removed from the natural conditions.

Similar misconceptions occurred in the attempts to develop drag-reducing coatings. In the United States, the approach was to investigate a wide range of elastic and viscoelastic coatings, then available in industry. Other researchers investigated the

mechanical properties and controllability of live marine animal integument in their natural swimming condition, and then developed materials with similar properties. The latter approach has had much more encouraging results and serves not only as a more rigorous scientific approach, but also as a model for bionics research. Success will follow a multiple disciplinary team that recognizes the multi-functional aspect of most biological systems and that has members who are both creative and well versed in all of the relevant science.

APPENDIX F

LOW-SPEED MANEUVERING—LESSONS FROM BIO-HYDRODYNAMICS

Dr. Promode R. Bandyopadhyay

Naval Undersea Warfare Center
Newport, RI 02841
(401) 832 - 2712
BandyopadhyayPR@Npt.NUWC.Navy.Mil

OVERVIEW

The focus of this work is on maneuvering and not propulsion, which is well developed in underwater vehicles. Navy has many important low-speed maneuvering needs. After they are launched, there is a need to steer small vehicles away from a submarine at low speeds to minimize alertment noise. This is a very important area where contributions are needed. Due to the contemporary focus on littoral areas, the following typical issues related to low-speed maneuvering hydrodynamics have assumed importance: a faster response to turning/angle-of-attack command in a vehicle, a lowering of turning/dive radius and speed, need for backward motion, and the prevention of tangling of arrays of towed cables. The present work originated from the vision, namely that, because a fish habitat is a predator-prey domain where stealth and maneuvering ability are vital to survival, their studies may give us a clue to novel control surfaces and new approaches to solving the above mentioned low-speed underwater hydrodynamics problems. Although difficult, the approach, namely learning from biology specifically for application to engineering, has many appeals. It was thought that the present work may also shed some light on the fundamental philosophical differences between biolocomotion, which is unsteady, force-based-control and survival-oriented in nature, and current vehicle hydrodynamics / aerodynamics which is steady state, moment-based-control and largely safety-oriented. A series of investigations combining hydrodynamics, biology and theoretical control, were carried out addressing these issues. They are reported here. The gap in maneuvering ability of fish and small underwater vehicles has been quantified and serves as a target for future improvement. The head and tail movements of a fish and their phased interaction have been simulated experimentally on a rigid cylinder. Extensive dynamic measurements of forces and moments on bodies appended with the fish-inspired control surfaces have been carried out and analyzed. Phase-matched measurements of vorticity-velocity vectors of shed vortices of flapping foil maneuvering devices, and their dye flow visualization have been carried out. The general conclusion is that, the mechanism of discrete and deterministic vortex shedding from oscillating control surfaces has the property of large amplitude unsteady forcing and an exquisite phase dependence, which makes it inherently amenable to active control for precision maneuvering. Several fish-inspired maneuvering control surfaces have been demonstrated on rigid cylindrical bodies. Finally, a novel low-speed precision maneuvering vehicle, that synthesizes many

of the key features of fish swimming, has been conceived and its swimming demonstrated. Patents have been generated. The research has been transitioned to the ONR 342 Biomimetics SBIR Program.

1. Questions

Specific *scientific* questions addressed in this research include:

- What is the quantitative gap in maneuvering ability between agile species of fish and small underwater vehicles? (Bandyopadhyay, Castano, Rice, Philips, Nedderman & Macy 1997)

- What general control surfaces characterize the maneuvering ability of fast or slow, yet agile species of fish? (Bandyopadhyay, Castano, Rice, Philips, Nedderman & Macy 1997, Bandyopadhyay, Nedderman & Dick 1999a)

- Is the flapping foil mechanism a signature suppressing / stealth mechanism? (Bandyopadhyay & Donnelly 1999)

- How different, phenomenologically, is the flapping foil mechanism of maneuvering and propulsion applied to a rigid cylinder, compared to a flexible bodied fish? (Bandyopadhyay & Donnelly 1999)

- Is there any gain to be had if the head and tail swaying of a fish are related? (Bandyopadhyay & Donnelly 1999)

- What philosophical design traits distinguish fish maneuvering and propulsion with those of man made engineering vehicles? (Bandyopadhyay, Singh & Chockalingam 1999b, Bandyopadhyay, Nedderman & Dick 1999a)

Specific *applied* questions addressed in this research include:

- Because fish are known for fast starts and stops, what of their control surfaces is suitable for brisk maneuvering of underwater bodies? (Bandyopadhyay, Castano, Rice, Philips, Nedderman & Macy 1997)

- Is it possible to demonstrate a precision maneuvering control of a rigid cylinder in a disturbed ocean environment by means of biologically-inspired active control surfaces? (Bandyopadhyay, Singh & Chockalingam 1999b)

2. Background

Interest in flapping foil propulsion dates back to the early part of this century (see Jones et al. 1996). During WW2, German scientists had built a torpedo on this principle (see Ref. HSVA ...). The first comprehensive review of the inviscid momentum theory of fish

propulsion was given by Lighthill (1969). Simultaneously, non-linear inviscid analytical treatments were developed by Chopra (1977) and Wu (1971). Apparently a modern review, containing experimental and numerical development, as well as in-water application, is being written by Triantafyllou. He has conducted a series of experiments showing the propulsive mechanism. His work has placed discrete vortex shedding from the tail and its Strouhal number squarely at the center of the jet producing mechanism (Wolfgang et al. 1998; Anderson et al. 1998; Triantafyllou & Triantafyllou 1995; Triantafyllou et al. 1993). Biolocomotion has been explained by biologists like Fish (1998), Ellington (1995) and Webb (1978) in a manner that is more understandable by engineers. Recently, there has been increased interest and success in computing the flapping foil experimental observations. For example, vortex-lattice method has been used to compute the flapping foil thrust flow, by Kato (1999), Isogai et al. (1999), Kagemoto et al. (1999). Ramamurti & Sandberg (1996) and Karniadakis (1998 unpublished) have conducted simulation and visualization of the MIT 'robotuna'. The experiments indicate that flapping foil mechanism may be viewed as a method of vectoring a jet at the tail either in directions downstream (thrust) or upstream (drag) or at intermediate angles (maneuvering), by simply adjusting the relative phase of successively shed vortices. This reliance on deterministic and discrete vortex shedding and phase gives this approach several inherent capabilities. They are, namely the production of large forces compared to steady state techniques (Bandyopadhyay & Donnelly 1999) and amenability to active control (Bandyopadhyay et al. 1999b). Due to these reasons, the present work highlights the suitability of fish based control surfaces to applications in maneuvering, rather than propulsion as pursued almost exclusively by other researchers (Bandyopadhyay et al. 1997, Bandyopadhyay & Donnelly 1999).

3. Characteristics of Low-speed Maneuvering of Fish and Small Underwater Bodies

To determine the morphological features of the control surfaces common to fish endowed with maneuvering ability, twenty nine species were first examined (Bandyopadhyay et al. 1997). They were grouped into three categories: slow and highly maneuverable (coral fish), fast and poorly maneuverable (open water fish) and an over-lapping category, namely fast yet maneuverable. Several characteristic features were found.

An engineering biology experiment was then carried out to compare the maneuvering ability of fish to small underwater vehicles (Bandyopadhyay et al. 1997). Digital video taping of fast yet maneuverable species of fish like bluefish and mackerel in a 'mazed' tank were carried out. The turning characteristics were compared with those of small underwater vehicles. The gap in turning ability, which is large, was thus quantified and serves as a target for future progress. It was found that the gap has been greatly reduced from the 1950s to the 1990s vehicles. This can be attributed to improved control technology, but not to hydrodynamic technology. It is thus suggested that further closing of the gap may be achievable by incorporating biology-based (biomimetic) maneuvering surfaces operated actively by modern digital control technology.

4. Fish-Inspired Control Surfaces Appended to a Rigid Cylinder

Four fish-inspired control surfaces were demonstrated. They are a brisk maneuvering dorsal fin device, a dual flapping foil device, a tiny but sensitive nose vortex shedding device (called nose-slider here), and a surface wave action stabilizing pectoral wing device.

The knowledge of the control surfaces special to fish with maneuvering ability was used to find a method of reducing the response time to maneuvering control of current tactical scale underwater vehicles. A brisk maneuvering device was then scaled on dorsal fins, built and demonstrated on a rigid cylinder.

The dual flapping foil and the nose slider, described in the next section exploit the phased-interaction of discrete shed vortices, from the nose and tail, to produce maneuvering cross-stream forces.

The effectiveness of attaching a pair of small pectoral wings to a rigid cylinder to improve maneuverability was studied. Measurements have been carried out in a tow tank on cylindrical bodies submerged in proximity of traveling surface waves. Two bodies are considered: a reference plain cylinder and another cylinder containing a pair of wings (or hydrofoils) below the cylinder, not above. The latter body owes its origin to certain species of fish which has small wings for maneuverability. The wavelength of the surface waves (λ) is of the order of the cylinder length (L) or higher ($1 < \lambda/L < 10$). Temporal measurements of axial and vertical forces and pitching moments, phase matched to the surface elevation of traveling waves, have been carried out. The time periods of the waves and depth of water pertain to deep water and intermediate depth waves. The forces and moments exhibit characteristic phase relationship with water elevation. Towing affects only vertical forces in the speed range of *0 to 1 m/s*. The effect of towing and surface waves on vertical forces is roughly additive. Within the low speed range of towing evaluated, the effects of surface waves dominate those of towing. The presence of the hydrofoil and intermediate depth waves bring in some additional effects which are not well understood. In intermediate depth waves, a small plain cylinder may encounter a resonance with traveling waves which can be averted by attaching a pair of small wings to dampen pitching moment and make it speed invariant, although at a cost of increased vertical forces.

5. Detailed Experimental Simulation of Fish-Inspired Unsteady Hydrodynamics on a Rigid Cylinder

The unsteady hydrodynamics of the tail flapping and head oscillation of a fish, and their phased interaction, are considered in a laboratory simulation. Two experiments are described where the motion of a pair of rigid flapping foils in the tail and the swaying of the forebody are simulated on a rigid cylinder. Two modes of tail flapping are considered:

waving and clapping. Waving is similar to the motion of the caudal fin of a fish. The clapping motion of wings is a common mechanism for the production of lift and thrust in the insect world, particularly in butterflies and moths. Measurements carried out include dynamic forces and moments on the entire cylinder-control surface model, phase-matched laser Doppler velocimetry maps of vorticity-velocity vectors in the axial and cross-stream planes of the near-wake, as well as dye flow visualization. The mechanism of flapping foil propulsion and maneuvering is much richer than reported before. They can be classified as natural or forced. This work is of the latter type where discrete vortices are forced to form at the trailing edge of flapping foils via salient edge separation. The transverse wake vortices that are shed, follow a path that is wider than that given by the tangents to the flapping foils. The unsteady flap-tip axial vortex decays rapidly. Significant higher order effects appear when Strouhal number (*St*) of tail flapping foils is above *0.15*. Efficiency reaches a peak below the *St* range of *0.25 - 0.35*. Understanding of two-dimensional flapping foils and fish reaching their peak efficiency in that range is clarified. Strouhal number of tail flapping does emerge as an important parameter governing the production of net axial force and efficiency, although it is by no means the only one. The importance of another Strouhal number based on body length and its natural frequency is also indicated. The relationship between body length and tail flapping frequency is shown to be present in dolphin swimming data. The implication is that, for aquatic animals, the longitudinal structural modes of the body and the head/tail vortex shedding process are coupled. The phase variation of a simulated and minute head swaying, can modulate axial thrust produced by the tail motion, within a narrow range of $\pm 5\%$. The general conclusion is that, the mechanism of discrete and deterministic vortex shedding from oscillating control surfaces has the property of large amplitude unsteady forcing and an exquisite phase dependence, which makes it inherently amenable to active control for precision maneuvering.

6. Biologically-Inspired Theoretical Control of Maneuvering

The theoretical control of low-speed maneuvering of small underwater vehicles in the dive plane using dorsal and caudal fin-based control surfaces is considered. The two dorsal fins are long and are actually mounted in the horizontal plane. The caudal fin is also horizontal and is akin to the fluke of a whale. Dorsal-like fins mounted on a flow aligned vehicle produce a normal force when they are cambered. Using such a device, depth control can be accomplished. A flapping foil device mounted at the end of the tailcone of the vehicle produces vehicle motion that is somewhat similar to the motion produced by the caudal fins of fish. The moment produced by the flapping foils is used here for pitch angle control. A continuous adaptive sliding mode control law is derived for depth control via the dorsal fins in the presence of surface waves. The flapping foils have periodic motion and they can produce only periodic forces. A discrete adaptive predictive control law is designed for varying the maximum tip excursion of the foils in each cycle for the pitch angle control and for the attenuation of disturbance caused by waves. Strouhal number of the foils is the key control variable. The derivation of control laws requires only imprecise knowledge of the hydrodynamic parameters and large uncertainty in system parameters is allowed. In the closed-loop system, depth trajectory

tracking and pitch angle control are accomplished using caudal and dorsal fin-based control surfaces in the presence of system parameter uncertainty and surface waves. A control law for the trajectory control of depth and regulation of the pitch angle is also presented, which uses only the dorsal fins and simulation results are presented to show the controller performance.

7. Synthesis of Lessons into Application

The knowledge gained was used to build two small tethered model vehicles. One of them termed an "agile vehicle" is described in the Bandyopadhyay references. The other is shown in Fig. 1 and described in the caption. A 4-channel software controlled digital circuitry (not shown) was also built to adjust the phase of the flapping foils for maneuverability. The opposing diagonal pairs of flapping foils may be operated out of phase to generate high levels of force at all times. A video demonstrating the swimming of this quiet low-speed vehicle has been made. Due to its precision maneuverability and ability to cancel imposed perturbations, the vehicle may be used as follows: a programmable mine; mapping of sea floor; towing of sensor cables from the tail core; and, the photographing and sampling of muddy floors due to its seeming quiet nature.

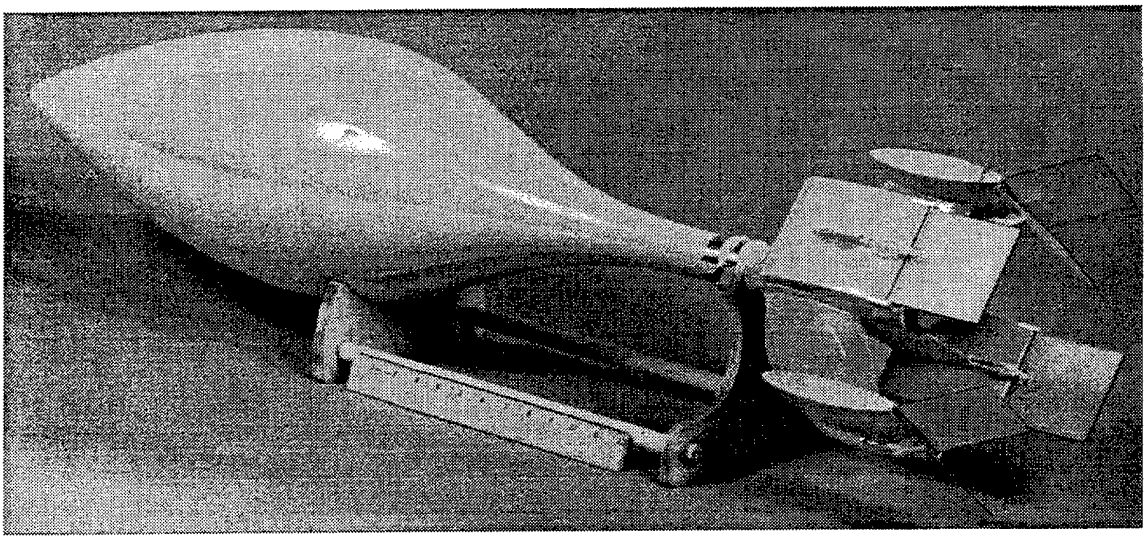

Figure 1. The 'quiet low-speed swimmer'. Four pairs of flapping foils attached to a so called 'B1-shaped' low-drag fore-body. Note the availability of the non-rotating tail center for towing sensor cables, unlike those in unmanned undersea vehicles with rotating propulsors.

8. Summary

A series of experiments and control simulations have been carried out to understand the maneuvering mechanism in fish propulsion, and also to build novel control surfaces for attachment to rigid cylindrical vehicles. The gap in maneuvering ability of fish and small underwater vehicles has been quantified and serves as a target for future improvement. Extensive dynamic measurements of forces and moments on bodies appended with several fish-inspired control surfaces have been carried out and analyzed. Phase-matched

measurements of vorticity-velocity vectors of shed vortices of flapping foil maneuvering devices, and their dye flow visualization have been carried out. The general conclusion is that, the mechanism of discrete and deterministic vortex shedding from oscillating control surfaces has the property of large amplitude unsteady forcing and an exquisite phase dependence, which makes it inherently amenable to active control for precision maneuvering. Several fish-inspired maneuvering control surfaces have been demonstrated on rigid cylindrical bodies. A novel low-speed precision maneuvering vehicle, that synthesizes many of the key features of fish swimming, has been conceived and its swimming demonstrated.

The future plan is to achieve a closed-loop active control and the development of ion-exchange polymer-metal composites as biomimetic actuators that mimic the functions of muscles. This would be for Naval application for quiet maneuvering, control of towed cables and also for the quieting of commercial turbomachines (Bandyopadhyay 1997).

ACKNOWLEDGMENT

The principal investigator would like to thank Dr. William Macy of the Graduate School of Oceanography, University of Rhode Island, Narragansett Campus for collaboration on the fish biology work. He would like to thank Professor S. N. Singh of the Department of Electrical Engineering and Computer Sciences, University of Nevada, Las Vegas, for collaboration on theoretical control of maneuvering. He would like to thank Dr. Martin Donnelly of the Department of Engineering Sciences, VPI & SU for collaboration on phase-matched laser Doppler measurements of vorticity-velocity vectors.

REFERENCES

Anderson, J. M., Streitlien, K., Barrett, D. S. & Triantafyllou, M. S. 1998 "Oscillating Foils of High Propulsive Efficiency," *Jou. Fluid Mech.*, vol. 360, 41-72.

Bandyopadhyay, P. R. 1997 "A Biomimetic Propulsor with Digital Vortex Management," *Navy Case Number 78880.*

Bandyopadhyay, P. R. & Donnelly, M. J. 1999 "Experimental Simulation of Fish-Inspired Unsteady Vortex Dynamics on a Rigid Cylinder," *ASME Journal of Fluids Engineering*, (subjudice).

Bandyopadhyay, P. R., Singh, S. & Chockalingam, F. 1999b "Biologically-Inspired Bodies Under Surface Waves. Part 2: Theoretical Control of Maneuvering", *ASME Journal of Fluids Engineering*, Vol. 121, No. 2, pp. (in Press).

Bandyopadhyay, P. R., Nedderman, W. H. & Dick, J. 1999a "Biologically-Inspired Bodies Under Surface Waves. Part 1: Load Measurements", *ASME Journal of Fluids Engineering*, Vol. 121, No. 2, pp. (in Press).

Bandyopadhyay, P. R., Castano, J. M., Rice, J. Q. Philips, R. B., Nedderman, W. H. & Macy, W. K. 1997 "Low-speed Maneuvering Hydrodynamics of Fish and Small Underwater Vehicles" *ASME Journal of Fluids Engineering*, V119, pp. 136-144.

Chopra, M. G. 1977 "Hydromechanics of Lunate Tail Swim-ming Propulsion," *J. Fluid Mech.*, **7**, 46-69.

Ellington, C. P. 1995 "Unsteady Aerodynamics of Insect Flight," *Biological Fluid Dynamics*, Sympo. of the Soc. for Experimental Biology, No. XLIX, pp. 109-129.

Fish, F. 1998 "Imaginative Solutions by Marine Organisms for Drag Reduction," *Proc. International Sympo. on Seawater Drag Reduction*, NUWC, Newport, RI, 443-450.

Gopalkrishnan, R., Triantafyllou, M. S., Triantafyllou, G. S. & Barrett, D. 1994 "Active Vorticity Control in a Shear Flow Using a Flapping Foil," *J. Fluid Mech.*, **274**, 1-21.

"HSVA Towing Tests on a G7e Torpedo with SSR-Drive and with Normal Propeller Drive," PG/21600, translated by the British from the German, September 1944.

Isogai, K., Shinmoto, Y. & Watanabe, Y. 1999 Effects of Dynamic Stall Phenomena on Propulsive Efficiency and Thrust of a Flapping Airfoil," *AIAA Jou.*, (due to appear).

Jones, K. D., Dohring, C. M. & Platzer, M. F. 1996 "Wake Structures Behind Plunging Airfoils: A Comparison of Numerical and Experimental Results, Paper No. AIAA 96-0078.

Kagemoto, H., Yue, D. K. P., Triantafyllou, M. S. 1999 "Force and Power Estimation in Fish-Like Locomotion Using a Vortex-Lattice Method," *ASME Jou. Fluids Engrg.*, (due to appear).

Kato, N. 1999 "Hydrodynamic Characteristics of Mechanical Pectoral Fin," *ASME Jou. Fluids Engrg.* (due to appear).

Lighthill, M. J. 1969 "Hydrodynamics of Aquatic Animal Propulsion," *Annual Rev. Fluid Mech.*, Vol. 1, pp. 413-446.

Ramamurti, W. C., Sandberg, W. C. & Lohner, R. 1996 "Computation of unsteady flow past a tuna with caudal fin oscillation", *Advances in Fluid Mechanics*, Eds. M. Rahman & C. A. Brebbia, Vol. 9, pp. 169-178.

Triantafyllou, M. S. & Triantafyllou, G. S. 1995 "An Efficient Swimming Machine," *Scientific American*, **272**, 64-70.

Triantafyllou, G. S., Triantafyllou, M. S. & Grosenbaugh, M. A. 1993 "Optimal Thrust Development in Oscillating Foils with Application to Fish Propulsion," *J. Fluids and Structures*, **7**, 205-224.

Triantafyllou, M. S., Triantafyllou, G. S. & Gopalkrishnan, R. 1991 "Wake Mechanics for Thrust Generation in Oscillating Foils," Phys. Fluids, *3*(12), 2835-2837.

Webb, P. W. 1978 "Hydrodynamics: Nonscombroid Fish," in *Fish Physiology, Vol. VII,* eds., W. S. Hoar & D. J. Randall, Academic Press, 189-237.

Wolfgang, M. J., Tolkoff, S. W., Techet, A. H., Barrett, D. S., Triantafyllou, M. S., Yue, D. K. P., Hover, F. S., Grosenbaugh, M. A. & McGillis, W. R. 1998 "Drag Reduction and Turbulence Control in Swimming Fish-like Bodies," *Proc. NUWC Intl. Sympo. on Seawater Drag Reduction*, July 22-24, 1998, held in Newport, RI.

Wu, T. Y. 1971 "Hydromechanics of Swimming Propulsion," *J. Fluid Mech.*, **46**, 337-355.

REPORT DOCUMENTATION PAGE

Form Approved
OMB No. 0704-0188

1. AGENCY USE ONLY *(Leave blank)*	2. REPORT DATE	3. REPORT TYPE AND DATES COVERED
	August 1999	Final

4. TITLE AND SUBTITLE
REVIEW OF DOLPHIN HYDRODYNAMICS AND SWIMMING PERFORMANCE

5. FUNDING NUMBERS
PE: 0603763E
AN: DN309253
WU: MM10

6. AUTHOR(S)
F. E. Fish
West Chester University

J. J. Rohr
SSC San Diego

7. PERFORMING ORGANIZATION NAME(S) AND ADDRESS(ES)
SSC San Diego
San Diego, CA
92152–5001

West Chester University
West Chester, PA 19383

8. PERFORMING ORGANIZATION REPORT NUMBER
TR 1801

9. SPONSORING/MONITORING AGENCY NAME(S) AND ADDRESS(ES)
Defense Advanced Research
Projects Agency (DARPA)
3701 North Fairfax Drive
Arlington, VA 22203–1714

10. SPONSORING/MONITORING AGENCY REPORT NUMBER

11. SUPPLEMENTARY NOTES

12a. DISTRIBUTION/AVAILABILITY STATEMENT
Approved for public release; distribution is unlimited.

12b. DISTRIBUTION CODE

13. ABSTRACT *(Maximum 200 words)*

The principal objective of this project was to perform a comprehensive review of performance, kinematics, and swimming hydrodynamics by dolphins and other cetaceans. This report describes information obtained from the available literature including published research and technical reports from English-speaking and Russian sources. The project team specifically studied routine and maximum swimming speeds, morphological design related to hydrodynamic performance, drag reduction, swimming kinematics, thrust production and efficiency, behavioral strategies employed for energy economy when swimming, and maneuverability.

14. SUBJECT TERMS
Mission Area: Marine Mammals
dolphin swimming
dolphin leaping
wave drag

15. NUMBER OF PAGES
196

16. PRICE CODE

17. SECURITY CLASSIFICATION OF REPORT	18. SECURITY CLASSIFICATION OF THIS PAGE	19. SECURITY CLASSIFICATION OF ABSTRACT	20. LIMITATION OF ABSTRACT
UNCLASSIFIED	UNCLASSIFIED	UNCLASSIFIED	SAME AS REPORT

21a. NAME OF RESPONSIBLE INDIVIDUAL	21b. TELEPHONE *(include Area Code)*	21c. OFFICE SYMBOL
J. J. Rohr	(619) 553–1604 e-mail: rohr@spawar.navy.mil	Code D363

INITIAL DISTRIBUTION

D0012	Patent Counsel	(1)
D0271	Archive/Stock	(6)
D0274	Library	(2)
D027	M. E. Cathcart	(1)
D0271	D. Richter	(1)
D3503	S. H. Ridgway	(1)
D363	J. J. Rohr	(35)

Defense Technical Information Center
Fort Belvoir, VA 22060–6218 (4)

SSC San Diego Liaison Office
Arlington, VA 22202–4804

Center for Naval Analyses
Alexandria, VA 22302–0268

Navy Acquisition, Research and
Development Information Center
Arlington, VA 22244–5114

Government Industry Data Exchange
Program Operations Center
Corona, CA 91718–8000

Office of Naval Research
Arlington, VA 22217–5660 (2)

Naval Undersea Warfare Center
Division Newport
Newport, RI 02841–5047

Defense Advanced Research
Projects Agency
Arlington, VA 22203–1714 (5)

University of California, Santa Cruz
Long Marine Laboratory
Santa Cruz, CA 95064

Texas A & M University
Department of Marine Biology
Galveston, TX 77553

Vassar College
Department of Biology
Poughkeepsie, NY 12601

Sea World
Orlando, FL 32821–8097

University of North Carolina at Wilmington
Biological Sciences
Wilmington, NC 28403

Northeastern Ohio Universities
College of Medicine
Rootstown, OH 44272–0095

Duke University
Department of Zoology
Durham, NC, 27706

University of Michingan
Department of Biology and School of
Natural Resources
Ann Arbor, MI 48109–1115

Technion
Department of Aeronautical Engineering
Technion City, Haifa 3200, Israel

University of California, Santa Cruz
Department of Biology
Santa Cruz, CA 95064

Slippery Rock University
School of Physical Therapy
Slippery Rock, PA 16057–1326

Smithsonian Institution
Museum of Natural History
Mammal Division
Washington, DC 20560

Abteilung Meereszoologie
Institut fur Meereskunde an der
Universitat Kiel
D–24105 Kiel, Germany

University of Washington
Department of Zoology
Seattle, WA 98250

University of California, Los Angeles
Department of Biology
Los Angeles, CA 90095–1606

NASA Langley Research Center
Hampton, VA 23681–0001

The University of Sydney
Department of Mechanical and
Mechatronic Engineering J07
New South Wales 2006, Australia

Massachusetts Institute of Technology
Department of Ocean Engineering
Cambridge, MA 02139–4307

Electric Boat
Groton, CT 06340–4989

West Chester University
Schmucker Science Center
Biology Department
West Chester, PA 19383 (10)

The Charles Stark Draper Laboratory, Inc.
Cambridge, MA 02139